Development of OTM Syngas Process and Testing of Syngas Derived Ultra-clean Fuels in Diesel Engines and Fuel Cells

Final Report

For Reporting Period Starting January 1, 2001 thru December 31, 2004

Principal Authors:
E.T. (Skip) Robinson, Principal Investigator, Torix
John Sirman, Program Administrator, Praxair
Prasad Apte, Ceramic Manufacturing Manager, Praxair
Xingun Gui, Chief Engineer, Advanced Combustion and Control,
International Truck and Engine Corp.
Tytus R. Bulicz, Project Development Engineer,
International Truck and Engine Corp.
Dan Corgard,, Senior Development Engineer, Future Technology,
International Truck and Engine Corp.
John Hemmings, Director, Technology and Chemicals, Foster Wheeler

Report Issue Date: May, 2005
DOE Cooperative Agreement No. DE-FC26-01NT41096

Submitting Organizations:

Primary: Praxair, Inc.
P.O. Box 44
175 East Park Drive
Tonawanda, NY 14150

Subcontractors:

Statoil ASA
Postuttak
N-7005 Trondheim, Norway

Torix, Inc
7165 Hart St., Suite B
Mentor, OH 44060

International Truck and Engine Corp.
10400 W. North Avenue
Melrose Park, IL 60160
Naperville, IL 60566

BP America Production Company
150 W. Warrenville Road
Mail Code H-5,

Foster Wheeler USA Corporation
2020 Dairy Ashford Road
Houston, TX 77077

DISCLAIMER

ABSTRACT

This final report summarizes work accomplished in the Program from January 1, 2001 through December 31, 2004

Most of the key technical objectives for this program were achieved. A breakthrough material system has lead to the development of an OTM (oxygen transport membrane) compact planar reactor design capable of producing either syngas or hydrogen. The planar reactor shows significant advantages in thermal efficiency and a step change reduction in costs compared to either autothermal reforming or steam methane reforming with CO_2 recovery.

Syngas derived ulltra-clean transportation fuels were tested in the Nuvera fuel cell modular pressurized reactor and in International Truck and Engine single cylinder test engines. The studies compared emission and engine performance of conventional base fuels to various formulations of ultra-clean gasoline or diesel fuels. A proprietary BP oxygenate showed significant advantage in both applications for reducing emissions with minimal impact on performance. In addition, a study to evaluate new fuel formulations for an HCCI engine was completed.

TABLE OF CONTENTS

List of Tables Page

List of Figures

List of Acronyms

ATR	Auto-thermal reforming
BDC	Bottom dead center
BPO	BP Oxygenate
BSFC	Brake Specific Fuel Consumption
CI	Compression ignition
CIDI	Compression ignition, direct injection
ECR	Effective compression ratio
EGR	Exhaust gas recirculation
F-T	Fischer-Tropsch
FTGTL	Fischer Tropsch Gas to Liquids
GHR	Gas heated reformer
IMEP	Indicative Mean Pressure
IVC	Intake valve closing
IVO	Intake valve opening
HCCI	Homogeneous Charge Compression Ignition
LCM	Lead candidate material
MCTE	Multi-Cylinder Test Engine
MM	Alternative material systems
OTM	Oxygen Transport Membrane
OTM-2	Compact planar reactor design optimized for F-T syngas production
OTM-3	Compact planar reactor design optimized for low emission hydrogen production
P-0	Small bench scale test reactors capable of testing single OTM tubes up to 8 inches in length at elevated pressures and temperature.
SCTE	Single Cylinder Test Engine
SMR	Steam methane reforming
TDC	Top dead center
TF	Target Flux
TFd	Target flux for dense disks
TFc	Target flux for composite systems
TP	Target Pressure
TT	Target Temperature
ULS	Ultra-low Sulfur
ULSD	Ultra-low Sulfur Diesel
VVA	Variable valve actuation

1.0 Executive Summary

Continued concerns about environmental quality are driving the need for development of ultra-clean transportation fuels (UCTF) and low emission vehicle propulsion systems. Natural gas is an attractive feed for the production of UCTF because it can be converted into an array of sulphur free fuels including synthetic gasoline, synthetic diesel, methanol, and other oxygenates. These fuels, when used neat or blended with conventional petroleum products have the potential to dramatically reduce emissions while providing an alternative (non-petroleum) energy source.

The processes for producing UCTF all utilize a common first step whereby natural gas is converted to syngas, a mixture of hydrogen, carbon monoxide, carbon dioxide and water. The syngas can be converted to synthetic gasoline and diesel via the Fischer Tropsch process or to methanol or other oxygenates by proprietary technologies. In all cases, over 50% of the capital cost and a significant fraction of the operating costs are associated with syngas production.

This program had two primary objectives: 1) develop an advanced, syngas technology based on ceramic oxygen transport membranes that will provide a step change reduction in the conversion costs of natural gas to syngas and 2) evaluation of syngas derived ultra-clean fuels in fuel cells; and the development of advanced compression ignition engines/after treatment /ultra-clean fuel systems. The first objective was expanded in Budget Period 3 to include OTM based hydrogen production, which is another type of UCTF. The second objective was modified in Budget Period 2 to include preliminary development work on a HCCI (homogenous charged compression ignition) engine. Some envisage the HCCI as the next generation internal combustion engine to replace conventional diesel engines.

The OTM Alliance team assembled to address these issues includes fuel producers, an industrial gas supplier and vehicle and engine manufacturers. Praxair (industrial gas), BP (oil/energy), and Statoil (oil/energy) focused on OTM syngas development and fuel production. Nuvera Fuel Cells and International Truck and Engine joined the team to evaluate the syngas derived fuels in fuel cells and internal combustion engines.

The program initially consisted of 10 tasks, but after the first 9 months several tasks were eliminated due to material issues which impeded further large scale pilot plant activities (Tasks 6 and 7). The program was restructured to focus the OTM syngas development work on material improvement and reactor design. The fuel testing program was not affected, and in fact was expanded to include HCCI development work. The program was also extended from three to four years, although the spend rate per year was reduced. The program was concluded in December 2004.

The program made great progress in resolving the material issues encountered during the operation of the P-1 pilot plant. An entirely new class of composite materials with dissimilar film and substrates was developed. Techniques for applying the new film materials to the more robust inert substrates were also developed. The new material system is amenable to planar designs, whereas the former material system was best deployed in a tubular architecture. The more robust planar system is also less expensive than earlier tubular designs. We project the planar system to have a very substantial (28 to 44%) capital cost advantage over conventional ATR (autothermal reforming) syngas technology utilizing cryogenic oxygen, thus meeting most of the requirements of the first program objective.

The planar reactor concept was modified for hydrogen production and found to have significant advantage relative to steam methane reforming with CO_2 capture. At equivalent hydrogen production costs, the OTM hydrogen reactor can reduce CO_2 sequestration costs by over 50% when compared to conventional amine scrubbing processes.

Fuels for evaluation in fuel cells and diesel engines were procured from Sasol and BP. Fischer Tropsch (FT) naphtha and diesel fuels were obtained from Sasol/Chevron and a proprietary oxygenate material (BPO) was obtained from BP. BP blended most of the fuels tested in the program.

Tests at Nuvera Fuel cells compared a FT naphtha and the same FT naphtha with BPO to a California Phase II reformulated low sulfur gasoline in burner module tests. The FT naphtha with BPO had the lowest CO, THC and NOx emissions than the other two fuels during start-up, and significantly lower NOx emissions during steady state operation.

Engine tests at International Truck and Engine showed similar advantages for the BPO when blended with ultra-low sulfur diesel fuel. 5% BPO in an ultra low sulfur (ULS) diesel fuel showed across the board reduction in soot, and mixed results for NOx and fuel consumption when compared to the neat ULS.

Finally, a matrix of fuel components were evaluated and three blends chosen for testing in a single cylinder HCCI test engine. This preliminary work showed that the HCCI engine will require a fuel with a vapor pressure of about 2 psi, but can tolerate low cetane components. The HCCI holds promise to be the next generation engine with the potential to substantially lower in-cylinder soot and NOx formation and no loss of efficiency. Thus all requirements of the second objective were met.

2.0 Introduction

The DOE’s Office of Fossil Energy created strategic partnerships targeted at the development and verification of advanced fuel-making processes that utilize fossil feedstocks. These processes will enable the production of ultra-clean transportation fuels that improve the environment, while also expanding and diversifying the fossil resource base. In response to the DOE’s solicitation (DE-PS26-00NT40758) for research and development leading to the production of ultra-clean transportation fuels from fossil resources, Praxair was awarded Cooperative Agreement number DE-FC26-01NT41096 for work entitled “Development of OTM Syngas Process and Testing of Syngas-Derived Ultra-clean Fuels in Diesel Engines and Fuel Cells” .

The objectives of this project are: (1) develop an advanced syngas technology, based on Oxygen Transport Membranes (OTMs), that will provide a step change reduction in the cost of converting natural gas to a spectrum of liquid transportation fuels and thereby improve the prospects for meeting vehicle emissions targets with cost competitive ultra clean transportation fuels (UCTFs); (2) evaluate the performance of, and emissions from selected syngas-derived UCTFs in advanced vehicle propulsion systems, including advanced diesel engines with post treatment and fuel cells; and 3) develop an optimized UCTF/diesel engine/exhaust after treatment system capable of meeting emission regulations beyond 2007.

The scope of work was modified for Budget Period 3 to include development of the OTM syngas technology for hydrogen production. Hydrogen is an ultra-clean fuel and a co-product of syngas, and is an integral part of the OTM commercialization roadmap.

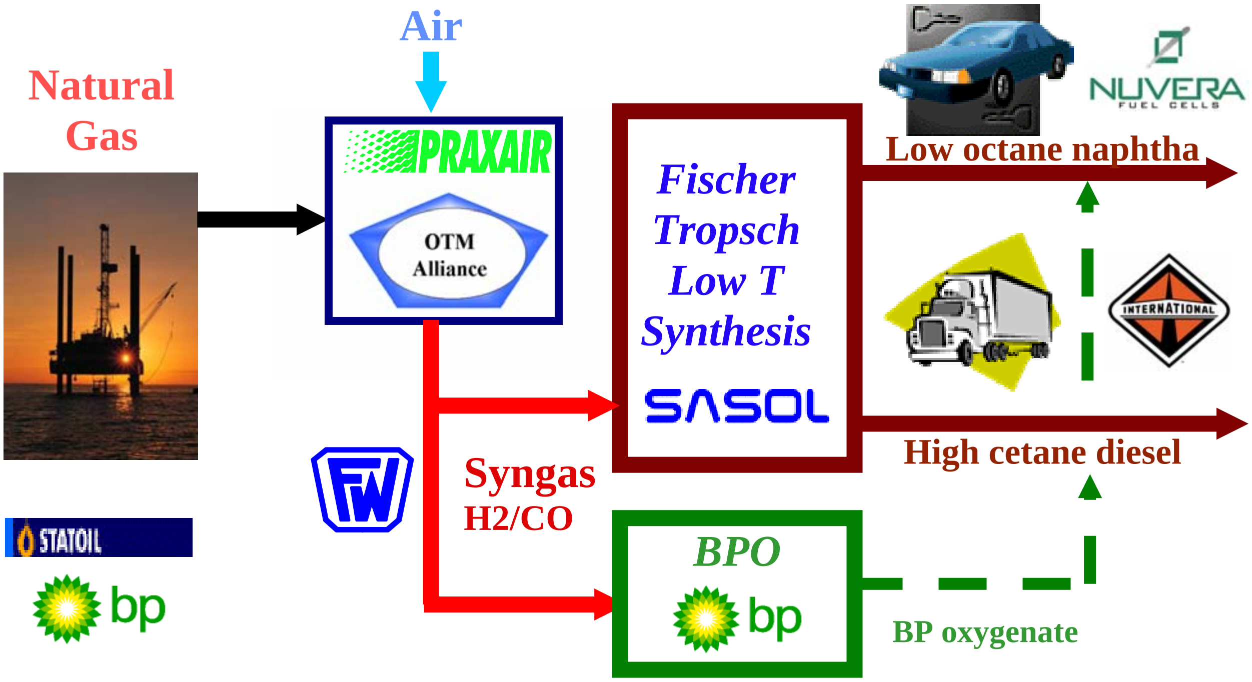

Figure 1: Program participants and contribution

To achieve these objectives, Praxair partnered with BP, Statoil, Sasol, Nuvera Fuel Cells, International Truck and Engine and Foster Wheeler Corp, Inc. as shown in Figure 1. Praxair, Statoil and BP focused on the syngas materials and reactor design. Foster Wheeler contributed to the development of the OTM reactors and syngas processes, and conducted benchmarking studies for both hydrogen and syngas production. BP and Sasol provided ultra-clean and base line fuels for testing. And Nuvera and International tested the fuels in their respective technologies.

3.0 Results and Discussion

3.1 Task 1: Materials Development

3.1.1 Goal - Task 1

The Recipient shall fabricate, test and characterize OTM film and substrate materials with the goal of developing a more robust and cost effective OTM element in comparison to the lead candidate material, LCM1.

3.1.2 Experimental - Task 1

The experimental facilities and methods in Task 1 were described in detail in the Topical Report for Budget Period 1 [Appendix I].

3.1.3 Task 1 Results and Discussion

The goal of this task is to develop superior materials for fabricating OTM elements. The approach is to develop two types of materials with different functions– a robust substrate for mechanical strength and an OTM film material for oxygen transport. Both materials must be chemically and physically compatible.

3.1.3.1 Substrate materials

Two robust substrate materials LCM65 and MM2 were discovered and optimized. Both of these materials have little or no chemical expansion and exhibit excellent high temperature strength and creep properties. MM2 was found to be amenable to planar construction and is the basis for the new material systems utilized in the planar type reactors, which are discussed further under Task 4.

3.1.3.2 Membrane materials

The focus of this subtask is to develop OTM film materials that are robust and compatible with LCM29 and MM2. To this end forty-nine new membrane materials were fabricated and characterized in Budget Period 3. Although some of these materials are single phase[1], many of these materials contain two or more phases to optimize flux, strength and other physical properties.[2],[3],[4],[5],[6] Several materials were discovered that are compatible with LCM29 and MM2, but have varying windows of operability. Thermal expansion properties of LCM61 are an excellent match with MM2 (Appendix III, Fig. 2) and have shown to be chemically compatible. LCM61 is suitable for long term operations up to about 0.8TT. Other materials under development (LCM89 to LCM97) show potential for very high temperature applications.

3.2 Task 2: Composite Element Development

3.2.1 Goal – Task 2

Develop advanced composite OTM elements and the techniques for fabricating these elements at the bench scale. The goal is to develop robust, low cost, high flux tubes or planar elements that can survive multiple cycles in temperature and fuel composition while maintaining structural integrity at target pressure differentials.

3.2.2 Experimental – Task 2

Experimental techniques are described in Appendix I, pg 13 and Appendix II, pg 20.

3.2.3 Results and Discussion – Task 2

In this task, composite elements (disk and tubes) are built using proprietary fabrication techniques. Some disk testing is also included in this task. The composite element consists of a robust porous substrate and a dense oxygen transport membrane. Oxygen flux is primarily controlled by two mechanisms in series: ambipolar diffusion of oxygen across the dense membrane and diffusion of the reaction species through the porous substrate layer. (Oxygen surface exchange rates on the air side and oxygen desorption or reaction on the fuel side may also be rate controlling, depending on process conditions) Both material properties, as discussed in Task 1, and element architecture (layer dimensions, pore structure, etc) are important factors affecting the performance and durability of the composite system.

Two types of composite elements have been developed based on the LCM family of materials and the MM family of materials. Each type requires different fabrication techniques. Both types promise excellent high temperature performance.

The MM2 substrate in combination with various film materials underwent numerous flux, cycling and life tests. The most successful system is LCM61/MM2. Flux and cycle tests conducted at atmospheric pressure (Appendix III, Figure 3 and 4) show good performance at TT over 500 hours, with no apparent signs of degradation, and thus attaining an important program milestone. However, success was not achieved at high pressure, an obvious setback. Further work is needed to develop a membrane that is robust at the most extreme conditions anticipated.

The methods of deploying the film on planar MM2 are considerably different than those used to apply films to tubular LCM29. These techniques are proprietary and represent a significant advance. Several techniques have been patented[7] or are pending[8].

3.3 Task 3: Tube Fabrication

3.3.1 Goal – Task 3

The main goal is to scale-up the manufacturing process and supporting technologies for building large-scale composite tubular elements. This team will also supply elements for testing in the P-0 (6 to 8 inches), LTT, P-1 (4 to 6 feet) and P-2 reactors (6 to 10 feet).

3.3.2 Experimental – Task 3

The fabrication techniques and testing methods are described in Appendix I, pg 15-16

3.3.3 Results and Discussion – Task 3

This task was important in Budget Period 1 while tube testing was underway in the P-1 pilot plant. A number of techniques for coating and fabricating closed end tubes[9] were developed, including isopressing[10],[11],[12] and thermal spray methods[13]. However, with termination of the large pilot plant testing programs, this task was reduced to making small elements for the P-0 reactors, which was then rolled into Task 2 for Budget Period 2 and 3.

3.4 Task 4: Reactor Design and Process Optimization

3.4.1 Goal - Task 4

Develop the commercial OTM syngas and hydrogen processes, including reactor design and catalyst deployment, reactor components (seals, internals, isolation devices, high temperature tube sheet, etc), and ancillary processes (feed pre-treatment, pre-heat, syngas cooling). Task 4 includes the operation of bench scale units, P-0, which are used to evaluate small OTM elements (tubes or disks) at high pressure. Task 4 also includes mathematical modeling, process scale up and economic evaluation.

3.4.2 Experimental - Task 4

The experimental facilities and methods in Task 4 were described in detail in the Topical Report0 for the Period Jan. 1 through Oct. 31, 2001 [Appendix I].

3.4.3 Results and Discussion

3.4.3.1 OTM Reactor

Early reactor design concepts focused on arrays of large closed-end tubular OTM elements.[14] . These designs required the development of special sealing devices to secure the ceramic OTM tubes to a metallic tube sheet. The seals must address the obvious problems of differential thermal expansion between ceramic and metal, constraining a brittle ceramic material while containing gas pressure differentials of 20 bar or more. Several seal designs were developed and proven in pilot plant operation.[15],[16]

Reliability and safety issues inherent to ceramic elements must also be addressed. A tube isolation device was developed, which in the event of a tube failure, would shut-off gas flows to the tube[17].

Several tubular reactor designs were developed with internal heat exchange and multiple feedstock injection ports to recover thermal energy and provide local temperature and process control[18],[19] ,[20]. In addition, an element architecture has been developed that inherently resists thermal runaway as demonstrated by a very flat response of oxygen flux to temperature[21].

However, the development of a new class of OTM materials permitted us to reevaluate the tubular OTM element strategy. These new materials are amenable to planar geometries with small channels and passages. Consequently, a new reactor design was developed in Budget Period 3, which employs a fundamentally new architecture based on planar, not tubular element fabrication. Details of this reactor design are proprietary and patent pending. The compact design has unique advantages in terms of thermal efficiency, emissions control and obviously plant size and footprint area. Computer modeling of the chemical and physical processes (heat and mass transfer) has shown that the limiting design parameter is heat transport, not oxygen flux.

Two planar reactor designs have been developed. The OTM-2 reactor is optimized for producing high pressure syngas for FTGTL applications. The OTM-3 reactor is optimized for producing hydrogen and sequestering CO_2. The OTM membrane operates at a much lower pressure differential than the OTM-2 reactor configuration.

The reactor design is staged[22] to allow optimal use of materials based on process severity. A low temperature inlet region will employ less expensive structural and OTM materials. The high temperature stage, if required, (it depends on product application) will employ suitable structural and OTM materials, which generally become more expensive as design temperature increases.

Currently the LCM61/MM2 system is adequate for the low temperature stage. Some improvements in film durability are required for the second stage

3.4.3.2 Foster Wheeler OTM Hydrogen Study

Foster Wheeler has completed an evaluation of OTM technology for producing hydrogen from natural gas. The base case is a 100 MMSCFD Gulf Coast steam methane reforming (SMR) hydrogen plant utilizing Foster Wheeler furnace technology and a conventional PSA for hydrogen purification. The study also compared advanced OTM designs to an SMR plant with a gas heated reformer (SMR/GHR). This configuration will produce the highest yield of hydrogen per mole of methane feed. An OTM process configuration and reactor design was developed that exceeded the SMR/GHR hydrogen yield efficiency and almost eliminates the production of NOx. In addition, all waste gases are nitrogen free, thus greatly facilitating carbon dioxide sequestration. A comparison of the cases is shown in Appendix III, Table 5.

The results show that OTM is efficient at converting methane to hydrogen and can do so without direct air combustion of fuel, which will create NOx. The OTM however requires a large blower to supply air to the membranes and thus has a non-trivial power cost penalty. This can be reduced by lowering the pressure drop of air through the OTM reactor membrane passages and improving the recovery of oxygen in the reactor.

This study showed that the OTM process has a distinct thermal efficiency advantage for producing hydrogen from natural gas. In addition, the OTM-3 planar reactor , which is explained in more detail in Appendix III, pg 18, has an added benefit of producing almost zero NOx while easily sequestering over 95% of the potential CO_2 emissions. A follow-up study by Foster Wheeler shows that the cost of capturing CO_2 with the OTM GSR is well under 50% of the cost of conventional amine scrubbing technology when more or less complete CO_2 capture is required. Further this system will recover 100% of the available CO_2 (compared to 92% for the most efficient amine configuration), will emit almost no NOx and yield considerably more hydrogen than conventional SMR. These results are shown below in Table 1.

Table 1. Economic Comparison of OTM-3 and Conventional SMR for hydrogen production with CO2 recovery and compression.

Parameter	**Units**	**SMR with CO_2 recovery of syngas and flue gas**	**OTM-3 Case**
H2 yield	Mole H_2 /Mole CH_4	1.45	2.57
Electricity	KW	2,663	18,220
CO2 production	TPD	3,359	2,018
CO2 emissions	TPD	284	-
CO2 Recovery		92%	100%
Estimated NOx emissions	Ton/Yr	346.2	Nil

TOTAL COSTS	$/year	181,599,405	112,330,036
Hydrogen cost	$/MSCF	2.49	2.49
CO_2 Cost w/compression	$/T	76.09	31.31

3.4.3.3 FTGTL Application

Foster Wheeler completed a study of a 25,000 BPD OTM based Fischer Tropsch Gas to Liquids plant (FTGTL). The purpose of this study was to update our understanding of the economic incentives, cost and performance targets for the new planar OTM technology

The OTM-2 reactor was sized and costed for the above 25,000 BPD GTL plant. Two reactor designs were evaluated. The “A” design employs a single high temperature material for the entire reactor length. The “B” design stages the reactor so that less expensive materials can be used in lower temperature regions of the reactor. In addition, the “B” reactor is configured so that ID and FD fans can be used to supply fresh air and remove the depleted air from the reactor. A cost comparison is shown below in Table 2. The OTM-2 planar reactor design shows cost reductions relative to conventional ATR with cryogenic oxygen of 28 to 44%. This shows that the economic potential for the OTM planar type reactor is very robust.

Table 2: Cost Comparison of OTM-2 Syngas Process and Conventional ATR

	ATR Case $MM	**OTM -2 (A) with 20 psi blower $MM**	**OTM -2 (B) staged $MM**
ASU/ATR (including extra power supply)	**164.75**		
OTM Modules, Installed		**71.70**	**62.42**
Air/DA Exchangers		**12.52**	**12.52**
Syngas Cooling to 1250oF		**3.75**	**3.75**
Balance of Syngas Island	**25.40**	**19.61**	**21.65**
Air moving equipment		**30.00**	**6.25**
TOTAL	**190.15**	**137.57**	**106.58**
Saving compared to ATR		**28%**	**44%**

3.4.3.4 Other Results

In Budget Period 1, when the tubular design was the leading architecture for the OTM syngas process, considerable advances were made in developing seals between a ceramic OTM tube and a metallic tube sheet.

In addition, several small scale (15 to 20 cm.) tube (P-0) tests were successfully completed, which gave confidence for scaling up to the P-1 reactor with 120 to 152 cm. tube lengths. Tube failures in P-1 were largely attributed to stresses which were created by thermal and chemical expansion. Thermal and chemical (oxygen partial pressure) gradients that create stress are more problematic as the size of the tubular element increases. It was recognized that the root cause of the P-1 failures was the physical properties of the OTM material—i.e. high temperature creep and expansion or contraction in response to changes in either temperature or oxygen partial pressure.

Advanced CFD models of the P-0 and P-1 reactor were developed to understand the complex physics (gas flow, heat transport, mass transport) and chemistry (oxygen flux, oxidation, reforming, and shift reactions) occurring within the reactor, and specifically at the tube surface. These models were used to interpret P-0 and P-1 data, and later were modified to study other architectures and OTM materials.

3.5 Task 5: Catalyst Development

3.5.1 Goal – Task 5

Develop the steam reforming catalyst system (and other catalysts, if so needed) employed in the OTM reactor. At least three methods of catalyst deployment will be evaluated.

3.5.2 Experimental – Task 5

Experimental apparatus and technique are described in Appendix I, pg 26-27

3.5.3 Results and Discussion – Task 5

The purpose of a catalyst in this reactor system is to promote both steam methane reforming and the water-gas shift reactions

Four types of catalyst systems were studied in this program: CatA, CatB, CatC and CatD.[23] Reaction rates are measured and fitted for each catalyst systems. The kinetic rates are then incorporated into various reactor models to determine the effectiveness of that catalyst under a variety of expected process and flow conditions. Cat A and Cat B were studied extensively. Each catalyst exhibits activity levels above that needed for operation of P-1, as shown in Appendix I, Figure 14 for CatA over a wide range of feed methane concentrations and temperatures. (Each curve representatives a different T and/or pressure) CatB exhibited a similarly robust activity profile.

In addition, (CatA and CatB) performed well in cycling and aging studies. It was concluded that Cat A and Cat B were both adequate for large scale pilot plant testing. However since the P-1 and P-2 tasks were cancelled after Budget Period 1, the catalyst development work was postponed. For convenience, subsequent tests in the P-0 or disk reactors utilized commercial steam methane reforming catalysts, if a catalyst was needed.

3.6 Task 6: P-1 Operation

3.6.1 Goal – Task 6

Run the newly constructed P-1 to demonstrate the technical feasibility of the OTM syngas technology under steady state and transient conditions. P-1 will be commissioned, shaken down, and operated with several tubes in BP1. The unit will be revamped end of year and outfitted with a full complement of tubes. (The composition, design and fabrication technique of these tubes will have been validated in the LTT).

3.6.3 Experimental – Task 6

See Appendix I, Appendix 4 page A-4 for a description and picture of P-1.

3.6.4 Task 6 Results and Discussion

A number of P-1 operating campaigns were carried out during Budget Period 1. The longest runs were a 60-hour test and a 100-hour test. This testing was conducted with a low number of OTM elements installed in the reactor and utilized inert fill rather than active reforming catalyst. Since the goal was to achieve steady state operation, effort was made to identify and eliminate causes of plant shutdowns and unacceptable process deviations. The work also included the identification and automation of operating protocols. Both the plant improvements and operating protocols were necessary to ensure the survival of the ceramic OTM elements.

After the implementation of a number of equipment and control system modifications for enhanced system operability and reliability, steady state operation of P1 was achieved using 1st generation materials, elements and inert catalyst. However it became clear that the major factor impeding successful pilot plant operation was tube robustness and durability. Consequently, with DOE approval, the P-1 campaign was terminated until such time when more robust elements could be fabricated.

3.7 Task 7: P-2 Build and Operation

3.7.1 Goal – Task 7

The purpose of the P-2 pilot plant is to demonstrate the commercial (technical and economic) feasibility of the OTM syngas technology. P-2 will be sized to demonstrate key scale-up risks and economic variables.

3.7.2 Results and Discussion – Task 7

The P-2 pilot plant was not designed or built due to the aforementioned tube durability and robustness issues.

3.8 Task 8: Fuels and Engine Testing

3.8.1 Goal -- Task 8

The goal of this task is to understand the relationship between ultra-clean fuel properties and their impact on the emissions and performance of a Nuvera fuel cell; and an advanced CIDI and exhaust treatment system under development by International Truck and Engine. The task was later expanded in Budget Period 2 to include the initial co-development of an HCCI engine and fuel.

3.8.2. Results and Discussion – Task 8

3.8.2.1 Diesel engine and ultra-clean diesel fuel

Six SCTE tests were completed to evaluate the effect of FT diesel and BPO on engine performance and emissions. The six tests were carried out in three campaigns during Budget Period 2 and 3. Each test evaluated obtained emission (soot, NOx and THC) and fuel consumption (BSFC) under four driving modes (Modes 4,6,7,8) per the HD FTP emission certification protocol.

The first set compared No. 2 diesel fuel to FT diesel. The No.2. Diesel is conventional petroleum based “low sulfur” fuel with ~ 350 ppm sulfur. The FT diesel was obtained from Sasol, LTD. Results of this test, discussed in Appendix II pg 32, 41 – 46, show across the board reductions of all three pollutants and demonstrate the real value of FT diesel as a petroleum substitute.

Table 3: Single cylinder diesel engine fuel test matrix

	Set 1—BP2		Set 2—BP2		Set 3—BP3	
	No. 2 Diesel	**FT Diesel**	**ULS**	**ULS + 10% BPO**	**ULS**	**ULS + 5% BPO**
API Gravity	36.0	49.9	36.5	34.8	36.5	35.0
IBP	370	327	364	317	364	339
50	503	480	488	502	488	517
Endpoint, F	642	672	666	646	666	653
Sulfur wt., ppm	370	<5	<10	<10	<10	<10
Cetane number	47.6	>70	65	68	65	66.7
Net heat of combustion, BTU/Lb	18,457	18,884	18,667	16,458	18,667	17,659

The second test set compared a petroleum based ultra-low sulfur diesel fuel to the same fuel with 10% BPO. BPO is a proprietary oxygenate developed by BP. It has a lower heating value than petroleum due to its high oxygen content. The molecular weight of the BPO can be adjusted so that its volatility can be matched with most fuel base stocks. The BPO however will lower the energy content of fuel. To ensure a meaningful and comprehensive comparison of the two fuels, the standard tests were run twice. The first test kept fuel rates constant while the second test adjusted fuel rates to keep torque constant. The results of these tests are discussed in detail in

Appendix II, pg 33 and 46-50. Surprisingly, the BPO had a positive effect on reducing soot and NOx under most modes of operation. However, The BSFC increased; and sometimes more than the 12% reduction in heating value of the 10% BPO blend. This suggests that the combustion chemistry is affected in ways that we do not yet fully understand. The result of this test campaign suggested that a lower BPO content should be investigated. This led to a third test set which was completed in Budget Period 3.

The third test set compared the same ULS to a ULS blend with 5% BPO. Since the engine configuration was modified during the elapsed time, the results of Set 2 and Set 3 cannot be compared rigorously. The engine modifications are described in Appendix III, g 23 and the results of the tests are shown in Appendix III, pg 24-26 and pg 38-43. Some test durations were abbreviated due to lack of fuel, and only one mode of operation, “constant fuel”, could be examined (BPO is not commercially produced, so we were limited to a fixed quantity form a pilot plant campaign). The results of these tests again showed that even 5% BPO can have a significant reduction of soot and NOx. And deterioration of BSFC was not as severe, sometimes resulting in actual improvements up to 18%. Thus operating conditions play an important role in fuel consumption and emissions.

All of these test were originally focused on meeting 2007 EPA regulations for diesel engines. These regulations will require soot traps and NOx traps. Subsequent improvements should focus on fundamental changes in the engine and fuel to reduce or eliminate these after treatment systems. One promising technology for reducing in-cylinder emissions is the HCCI (homogenous charged compression ignition) engine. International Truck and Genie are exploring the HCCI as a potential candidate to meet air standards after 2010.

3.8.2.2 HCCI engine and compatible fuel

The HCCI engine is described in Appendix III, pg 26. Engine simulation studies were undertaken to determine optimal modes for operating intake and exhaust valves (pg27-31). The HCCI engine requires a significantly different fuel than either the conventional gasoline or diesel engine now requires. A blending study was undertaken by BP to provide three fuels for testing. (Appendix III, pg 31-33 and 54-63). The three fuels spanned a range of aromatics (29 to 60 vol.%) and cetane number. Volatility varied somewhat, the RVP of all fuels was in the range of 1.5 to 2.6 psi.

The three fuels were compared to the same ULS diesel used in the above SCTE tests. Results of these tests are shown in Appendix III, pg 33 and pg 44-53. The tests demonstrated the potential for an HCCI type engine to reduce emissions and improve efficiency. Fuels #2 and #3, at their *best test points* reduced BSNOXg/hp-hr by 33 to 43% and SOOT by 85 to 92% in comparison to the ULS diesel fuel. In order to fully evaluate this technology, a much more extensive engine mapping exercise is required.

3.8.2.3 Nuvera Fuel cell and ultra-clean naphtha fuel

Growing interest in PEM fuel cells as a potential propulsion system for transportation vehicles initiated development of the advanced fuel-making technologies for improving environment and meeting fuel vehicles emission targets. These technologies will enable production of ultra-clean transportation fuels, alternative to gasoline but utilizing it's infrastructure and being cost competitive at the same time. Nuvera Fuel Cells have been investigating autothermal reforming for the series of fuels such as gasoline, methanol, ethanol, diesel and naphthas. Previous efforts were concentrated on the parametric study of syngas production efficiencies and reforming operating conditions. The purpose of the current project was to understand effect of UCTF on the fuel cell system and possibly reduce emissions on a per mile basis.

The Nuvera fuel cell tests wee conducted in two phases:

- Phase I commenced in 2001 (Budget Period 1) and was purposed to demonstrate DC power in Nuvera's state-of-art disintegrated fuel cell power train with autothermal (ATR) fuel reforming. Single ultra-clean synthetic fuel was selected for this task and then compared to conventional California Phase II Gasoline fuel for hydrogen and power production efficiency.
- Phase II was completed in 2002 and scoped testing selected fuels in Nuvera's state-of-art burner module. Three fuels including two synthetic fuels and conventional gasoline were compared in terms of start-up and steady state emissions to the environment.

The final report (Appendix II, pg 52-74) summarizes work conducted within the scope of both phases. Performance of all synthetic fuels tested was referenced to the performance of conventional gasoline fuel, which served the benchmark in the current program and in Nuvera's automotive state-of-art fuel processors. All studied fuels were successfully processed in Nuvera's Modular Pressurized Reactor (MPR) facility and resulted in electrical power produced by the fuel cell stack. The fuels under study were compared in terms of process efficiencies, operating conditions, reformate compositions along the power train and potential emissions to the environment. The reformate gas was analyzed for bulk composition and traces of species, representing poisons to the fuel cell stack and environment. The fuel cell stack polarization curves were recorded and the derating factors on fuel reformates were estimated relatively to operation on pure hydrogen and air. The process condensates have been analyzed at different locations for understanding potential emissions and contaminants to fuel cells and environment.

3.9 Task 9: System Commercialization and Marketing Study

3.9.1 Goal – Task 9

The goal of this task is to understand marketing and commercialization hurdles and to develop plans to bring the ultra-clean fuel system to market.

3.9.2 Results and Discussion – Task 9

This task was not undertaken in the first three budget periods, as it was intended to be a closure activity in the final budget period, which until recently was thought to be Budget Period 4. This program has shown that Fischer-Tropsch liquids (naphtha and diesel), neat or in combination with BPO are viable ultra-clean fuels which can out perform comparable ultra-low sulfur petroleum fuels. However significant commercialization issues remain as discussed below.

The FT naphtha is too low in octane to be considered as a neat fuel for gasoline engines. However it is an excellent fuel for transportation fuel cells. The key hurdle to commercialization of this system is development and acceptance of a viable fuel cell for automotive use. Recent status report of fuel cell cars[24] concludes that large scale production of fuel cell automobiles is at least 10 years off. Key issues include fuel cell cost, reliability, hydrogen supply, storage (directly influencing automobile range) and distribution. The on-board reformer under development at Nuvera addresses the hydrogen supply and range issue; however the fundamental fuel cell cost and reliability issues must still be resolved.

FT diesel with lubricity and other additives is also an excellent ultra-clean fuel, which can be enhanced with the addition of BPO. The current supply of FT diesel is insufficient to warrant marketing it as a separate neat fuel. However FT diesel, with or without BPO, could in theory be blended with low sulfur petroleum diesel fuel to extend supplies and improve performance. This may in fact occur towards the end of this decade as more FTGTL plants come on stream in Qatar and elsewhere.

The ultimate ultra-clean fuel/IC engine system for the next decade may in fact be the HCCI engine, powered by a broad cut of FT naphtha and diesel blended with appropriate petroleum middle distillates. Although this engine is still in its infancy, sufficient emission and performance advantages have been demonstrated in single cylinder tests to warrant further development outside of this program. A key hurdle for commercialization of the HCCI engine is the volatility requirement of ~ 2 psi Reid vapor pressure. This fuel is reminiscent of a JP4 type fuel, which poses flammability hazards that are more serious than either gasoline or diesel fuel. Gasoline has a high vapor pressure which results in a fuel rich vapor space above the liquid fuel that is difficult to ignite. Conversely, diesel has a very low volatility that creates a very fuel lean vapor space that is again difficult to ignite. However, the 2 RVP fuel creates a vapor space that is flammable over a wide range of atmospheric conditions and is thus more problematic to transport, store and handle. All vessels and lines that the fuel comes into contact must be grounded to avoid unwanted static spark ignition. The fuel will not be fungible with other common transportation fuels and thus will pose a whole new set of storage, distribution and retailing logistical issues. This may be the most serious threat to commercialization of an HCCI engine vehicle.

3.10 Task 10: Project Management

3.10.1 Goal – Task 10

The goal of this task is to provide technical leadership and management direction to ensure that the program achieves deliverables on time, within budget, and in a safe and environmentally acceptable manner. A further requirement is to maintain good communications among the DOE, stakeholders, participants and subcontractors.

3.10.2 Results and Discussion – Task 10

The program scope and direction was modified at the completion of Budget Period 1 to address OTM material and tube reliability and robustness issues. Although all of the original goals were not achieved, the two primary objectives (step change cost reduction in syngas technology and demonstration of UCTF in advanced engine systems) were met at a considerably lower cost than originally projected. All communication and reporting requirements were satisfied. Two public papers were presented (ACS, Spring, 2003[21] and AIChE, Spring, 2004[6]). The program received favorable comments from a peer review conducted in Houston in June, 2003.

4.0 Conclusions

- An advanced material system LCM61/MM2 has met our flux, life and cyclabiltiy targets. This material system is suitable for the first stage of a high pressure OTM hydrogen or syngas process; a more robust film material is required for the higher temperature second stage.
- Several promising high temperature OTM film material candidates have been fabricated and are undergoing testing.
- A new fabrication technique has been developed that allows the manufacture of thin, dense OTM films on porous substrates.
- The OTM-2 reactor shows potential to reduce ATR syngas capital costs by 28 to 44% based on a 25,000 BPD FTGL plant with cryogenic oxygen.
- A very efficient hydrogen reactor has been developed; the OTM-3 reactor has been shown to have a very high hydrogen yield with almost no NOx emissions. .
- The OTM-3 will reduce the costs of recovering the carbon dioxide created from reforming natural gas .by 50% or more. This device could be a BACT candidate for hydrogen production if NOx and CO2 are regulated pollutants and would therefore be significantly advantaged over SMR.
- Adding the BP oxygenate at a 5% oxygen level to conventional ultra-low sulfur diesel fuel significantly reduces soot and NOx emissions with only minimal impact on fuel consumption and engine efficiency.
- The HCCI engine promises to be the next generation internal combustion engine, capable of meeting 2010 EPA emission regulations. The engine has demonstrated the potential to reduce soot and NOx formation in the cylinder with no loss of efficiency, thereby reducing the need or complexity of after-treatment technology.
- VVA system capable of simultaneous control of intake valve closing and intake valve lift at fixed intake valve opening has a significant potential for becoming the HCCI enabling technology.
- The HCCI fuel will likely resemble JP4 in volatility, but will have specific ignition delay and cetane requirements to achieve optimal performance.
- The best HCCI fuel found in this study has an aromatic content of ~ 45 volume percent and a Reid vapor pressure of ~ 2 psi. with an estimated IQT cetane of 25
- In Nuvera fuel cell burner tests, BPO oxygenate added to FT naphtha reduces start-up emissions of NOX, soot and hydrocarbons and reduced steady state emissions of NOx.
- FT naphtha appears to be a superior fuel for transportation fuel cells. In Nuvera fuel reforming and cell stack tests, hydrogen yield and reforming efficiency were improved when FT naphtha was compared to low sulfur California Phase II RFG (reformulated gasoline). FT naphtha has the added advantage of being sulfur free, thus eliminating sulfur traps. Power production from the fuel cell stack was similar for both the RFG and FT naphtha, but emissions are reduced with the FT naphtha.

5.0 References

---

[1] U.S. Patent 5,306,411 Mazanec, T.M., et al "Solid multi-component membranes, electrochemical reactor components, electrochemical reactors and use of membranes, reactor components, and reactor for oxidation reactions"
[2] U.S. Patent 6,332,964 B1, Chen, "Multi-phase solid ion and electron conducting membrane with low volume percentage electron conducting phase and methods for fabricating"
[3] U.S. Patent 5,911,860 , Chen, et al " Solid electrolyte membrane with mechanically-enhancing constituents"
[4] U.S. Patent 6,514,314 Sirman, J, "Ceramic membrane structure and oxygen separation method"
[5] U.S. Patent 6,287,432 Mazanec, et al, " Solid multi-component membranes, electrochemical reactor components, electrochemical reactors and use of membranes, reactor components, and reactor for oxidation reactions"
[6] Robinson, E.T., Aasland, S, Chen, J, "The application of oxygen transport membranes for syngas or hydrogen production" AIChE Spring 29044 National Meeting, Synthesis Gas Generation, April 26, 2004
[7] U.S. Patent 6,165,553, Chen, et al, " Method of fabricating ceramic membranes"
[8] U.S. patent application 2005/0013933A1, Chen, H. et al, "Method of forming ion transport membrane composite structure", pub.. Jan. 20, 2005
[9] U.S. Patent 6,558,597 B1, Corpus, "Process for making closed end tubes"
[10] U.S Patent 6,524,421 B1, Chen, et al, " Cold isopressing method"
[11] U.S Patent 6,372,165 B1, Apte, et al., " Cold isopressing method"
[12] U.S. Patent 6,776,941 B1, Apte, et al, "Cold isopressing method and mold"
[13] U.S Patent 6,638,575 B1, Chen, et al, "Plasma sprayed oxygen transport membrane coatings"
[14] U.S Patent 6,139,810, Gottzmann, et al, "Tube and shell reactor with oxygen selective ion transport ceramic reaction tubes"
[15] U.S Patent 6,547,286 White, et al, "Joint for connecting ceramic element to a tubesheet"
[16] U.S Patent 6,454,274 White, et al, "Joint assembly for joining a ceramic membrane to a tube sheet"
[17] U.S. patent application 2004/0221722, Prasad, et al, "Ion transport membrane isolation devise
[18] U.S. patent application 2003/0039601, Halvorsen, G, et al, "Oxygen ion transport membrane apparatus and process for use in syngas production"
[19] U.S patent 5,820,655 Gottzmann, et al, "Solid Electrolyte ionic conductor reactor design"
[20] U.S patent 6,010,614 Keskar, et al., "Temperature control in a ceramic membrane reactor"
[21] Robinson, E.T., "Oxygen transport membranes for ultra-clean fuel production", ACS Fuel Chemistry Division Preprints, March 23-27,2003, 47(1)
[22] U.S. Patent 6,695,983, Prasad, et al, "Syngas production method utilizing an oxygen transport membrane"
[23] U.S. patent application 2003/0218891 A1, Besecker, et al , "Membrane systems containing an oxygen transport membrane and catalyst", pub. Nov. 27, 2003
[24] Ashley, S. "On the Road to Fuel-Cell Cars", Scientific American, Vol. 292, No. 3, pg 62-69

FINAL REPORT APPENDIX I
Topical Report – Budget Period 1

Development of OTM Syngas Process and Testing of Syngas-Derived Ultra-clean Fuels in Diesel Engines and Fuel Cells

Budget Period 1

Topical Report

For Reporting Period Starting January 1, 2001 and Ending October 31, 2001

Principal Authors:

E.T. (Skip) Robinson, Principal Investigator
James P. Meagher, Program Administrator
Ravi Prasad, Corporate Fellow

Report Issue Date: October 2001

DOE Cooperative Agreement No. DE-FC26-01NT41096

Submitting Organizations:

Primary:
Praxair, Inc.
P.O. Box 44
175 East Park Drive
Tonawanda, NY 14150

Subcontractors:
BP Amoco
150 W. Warrenville Road
Mail Code H-5
Naperville, IL 60566

Torix, Inc.
7165 Hart St., Suite B
Mentor, OH 44060

International Truck and Engine Corp.
10400 W. North Avenue
Melrose Park, IL 60160

Nuvera Fuel Cells
15 Acorn Park
Cambridge, MA 02140

FINAL REPORT APPENDIX I

Topical Report – Budget Period 1

DISCLAIMER

ABSTRACT

This topical report summarizes work accomplished for the Program from January 1 through September 15, 2001 in the following task areas:

- Task 1 Materials Development
- Task 2 Composite Element Development
- Task 3 Tube Fabrication
- Task 4 Reactor Design and Process Optimization
- Task 5 Catalyst Development
- Task 6 P-1 Operation
- Task 8 Fuels and Engine Testing
- Task 10 Project Management

OTM benchmark material, LCM1, exceeds the commercial oxygen flux target and was determined to be sufficiently robust to carry on process development activities. Work will continue on second-generation OTM materials that will satisfy commercial life targets.

Three fabrication techniques for composite elements were determined to be technically feasible. These techniques will be studied and a lead manufacturing process for both small and large-scale elements will be selected in the next Budget Period.

Experiments in six P-0 reactors, the long tube tester (LTT) and the P-1 pilot plant were conducted. Significant progress in process optimization was made through both the experimental program and modeling studies of alternate reactor designs and process configurations.. Three tailored catalyst candidates for use in OTM process reactors were identified.

Fuels for the International diesel engine and Nuvera fuel cell tests were ordered and delivered. .Fuels testing and engine development work is now underway.

FINAL REPORT APPENDIX I

Topical Report – Budget Period 1

Development of OTM Syngas Process and Testing of Syngas-Derived Ultra-clean Fuels in Diesel Engines and Fuel Cells

Budget Period 1

TABLE OF CONTENTS

List of Tables Page

List of Figures

List of Acronyms

A tubes	Tube with a large nominal outside diameter
B tubes	Tube with a small nominal outside diameter
CFD	Computational Fluid Dynamics
LCM	Lead Candidate Material
LTT	Long Tube Tester, single tube pilot plant
OTM	Oxygen Transport Membrane
P-0	Small bench scale test reactors capable of testing single OTM tubes up to 8 inches in length at elevated pressures and temperature.
P-1	Multi-tube pilot plant

FINAL REPORT APPENDIX I

Topical Report – Budget Period 1

Executive Summary

This program has two primary focuses: 1) development of an advanced, low cost syngas technology based on ceramic oxygen transport membranes and 2) the evaluation of syngas derived ultra-clean fuels in Nuvera fuel cells; and the development of advanced compression ignition engines /after- treatment/ultra-clean fuel systems. Although the program had a late start, significant progress has been made in the OTM syngas tasks. The fuels and engine development (Task 8) work was initiated in August.

Task 1, Materials Development has created and fabricated a number of OTM materials that promise to deliver both the target oxygen flux and superior mechanical properties required for a long-term commercial operation. Two new materials were completely characterized. Five other materials are in various stages of fabrication or testing. All of these materials satisfy the oxygen flux requirement; several have demonstrated superior mechanical properties such as creep, fracture toughness and thermal and compositional expansion. The benchmark material, LCM1, exceeds the commercial oxygen flux target and is sufficiently robust to carry on with process development and pilot plant activities Work will continue to develop materials that satisfies commercial life targets.

Task 2, Composite Element Development has focused on optimizing element parameters such as oxygen flux and strength while developing the fabrication techniques to commercially manufacture these elements. Experiments to quantify the role of element morphology and temperature effects were completed. Three manufacturing techniques for making robust composite tubes have proven technically feasible based on the capability to make leak free composite elements with uniform geometry. The advantages and disadvantages of each technique are being studied; a decision to select the lead manufacturing process has been postponed until the next budget period, pending selection of commercial material(s) in Task 1.

Work continued on the scale-up of manufacturing techniques for producing both small and large-scale ceramic OTM elements (Task 3). A number of composite elements with inside dense films were made for P-0 tests. Large tubes (up to 140 cm in length) for the LTT and P-1 pilot plants were made and are being tested. These tubes incorporate a special open end for sealing and exhibit excellent straightness and roundness. Three technically viable techniques for making composite elements with inside films are under development. Final selection of the commercial manufacturing technique is pending selection of the commercial materials. However work with the current candidates LCM1 and LCM2 will enable rapid changeover to the new material when it is available.

Significant progress has been made in developing process models of the OTM reactor (Task 4). A CFD code has been developed that includes hydrodynamic descriptions of the reactor internals, and kinetic descriptions for both oxygen diffusion through the ceramic OTM and heterogeneous catalysis of steam methane reforming and water gas shift reactions. Fluid flow, heat and mass transfer and reaction kinetics are coupled to give an accurate representation of the reactor performance. The model is being validated against P-0, LTT and P-1 results. These models, plus simpler codes are being used to evaluate alternative reactor designs and process configurations.

Seals to hold the ceramic elements in the reactor and maintain a large pressure difference have been developed and are in use in all of the bench scale and pilot plant units. Two design types are being developed. Both types can be pressure and thermally cycled and can accommodate the thermal and compositional expansion characteristics of the OTM elements.

P-0 tests in six reactors are evaluating alternative element architectures and materials, as well as studying effect of process conditions and tube morphology on temperature profiles and element performance.

Construction of a new pilot plant, the Long Tube Tester (LTT), was completed at the end of June. This unit is capable of testing OTM elements up to ~six feet in length with a variety of process gases and flow configurations at target temperatures and pressures. Commissioning of all systems is complete and the unit is in start-up mode.

The P-1 Pilot Plant (Task 6) achieved a milestone operation of 100 hours, including successful start-up and shutdown without a tube failure. This run utilized two OTM elements. The unit is now configured with 15 OTM elements, 140cm length, and is undergoing start-up.

Development of tailored catalysts (Task 5) suitable for the unique operating environment of an OTM process reactor has successfully yielded three candidates, all of which can satisfy activity targets. At least one catalyst system qualifies for the P-1 application, meeting the milestone target for this budget period. Work continues to optimize the performance, cost and life characteristics of a commercial catalyst system. A detailed model based on intrinsic kinetic experiments has been completed for one of the catalyst candidates. This model is incorporated in the reactor CFD code.

Fuels testing and engine development work (Task 8) is now underway at Nuvera Fuel Cells and International Truck and Engine. Experimental plans have been finalized and Fischer Tropsch-based fuels (an FTL naphtha for Nuvera and a FTL diesel for International) have been delivered to both sites.

Program Management (Task 10) has been successful in kicking off all sub-contractor work in a timely fashion after the DOE /Praxair contract was signed on May 21, 2001. Contracts with BP Amoco, Nuvera Fuel Cells and International Truck and Engine were completed by August and work is underway at all sites. In addition, very long lead fuel requirements were anticipated and delivered to the subcontractors in time to prevent delays in Task 8.

Introduction

The DOE's Office of Fossil Energy created strategic partnerships targeted at the development and verification of advanced fuel-making processes that utilize fossil feedstocks. These processes will enable the production of ultra-clean transportation fuels that improve the environment, while also expanding and diversifying the fossil resource base. In response to the DOE's solicitation for research and development leading to the production of ultra-clean transportation fuels from fossil resources, Cooperative Agreement number DE-FC26-01NT41096 for work entitled "Development of OTM Syngas Process and Testing of Syngas-Derived Ultra-clean Fuels in Diesel Engines and Fuel Cells" was awarded to Praxair.

The objectives of this project are: (1) develop an advanced syngas technology, based on Oxygen Transport Membranes (OTMs), that will provide a step change reduction in the cost of converting natural gas to a spectrum of liquid transportation fuels and thereby improve the prospects for meeting vehicle emissions targets with cost competitive ultra clean transportation fuels (UCTFs); (2) evaluate the performance of, and emissions from selected syngas-derived UCTFs in advanced vehicle propulsion systems, including advanced diesel engines with post treatment and fuel cells; and 3) develop an optimized UCTF/diesel engine/exhaust after treatment system capable of meeting 2007 emission regulations.

The program follows a systems approach as shown in Figure 1, encompassing natural gas pre-treatment, syngas generation, liquid fuel production, product work-up/blending, and validation of the UCTF in engine tests including aftertreatment of emissions.

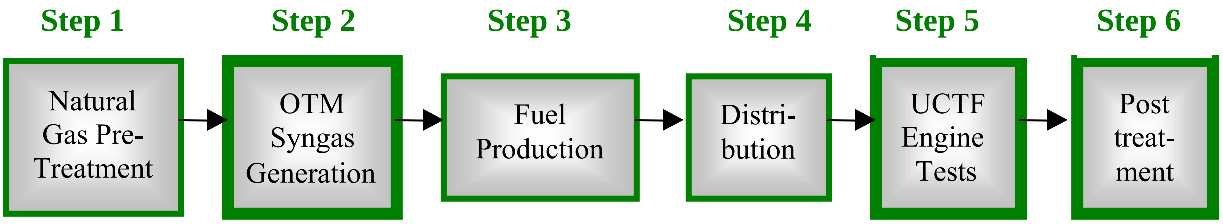

Figure 1. *Systems Approach to UCTF*

The 48-month project includes three parallel development or testing programs: 1) OTM syngas reactor and reactor components, OTM element fabrication and OTM syngas process development; 2) testing and co-optimization of UCTF in International Truck and Engine advanced diesel engines with exhaust post treatment; and 3) emission testing of UCTFs in a Nuvera transportation fuel cell power system. Performance objectives include:

- OTM Syngas Technology: lower capital costs, lower operating costs, lower emissions and smaller footprint compared to conventional syngas plants.
- UCTF in Advanced Diesel Engines: co-optimized system of syngas derived UCTF, diesel engine and post treatment technology targeting proposed 2007

regulations for light and medium duty engines i.e. diesel fuel sulfur < 15 ppm; light duty engine emissions: NOx < 0.2 g/mi, PM < 0.01 g/mi; and heavy duty engines NOx < 0.2 g/mi and PM < 0.02 g/bhp. UCTF should enable compliance with these objectives and/or lower vehicle costs.

- UCTF in a Nuvera fuel cell system: lower air emissions (on a per mile basis) based on UCTF properties such as ultra low sulfur, high aliphatic content and oxygen content.

The program has 10 major tasks, seven of which are focused on syngas technology development, one task is devoted to fuel and engine testing and optimization, one task addresses the marketing and commercialization of an UCTF system, and the final task is for program management and cost control.

The Cooperative Agreement was signed by the DOE's Contracting Officer on May 21, 2001. Budget Period 1 is January 1, 2001 through October 30, 2001. This Topical report will include results and discussions for work conducted January 1, 2001 through September 15, 2001.

3.0 Progress and Results by Task

3.1 Task 1: Materials Development

3.1.1 Goal – Task 1

The Recipient shall fabricate, test and characterize OTM film and substrate materials with goal of developing a more robust and cost effective OTM element in comparison to the lead material candidate, LCM1.

3.1.2 Milestones – Task 1

This budget period: 1Q01--Select 2nd generation material for scale-up
Status: Alternate materials have been developed with improved properties over our first generation material, LCM1. LCM1 exceeds our oxygen flux target and is suitable for continuing process and reactor development. However, a second-generation material(s) with superior mechanical properties that can withstand long-term commercial operations has not yet been selected for scale-up.

3.1.3 Experimental – Task 1

The search for advanced materials requires satisfying simultaneously proprietary targets in oxygen flux, creep, and thermal and compositional expansion. In addition, fracture toughness and indentation hardness are important physical characteristics, which must be optimized.

Task 1 is following an experimental plan based on proprietary knowledge of OTM materials acquired over nearly 15 years of relevant experience in the field. A number of material compositions were developed and tested during this reporting period.

3.1.3.1 Oxygen Flux

Small disk samples of the new material are fabricated for measuring oxygen flux in a permeation cell. (See Appendix pageA-1 for description and picture.) Similar cells are operational at both BP and Praxair.

3.1.3.2 Creep Measurements

A uniaxial compressive creep testing apparatus was modified at UDRI for testing ceramic pieces under a separate program with Praxair and BP. Creep measurements can be carried out at different temperatures and different loads [1]. A similar apparatus was also constructed at Praxair and is used to conduct additional tests.

3.1.3.3 Dilatometry

Dilatometry is used to measure dimension changes because of heating or changing gas composition. Thermal and chemical expansion is determined by conducting temperature and compositional scans of the subject materials in a Netzsch DIL 402E dilatometer.

3.1.3.4. Fracture Toughness

Vickers hardness was measured at loads 300, 500 and 1000g and held for 5 seconds using Model VTD11, Wolpert, Germany.

3.1.4. Task 1 Results and Discussion

3.1.4.1 Oxygen Flux

Oxygen flux is the most important property and first target to be reached in the development of an OTM reactor. Oxygen flux of dense discs of LCM1 and some alternative membrane candidates are given in Figure 2. It is clearly shown that the oxygen flux of LCM1 is higher than for other candidates. However according to the flux target for these discs, several of the alternative materials have sufficiently high flux to be considered as a candidate for composite membranes.

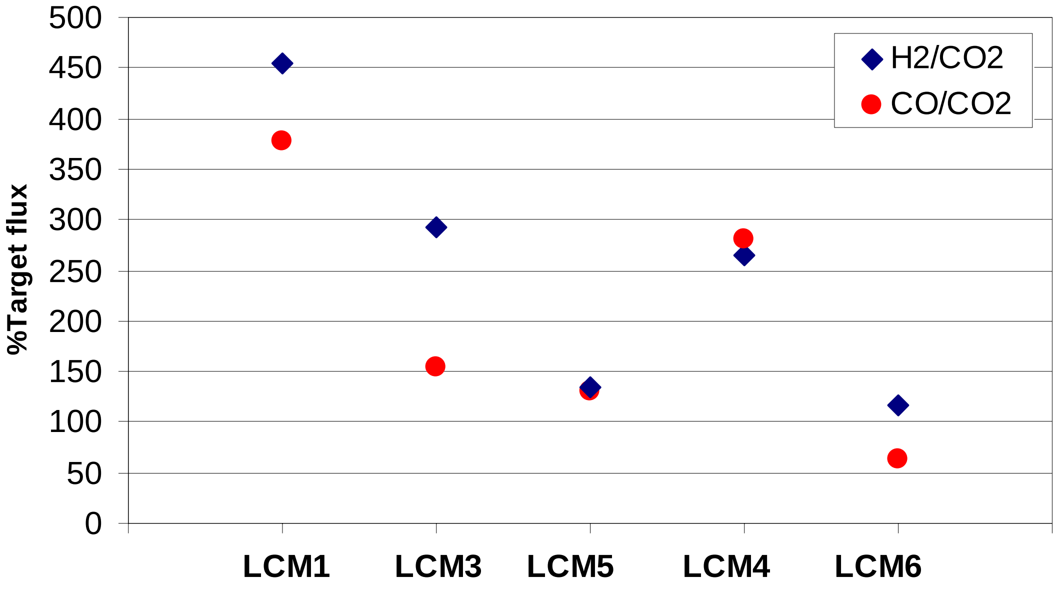

Figure 2. *Flux of Lead Commercial Material Candidates*

3.1.4.2 Creep Measurements

Creep has been measured for dense LCM1, LCM2 and LCM3 at UDRI and for porous LCM1 at Praxair within this program [2]. The creep rate increases with stress (load) and temperatures as shown in Figure 3.

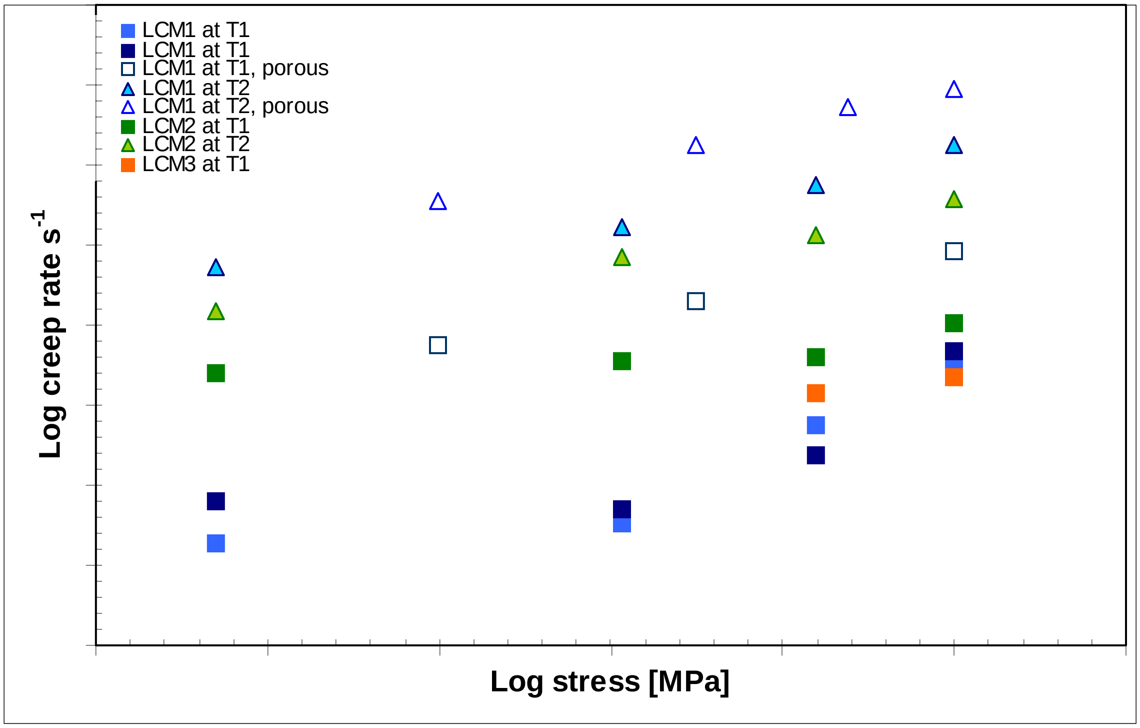

Figure 3. *Creep Rate of Lead Materials as a Function of Temperature and Stress (The target temperature is T1 and T2> T1)*

At the target temperature, the lowest creep rate was measured for LCM1. A lower creep rate was expected for LCM2, however the quality of the LCM2 sample was not optimized; the creep measurement should be repeated for this sample.

The reproducibility of the creep rate was found to be good for LCM1. Porous LCM1 has about an order of magnitude higher creep rate than dense LCM1.

3.1.4.3 Thermal expansion

The expansion of a material during heating is the results of an increase in the amplitude of vibration between the atoms in the material. The thermal expansion depends on the bond strength of the material and decreases with increasing bond strength. An interesting correlation has been observed between linear thermal expansions and melting temperature of relatively close packed metal and ceramic structures. For cubic close packing, the bond strength generally increases with decreasing ionic sizes in a series of compounds with the same structure.

The thermal expansion of oxygen conducting materials includes chemical expansion from oxygen loss at higher temperatures in addition to the normal thermal expansion due to increased thermal vibrations. An example is given in Figure 4 for LCM3, the thermal expansion coefficient is 13 X 10^{-6} 1/K below 600°C and increases to 19.3 10^{-6} above 800°C [3]. The chemical expansion addition to the thermal expansion is supposed to increase with the increasing number of oxygen vacancies created during heating of the membrane material. Thus, materials with high oxygen flux will also have high thermal expansion above 600°C, where the material starts to lose oxygen. The thermal expansion coefficients for a few membrane and substrate materials are given in Table 1 [4].

Table 1. *Thermal Expansion Coefficients of Lead Material Candidates*

Material	**TEC** **α 10^6 [K^{-1}]**	**Temperature interval** **°C**
LCM1	16.9	25-950
LCM3	14.4	25-950
LCM6	10	25-1000
LCM5	14	25-1000
LCM7	12.3	25-1000
LCM8	11.5	25-700
ZrO_2	~10	Average TEC
YSZ	10.3	25-1100

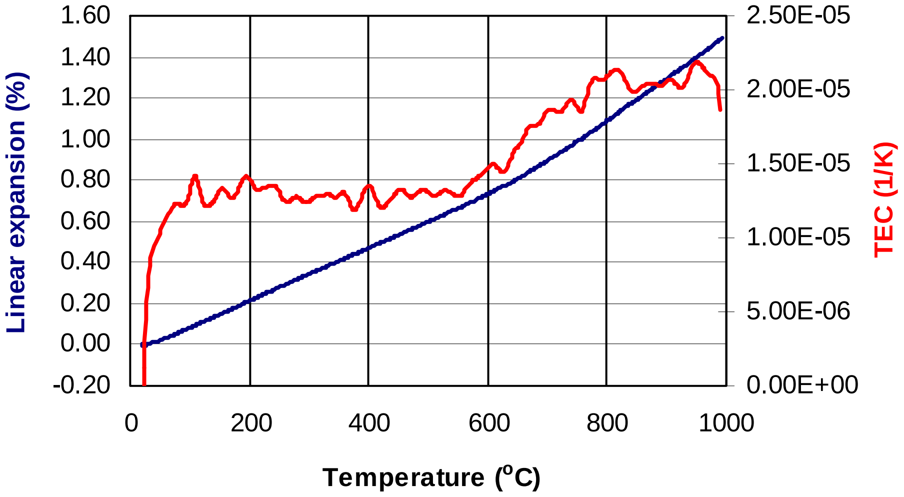

Figure 4. *Thermal expansion of LCM3 as a Function of Temperature*

3.1.4.4 *Chemical expansion*

Chemical expansion of oxygen conducting materials is caused by loss of oxygen. The oxygen content is lower at higher temperatures and at lower partial pressures of oxygen. Thus by heating the materials or lowering the pO_2, the materials will expand. Chemical expansion is treated as the expansion caused by decrease in pO_2. Chemical expansion of LCM1, LCM3 and LCM7 is shown in Figure 5 [5]. High chemical expansion gives rise to stresses in the membrane which is exposed to a gradient in pO_2 with air on one side and fuel ($pO_2 = 10^{-16}$) on the other side. Thus it is important that the chemical expansion is as low as possible. For a dual phase or layered membrane, the match in thermal and chemical expansion is also very important. From Figure 5, one can see that there is a large mismatch in CEC of LCM1 and LCM7 at low pO_2, which can be a problem with using these materials together.

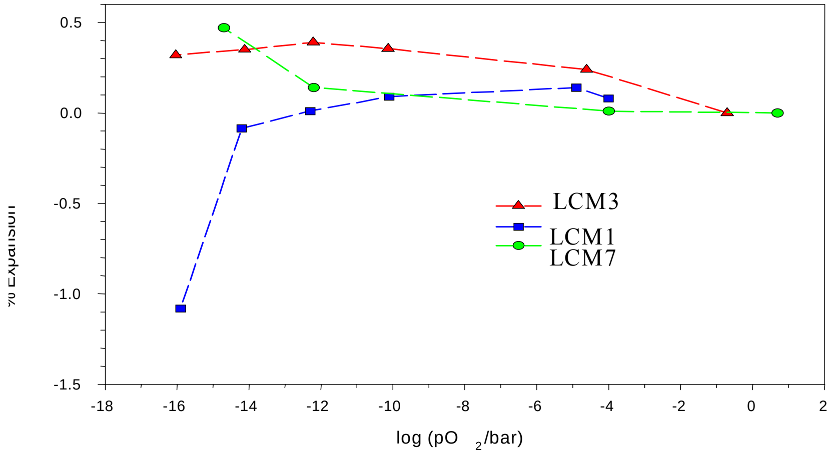

Figure 5. Chemical Expansion of LCM1, LCM3 and LCM7 vs. pO_2

Measurement of the chemical expansion of a material is time consuming; the complete chemical expansion vs. pO_2 has only been measured for a few membrane materials. In the future it will be important to measure the chemical expansion coefficient of a number of candidate materials as this it is crucial to match this property for a layered and/or dual phase membrane system.

3.1.4.5. Chemical stability

The chemical stability of LCM1 and other membrane materials can be calculated from thermo dynamical data using some simple estimates for the activity of the alkaline earth metal. Methods to improve chemical stability by varying material composition are under study.

3.1.4.6. Other mechanical and thermal properties

Vickers indentation method has been used to measure hardness and fracture toughness of different membrane materials as given in Table 2 [6]. The fracture toughness is slightly higher for LCM5 and LCM3 compared to LCM1 and LCM6. Slow crack growth of ceramics is largely determined by the fracture toughness values.

Table 2. *Vickers Indentation Method Measurements*
(Number of indentations/cracks measured is given in brackets).

Note: All results normalized to LCM1	**Relative Vicker's Indentation Hardness**	**Relative Vicker's Fracture Toughness E = GPa1** (Estimated)	**Relative Vicker's Fracture Toughness E =GPa $_2$** (Estimated)
LCM1	1 (26)	1 (11)	1
LCM6	1.03 (12)	0.78 (12)	0.78
LCM3	1.17 (12)	1.05 (8)	1.07
LCM5	1.15 (12)	1.07 (7)	1.08

A Young's modulus of LCM1 has been measured at room temperature. Measurements at higher temperatures are in progress.

The strength of LCM1 has been measured at room temperature and measurements at higher temperatures are in progress. The mechanical properties (strength) of ceramics is known to weaken with increasing flaw size according to Griffith's equation:

$$\sigma = A\,(E\gamma/c)^{1/2} \qquad (1)$$

where σ is the fracture stress, E the elastic modulus, γ the fracture energy, c the flaw size and A a constant. Generally, the flaw sizes equals the grain size of the ceramic and thus the strength decreases with increasing grain size. Thus grain size is an important parameter which must also be considered when measuring and improving strength properties.

Thermal conductivity of LCM1 has been measured at room temperature and higher temperatures. The thermal conductivity closely resembles the values of alumina.

3.1.5 Task 1 Conclusions

Physical characterization of three candidate materials has been completed. Nearly all new material candidates under study exceed the commercial oxygen flux target. Key mechanical properties such as creep, thermal and chemical expansion and fracture toughness can be manipulated by changing the material crystalline composition. Work will continue to optimize these properties in the search of a superior material suitable for long-term commercial operations.

3.2 Task 2: Composite Element Development

3.2.1 Goal – Task 2

Develop advanced composite OTM elements (tubes) and the techniques for fabricating these elements at the bench scale. The goal is to develop robust, low cost, high flux tubes that can survive multiple cycles in temperature and fuel composition while maintaining structural integrity at target pressure differentials.

3.2.2 Milestones – Task 2

This budget period: 3Q01-- Select composite structure and manufacturing technique for 2nd generation material
Status--Several methods have been developed that are suitable for manufacturing advanced element designs. However since a 2nd generation material or suites of materials have not yet been selected, a fabrication technique cannot yet be decided.

3.2.3 Experimental – Task 2

In order to develop high quality OTM tubes, characterization and testing of incoming powders (Powder Quality Control) must be conducted. The following measurement apparatus will be utilized:

- Inductively Coupled Plasma Analysis (ICP) - Stoichiometry and impurities
- X-ray Diffraction (XRD) - Phase purity
- Microtrac - Particle size distribution
- BET - Surface area
- Scanning electron microscope (SEM) - Particle morphology
- Thermo-gravimetric Analysis (TGA) - Organic content and water loss

After characterization, the powders are mixed into workable pastes and formed into disks or tubular shapes utilizing methods developed in previous Praxair programs. The OTM disks or tubes are then sintered in a controlled atmosphere at a controlled rate of heating in a high temperature muffle furnace. The sintered tubes then undergo tube characterization where a battery of tests are conducted to determine strength, diameter, straightness, flaws, phase purity and absence of leaks.

3.2.4 Task 2 Results and Discussion

Composite membrane structures are under study as a means to satisfy both the flux and strength requirements of a commercial ceramic OTM element. A composite structure employs a dense OTM film on a porous substrate. The porous substrate allows feed gases to permeate to the dense film where oxygen exchange and bulk diffusion through the ceramic OTM material occurs. Figure 6 is a plot of oxygen flux versus substrate thickness for two levels of dense film thickness at the commercial target temperature. For these conditions, the oxygen flux is proportional to substrate depth and insensitive to dense film thickness.

Oxygen flux through a composite membrane is a strong function of both temperature and composite membrane architecture. Figure 7 shows that the target oxygen flux can be met with a variety of composite membrane architectures and a significant range of temperatures.

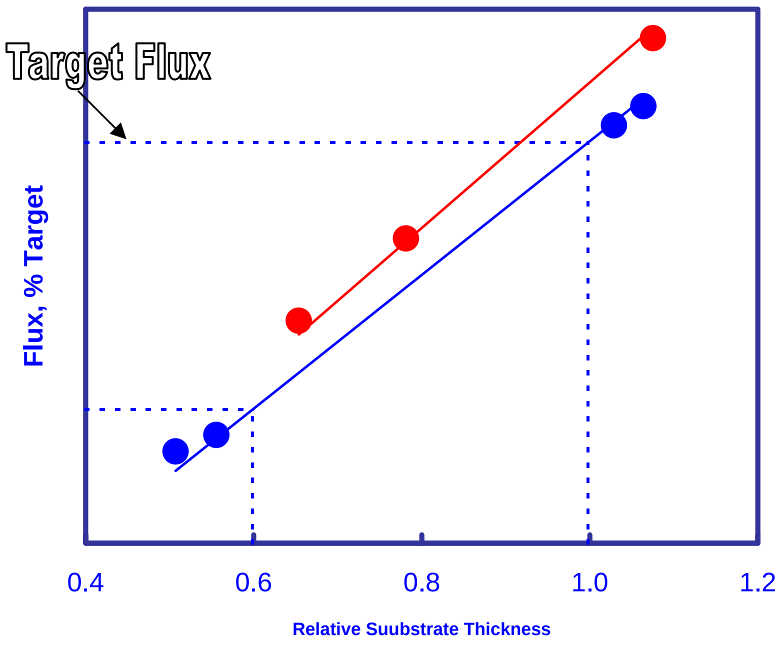

***Figure 6.** Flux of LCM1 and LCM2 Disks versus Substrate Thickness*

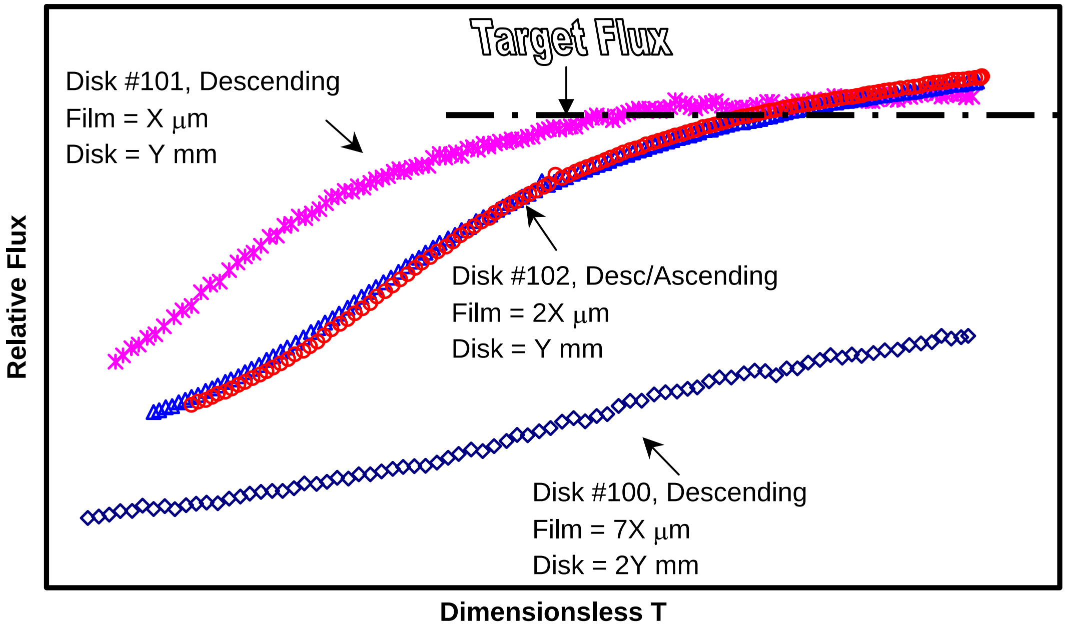

***Figure 7.** Flux of LCM2 Disks versus Temperature*

Three proprietary methods of fabricating composite membrane structures are currently under study. All methods have proven capable of applying leak free dense films to porous substrates. Differentiating parameters include costs, yield of leak free tubes, dimensional consistency and tube robustness, among others. So far, the method of fabrication has not had a large observable effect on the flux performance of the elements. A key milestone is selection of the best method for scale-up in the next budget period.

3.2.5 Task 2 Conclusions

Flux is influenced by both temperature and tube architecture. Target oxygen fluxes can be met with a variety of tube architectures and fabrication methods. At least three fabrication techniques are capable of making leak free composite tubes. One of these methods will be selected for scale-up to produce large elements for large scale pilot plant testing.

3.3 Task 3: Tube Fabrication

3.3.1 Goal – Task 3

The main goal is to scale-up the manufacturing process and supporting technologies for building large-scale composite tubular elements. This team will also supply elements for testing in the P-0 (6 to 8 inches), LTT, P-1 (4 to 6 feet) and P-2 reactors (6 to 10 feet).

3.3.2 Milestones – Task 3

This budget period: None.

Status: Prototypical membranes with dense layers ranging from X to 3X micron and porous layers ranging from Y to 1.67Y micron have been produced as tubes ranging from 20 to 140 cm long from LCM1 and LCM2 candidate materials.

Next Milestone: Scale-up second-generation material to make tubes adequate for P1 size reactor.

Status: Scale-up has been hampered by the delay in finalizing the chemistry of the second-generation material. However, substantial progress has been made with generic materials to enable rapid change over to the new material.

3.3.3 Experimental – Task 3

3.3.3.1 Green Forming: The scale-up effort centered on isostatic pressing as the green forming process to make the substrate. The dense film was then applied to the substrate using a variety of different processes. The different processes have limitations on the minimum and maximum layer thickness and hence the appropriate technique can only be finalized after the tube architecture and material are finalized.

The isostatic press is capable of making up to 3500cm long tubes and is large enough to handle about 5 tubes simultaneously. The press has a maximum operating pressure of 345 Mpa. [50ksi] pressure, which is adequate for most ceramic processes.

This press is generally reserved for making longer elements. The tubes for the shorter P-0 reactors are made in a smaller press which is capable of a larger range of pressures. Isostatic pressing enables the making of tubes with an open end designed to assist in sealing.

The isostatic press and an example of a green pressed tube are shown in Appendix 5.a. page A-5.

3.3.3.2 Sintering: Sintering is performed in vertical furnaces where the tubes are hung from refractory supports. The furnaces are loaded and unloaded from the top and the atmosphere in the furnace can be controlled. Typically, the sintering process starts with slow heating in air to oxidize, evaporate and or burn the organic additives, the adsorbed water. This step has to be slow in order to ensure that the departing species do not physically damage the ceramic component, which is weakened by the removal of the binders.

After the organic constituents are removed, the furnace atmosphere can be changed to ensure that the stresses introduced by the thermal and compositional effects do not affect the ceramic. The tubes are sintered at a temperature above the target temperature, held at the temperature for 4 hours and then cooled gradually to room temperature. The temperature and the oxygen partial pressure inside the furnace are monitored continually. The sintering process results in shrinkage of about 20% in the length of the tubes. . A picture of the sintering is shown in Appendix 5.b on page A-6.

3.3.4 Task 3 Results and Discussion:

The experimental work has been useful in defining the processing route for the Lead Candidate Material #1 (LCM1). Several process improvements were made; new fixtures were designed and made to enable the green forming, extraction and handling of the green tubes. Two critical issues remain in this area: wall thickness uniformity and control over pore former segregation along the length of the substrate. Since the pore former has a size distribution, there is always a possibility that a larger piece will be in an area immediately behind the dense film creating a region of local weakness after sintering.

Sintering of short tubes is performed in smaller furnaces where the tubes are supported on a ceramic sagger. Thus, the side of the tube in contact with the sagger behaves differently than the rest of the tube because of friction during shrinkage and the difficulty in the removal of organic material. The weight of the tube results in some deformation during sintering. The yield of composite tubes is therefore quite low [20%] but is adequate for small scale testing.

Longer elements are sintered in hang fire furnaces in Indianapolis. The challenge there is to support the tubes without creating high local stresses which could break the tube after the binder is removed but before the tube is sintered. The support also has to ensure that the tube shrinks uniformly and thus remains straight.

The experiments have also provided some guidance that will be useful to accelerate the scale up work on the second-generation material. This was accomplished by developing some sintering experience on generic LCM2 materials. Further development work will continue upon specification of the second-generation material.

3.3.5 Task 3 Conclusions

The ability to manufacture long composite elements with an open end designed for sealing has been developed. This process has been used to make membrane elements for evaluation in the P-0, LTT and P-1 reactors. The elements have excellent straightness and roundness.

Deposition of the dense film on the inside has also been successfully demonstrated. One important finding was that when the dense layers are thin the yield after sintering is low. Future work will be directed at finding ways to improve the yield.

3.4 Task 4: Reactor Design and Process Optimization

3.4.1 Goal – Task 4

Develop the commercial OTM syngas process including reactor design and catalyst deployment, reactor components (seals, internals, isolation devices, high temperature tube sheet, etc), and ancillary processes (feed pre-treatment, pre-heat, syngas cooling). This team shall develop and employ mathematical models to simulate process conditions (reactor flow conditions, kinetics, heat and mass balances) and the mechanical, thermal and compositional stresses on the reactor components and elements. These models will enable evaluation of various conceptual designs and facilitate detailed design and evaluation of preferred options. Task 4 includes the operation of the small bench scale units, P-0, which are used to evaluate small OTM elements (6 inches long) and develop engineering data for reactor scale-up. It also includes the resources to build and operate the long tube tester.

3.4.2 Milestones – Task 4

This budget period: 2Q01: Start-up the Long Tube Tester (LTT)
Status--Start-up began in early 3rd quarter. Shakedown continues, with ceramic (OTM) tube tests expected to commence before the end of September.
Next budget period: 4Q01: CFD model validated; conceptual commercial design complete.

3.4.3 Experimental – Task 4

3.4.3.1 P-0 Tests

The single tube tester consists of a tubular shell inside a tubular furnace that provides heat and temperature control. The shell is capable of allowing pressurized tests. The tube is sealed to fittings that separate the two sides of the membrane and prevent flow communication. Inlet gas composition, pressure, and temperature are controlled and outlet gas composition, pressure, and temperature are measured. Thermocouples are also located inside the reactor to monitor temperature. A gas chromatograph is used to measure gas compositions. See Appendix 2 page A-1 for an example of a single tube reactor.

3.4.3.2 Long Tube Tests

The Long Tube Tester (LTT) is designed to test a commercial scale ceramic oxygen transport membrane (OTM) in the production of synthesis gas using natural gas, air and steam. The LTT consists of an electrically heated reactor, a feed heater, discharge coolers and various controls, all of which are located within a ventilated enclosure. The unit will demonstrate the viability of most aspects of the OTM technology including the membranes, catalysts, seals and process parameters. For a view of the LTT see Appendix 3 page A-3.

3.4.3.3 Seal Tests

The unique material properties of the OTM elements make sealing a particularly challenging task, especially in the application of bonded seal technology such as diffusion joints, brazes, or glass sealants. For this reason, the OTM alliance has focused primarily on non-bonded compression joints. Although the compression joints generally are not as leak-tight as bonded seals, they are more versatile and can better accommodate the current OTM elements. At this time, versatility in the seal technology is particularly important since the OTM elements are themselves still under development.

OTM alliance compression seal performance is tested in single element P-0 reactors (described above), the multi-element P-1 reactor, and designated seal test reactors. The latter are used to evaluate new concepts and address important issues related to longevity and thermal cyclability of the seals.

As in P-0 reactor tests, small OTM elements (6-8 inches long) are used in seal test reactors, which include replicas of the seal fixtures used in the multi-element P-1 reactor. Seal tests are performed at up to target temperature and a pressure differential up to slightly greater than target pressure in either air or nitrogen. Mass flow measurements are used to determine leak rates. In addition, coupon tests under compression are performed to study interaction between sealant and OTM materials.

3.4.3.4 Modelling Studies

A computational fluid dynamics (CFD) model has been developed for the P-0 reactor. This is a traditional laboratory scale reactor with axial flow in a cylindrical pipe heated by a radiation furnace. Inside the reactor shell, on the axis of symmetry, is a closed end oxygen transport membrane (OTM) tube. To enable axial circulation of air inside the OTM tube, an opened end lance tube is inserted as depicted in Figure 8. Typically, air at low pressure flows up through the annulus formed by the lance and OTM and down through the lance. Fuel at high pressure flows down through the annulus formed by the OTM and the reactor shell. As a result of the difference in chemical potential across the membrane, oxygen permeates through the wall and reacts with the fuel on the surface of the OTM tube.

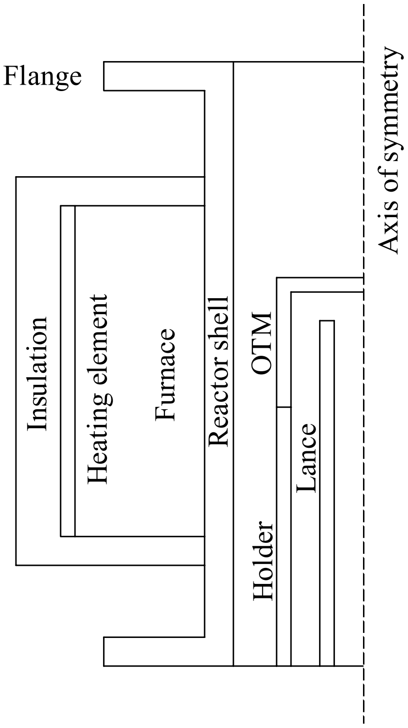

Figure 8. *Schematic Diagram of P-0 Reactor*

The flow fields inside the reactor are axisymmetric, but not one dimensional, because the air stream changes from upflow to downflow at the top of the lance and the fuel stream has a radial velocity component at the top of the OTM tube. Both streams must be treated as multi-component because the oxygen concentration in the air stream is changing due to permeation and the fuel stream composition is changing due to combustion and reforming reactions. The computational model is complex because the physical and chemical processes in the two streams are coupled due to oxygen permeation and heat transfer through the OTM wall.

When oxygen permeates through the membrane, combustion reactions occur on the outside surface of the OTM, and the heat of reaction must be dissipated by conduction in the OTM, convection to the fluid streams and radiation to both the lance and the reactor shell. In this event, the radiation flux from the OTM to the reactor shell is significantly greater than the radiation flux from furnace to the reactor shell. Since the shell temperature is determined by the net radiation flux, it is necessary to include the radiation furnace in the reactor model. In addition, end losses of thermal radiation in the fuel stream cannot be ignored because the OTM tubes are relatively short compared to the reactor diameter. As a result of these two features, a very sophisticated radiation code is required to handle the radiation exchange between surfaces.

The P-0 reactor model is implemented in a commercial CFD code called CFX-4. The radiation problem is handled in a separate code called CFX Radiation which interfaces with CFX-4. Both codes were developed and are sold by AEA Technology.

The equations in CFX-4 are derived from the basic conservation laws for momentum, energy, total mass balance and species mass balance. These equations are supplemented by empirically based chemical kinetics equations for the combustion and fuel reforming reactions. Another key component is the oxygen transport model which calculates the oxygen flux through the membrane as function of the difference in chemical potential across the membrane. Fluid properties are treated as functions of temperature and composition.

3.4.4 Task 4 Results and Discussion

3.4.4.1 P-0 Tests

P-0 tests in 2001 have concentrated on meeting the life (1000 hour continuous operation at pressure) and cycling (10 complete thermal and compositional cycles) goals of Phase 2. Neither of these goals has been accomplished yet, but there has been substantial progress made in both areas.

A tube has been running for over 750 hours with a flux close to 70% of the Phase 2 target flux using the standard fuel mixture at 100 psi. The tube surface temperature is higher than the furnace temperature, indicating that the exothermic oxidation reaction is providing heat to the membrane. The test also included one complete compositional cycle. Another tube survived 310 hours at medium pressure. The initial flux met the Phase 2 target flux, but declined to about 70% of the target flux where it stabilized. Another tube survived for about 150 hours at medium pressure with no fuel, an additional 175 hours at low pressure with no fuel, and then 125 hours under the standard fuel mixture at a slightly lower pressure before it failed. The initial oxygen flux with the standard fuel mixture was about 80% of the Phase 2 target flux.

A thermal cycling test completed seventeen thermal cycles between room temperature and 70-100% of target temperature without leakage, but during the 18th cycle, a system failure unrelated to the membrane or seal caused the seal to fail. The total test time was almost 1000 hours. High differential pressure was maintained throughout the test. There was no leakage using the new seal design. The flux was almost half of the Phase 2 target flux and did not change significantly with pressure. The tube was removed intact upon shutdown. Another test completed 5 thermal cycles and one process gas cycle before failure after about 150 hours. Other tests have completed two or three compositional and thermal cycles. Cycling tests continue.

The single tube reactors have also accomplished other important program goals in 2001.

At the beginning of the year, corrosion was considered an important issue. No corrosion or other new phases were found on a tube after 430 hours on stream under dynamic conditions at 90% of target temperature. The color of the tube changed slightly, probably because of some surface roughening as seen in SEM. The results from the static corrosion test in the P-0 reactor are in good agreement with earlier tests under similar conditions (same T, P, and composition) in the SCTU reactors.

Sealing the membrane was also an important issue. A P-0 reactor was modified to operate at high pressure. The tube held high pressure at 96% target temperature for 24 hours after which the pressure was reduced to medium-high pressure and reactor temperature increased to the target temperature for 72 hours. A very small helium leak was observed.

The single tube reactors are also required to assist in the design and operation of the multi-tube reactors. A startup/shutdown protocol was specified for P-1. A much more aggressive startup procedure has been demonstrated in P-0. The oxygen flux vs. utilization was measured. The flux decreased significantly as the O_2 in the inlet dropped below a threshold inlet concentration. Lower inlet oxygen concentrations led to very low oxygen concentrations at the outlet. This provided important information to the reactor design for large-scale reactors. The catalyst for the pilot reactor was specified and will be deployed on the process gas side of the membrane. The catalyst was tested with an alumina tube and gave a high, stable methane conversion at 93% of target temperature with a total fuel flow of 1.8 lpm at atmospheric pressure. The catalyst deactivated slowly during the first 200 hours on stream, both in fuel and inert, but stabilized after 200 hours. The total length of the run was 360 hours.

3.4.4.2 Long Tube Tests

October has been reserved for testing the background activity of the cross flow reactor. In addition a 250 hour life test will be pursued at target pressure using the 'standard gas mixture'. The test will be performed at low oxygen utilization and methane conversion in order to take advantage of a higher heat removal rate under those operating conditions. The furnace temperature will be controlled to such a value that the membrane wall temperature will be below target temperature. All OTM tubes selected will be helium leak tested in order to enhance our chances for a successful test.

3.4.4.3 Seal Tests

Efforts in 2001 have been focused on deploying compression seals in the P-1 reactor and improving the ability of these seals to undergo thermal cycling. The OTM compression seal has been used successfully in a number of P-1 reactor tests with full size OTM elements. Thermal cycling has also been demonstrated in P-0 and seal reactors; however, a number of issues have hindered consistency in cycling, especially in the P-1 reactor.

One obstacle to thermal cycling has been adverse chemical interaction between the seal materials and OTM elements. Such interactions can lead to undesirable chemical bonding, stress accumulation during cycling, and failure in the OTM elements. As expected, this becomes more problematic as the operation temperature is increased.

Several promising techniques that reduce or eliminate adverse interactions between the sealant materials and OTM elements have been investigated. The ability to make OTM compression seals that can survive thermal cycling and maintain leak rates well below the target is shown in Figure 9. Figure 10 includes data from several different seal tests that were cycled between ambient and several temperatures including the target temperature.

The seal cycled to the target temperature included one of the techniques to prevent chemical interaction.

In addition to reducing chemical interaction between the seal materials and OTM elements, design modifications to key seal components have also improved consistency. These modifications have especially been beneficial in the ability to form seals for OTM element life-tests in the P-0 reactor. Leak rates as a function of time for seals from P-0 and seal reactor tests are shown in Figure 10. In each test, the temperature of the seal was maintained between approximately 87-100% of target temperature.

A number of other seal options are being investigated by the OTM alliance. Along with alternative compression seal designs, bonded seal technologies are also being evaluated. Bonded seals are expected to become more feasible with advances in the OTM element technology and ultimately provide the best commercial sealing option.

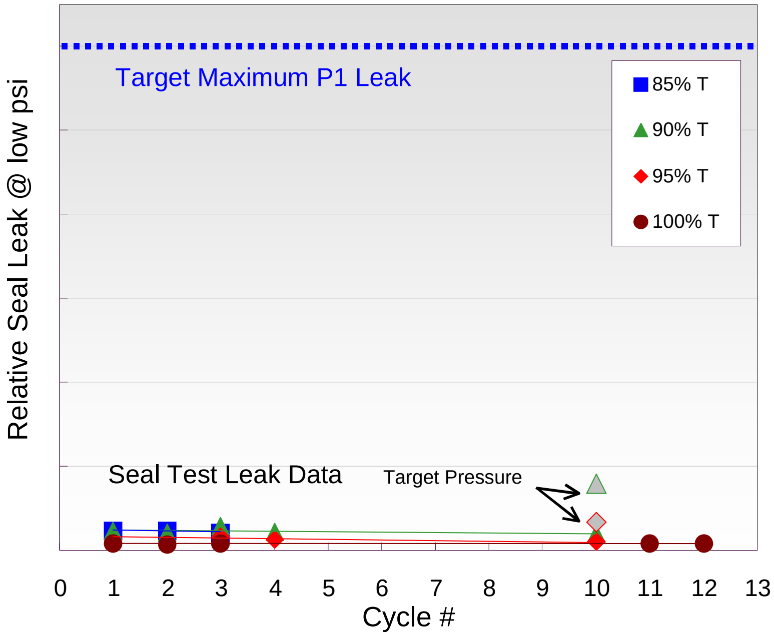

***Figure 9**. Relative Leak Rates of OTM Seals after Thermal Cycling*
The blue dashed line indicates the target maximum leak rate for the P1 reactor.

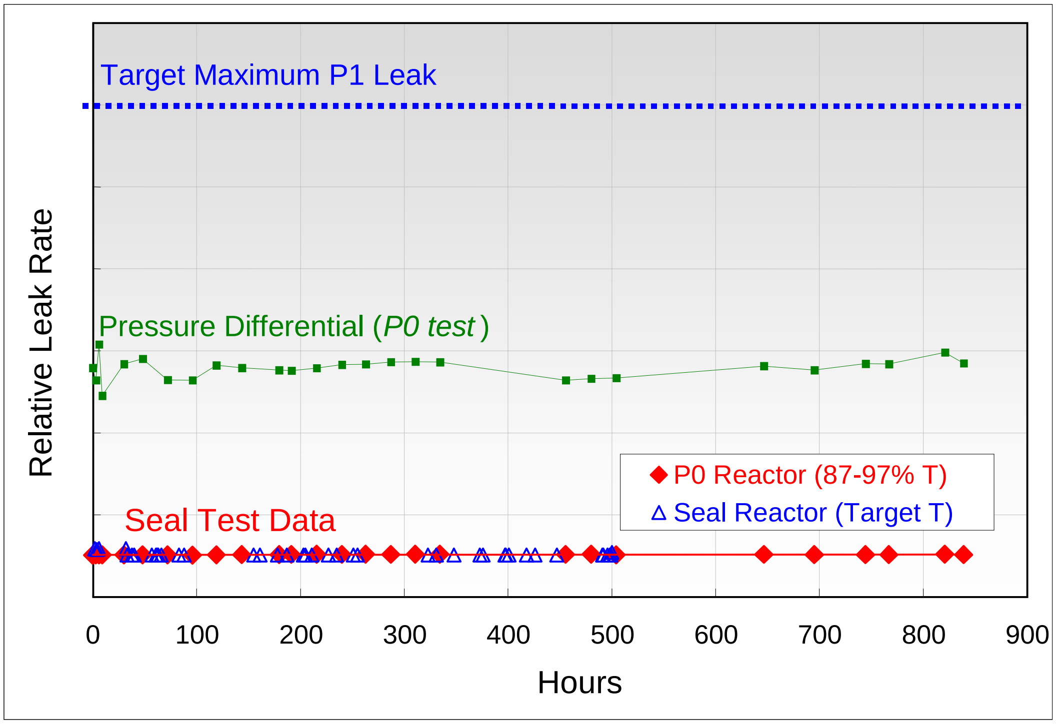

Figure 10. *Relative Leak Rate as a Function of Time for OTM Seals used in the P0 (red) and seal test (blue) reactors. The blue dashed line indicates the target maximum leak rate for the P1 reactor.*

3.4.4.4 Modelling Studies

The P-0 model predicts the flow fields inside the reactor for both the air and fuel streams. As an example, Figure 11 shows a view of the weak counter flow vortex produced by the turning air stream at the top of the lance tube. This phenomenon produces very low velocities and oxygen concentrations above the lance. The momentum equations also give the pressure loss in each of the fluid streams.

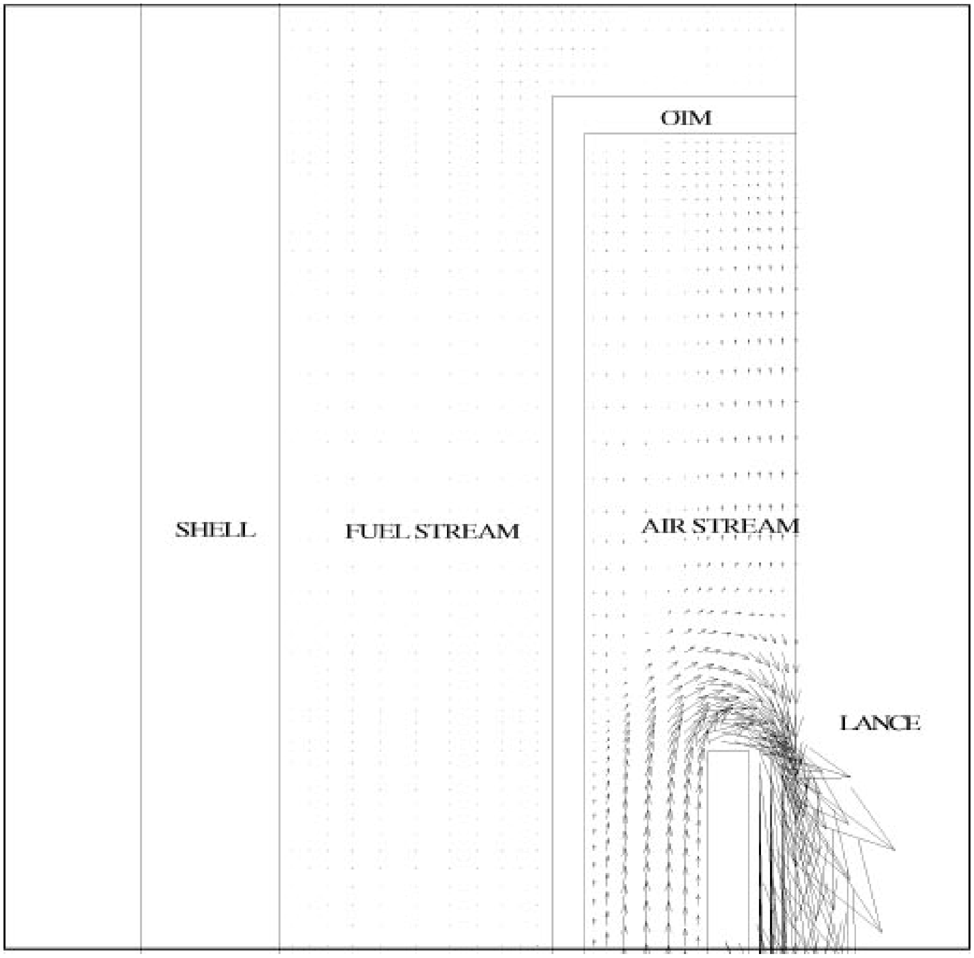

Figure 11. *Velocity Vectors Showing the Recirculation Zone above the Lance Entrance*

Another important parameter is the temperature distribution in the OTM wall. This is a two-dimensional field varying in both the radial and axial direction. It is computed by the CFD code from an energy balance which accounts for the heat of reaction, conduction, convection and radiation exchange with the surroundings. Figure 12 shows the temperature contours near the top of the OTM tube. In this case the temperatures range from a low of about 86% of target temperature in the fuel stream to a high of about 116% of target temperature in the OTM tube. The contour lines are separated by 20^{o}C intervals. The wall temperature is important because it affects the rate of oxygen permeation, and more importantly, it affects the structural stability of the OTM tube.

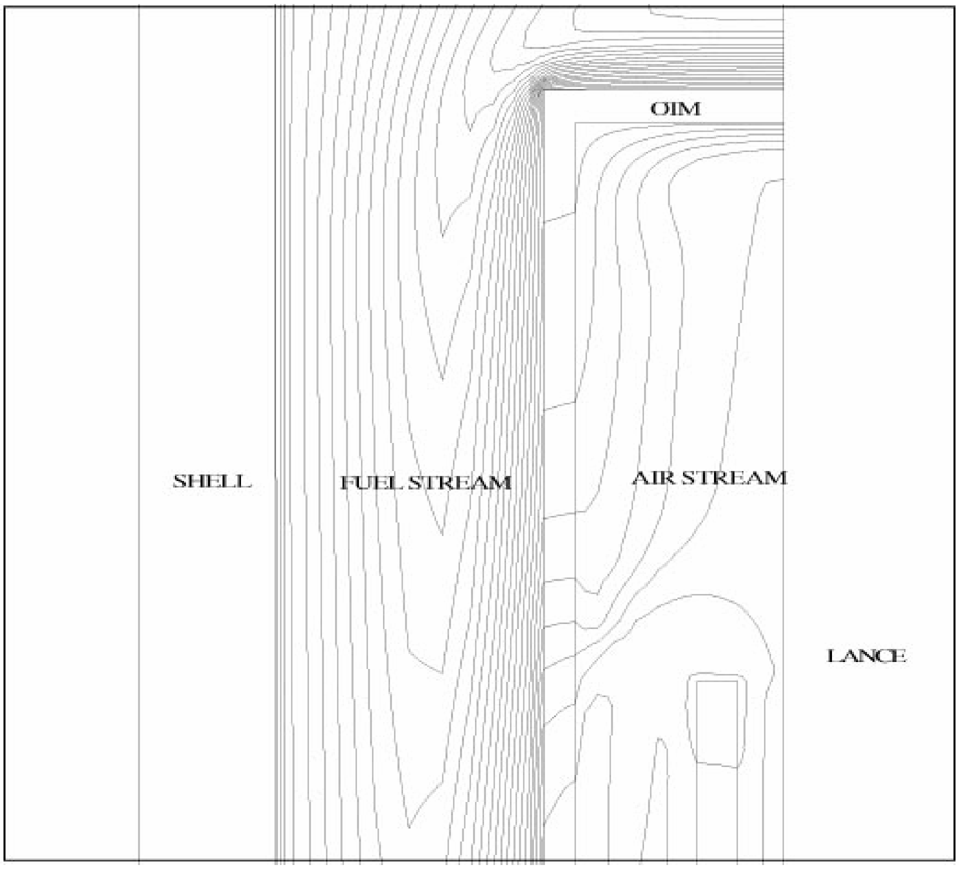

Figure 12. *Temperature Contours at the Top of the OTM Tube*

The model is also capable of predicting the oxygen concentration in the air stream and the species concentrations in the fuel stream. These concentrations change as a function of axial and radial position as a result of oxygen permeation and chemical reactions. The reaction rates are determined in separate laboratory experiments, and then are inserted into the CFD code as empirical correlations. This capability enables one to examine the effect of operating conditions and design parameters on the performance of the reactor.

As discussed in the above paragraphs, the purpose of the computational model is to provide insight into the complex physical and chemical processes occurring in the P-0 reactor. Often the parameters affecting the performance of the reactor are not easily measured in the laboratory or are very expensive to measure. In this case the computational model provides a cost effective alternative tool. It is also useful in optimizing the performance of the reactor under changing operating conditions and design features. Finally, it provides a diagnostic tool for investigating operational problems in experimental work. Stimulation runs using the model are often the only means for understanding the source of a test failure.

3.4.5 Task 4 Conclusions

Significant progress was made in modelling of the OTM performance in the reactor. The tube wall temperature was shown to be a critical variable impacting tube life. The tube wall temperature was shown to be primarily controlled by the oxygen flux and the heat transfer mechanisms from the surface. The importance of radiation and convection was delineated and preferred means to control wall temperature were identified. A novel strategy for preheating the feed gas was identified. The conceptual design of commercial reactor has been postponed

Seal and TID developments are on track. Leak rates below target and ability to cycle multiple times without seal degradation was demonstrated. A proof of concept TID was fabricated and performed well in room temperature lab tests.

While P-0 tests are behind schedule, there was significant progress in running high pressure tests with gas mixtures simulating reactor operation. The P-0 reactors have been heavily instrumented to permit detailed mapping of the thermal fields inside and outside the tube. This has permitted close control of the tube wall temperature greatly enhancing the success rate in the tests. A life test at medium pressure and target temperature is in progress and has exceeded 500 hours.

3.5 Task 5: Catalyst Development

3.5.1 Goal – Task 5

Develop the steam reforming catalyst system (and other catalysts, if so needed) employed in the OTM reactor. At least three methods of catalyst deployment will be evaluated.

3.5.2 Milestones – Task 5

This budget period: 2Q01--2nd generation catalyst system chosen for testing
Status--Completed--Chose Cat A for testing
Next budget period: 4Q01--2nd generation catalyst system installed in P-1

3.5.3 Experimental – Task 5

Kinetics experiments were performed in an Incoloy-800HT tubular reactor (ID= 12mm, length = 20in) heated by a three-zone Thermcraft furnace. Gases (CH_4, H_2, CO, CO_2, He) were fed to the reactor using Brooks mass flow controllers. Steam was supplied to the reactor using an ISCO pump and heat-traced sample lines. The water vaporization section of the reactor was maintained at 175°C with heating tape. 1/16" stainless steel tubing was used to connect the ISCO pump outlet to the water vaporization inlet in order to assure a steady flow of liquid water into the reactor system. The inlet gases were mixed with the steam in the water vaporization section. Steady flow of water into the system is essential for stable operation. The high surface tension of water results in a tendency to form large drops of liquid. This can result in intermittent bursts of steam into the reactor system. Steady state gas flow out of the reactor provides a good indication that the bursting effect is minimized.

The tubular reactor was lined with an alumina sleeve (11mm OD, 8mm ID) in order to minimize gas contact with the active metal surface. Background runs with no catalyst in the system consistently showed low activity for methane conversion (<5%). Zirconia wool was used to plug the alumina tube near the reactor outlet and alumina powder

(50/60 mesh) was layered on top of the zirconia wool up to the axial location desired for the catalyst bed (close to the center of the furnace). A thermocouple was fed through the top of the reactor and adjusted to rest in the center of the catalyst volume.

Steam was condensed out of the effluent in a stainless steel vessel immersed in an ice bath. Condensation occurred before a backpressure regulator valve released the gases to atmospheric conditions. The gases were analyzed using an MTI gas chromatograph equipped with a TCD detector. Water flow was calibrated gravimetrically. Gas flows were measured under ambient conditions using a digital bubble-meter and corrected to STP conditions. Carbon balances were generally 95% or greater.

Catalyst samples were cut and in some cases crushed to fit in the reactor. The samples were arranged in the reactor to minimize reactant gas bypass and allow for flow-through conditions. The mass of catalyst tested was usually in the range of 0.1-0.5 g. Flow rates were scaled from the values expected for commercial reactor designs.

3.5.4 Task 5 Results and Discussion

The purpose of a catalyst in this reactor system is to promote both steam methane reforming and the water-gas shift reactions:

$$CH_4+H_2O \leftrightarrow CO + 3H_2 \qquad (2)$$

$$CH_4+2H_2O \leftrightarrow CO_2 + 4H_2 \qquad (3)$$

Note that Equation (3) is simply Equation (2) plus the water gas shift reaction. The empirical rate equations are of the following form:

$$\textbf{CO Reaction Rate} = k_{o1}\exp\left(\frac{-Ea_1}{RT}\right)P_{CH4}^{a1}P_{H2O}^{b1}P_{H2}^{c1}P_{CO}^{d1}\left[1-\frac{P_{H2}^{3}P_{CO}}{K_{smr1}P_{CH4}P_{H2O}}\right] \qquad (4)$$

$$\textbf{CO}_2\textbf{ Reaction Rate} = k_{o2}\exp\left(\frac{-Ea_2}{RT}\right)P_{CH4}^{a2}P_{H2O}^{b2}P_{H2}^{c2}P_{CO}^{d2}\left[1-\frac{P_{H2}^{4}P_{CO2}}{K_{smr2}P_{CH4}P_{H2O}^{2}}\right] \qquad (5)$$

where P_{CH4}, P_{H2O}, P_{H2}, P_{CO}, P_{CO2} are partial pressures in atmospheres, T is temperature in Kelvin, K_{smr1} and K_{smr2} are the equilibrium constants for Reactions (2) and (3) in atmospheres^2, R is the gas constant, and k_{o1}, k_{o2}, Ea_1, Ea_2, a1, a2, b1, b2, c1, c2, d1, and d2 are empirical constants whose values are determined by standard regression techniques. Reaction rates calculated from Equations (4) and (5) are in units of moles/m^3 reactor/s. Rates for the other gas components can be determined from the CO and CO_2 rates using the reaction stoichiometry. By taking the logarithm of both sides of Equation (4) and (5), the reaction rates predicted by the catalyst model can be correlated to the various pre-exponential factors, activation energies, and pressure exponent terms using multiple linear regression. This yields a simpler model, which is more readily deployed in our advanced CFD reactor models. A comparison of the rigorous model and the regressed model is shown below in Figure 13.

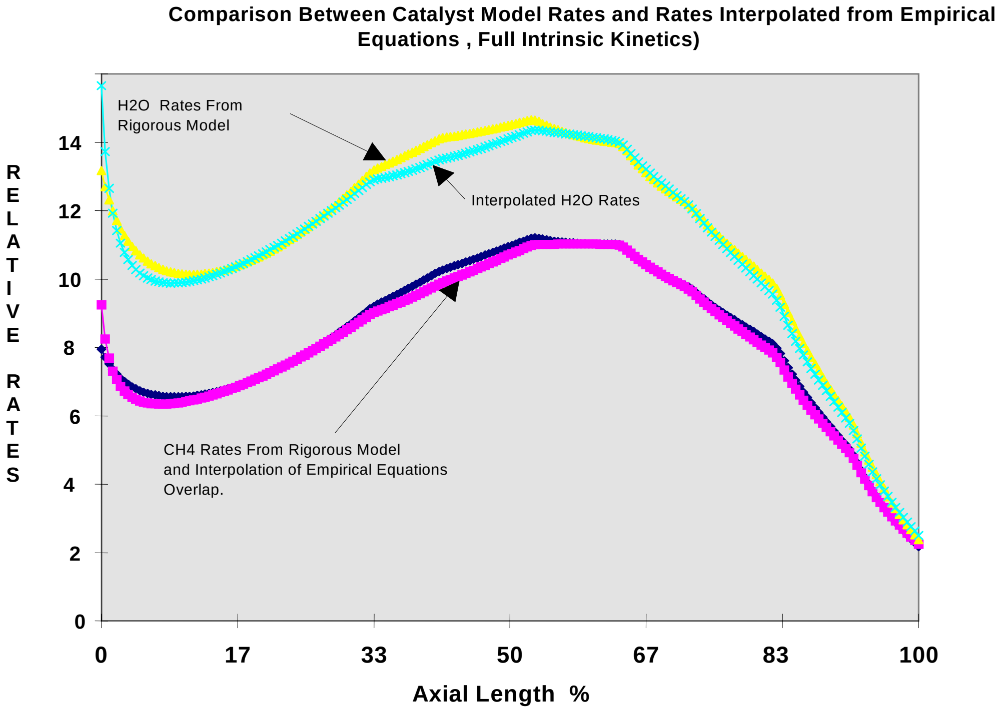

Figure 13. *Comparison of Rigorous and Empirical Kinetic Model*

Four types of catalyst systems are under study for this program, CatA, CatB, Cat C and Cat D. Reaction rates are measured and fitted to equations 3 and 4 for each these catalyst systems utilizing the apparatus and methods described above. The kinetic rates are then incorporated into various reactor models to determine the effectiveness of that catalyst under a variety of expected process and flow conditons. So far, Cat A and Cat B have been studied extensively. Each catalyst exhibits activity levels above that needed for operation of P-1, as shown below in Figure 14 for CatA over a wide range of feed methane concentrations and temperatures. (Each curve representatives a different T and/or pressure) CatB exhibited a similarly robust activity profile.

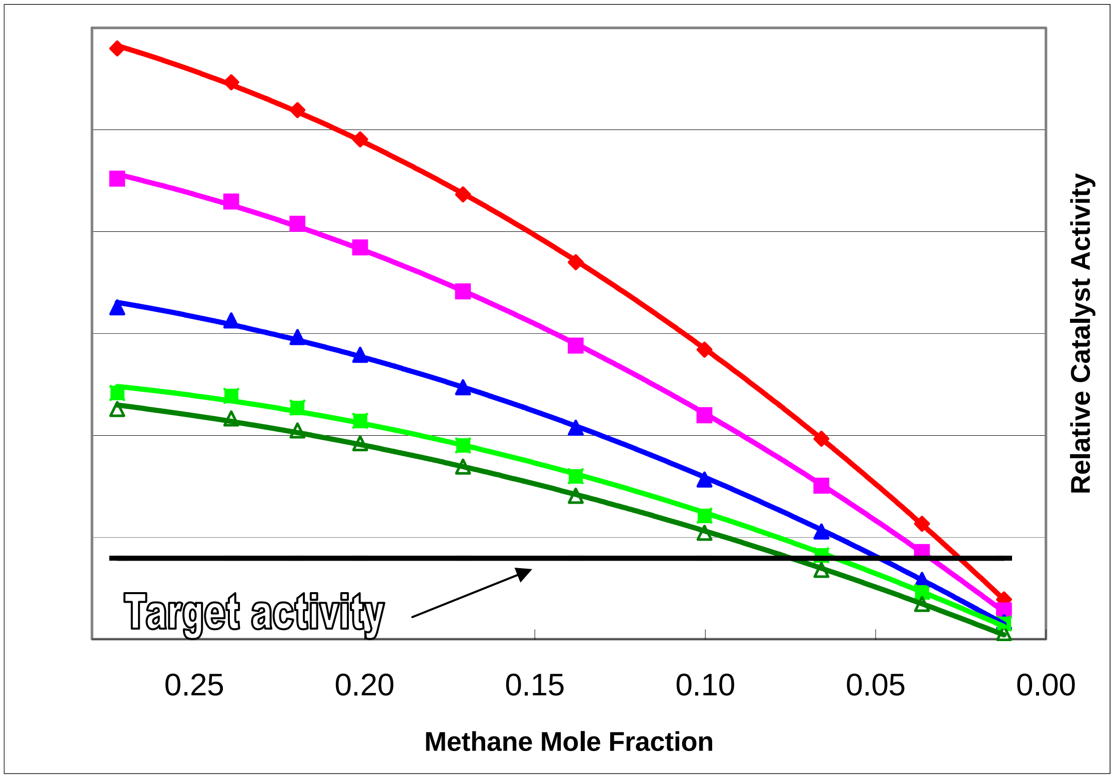

Figure 14. *CatA Relative Activity versus Target Activity over a Range of Temperature*

In addition, cycling and aging studies are underway to determine catalyst life and stability during both steady state and transient conditons. Although these studies are still underway, both catalyst systems (CatA and CatB) are performing well. Each catalyst appears to have sufficient activity, life and stability for P-1 operations. CatA has been chosen for near term test work in the LTT and P-1 based on it's availability, cost, activity, ease of use and compatibility with OTM elements and reactor components

Work will continue to assess life and stability of CatA and CatB. Similar evaluations of CatC and CatD will be undertaken in Budget Period 2. Final selection of a catalyst system for a commercial process will be based on a number of factors, including cost, ease of deployment, regeneration or replacement, life, stability, activity, susceptibility to and compatibility with reactor components and OTM elements.

3.5.5 Task 5 Conclusions

The catalyst development program has yielded a number of exciting options for satisfying the catalytic needs of proposed OTM reactor designs with unique deployment requirements. Two catalyst systems, CatA and CatB, exhibit adequate activity, life and stability for use in P-1 pilot plant operations.

3.6 Task 6: P-1 Operation

3.6.1 Goal – Task 6

Run the newly constructed P-1 to demonstrate the technical feasibility of the OTM syngas technology under steady state and transient conditions. P-1 will be commissioned, shaken down, and operated with several tubes in BP1. The unit will be revamped end of year and outfitted with a full complement of tubes. (The composition, design and fabrication technique of these tubes will have been validated in the LTT).

3.6.2 Milestones- Task 6

This budget period: 3Q01--P-1 achieve steady state with low tube count of 1st generation materials, elements, and catalyst.
Status--Partially Complete--Steady state was achieved with two first generation tubes and an inert catalyst material. The unit achieved steady state operation for over 100 hours, but about 100°C below target temperatures. The unit was successfully cycled without a tube failure.

Next budget period: 4Q01--Design modifications for revamp of P-1 completed.

3.6.3 Experimental – Task 6

See Appendix 4 page A-4 for a description and picture of P-1.

3.6.4 Task 6 Results and Discussion

A number of P-1 operating campaigns were carried out during this reporting period. The longest of which were a 60-hour test and a 100-hour test. This testing was conducted with a low number of OTM elements installed in the reactor and utilized inert fill rather than active reforming catalyst. Since the goal was to achieve steady state operation, effort was made to identify and eliminate causes of plant shutdowns and unacceptable process deviations. The work also included the identification and automation of operating protocols. Both the plant improvements and operating protocols were necessary to ensure the survival of the ceramic OTM elements.

The following graph, Figure 15, illustrates the performance of the temperature ramping feature that was added as part of the automated operating protocol.

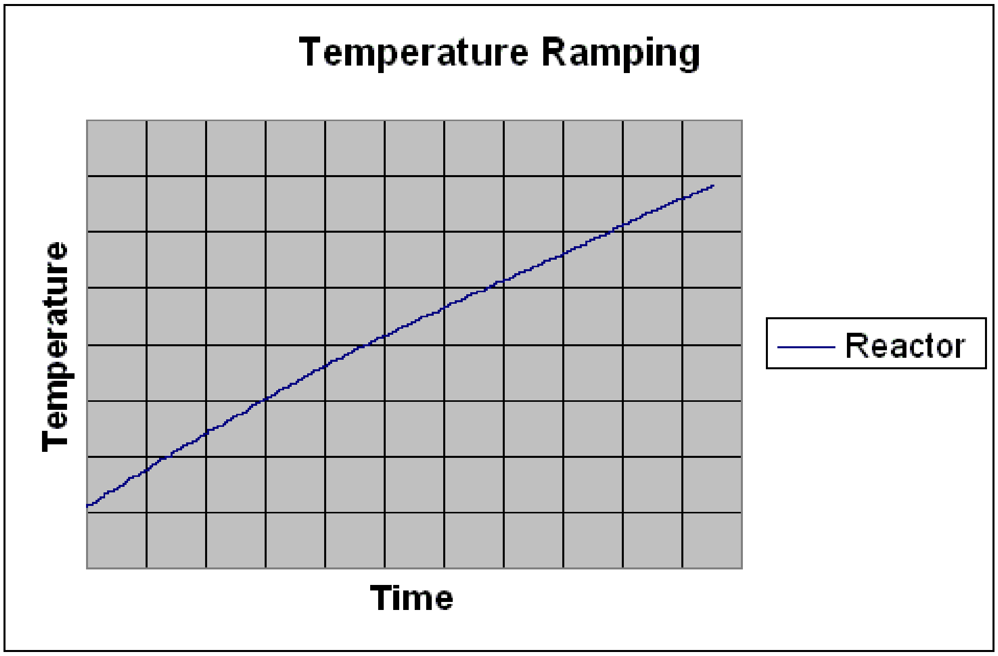

Figure 15. *Reactor Temperature Ramp*

3.6.5 Task 6 Conclusions

After the implementation of a number of equipment and control system modifications for enhanced system operability and reliability, steady state operation of P1 was achieved using 1st generation materials, elements and inert catalyst. Although more robust OTM elements would facilitate testing progress, P1 and the current OTM elements have been proven ready to begin the next stage of higher tube count testing.

3.7 Task 7: P-2 Build and Operation

3.7.1 Goal – Task 7

The purpose of the P-2 pilot plant is to demonstrate the commercial (technical and economic) feasibility of the OTM syngas technology. P-2 will be sized to demonstrate key scale-up risks and economic variables.

3.7.2 Milestones – Task 7

This budget period: None
Next budget period: 2Q02-- Submit NEPA documentation for P-2; 3Q02--preliminary design and cost estimate for P-2 completed.

3.8 Task 8: Fuel and Engine Testing

A matrix of UCTF will be prepared for testing at each engine (International Truck and Engine) or fuel cell developer (Nuvera Fuel Cells). The fuel matrix will include a base stock of syngas derived Fischer Tropsch liquids and will study the addition of advanced oxygenates supplied by BP. The result of the study will be the impact of fuel properties on emissions and engine (or fuel cell) system performance.

3.8.1 Diesel Engines and Exhaust Treatment

3.8.1.1 Goal - Diesel Engines and Exhaust Treatment

The goal of this task is to understand the relationship between ultra-clean fuel properties and their impact on the emissions and performance of an advanced CIDI and exhaust treatment system under development by International Truck and Engine.

3.8.1.2 Milestones - Diesel Engines and Exhaust Treatment

This budget period: 2Q01--define test matrix, order long lead fuels, kick-off program
Status--Fuels ordered and received, test matrix agreed, program started.

3.8.1.3 Experimental - Diesel Engines and Exhaust Treatment

A two-tier test program shall examine the effect of fuel composition (sulfur, oxygenates, hydrocarbon-type conventional diesel, or non-aromatic FT diesel) on engine performance and engine emissions. The first tier will be single cylinder tests with five fuel blends that will focus on in-cylinder emissions reduction. The second tier shall test various fuel compositions in an advanced multi-cylinder CIDI test engine with various after-treatment technologies. The single cylinder engine specifications are shown in Table 3.

Table 3. *Single Cylinder Engine Specifications*

Engine	V6 single cylinder engine
Bore x Stroke	95 x 105 mm
Compression Ratio	18.5
Displacement	0.744 L/cylinder
Injector	G2 SV2.5
Injector Nozzle	6 x 154 x 525
Valve Train	4 valves per cylinder

Pictures of International Truck and Engine Corporation's Facility are attached in Appendix 7 page A-8.

3.8.1.4 Diesel Engines and Exhaust Treatment Results and Discussion

Single cylinder engine test have just been begun; no results are available yet.

3.8.2 Nuvera Fuel Cells

3.8.2.1 Goal - Nuvera Fuel Cells

The goal is to understand effect of UCTF on this fuel cell system and possibly reduce emissions on a per mile basis.

3.8.2.2 Milestones - Nuvera Fuel Cells

This budget period: 2Q01--Order long lead items (fuels for testing); 3Q01--kick-off meetings Nuvera; Full power train tests on two fuels at Nuvera
Status--Fuels ordered and received, test matrix agreed, program underway
Next budget period: 4Q01--Complete burner studies

3.8.2.3 Experimental - Nuvera Fuel Cells

A schematic of the experimental setup is shown below in Figure 16. Pictures of the MPR Facility are attached in Appendix 6 page A-7.

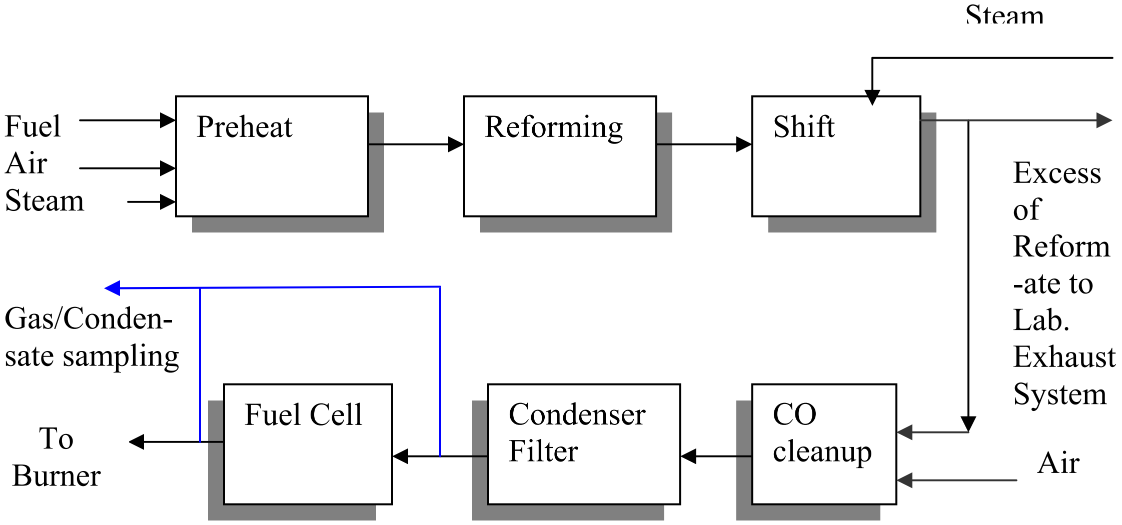

Figure 16. Nuvera Fuel Cells Modular Pressurized Reactor Schematic

The autothermal reforming of the specified fuels will be conducted in the MPR (Modular Pressurized Reactor) facility. The MPR test matrix is shown in Table 4.

Table 4. *MPR Test Matrix*

FUEL COMPOSITION	Cal. Phase 2 Gasoline, 35 ppm sulfur	FT/Naphtha blend 1
Air/Fuel Stoichiometry, φ	3.75	3.75
Water/fuel stoichiometry, Steam/Carbon	3.4	3.4
Power/throughput, KWth	60	60

The fuel cell stack testing matrix is described in Table 5.

Table 5. *Fuel Cell Test Matrix*

Stack temperature, C	70
Pressure, psig	20
Cathode humidification, %	80-100 at 65ºC
Cathode stoichiometry	2
Anode stoichiometry	1.5 – 2

The following data will be recorded during experiment:

- all operating conditions specified above;
- the dry bulk composition of the reformate at the exit of MPR clean-up section (vol. % of H2, CO2, CH4, N2)
- the dry bulk composition of the Fuel Cell anode exhaust (vol. % of H2, CO2, CH4, N2)
- the PPM levels of other components, if any, in the reformate stream at the exit of MPR clean-up section
- the PPM levels of other components, if any, in the Fuel Cell Anode Exhaust

3.8.2.4 Results and Discussion - Nuvera Fuel Cells

Two fuels were selected for the first series of tests on the MPR facility. One fuel is a CARB gasoline obtained from California. This commercially available fuel meets the current strict emission standards of the state of California. The second fuel is a Fischer Tropsch naphtha obtained from the Sasol-Chevron joint venture. This is a highly paraffin fuel with essentially no sulfur, nitrogen or aromatics.

Both fuels will be compared in the MPR as described above.

3.9 Task 9: Market Study

3.9.1 Goal – Task 9

The goal of this task is to understand marketing and commercialization hurdles and to develop plans to bring the ultra-clean fuel system to market.

3.9.2 Milestones – Task 9

Note--this study does not begin until Year 3, so there are no near term milestones.

3.10 Task 10: Program Management

3.10.1 Goal – Task 10

The Recipient shall provide technical leadership and management direction to ensure that the program delivers its goals on time, within budget, and in a safe and environmentally acceptable manner. Good communications with DOE, participants, and sub-contractors will be maintained.

3.10.2 Milestones – Task 10

A detailed briefing shall be presented within sixty (60) days after agreement award. The briefings shall be given by the Recipient to explain the plans, progress, and results of the project effort, both technical and administrative.
Status: Accomplished--detailed briefing was provided to the DOE on July 25, 2001.
Enlist subcontractors and initiate work plans within 90 days of award.
Status: Accomplished--subcontracts were let and work initiated by mid August.

3.10.3 Discussion – Task 10

The program award was finalized on May 21, 2001. In anticipation of ward closure, work at Praxair and BP had proceeded since January 1, 2001 and costs were accrued at their own risk. Other subcontractors were not enlisted until after the Praxair/DOE contract was finalized; however, arrangements were made to procure long lead fuel samples for Task 8. This included drum quantities of syngas derived Fischer Tropsch naphtha and diesel fuels obtained from the Sasol-Chevron joint venture. The fuels were delivered in time to avoid delays in the program.

Total program costs to date are tracking close to budget.

Technical progress is mostly on track with the exception of selecting a new lead commercial material. This is a critical path item, which can control advancements in other tasks, especially Task 3, Tube Manufacturing. Nonetheless good progress is being made with the current lead material (LCM1) which is sufficiently robust to enable progress in reactor and process development (Task 4) and tube manufacturing (Task 3).

4.0 Budget Period 1 Conclusions

Significant progress has been made in the OTM syngas tasks of this project during Budget Period 1. Due to subcontract negotiations and modifications in scope of work, the fuels and engine development (Task 8) work was initiated in August 2001.

In Materials Development work (Task 1), it was determined that the benchmark material, LCM1, exceeds the commercial oxygen flux target and is sufficiently robust for process development and pilot plant activities. In addition to LCM1, two new materials were completely characterized and five other materials are in various stages of fabrication or testing. All of these materials satisfy the oxygen flux requirement; and several have demonstrated superior mechanical properties. Work will continue to develop and select second-generation material(s) with superior mechanical properties that can withstand long-term commercial life targets.

Fabrication techniques to commercially manufacture composite elements (Task 2) while optimizing strength and oxygen flux were investigated this Budget Period. Three manufacturing techniques for making robust composite tubes have proven technically feasible based on the capability to make leak free composite elements with uniform geometry. Each manufacturing technique will be studied in detail next Budget Period. Selection of the lead manufacturing process for composite elements has been postponed until the next Budget Period, pending selection of commercial material(s) in Task 1.

Scale-up of manufacturing techniques for producing both small-scale and large-scale ceramic OTM elements (Task 3) was conducted this Budget Period. LCM1 and LCM2 composite elements for P-0 tests and tubes up to 140cm in length for LTT and P-1 pilot plant tests were fabricated and were tested. These elements exhibited excellent straightness and roundness and incorporated a special open end for sealing. Final selection of the commercial manufacturing technique will be determined in the next Budget Period pending selection of the commercial material(s).

Significant progress has been made in Task 4 (Reactor Design and Process Optimization). P-0 tests in six reactors evaluate alternative element architectures and materials, as well as studying effect of process conditions and tube morphology on temperature profiles and element performance.

Construction of a new pilot plant, the Long Tube Tester (LTT), was completed at the end of June. This unit is capable of testing OTM elements up to six feet in length with a variety of process gases and flow configurations at target temperatures and pressures. Commissioning of all systems is complete and the unit is in start-up mode.

The P-1 Pilot Plant (Task 6) achieved a milestone operation of 100 hours, including successful start-up and shutdown without a tube failure. This run utilized two OTM elements. The unit is now configured with 15 OTM elements, 140cm length, and is undergoing start-up.

Two seal design types are being developed. These seals hold the ceramic elements in the reactors and are in use in all of the bench scale and pilot plant units. Both types can be thermally and pressure cycled and can accommodate the thermal and compositional expansion characteristics of the OTM elements.

In modeling, a CFD code has been developed that includes hydrodynamic descriptions of the reactor internals, and kinetic descriptions for both oxygen diffusion through the ceramic OTM and heterogeneous catalysis of steam methane reforming and water gas shift reactions. Fluid flow, heat and mass transfer and reaction kinetics are coupled to give an accurate representation of the reactor performance. The model is being validated against P-0, LTT and P-1 results. These models, plus simpler codes are being used to evaluate alternative reactor designs and process configurations.

Development of tailored catalysts (Task 5) suitable for the unique operating environment of an OTM process reactor has successfully yielded three candidates, all of which can satisfy activity targets. At least one catalyst system qualifies for the P-1 application, meeting the milestone target for this Budget Period. Work continues to optimize the performance, cost and life characteristics of a commercial catalyst system. A detailed model based on intrinsic kinetic experiments has been completed for one of the catalyst candidates. This model is incorporated in the reactor CFD code.

Fuels testing and engine development work (Task 8) are now underway at Nuvera Fuel Cells and International Truck and Engine. Long lead-time for fuel requirements were anticipated and fuel orders were placed to prevent delays in Task 8. Experimental plans have been finalized and Fischer Tropsch-based fuels (an FTL naphtha for Nuvera and a FTL diesel for International) have been delivered to both sites.

Program Management (Task 10) has been successful in kicking off all sub-contractor work in a timely fashion after the DOE /Praxair contract was signed on May 21, 2001. Subcontracts with BP Amoco, Nuvera Fuel Cells and International Truck and Engine were executed in August 2001and work is underway at all sites. A detailed briefing was provided to the DOE during the program kick-off meeting held at the DOE NETL Morgantown, WV site on July 25, 2001.

5.0 References

1. G. Majkic, L. Wheeler, K. Salma, Acta. Mater. 48 (2000) p.1907-1917.

2. Private Communiqué, "Creep Results for LCM materials", T. Stephens, April, 2001
3. Private Communiqué, "Sintering Study of LCM3, LCM5 and LCM6", K. Kleveland, March, 2001
4. Private Communiqué, "Properties of Different Membrane and Substrate Materials, S Aasland and K. Kleveland, April 2001
5. Private Communiqué, "Properties of LCM3 compared to LCM1", J. Sirman, September 2001
6. Private Communiqué, "Vickers Indentation Hardness and Fracture Toughness of LCM1 and Other Materials", B. Krogh and K. Kleveland, April, 2001

Appendix 1. Disk Reactor

Permeation cells for measuring the oxygen flux of discs of OTM materials is in place at Praxair and BP. The permeation cell has an air feed stream passing over the surface of the membrane where oxygen is removed from the gas stream and incorporated into the OTM sample. On the other side of the disc a fuel, gas purge stream is passed over the membrane surface and oxygen is extracted from the OTM material at atmospheric pressure. The oxygen flux can be calculated by measuring the fraction of oxygen in the depleted air stream and the compositional changes in the fuel gas stream. Leaks are detected by monitoring nitrogen concentrations in the fuel purge stream. The sample is contained in a furnace allowing temperature dependence measurements. A view of a permeation cell is shown below.

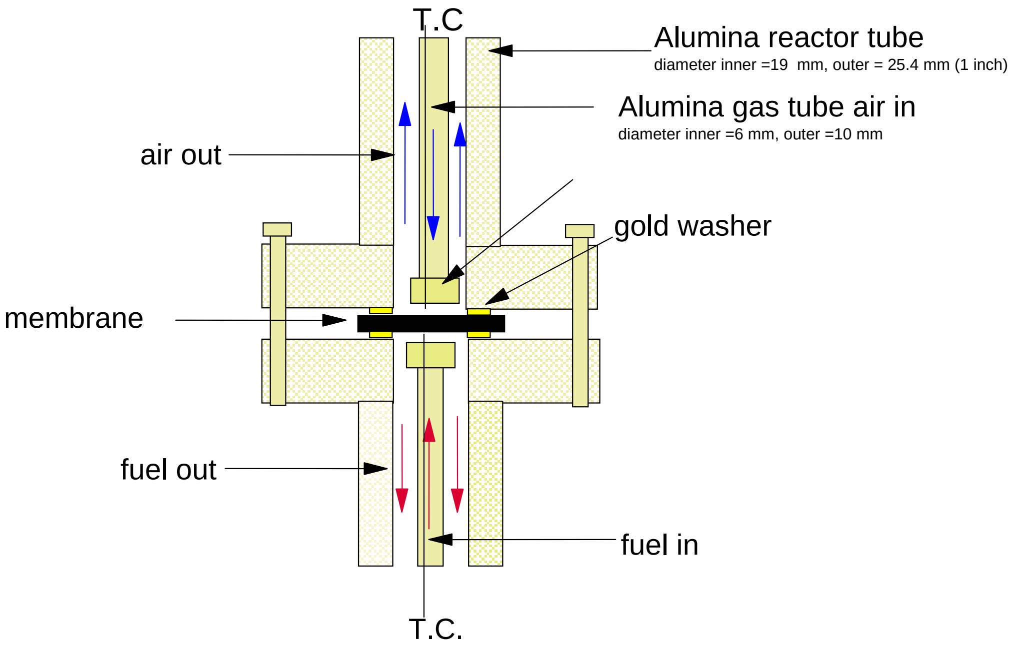

A1

Appendix 2. Description of P-0 Reactors and Test Methods

Six P-0 reactors are available for testing small OTM tubes. Each P-0 reactor includes the following: a three-zone furnace is used to heat the OTM to the operating temperature, between 800 and 1050ºC.; a gas manifold that delivers oxygen, nitrogen, air, and mixtures thereof to the OTM and backpressure regulators to control the pressure both at the air side and the fuel product side of the membrane. A paramagnetic oxygen analyzer is used to determine the level of oxygen depletion from the air stream.

The flux of oxygen through the OTM tube, J_{O_o}, is determined using Equation [A.1]:

$$J_{O_2} = \frac{y_{O_2} F_{purge}}{A_{OTM}} \qquad \text{Equation [A.1]}$$

where:

J_{O_2} = Average oxygen flux (sccm/cm^2)

y_{O_2} = Oxygen mole fraction in the purge gas as measured by the oxygen analyzer

F_{purge} = Volumetric flow rate of the purge gas as measured by the Flowmeter
A_{OTM} = OTM Area (cm^2)

Appendix 3. Description of Long Tube Tester

The Long Tube Tester (LTT) is designed to test a commercial scale ceramic oxygen transport membrane (OTM) in the production of synthesis gas using methane, air and steam. The LTT consists of an electrically heated reactor, a feed heater, discharge coolers and various controls, all of which are located within a ventilated enclosure. A view of the LTT is shown below with the analytical equipment and control panels visible on the side of the LTT enclosure.

Long Tube Tester Pilot Plant Facility

Appendix 4. Description of P-1 Pilot Plant

The P1 Pilot Plant (P1) is designed to demonstrate the technical feasibility of the OTM synthesis gas generation technology under steady state and transient conditions using commercial scale OTM's. P1 consists of a multi-tube reactor, feed heaters, discharge coolers and various controls, all of which are located within a ventilated enclosure. A view of the P1 reactor is shown below with a portion of the reactor vessel visible below the enclosure.

P-1 Pilot Plant

Appendix 5. Element Manufacturing Facilities

5. a. Green Forming Facilities

Iso-static pressing - Indianapolis

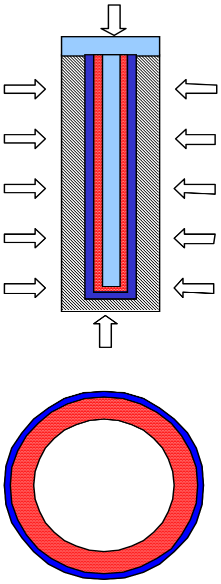

Isostatic Press

Example of long Green Tube [225cm]

A5

5. b. Sintering Facilities

Sintering Furnace

Appendix 6. Photographs of the Nuvera MPR Facility

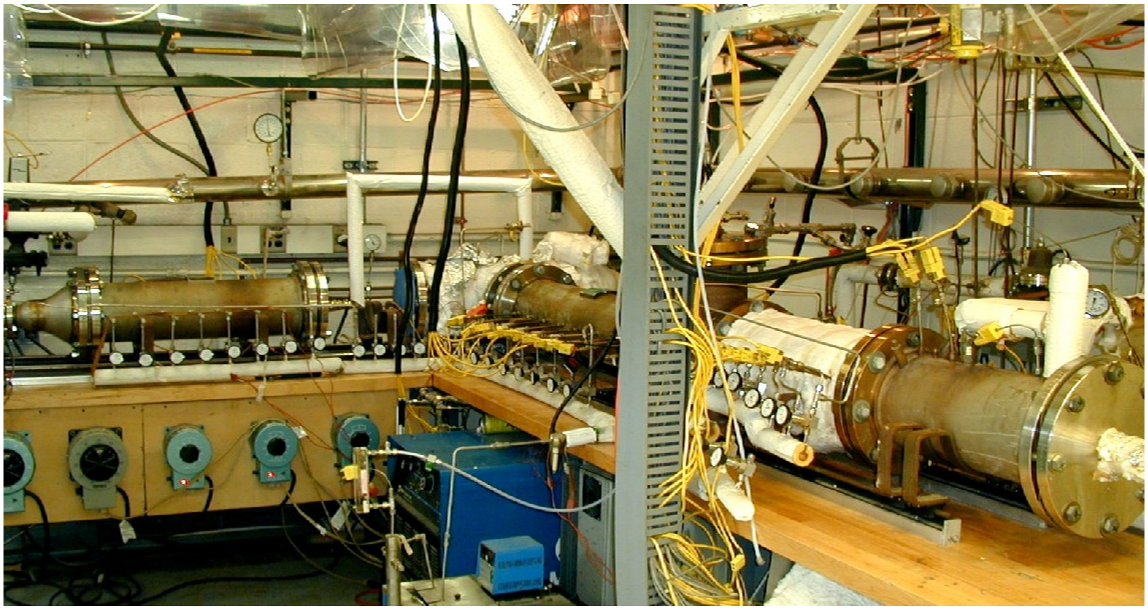

Nuvera MPR Facility: Pre-heat, Reforming, Shift and CO Cleanup Modules

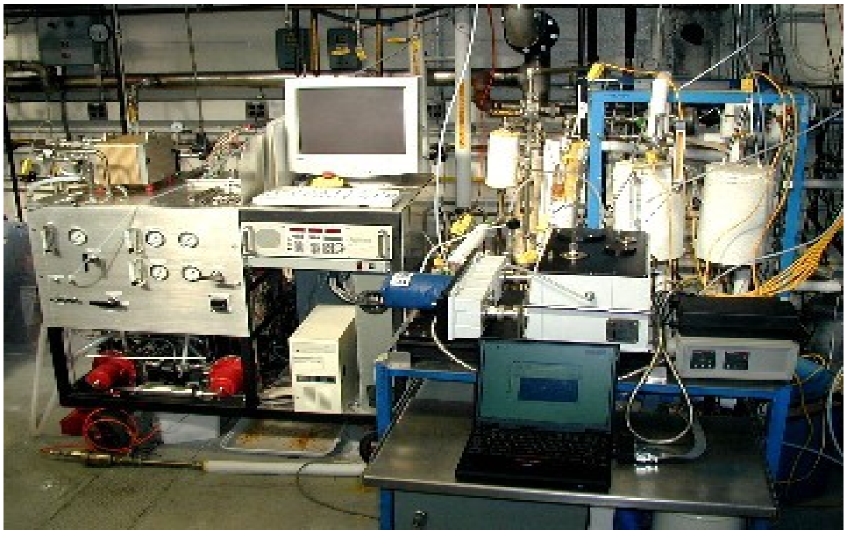

Nuvera MPR Facility: Fuel Cell Stack, Instrumentation and Controls

Appendix 7. International Truck and Engine Facility

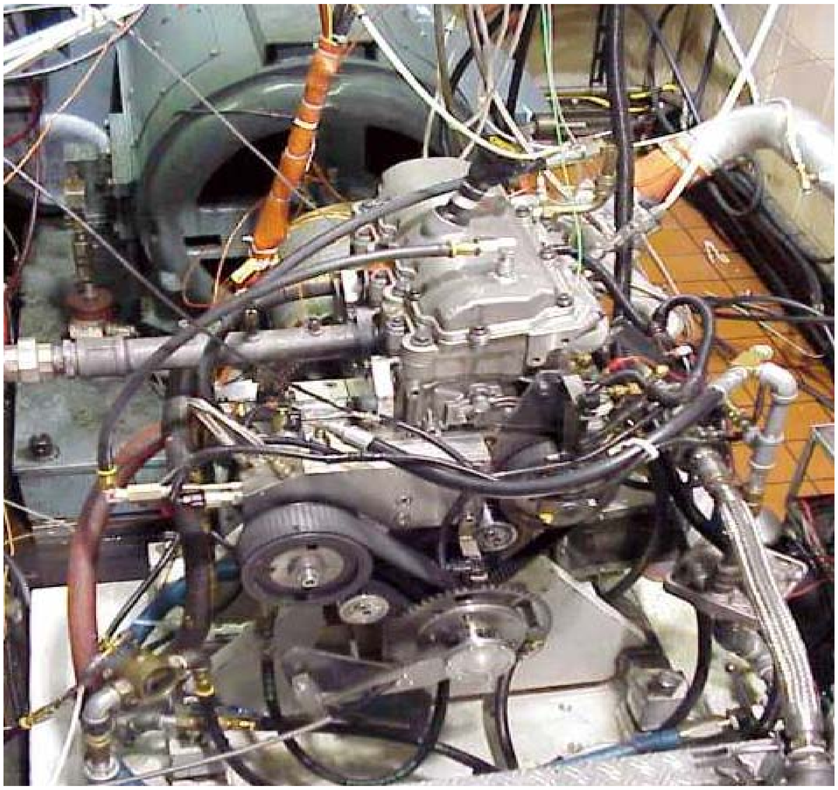

International's CIDI Engine

International's Data Acquisition and Control Panel

A8

FINAL REPORT APPENDIX I

Topical Report – Budget Period 1

FINAL REPORT APPENDIX II

Development of OTM Syngas Process and Testing of Syngas Derived Ultra-clean Fuels in Diesel Engines and Fuel Cells

Budget Period 2

Topical Report

For Reporting Period Starting November 1, 2001 and Ending December 31, 2002

Principal Authors:
E.T. (Skip) Robinson, Principal Investigator, Torix
James P. Meagher, Program Administrator, Praxair
Prasad Apte, Ceramic Manufacturing Manager, Praxair
Xingun Gui, Chief Engineer, Advanced Combustion and Control,
  International Truck and Engine Corp.
Tytus R. Bulicz, Project Development Engineer,
  International Truck and Engine Corp.
Siv Aasland, Staff Engineer, Statoil
Charles Besecker, Senior Chemist, BP America
Jack Chen, Senior Development Associate, Praxair
Bart A. van Hassel, Senior Development Associate, Praxair
Olga Polevaya, Manager Process Engineering, Nuvera Fuel Cells
Rafey Khan, Senior Engineer, Nuvera Fuel Cells
Piyush Pilaniwalla, Engineer, Nuvera Fuel Cells

Report Issue Date: February 2003
DOE Cooperative Agreement No. DE-FC26-01NT41096

Submitting Organizations:

Primary: Praxair, Inc.
P.O. Box 44
175 East Park Drive
Tonawanda, NY 14150

Subcontractors:

BP America Production Company
150 W. Warrenville Road
Mail Code H-5
Naperville, IL 60566

Torix, Inc.
7165 Hart St., Suite B
Mentor, OH 44060

International Truck and Engine Corp.
10400 W. North Avenue
Melrose Park, IL 60160

Nuvera Fuel Cells
15 Acorn Park
Cambridge, MA 02140

Statoil
Arkitekt Ebbels veg 10, Rotvoll
N-7005 Trondheim, Norway

DISCLAIMER

ABSTRACT

This topical report summarizes work accomplished for the Program from November 1, 2001 to December 31, 2002 in the following task areas:

Task 1: Materials Development
Task 2: Composite Development
Task 4: Reactor Design and Process Optimization
Task 8: Fuels and Engine Testing
    8.1 International Diesel Engine Program
    8.2 Nuvera Fuel Cell Program
Task 10: Program Management

Major progress has been made towards developing high temperature, high performance, robust, oxygen transport elements. In addition, a novel reactor design has been proposed that co-produces hydrogen, lowers cost and improves system operability.

Fuel and engine testing is progressing well, but was delayed somewhat due to the hiatus in program funding in 2002. The Nuvera fuel cell portion of the program was completed on schedule and delivered promising results regarding low emission fuels for transportation fuel cells. The evaluation of ultra-clean diesel fuels continues in single cylinder (SCTE) and multiple cylinder (MCTE) test rigs at International Truck and Engine. FT diesel and a BP oxygenate showed significant emissions reductions in comparison to baseline petroleum diesel fuels.

Overall through the end of 2002 the program remains under budget, but behind schedule in some areas.

FINAL REPORT APPENDIX II

Topical Report—Budget Period 2

TABLE OF CONTENTS

Page

List of Tables Page

List of Figures Page

List of Acronyms

BPO	BP Oxygenate
BSFC	Brake Specific Fuel Consumption
F-T	Fischer-Tropsch
HCCI	Homogeneous Charge Compression Ignition
LCM	Lead candidate material
MM	Alternative material systems
OTM	Oxygen Transport Membrane
P-0	Small bench scale test reactors capable of testing single OTM tubes up to 8 inches in length at elevated pressures and temperature.
SCTE	Single Cylinder Test Engine
MCTE	Multi-Cylinder Test Engine
TF	Target Flux
TFd	Target flux for dense disks
TFc	Target flux for composite systems
TP	Target Pressure
TT	Target Temperature
ULS	Ultra-low Sulfur
Target A	High severity process conditions
Target B	Low severity process conditions

FINAL REPORT APPENDIX II

Topical Report—Budget Period 2

1.0 Executive Summary

This program has two primary objectives: 1) development of an advanced, low cost syngas technology based on ceramic oxygen transport membranes and 2) the evaluation of syngas derived ultra-clean fuels in Nuvera fuel cells; and the development of advanced compression ignition engines /after- treatment/ultra-clean fuel systems.

This report covers the period November 1, 2001 through December 31, 2002. Under the revised scope of work for this budget period, work will be performed only in Tasks 1, 2, 4, 8 and 10.

Under objective 1, major progress has been made towards developing high performance, robust oxygen transport elements for high temperature operation. The operating window of these new systems has been expanded dramatically, with tests successfully completed at 1.1TT and 2.2TP. In addition, a new flexible, reactor design has been proposed that lowers cost, improves system operability and can co-produce hydrogen.

Under objective 2, the fuel cell portion of the program was completed. The evaluation of ultra-clean diesels continues in the SCTE and MCTE rigs. Both FT diesel and the BP oxygenate dramatically reduce emissions (NOX, unburned hydrocarbon) in comparison to a baseline No.2 diesel and an ultra-low diesel fuel without the BP oxygenate.

Task 1, Materials Development
Two new high temperature robust substrates, LCM29 and MM1, have been discovered. These materials exhibit low creep and excellent strength at high temperature. In addition, a new suite of high flux OTM materials has been developed with thermal expansion characteristics that are compatible with the new high temperature substrates. This new portfolio of substrate and membrane materials is key to developing high performance, long life OTM elements.

Task 2, Composite Element Development
Composite elements based on the two new substrates, LCM29 and MM1, and the advanced OTM materials have been fabricated and tested in disk reactors. Both systems have survived life tests that include multiple thermal cycles and extended operation (over 500 hundred hours) at extremely high temperatures, 1.1TT. Work is now focusing on developing and optimizing the element architecture to maximize oxygen flux and durability. Several new element architectures now under development have survived multiple rapid thermal cycles in an oven thermal cycling test. These designs will be evaluated under full flux conditions in the next quarter.

Task 4, Reactor Design and Process Optimization
Proprietary engineering studies evaluated the impact of porosity, tortuosity and wall thickness on flux rate. Design ranges for tube internal diameter, porosity, tortuosity and material creep rate were derived that satisfy both creep/buckling lifetime targets and oxygen flux targets.

A novel reactor design concept was modeled. This system offers lower capital cost, improved operability, and flexibility to produce hydrogen as well as syngas for FTGL applications.

A new high pressure P-0 rig has been commissioned and operated at BP. A dense LCM1 tube performed well at the extreme conditions of 2.2TP and 1 TT.

Task 8, Fuels and Engine Testing
SCTE evaluations of four fuels were completed: 1) No.2 diesel, 2) FT diesel, 3) an ultra-low sulfur (ULS) petroleum diesel and 4) the same ULS diesel with BP oxygenate blend to 10% oxygen. The test focused on the four modes of the HDFTP emission certification cycle (4, 6, 7, 8) considered to be the most significant contributors to air emissions. The FT diesel showed significant reductions in NOx and unburned hydrocarbon for all four test modes and operating conditions. Soot reductions were achieved for modes 6 and 7 and for most of the operating conditions in 4 and 8.
The effectiveness of a BP oxygenate (BPO) was evaluated in a ULS fuel blended to a 10% level of chemical oxygen. The oxygenated fuel showed significant reductions in soot and NOx at all modes and operating conditions tested. However brake specific fuel consumption increased due to the lower heating value of the fuel and perhaps other inefficiencies. More tests are planned at intermediate levels of oxygen.

The Nuvera fuel cell program was completed. The second phase of this program evaluated effect of three fuel candidates for transportation fuel cells: 1) a California Phase II RFG, 2) a GTL naphtha and 3) a GTL naphtha with BPO blended to 1.74% chemical oxygen. The BPO showed significant reductions in both start-up and steady state NOx levels in comparison to both the GTL naphtha and the RFG. The GTL naphtha was slightly better than the RFG in CO and slightly worse in THC.

Task 10, Project Management
The project remains under budget, but behind schedule in certain tasks.
All reports and briefings were completed on time. Some delays were incurred due to a 5 month hiatus between completion of Budget Period 1 and approval for Budget Period 2. More recently, availability of BPO for fuel blending has impacted schedule. Most tasks should be brought back on schedule in 2003.

2.0 Introduction

The DOE's Office of Fossil Energy created strategic partnerships targeted at the development and verification of advanced fuel-making processes that utilize fossil feedstocks. These processes will enable the production of ultra-clean transportation fuels that improve the environment, while also expanding and diversifying the fossil resource base. In response to the DOE's solicitation for research and development leading to the production of ultra-clean transportation fuels from fossil resources, Cooperative Agreement number DE-FC26-01NT41096 for work entitled "Development of OTM Syngas Process and Testing of Syngas-Derived Ultra-clean Fuels in Diesel Engines and Fuel Cells" was awarded to Praxair.

The objectives of this project are: (1) develop an advanced syngas technology, based on Oxygen Transport Membranes (OTMs), that will provide a step change reduction in the cost of converting natural gas to a spectrum of liquid transportation fuels and thereby improve the prospects for meeting vehicle emissions targets with cost competitive ultra clean transportation fuels (UCTFs); (2) evaluate the performance of, and emissions from selected syngas-derived UCTFs in advanced vehicle propulsion systems, including advanced diesel engines with post treatment and fuel cells; and 3) develop an optimized UCTF/diesel engine/exhaust after treatment system capable of meeting 2007 emission regulations.

The program will follow a systems approach as shown below, encompassing natural gas pre-treatment, syngas generation, liquid fuel production, product work-up/blending, and validation of the UCTF in engine tests including aftertreatment of emissions.

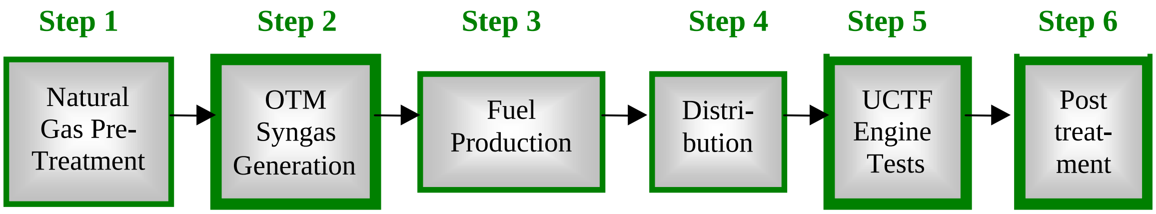

Systems Approach to UCTF

The 60-month project includes three parallel development or testing programs: 1) OTM syngas reactor and reactor components, OTM element fabrication and OTM syngas process development; 2) testing and co-optimization of UCTF in International Truck and Engine advanced diesel engines with exhaust post treatment; and 3) emission testing of UCTFs in a Nuvera transportation fuel cell power system. Performance objectives include:

- OTM Syngas Technology: lower capital costs, lower operating costs, lower emissions and smaller footprint compared to conventional syngas plants.
- UCTF in Advanced Diesel Engines: co-optimized system of syngas derived UCTF, diesel engine and post treatment technology targeting proposed 2007

regulations for light and medium duty engines i.e. diesel fuel sulfur < 15 ppm; light duty engine emissions: NOx < 0.2 g/mi, PM < 0.01 g/mi; and heavy duty engines NOx < 0.2 g/mi and PM < 0.02 g/bhp. UCTF should enable compliance with these objectives and/or lower vehicle costs.

- UCTF in Nuvera fuel cell system: lower air emissions (on a per mile basis) based on UCTF properties such as ultra low sulfur, high aliphatic content and oxygen content.

The program has 10 major tasks, seven of which are focused on syngas technology development, one task is devoted to fuel and engine testing and optimization, one task addresses the marketing and commercialization of an UCTF system, and the final task is for program management and cost control.

The Cooperative Agreement was signed by the DOE's Contracting Officer on May 21, 2001. This Topical Report includes results and discussions for work conducted November 1, 2001 through December 31, 2002.

3.0 Progress and Results by Task

3.1 Task 1: Materials Development

3.1.1 Goal - Task 1

The Recipient shall fabricate, test and characterize OTM film and substrate materials with goal of developing a more robust and cost effective OTM element in comparison to the lead candidate material, LCM1.

3.1.2 Experimental - Task 1

The experimental facilities and methods in Task 1 were described in detail in the Topical Report for Budget Period 1 [Ref. 1].

3.1.3 Results and Discussion – Task 1

The goal of this task is to develop superior materials for fabricating OTM elements. The approach is to focus on two subsets of materials, substrate materials and oxygen transport membrane (OTM) materials, for building composite or laminated elements. The substrate provides a robust foundation for the thin film OTM layer. Key characteristics of the substrate are: high temperature strength, creep resistant, stability in both oxidizing and reducing atmospheres and low reactivity with the OTM materials. The substrate does not have to conduct oxygen ions, but must be sufficiently porous to allow gas species to diffuse to the OTM membrane surface. Thus strength and permeability of the substrate material in porous form are equally important.

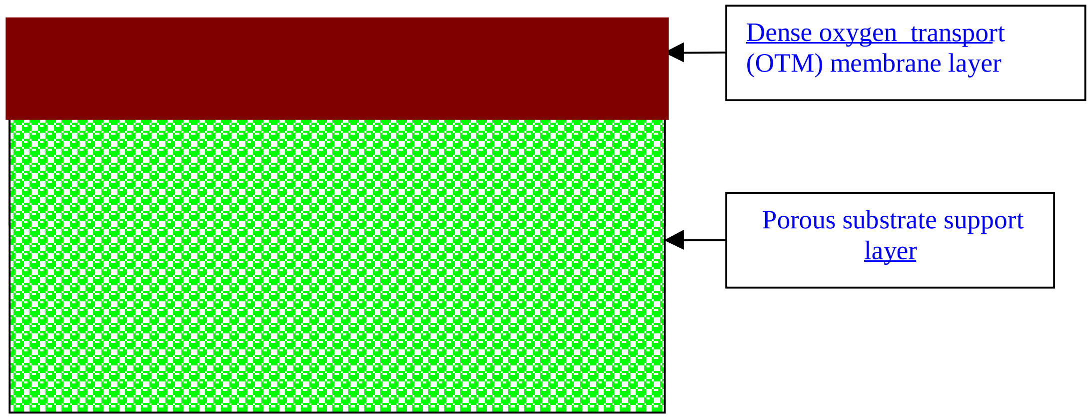

Figure 1: Schematic of a composite OTM

The OTM layer does the work of separating oxygen from air as shown in Figure 2. The dense OTM layer must seal the porous substrate, withstand a pressure differential of 15 to 40 bar and conduct oxygen. The key characteristics of OTM materials are oxygen ion and electronic conductivity (usually measured together and reported as oxygen flux), high temperature stability under both oxidizing and reducing conditions, high temperature strength, volumetric expansion or contraction in response to oxygen partial pressure and high temperature creep. Creep is less important because a proper substrate should provide the required high temperature strength and rigidity.

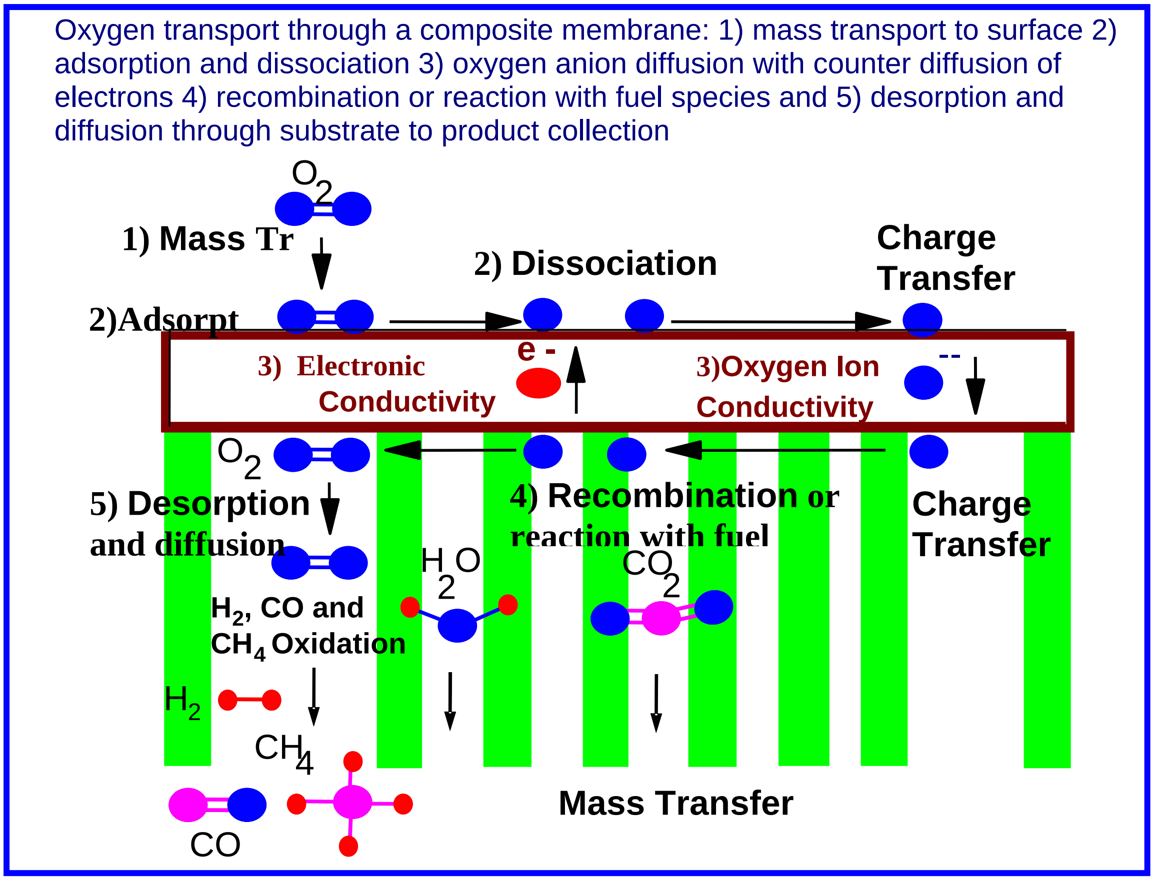

Oxygen transport through a composite membrane: 1) mass transport to surface 2) adsorption and dissociation 3) oxygen anion diffusion with counter diffusion of electrons 4) recombination or reaction with fuel species and 5) desorption and diffusion through substrate to product collection

Figure 2: Oxygen transport mechanism through an OTM composite element

The composite element, made of at least two dissimilar materials, must be capable of withstanding rapid changes in temperature and oxygen partial pressure to survive start-up, shutdown or other planned or unplanned process upsets. Ideally both the substrate and membrane materials would change volume in response to temperature in exactly the same way (or not at all) so that stresses caused by thermal expansion are minimized. Thus another important physical property of both membrane and substrate materials is the thermal expansion coefficient (TEC), measured by a dilatometer, over the temperature range of interest.

In Task 1 several new substrate and OTM materials have been developed that meet proprietary criteria for performance, durability and mutual compatibility. Results of this work are discussed below. In addition, another class of substrates materials, designated MM, do not require material development, but require development of compatible OTM materials and an architecture that will permit high oxygen flux while retaining high temperature strength and creep resistance. The development of these MM compatible OTM materials is included in Task 1. However development and testing of the MM substrate and MM composite systems are reported in Task 2, Composite Element Development.

3.1.3.1 Substrate materials

Twenty substrate materials (LCM 7-9, 11, 12, 21-31, 36, 41-43) were either made in-house or obtained from outside sources and evaluated. In 1Q02, LCM29 was selected as the primary substrate candidate. Subsequent work focused on characterization and optimization of this material.

3.1.3.1.1 High Temperature Creep Rates of Substrate Materials

Creep rates as a function of temperature for a number of substrate and membrane candidates are plotted in Figure 3. The red diamonds, A and B, designate target creep rates for a high temperature scenario (1.1TT) and the target temperature scenario (TT), respectively. The open blue squares show the creep rate of a porous LCM29; the dark blue squares are creep rates of dense samples of LCM29. The lines through these data show that porous LCM29 meets the TT target creep rate (within the error of the measurements) and dense LCM exceeds the creep requirements for TT. However neither dense or porous LCM meet creep targets for the extreme temperature case, point A. Note that the creep rates for these materials are so low, that very high temperatures and compressive loads must be used just to obtain a measurable rate within a reasonable time frame (~ 1 to 3 weeks). For dense LCM29, no creep rate could be measured at the target temperature, TT; rates at TT are extrapolated from higher temperature measurements. The low creep rate of LCM29 is one of the main reasons for selecting it as the prime substrate candidate. It is at least 2 to 3 orders of magnitude more creep resistant than LCM1.

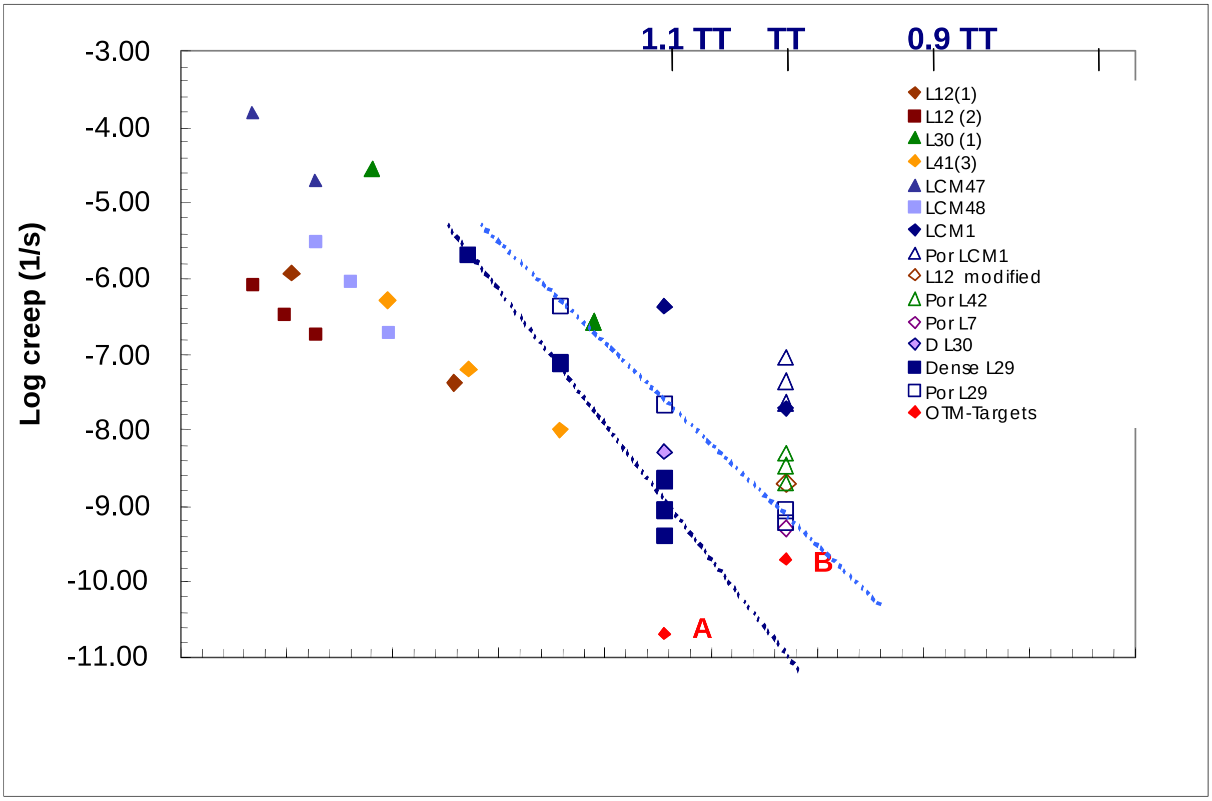

Figure 3: High temperature creep rates of substrate and membrane candidates

3.1.3.1.2 Thermal and chemical expansion of substrate materials

Thermal and chemical expansion behavior of both substrate and membrane materials as a function of temperature and oxygen partial pressure must be known to engineer a robust, low stress, composite element. LCM29 thermal expansion coefficient (TEC) is reported below in Table 1. It was discovered that LCM29 exhibited high volumetric expansion when subjected to low oxygen partial pressures at very high temperature, 1.1TT. Variations of LCM29, LCM 26 and 27, were fabricated and tested. Both of these materials reduced the chemical expansion by a factor of 10 with only a small impact on TEC. These materials will probably replace LCM29 as the substrate of choice for very high temperature applications. LCM23 was also found to have good high temperature chemical expansion behavior. However this material has other issues which preclude its selection as a substrate candidate at this time.

Table 1. Thermal and chemical expansion behavior of substrate candidates

Composition	**TEC 100-1.1TT (10^{-6}/K)**	**CEC at 1.1TT Air- 90CO/10CO_2 %**
LCM29	11.9±0.3	0.21
LCM26	11.6	0.02
LCM27	11.6	0.02
LCM23	11.5	0.00

3.1.3.1.3 Substrate fracture strength and slow crack growth

Fracture strength at high temperature is an important property for substrate materials because the membrane system must withstand high external pressure gradients and internal stresses created by thermal and chemical expansion. Slow crack growth has been measured at the target temperature (TT) in air for LCM29 in a 4-point bend apparatus by varying the displacement rate (and thereby the load rate) according to ASTM C1465. The sample sizes were 3x4x45mm and the fracture strength was measured at the deflection rates of 50, 5, 0.5, 0.05 mm/min. The slow crack parameters n= 68.2 and D=208.7 were calculated from the data illustrated in Figure 4. The data indicate that slow crack growth is negligible under the measurement conditions. However, slow crack growth may be different under reactor conditions. To be sure that slow crack growth is not a problem; the measurements should also be done in environments simulating reactor conditions on the fuel side. For example, elevated steam concentrations have been reported to increase the slow crack growth rates in other high temperature ceramics.

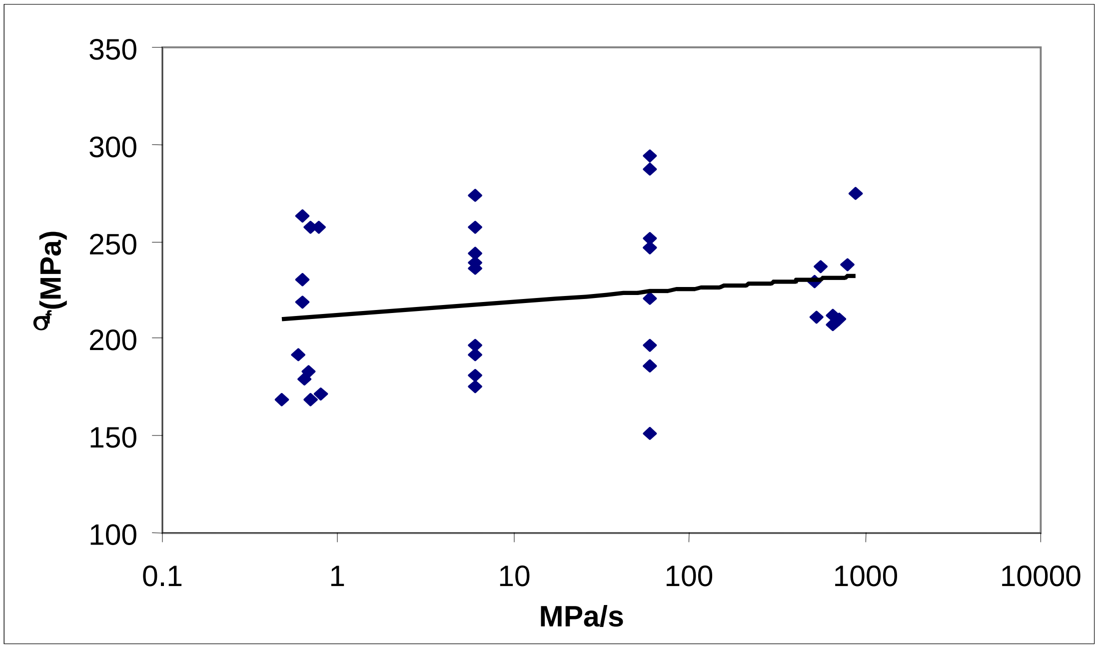

Figure 4: Fracture strength as a function of load rate for LCM29

3.1.3.1.5 Fracture toughness and hardness

Fracture toughness and hardness has been measured for a number of different materials by the Vickers indentation method. These properties are important for gauging the ability of a material to withstand physical shock and resist cracking. The data are summarized in Table 2. All the measured perovskites have fracture toughness values in the region 0.7-1.1 MPam$^{0.5}$, which is very low. The calculated fracture toughness values depend on the estimated Young's modulus and will increase somewhat if the Young's modulus is higher than estimated.

Table 2. Hardness and Fracture Toughness Data Measured at Statoil by the Vickers Indentation Method

Sample (wt%)	Average hardness [GPa]	Fracture toughness [MPa m$^{0.5}$]
LCM20	6.5 (0.5)	0.95 (0.14)*
LCM32	7.1 (0.1)	0.68 (0.06)*
LCM33	7.6 (0.2)	0.76 (0.11)*
LCM16	7.0 (0.3)	1.03 (0.18)*
LCM16 (another batch)	4.5 (0.6)	1.15 (0.26)*
LCM34	5.7 (0.4)	1.02 (0.12)*
LCM35	5.7 (0.3)	0.85 (0.34)*
LCM30	10.6 (1.5)	2.0 (0.5)**
LCM9	8.7 (0.2)	1.2 (0.1)**
LCM29	**8.8 (0.4)**	**> 10**

Estimated Young's modulus of 110* and 200** GPa.

The substrate material candidates LCM12, LCM30, and LCM9 all have fracture toughness values in the range 1-2 $MPam^{0.5}$ (similar crack lengths as the perovskites but higher Young's modulus). The materials which stand out with remarkably higher fracture toughness are LCM25 and LCM29, for which the fracture toughness could not be measured by the Vickers indentation method even with a 30 kg load. Fracture toughness values for LCM29 above 10 $MPam^{0.5}$ have previously been reported.

3.1.3.1.6 Phase stability of substrate materials

A number of different LCM29 samples were examined by XRD before and after heat treatment for 800 h at 1.1TT in order to investigate the phase stability of the materials. XRD analyses of the samples are given in Table 3.

Table 3. XRD analyses of samples before and after heat treatment at 1.1 TT*

Sample	Before*	After*
LCM 29 (Supplier 1)	x	Xx
LCM 29 (Supplier 2)	x	Xxx
LCM29 – variant 1	0	0
LCM29 –variant 2	0	0
LCM29 – variant 3	0	0

* One x marks a trace amount of second phase, the amount of second phase increases with number of x's. Zeros denote no second phase

The data shows the amount of second phase in LCM29 can vary by supplier, and there is some increase in this phase with a high temperature heat soak. However, there is no evidence that other, more deleterious phases are formed. Also, some variations of LCM29 result in no second phase with excellent high temperature stability.

3.1.3.2 Membrane materials

The main objective of the membrane development work is to find robust high flux OTM materials that are compatible with the lead substrate candidates, such as LCM29 and MM1. A systemic approach has been taken that focuses on the LCM_{ABC} system as shown in Figure 5. The points on the tertiary diagram show the compositions that have been synthesized. Each new material is measured for oxygen flux, electrical conductivity, thermal and chemical expansion. Proprietary correlations and trends have been developed that show how these properties are affected by compositional changes, such as atomic substitutions or variations in the A and B sites of the base perovskite material. (Note: A, B and C materials in Figure 5 do not necessarily correspond to the ABO_3 general formula for a perovskite.)

Results of this extensive material synthesis and testing work are summarized in the following sections.

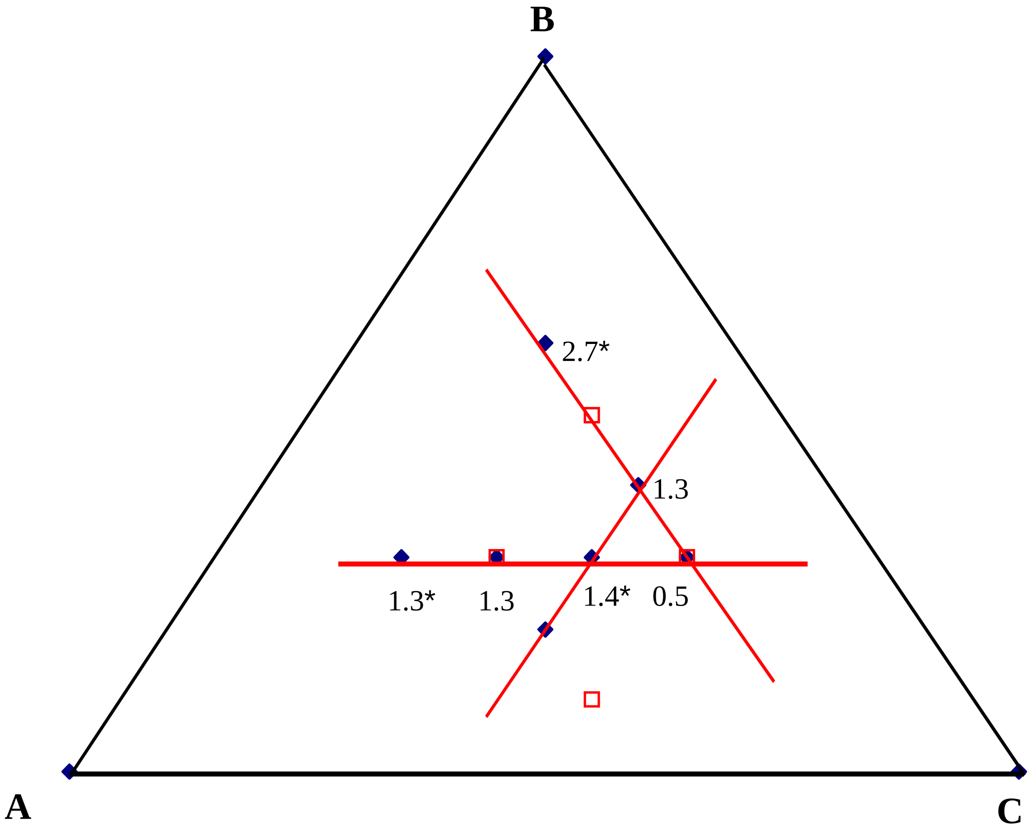

Figure 5: Synthesized compositions & relative flux results in the $\mathrm{LCM}_{\mathrm{ABC}}$ system

3.1.3.2.1 Oxygen Flux Testing of New Membrane Materials

Oxygen flux tests of a number of membrane material candidates are shown in Figure 5. All of these tests are of dense disk, ~ 1 mm thick, using a standard gas mixture, at the target temperature, TT. The fluxes are normalized to the target flux for a dense disk, TFd. Thus a flux of 2.7 means the flux is 2.7 times the target flux for a dense disk. Note that flux doubles as B increases relative to C or A. For reference, LCM1 flux is ~ 4.3 TFd.

The impact of A/B ratio was also studied for LCM 16. Flux versus A/B ratio is plotted below in Figure 6. Small variances in the A/B ratio can have a very significant impact on flux of a material. A sharp optimum is found exactly at A/B = 1.0

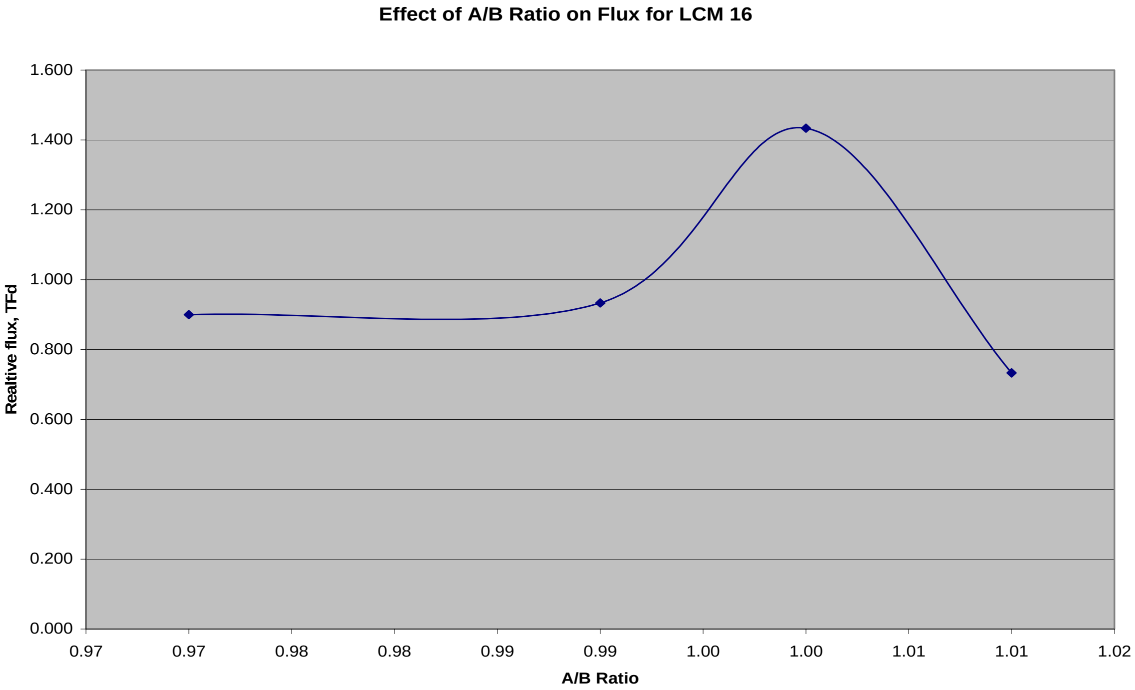

Figure 6: Effect of A/B ratio on the flux of LCM16

In addition to single phase OTM materials, multiphase mixtures of OTM materials were prepared and tested. Fluxes of three mixtures are reported below in Table 4. The goal is to develop materials that at least achieve the minimum flux criteria of 1.0TFd, while improving other properties such as TEC, chemical expansion or strength.

Table 4. Oxygen flux of dual phase materials

Material	70% H2 / 30% CO2	85% H2 / 15%CO2
LCM38	0.87TFd	0.87TFd
LCM39	1.37TFd	1.8TFd
LCM45	0.33TFd	

3.1.3.2.2 Thermal and chemical expansion of membrane materials

Thermal and chemical expansion of both the single phase and dual phase materials were measured using dilatometry. The goal is to develop membrane materials that closely match LCM29, MM1, or MM2 in thermal expansion properties while minimizing the chemical expansion at low pO_2, and achieving a flux of at least 1.0TFd. Several materials have been found that meet these criteria for LCM29 and MM1 as shown in Table 5. For the substrates LCM26 and 29, membrane materials LCM38 and 46 provide fairly good matches. For the substrate MM1, membranes LCM15 and 20 provide excellent TEC match, marginal chemical expansion (CE) and good flux properties.

Table 5. Summary of Expansion and flux properties for lead candidate materials

Material	TEC to 1.1TT (in air) $10^{-6}/^{o}K$	CE @ 1.1TT Air to Fuel, Vol. %	Flux @ TT TFd
LCM29 (S)	**11.9**	**0.21**	**0**
LCM26 (S)	**11..6**	**0.02**	**0**
LCM15	**15.2**	**0.11**	**1.35**
LCM16	15.8	~0.14	1.41
LCM20	**15.8**	**0.09**	**1.75**
LCM38	**11.7**	**TBD**	**0.87**
LCM39	13.5	0.12	1.80
LCM46	**12.6**	**0.06**	**TBD**
LCM1	18.1		4.3
MM1 (S)	**15.3**	**0.0**	**0**

(S) = substrates TBD = To be determined

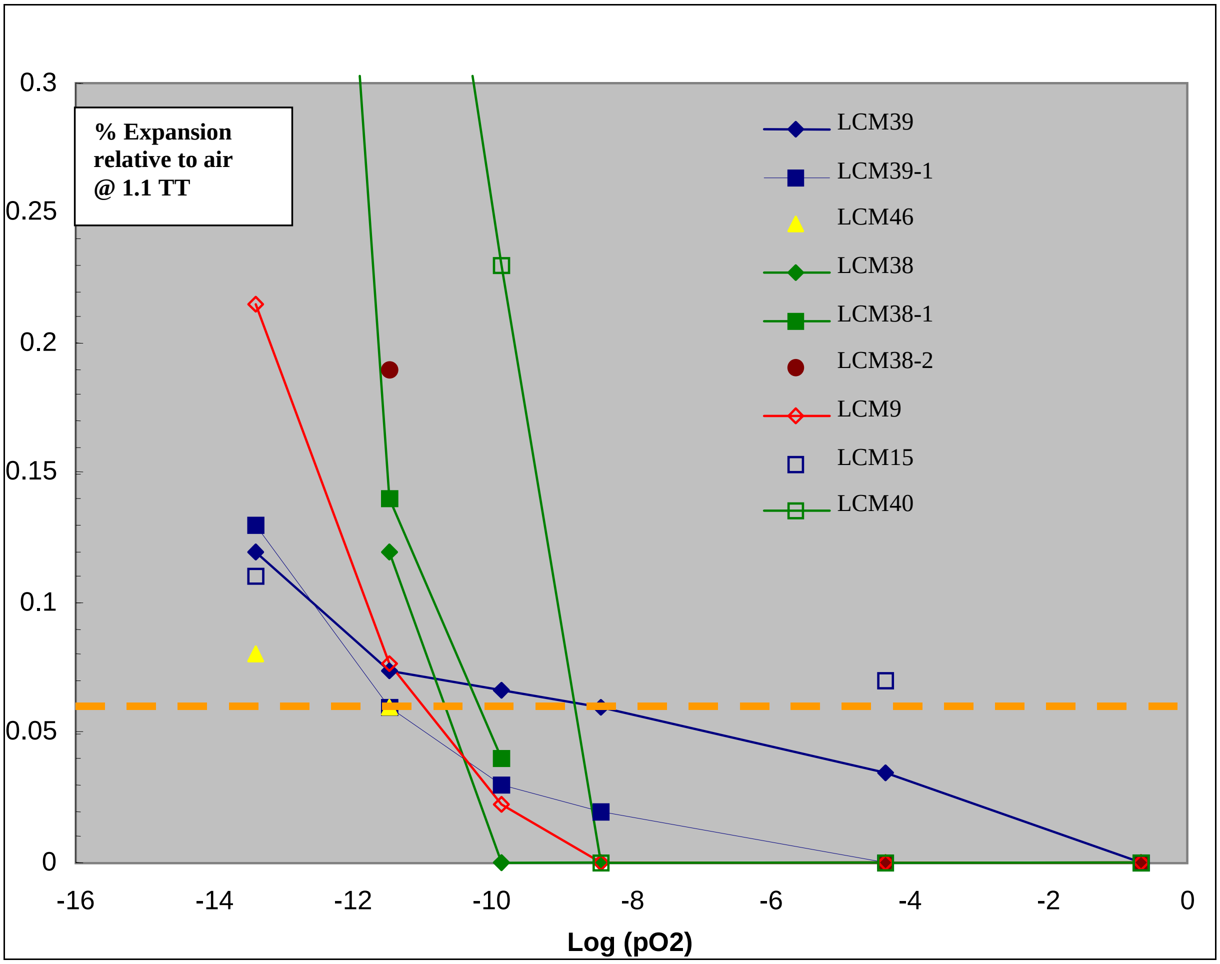

Figure 7: Chemical expansion of substrate and membrane materials versus pO2

The chemical expansion shown above is the change in volume recorded when a sample at 1.1TT is switched from air to a fuel gas containing 75%CO and 25% CO2. Chemical expansion generally increases as oxygen partial pressure decreases and temperature increase. The effect of oxygen partial pressure at 1.1TT is illustrated in Figure 7 for a number of membrane and substrate materials. This plot also shows that minor variations in composition of the component materials (LCM39 vs. 39-1; LCM 38 vs. 38-1, 38-2) changes can have significant impact on chemical expansion behavior. Thus at lower temperature and higher oxygen partial pressure chemical expansion may not be an issue for the lead candidates. And with some minor manipulation, it is believed that all of the key physical properties, CE, TEC and oxygen flux, can be improved further.

3.1.3.3 Interaction of Substrate and Membrane Materials

A robust composite system must be chemically stable over long periods of time. At very high temperatures adjacent layers of dissimilar materials can chemically react or inter-diffuse. Other phases can be formed that may physically weaken the substrate materials or adversely affect the membrane's ability to transport oxygen. However some reaction or diffusion is desirable to ensure a strong bond between adjacent layers.

Chemical reactivity of membrane and substrate candidates was determined by preparing diffusion couples of selected pairs of materials. The membrane candidates studied were LCM16, LCM20 and LCM40 versus substrate candidates LCM7, LCM9, CLM36, LCM30 and LCM29. The couples were exposed to stagnant air for 100 hours at 1.2 and 1.3TT. XRD was used to identify secondary phase formation. SEM and EDS analysis were also used to examine polished cross sections of selected samples sputtered with carbon. Results show that LCM16 was the least reactive of the membrane candidates and LCM36 was the least reactive of the substrate candidates.

Table 6. High temperature interaction test results

Material	LCM40	LCM20	LCM16
LCM36	Surface color chance **Diffusion**	Good adherence. **Diffusion**	No visible rx. **Diffusion**
LCM7	Surface color changed **Diffusion**	Good adherence. **Diffusion**	No visible rx. **Diffusion**
LCM9	**Secondary phases** **Diffusion**	Good adherence. **Secondary phases** **Diffusion**	No visible rx. **Diffusion**
LCM30	. **Secondary phases** **Diffusion**	Good adherence. **Secondary phases** **Diffusion**	**Secondary phases** **Diffusion**
LCM29	**Secondary phases** **Diffusion**	**Secondary phases** **Diffusion**	**Secondary phases** **Diffusion**

Material interactions of LCM29 with LCM30, LCM8 and LCM 9 were also studied. No visible reactions were observed for any of the diffusion couples after 100 h at 1.3TT.

3.2 Task 2: Composite Development

3.2.1 Goal - Task 2

Develop advanced composite OTM elements and the techniques for fabricating these elements at the bench scale. The goal is to develop robust, low cost, high flux elements that can survive multiple temperature and fuel composition cycles while maintaining structural integrity at target pressure differentials.

3.2.2 Experimental - Task 2

The experimental facilities and methods in Task 2 were described in detail in the Topical Report for the Period Jan. 1 through Oct. 31, 2001 [Ref. 1].

In addition, an oven thermal cycle test is being employed to test durability of the composite systems subjected to rapid changes in temperature. The procedure is:

- Heat the sample in air from room temperature to TT at $1^{O}C$/minute.
- Hold the sample at TT in air for 1 hour.
- Cool at $1^{O}C$/minute.
- Leak test sample by applying a differential pressure up to 50 psi and measuring the gas permeability rate, in cc/second. (This may not be performed after every cycle.)
- Repeat.

3.2.3 Results and Discussion - Task 2

In this task, composite elements (disk and tubes) are built using proprietary fabrication techniques and tested. The composite element, shown in Figure 1, consists of a robust porous substrate and a dense oxygen transport membrane. Oxygen flux is primarily controlled by two mechanisms in series: ambipolar diffusion of oxygen across the dense membrane and diffusion of the reaction species through the porous substrate layer. (See also Figure 2) Both material properties, as discussed in Task 1, and element architecture (layer dimensions, pore structure, etc) are important factors affecting the performance and durability of the composite system.

Two types of composite elements are under development: the LCM family of materials and the MM family of materials. Each type requires different fabrication techniques. Both types promise excellent high temperature performance.

3.2.3.1 LCM Composite Systems

Two LCM systems were fabricated and tested. Both systems utilize LCM 29 as the substrate. Each system is discussed below.

3.2.3.1.1 LCM38/LCM29

An LCM 38/LCM29 composite disk was fabricated and cycled in air using the oven cycling procedure. This disk did not exhibit any signs of stress cracking and the layers remained intact. Another 38/29 disk was subjected to a life test that included both thermal and chemical cycles as shown below in Figure 8. The test ran for over 800 hours. The first 24 hours were run at 1.0TT. Gas compositions were changed to reduce the pO2 in steps three steps. Flux increased as pO2 was reduced as expected.

Flux is calculated by two methods and both are shown in the figure as dark blue and mauve. The temperature was increased to 1.1TT for the remainder of the test. This is an extremely high test temperature intended to evaluate OTM syngas conditions in a commercial reactor. The flux increased from ~ 0.3 to ~ 0.5TFc. The flux remained constant for the next 500 hours, showing no significant degradation. Equally important, the fuel leak did not change, indicating the disk did not crack. The disk was then subject to five thermal cycles between 0.65TT and 1.1TT. The fuel leak rate did not change and the flux showed a slight degradation. Finally the disk was subject to a more severe cycling sequence where the end temperature was dropped to 0.2TT and the gas composition was switched to nitrogen. Under these conditions the disk developed a leak and the run was terminated after five severe cycles and over 800 hours at high temperature operation. Post mortem of the disk showed no deleterious interactions between the layers, but some cracks were formed in the membrane. It was also concluded that flux was inhibited by the architecture, which can be readily improved.

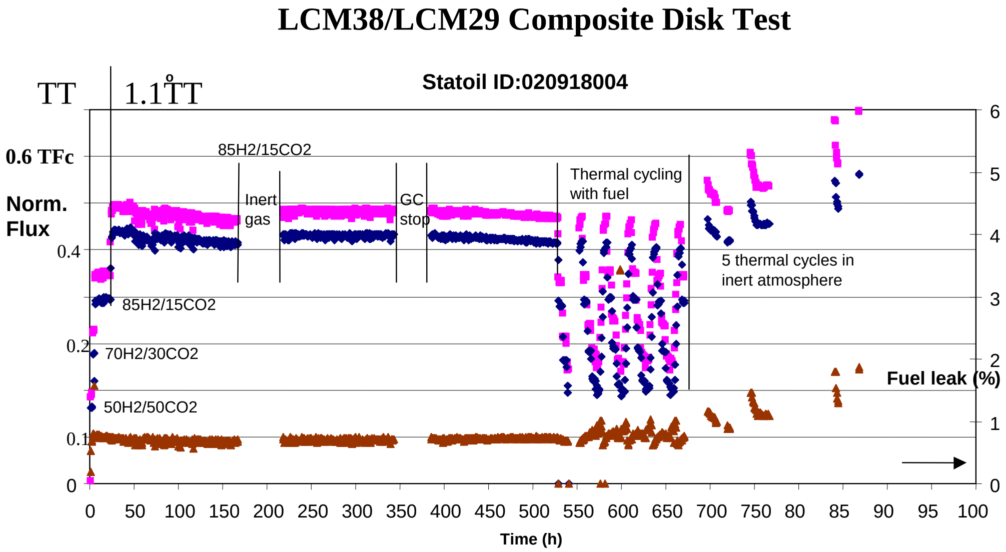

Figure 8: Composite disk LCM38/LCM29 life and cycle test results

3.2.3.1.2 LCM15/LCM29

A composite disk comprised of LCM15 and LCM29 was fabricated by improved techniques. This disk is currently the subject of a life test. At 1.0TT the disk has achieved a steady flux of ~ 0.8TFc for over 300 hours as shown in Figure 9. The leak rate has not increased and the test is on-going. This demonstrates that learnings from the prior life test were successfully applied and resulted in a doubling of the flux with no apparent degradation in the robustness of the disk. (Compare fluxes at 1.0 TT)

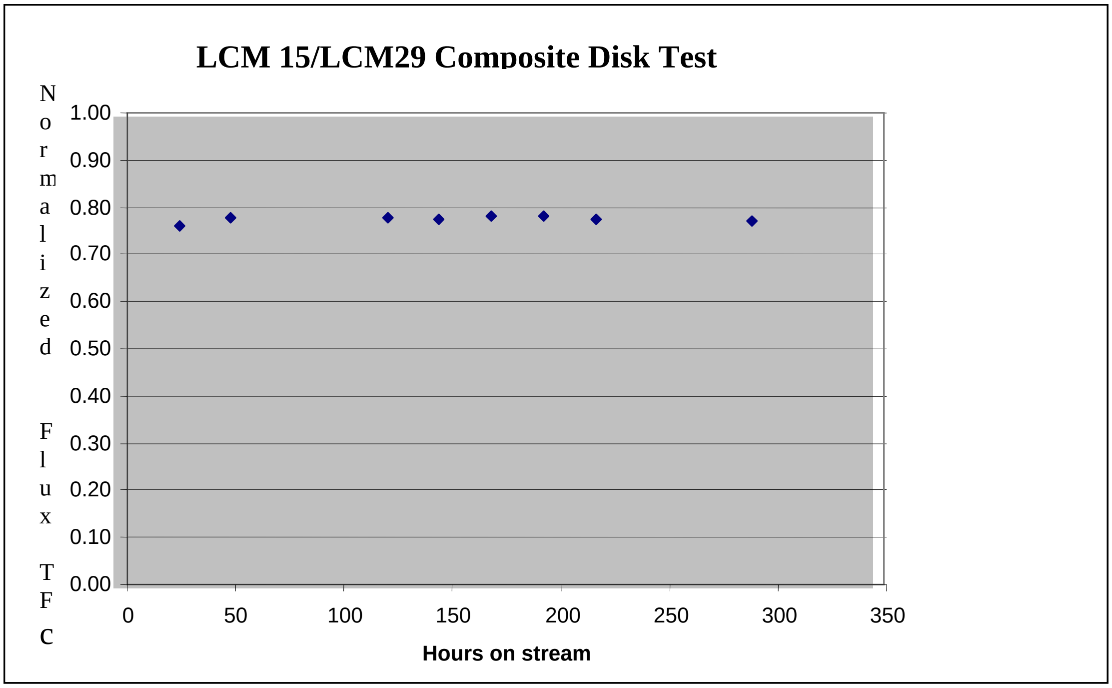

Figure 9: Composite disk LCM15/LCM29 life test results (in-progress)

3.2.3.2 MM Composite Systems

A second type of substrate, designated MM, is being explored that could provide certain fabrication advantages over our LCM materials. These materials are commercially available; work is focused on finding compatible membrane materials and a suitable architecture. Several membrane materials have been identified with similar thermal expansion properties, as shown in Table 5. Test disks of three systems have been fabricated using in-house proprietary techniques. The MM1 and MM2 systems are targeted for very high temperature operation, which are expected in an OTM reactor. The MM3 system is a lower temperature material more suitable for a hydrogen application. Each of these systems is discussed below.

3.2.3.2.1 LCM1/MM3 Composite Disk

Three samples of an LCM1/MM3 composite were fabricated utilizing different architectures and techniques. The performance of the discs, designated Disk 1, Disk 2 and Disk 3 is shown in Figure 10. Disk 1 and Disk 2 represents two different techniques while Disk 3 combines both of these techniques. All three disks begin with the same flux off ~ 0.7TFc, then performance rapidly diverges. Disk 2 begins to decline immediately while 1 and 3 appear to behave a bit erratically for the first 150 hours. Disk 1 then begins to decline at ~250 hours while Disk 3 maintains a steady flux for 350 hours. The tests show that the combined techniques are better than either alone, but further improvement is needed to sustain stability.

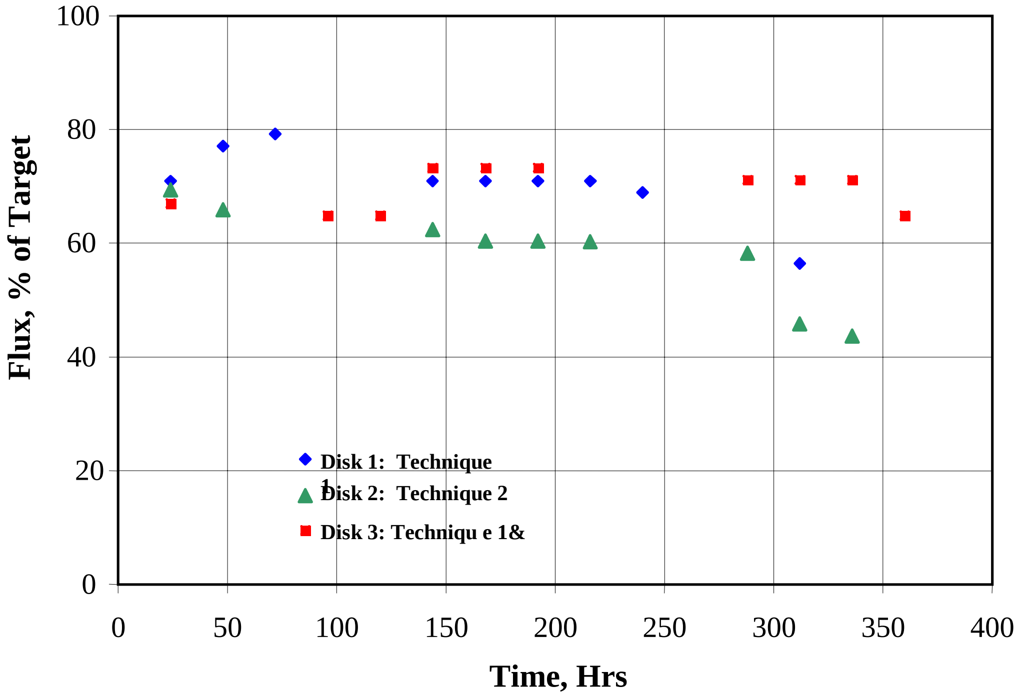

Figure 10: Performance of three LCM1/MM3 Composite Disks

Based on this and other learnings, another disk LCM1/MM3 disc was fabricated and tested in the same manner. Designated Disk 4, its test results are shown in Figure 11. The disk was tested at two temperatures, TT for the first ~ 100 hours and 1.1TT for another 220 hours. The disk was then slowly cooled to obtain flux data over a wider temperature range.

Flux and leak rate are plotted versus time on-stream in Figure 11. Flux is measured by two mass balance techniques; both methods are plotted as shown by the blue and red lines. Leak rate is measured as percentage of total fuel fed to the system. The calculated fluxes are normalized for the leak. (The error of the calculated flux rates will increase as the leak rate increases.)

This test showed that target fluxes can be obtained with this system at 1.1TT. Based on leak rate, the test also shows the system is relatively stable (over 300 hours). The leak rate jumped twice in this test; first when the temperature was increase by 10%, and second time when the system was cooling down. The latter case may be caused by the disk contracting, increasing leakage around the seals.

After the test, the disk was removed and examined by SEM. This disk shows a slight improvement in flux when compared to Disks 1-3 at TT. However, the disk shows a significant improvement in stability, especially given the test was run at the higher temperature, 1.1TT.

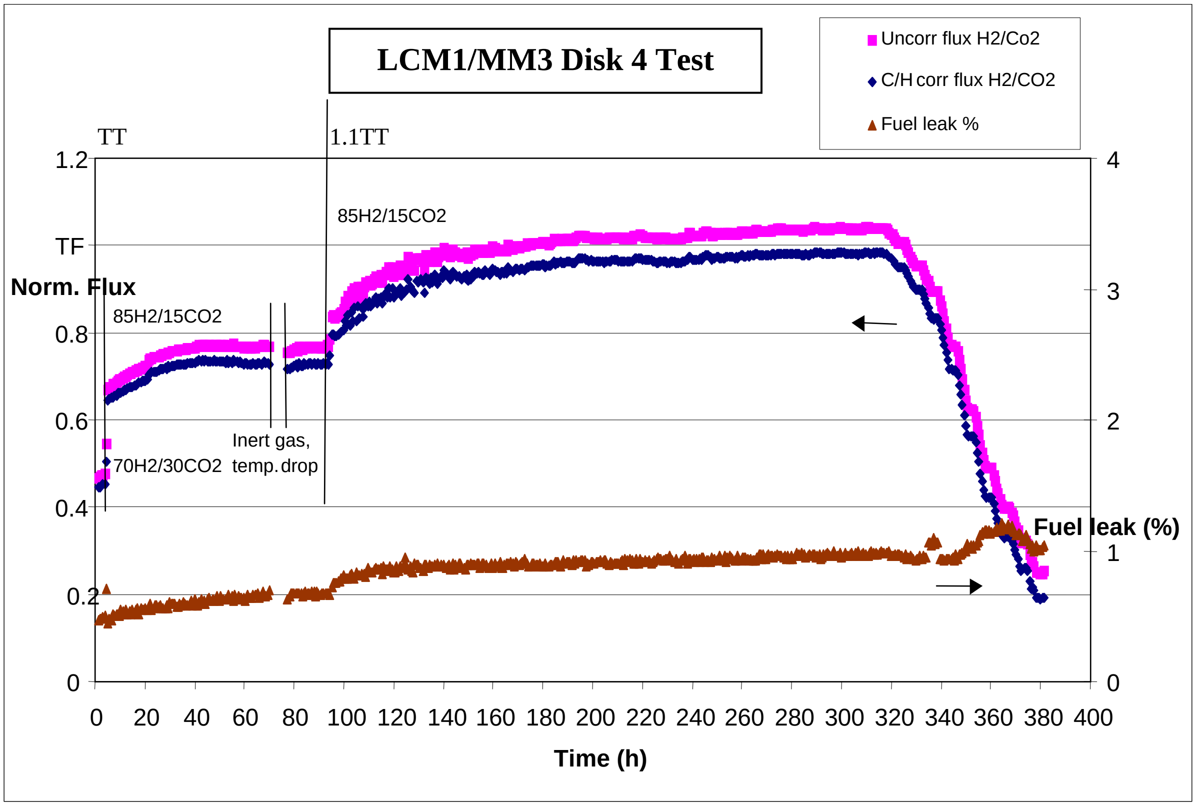

Figure 11: Performance of LCM1/MM3 Composite Disk 4

3.2.3.2.2 LCM1/MM1 System

The LCM1/MM1 system is intended for the very high temperature operating conditions that are expected in an OTM syngas reactor. An LCM1/MM1 disk was fabricated using techniques similar to those used to fabricate LCM1/MM3 Disk 4. This disk, designated LCM1/MM1 Disk 1 was tested for over 2000 hours as shown in Figure 12. The flux and temperature data are plotted versus time for the 2500-hour run. The reported fluxes on the left “Y” axis are relative to the composite target flux, TFc. The disk showed no significant degradation in flux after 2500 hours on stream and 10 thermal cycles. This satisfies a major milestone in demonstrating the viability of these types of systems.

Additional disk tests showed there was no effect of MM1 substrate thickness on flux. Nearly identical fluxes were measured for disks with 1.5 X and 0.5 X the substrate thickness of Disk 1.

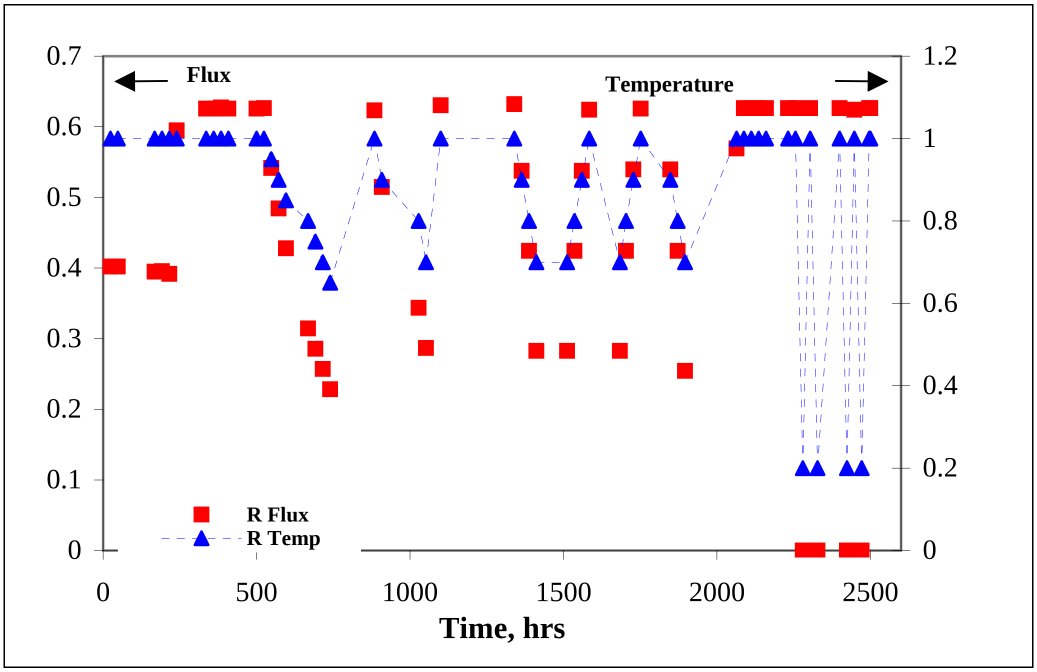

Figure 12: Performance of composite LCM1/MM1 Disk 1

In order to evaluate the effect of temperatures on the flux performance, the composite LCM1/MM1 Disk 1 was tested every 50 degrees from TT to 0.6TT until the flux data could no longer be recorded due to an increase in the leak rate on the air-side. The leak rate increases at low temperatures because the seals contract. The leak usually is abated when the temperature is ramped back up. As shown in Table 7, the flux decreased with temperature. At 0.65TT, the flux remained at 0.23TFc, which is still significant and may be adequate for some other applications, such as hydrogen.

Table 7. Flux test results of LCM1/MM1 Composite Disk 1 vs. temperature

Relative T	Relative Flux, TFc @ 85%H2:15%CO2
TT	0.63
0.95	0.54
0.9	0.48
0.85	0.43
0.8	0.31
0.75	0.28
0.7	0.26
0.65	0.23

Post mortem of the above disk showed some cracking in the dense film. This may have occurred during final cool-down or during one of the last few thermal cycles. Subsequently several architectural improvements for the LCM1/MM1 have been proposed. Two new architectures (Config. 1 and Config. 2) were fabricated and submitted for oven thermal cycle tests. Both test samples employed MM1 as a substrate and LCM1 as the dense membrane. Systems that survive this screening test are then advanced to disk tests, followed by pressurized tube tests.

The permeability test record for LCM1/MM1, Config. 1 is shown below in Figure 13. (The red line is a reference standard used to check the permeability apparatus.) The sample was leak tested before the sample was cycled (0 TC), then after the 3rd, 5th and 11th thermal cycle. In all cases the sample showed zero gas permeability over the pressure differential range tested (0 to 50 psi). This is very encouraging.

LCM1/MM1 Config. 2 is also undergoing thermal cycle tests by the same method. Config. 2 so far has survived one cycle; the test is on-going.

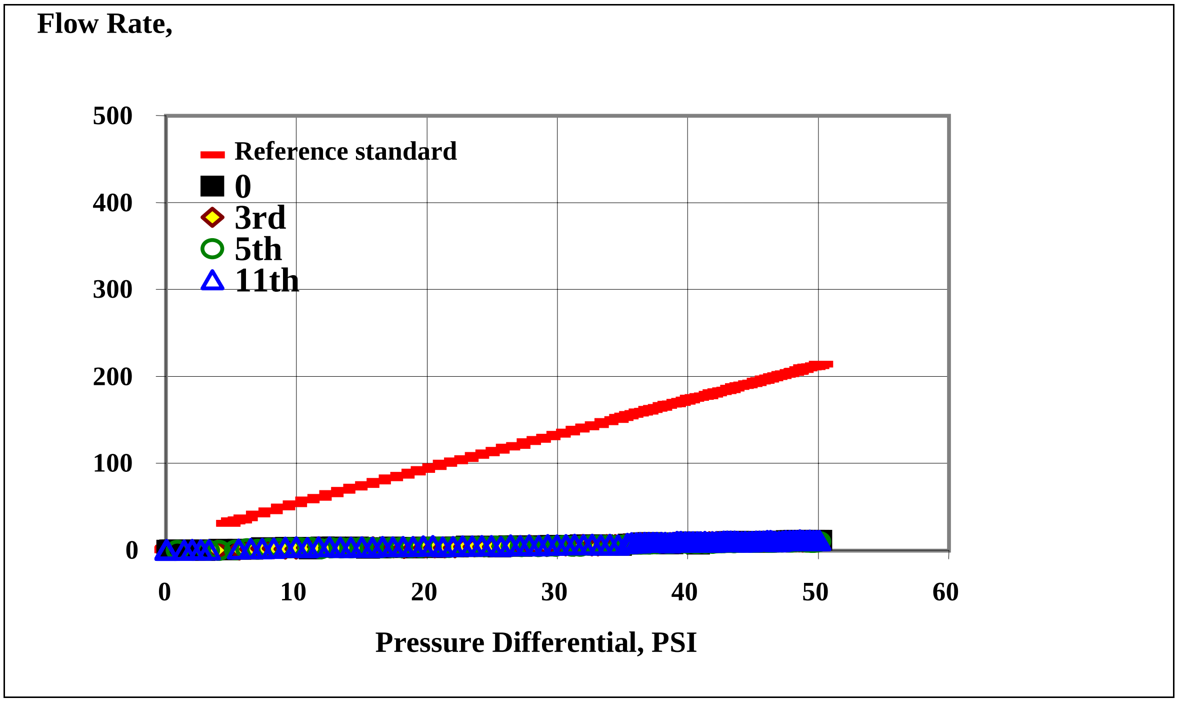

Figure 13: LCM1/MM1 Config. 1 thermal cycle permeability test results

It is expected that these architectural improvements in combination with the OTM material improvements discussed in Task 1, will lead to major advances in both performance and durability in the next program budget period.

3.3 Task 4: Reactor Design and Process Optimization

3.3.1 Goal - Task 4

Develop the commercial OTM syngas process including reactor design and catalyst deployment, reactor components (seals, internals, isolation devices, high temperature tube sheet, etc), and ancillary processes (feed pre-treatment, pre-heat, syngas cooling).

This team shall develop and employ mathematical models to simulate process conditions (reactor flow conditions, kinetics, heat and mass balances) and the mechanical, thermal and compositional stresses on the reactor components and elements. These models will enable evaluation of various conceptual designs and facilitate detailed design and evaluation of preferred options. Task 4 includes the operation of the small bench scale units, P-0, which are used to evaluate small OTM elements (6 inches long) and develop engineering data for reactor scale-up.

3.3.2 Experimental - Task 4

The experimental facilities and methods in Task 4 were described in detail in the Topical Report for the Period Jan. 1 through Oct. 31, 2001 [Ref. 1].

3.3.3 Results and Discussion

3.3.3.1 P-0 Test Results

P-0 reactors are small pressurized rigs capable of testing tubular elements up to 8 inches in length at pressures up to 0.6 TP. One reactor at BP was modified to operate safely at 2.2TP. Results of studies carried out in both types of rigs are discussed below. Except as noted, all P-0 test results are at 0.6TP.

3.3.3.1.1 High Pressure P-0 Test

A high-pressure test was carried out at the BP facility. A dense LCM1 tube was tested at 2.2TP. Flux was measured as a function of pressure and air flow rate. Air flow studies show that very high oxygen removal rates can be achieved at low air flow rates as shown in Figure 14 below.

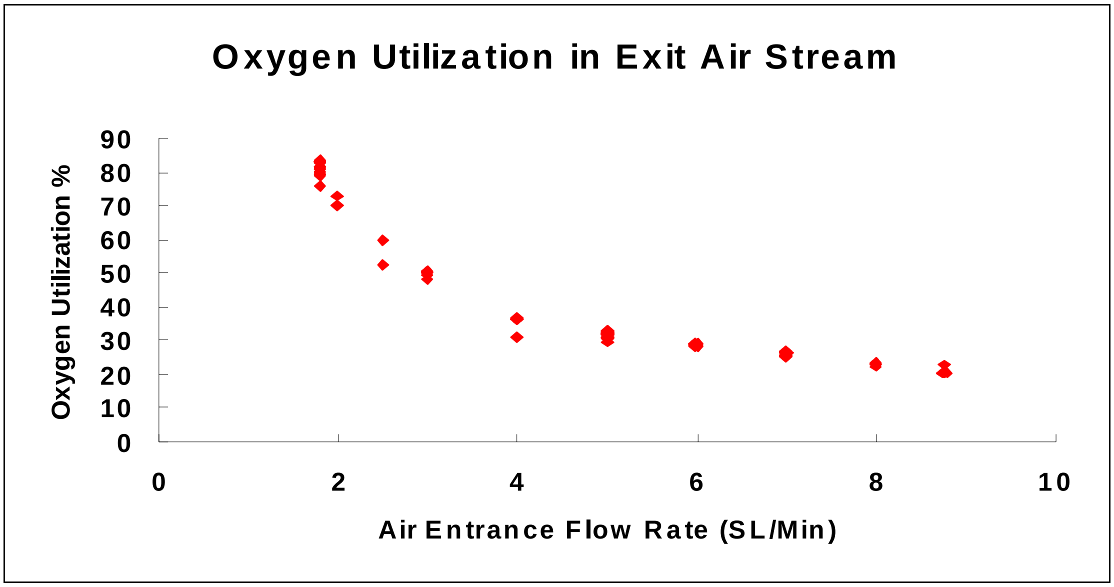

Figure 14: P-0 oxygen utilization test for a dense LCM1 tube at TT

Figure 15 shows the effect of high pressure on flux for the same LCM1 dense tube at TT. These tests confirmed the operability of the BP high Pressure reactor system. The data will be used to validate the P-0 process models.

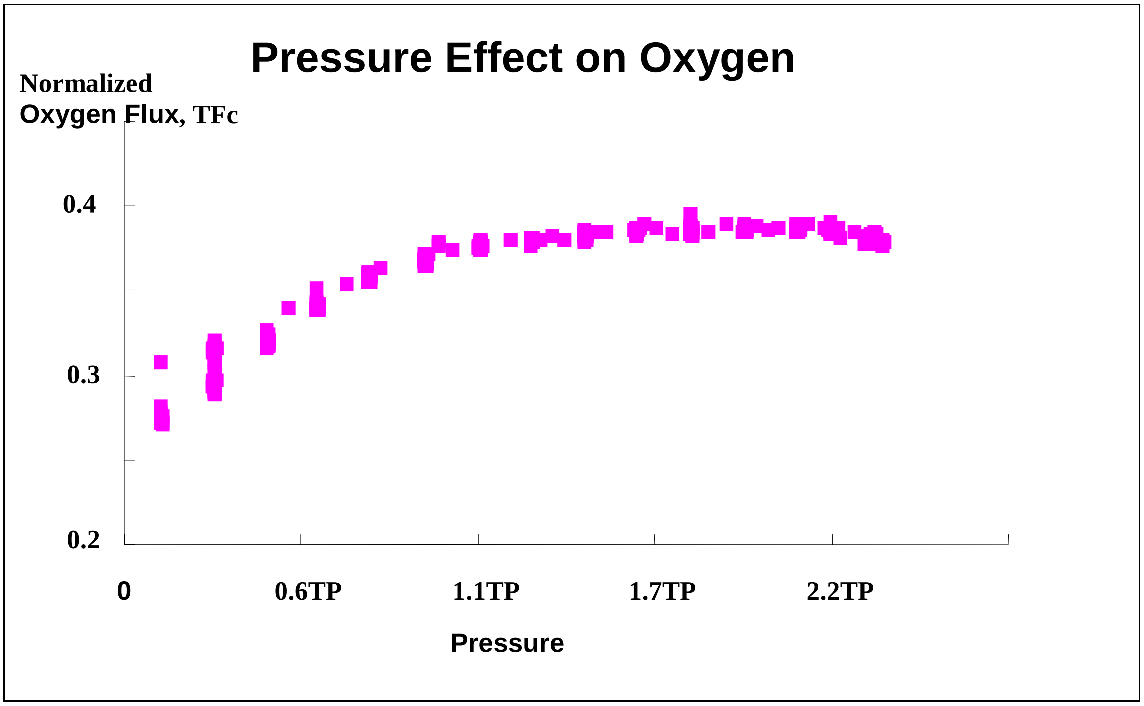

Figure 15: **Effect of pressure on flux in a P-0 reactor with an LCM1 dense tube**

3.3.3.1.2 New Tube Architecture Tests

Four tubes with different architectures (but all of the same LCM1 material) were prepared and tested in the Statoil P-0 rig. Oxygen flux was measured as a function of temperature and air flow rate. Results plotted in Figure 16 show an interesting insensitivity to element morphology--neither dense film nor substrate thickness appear to have a significant effect on the measured oxygen flux of the tube. Flux appears to be affected by airflow rate, suggesting that oxygen diffusion at the boundary layer may be limiting in this particular test rig. These data will be used to validate the fundamental oxygen transport model and the P-0 models.

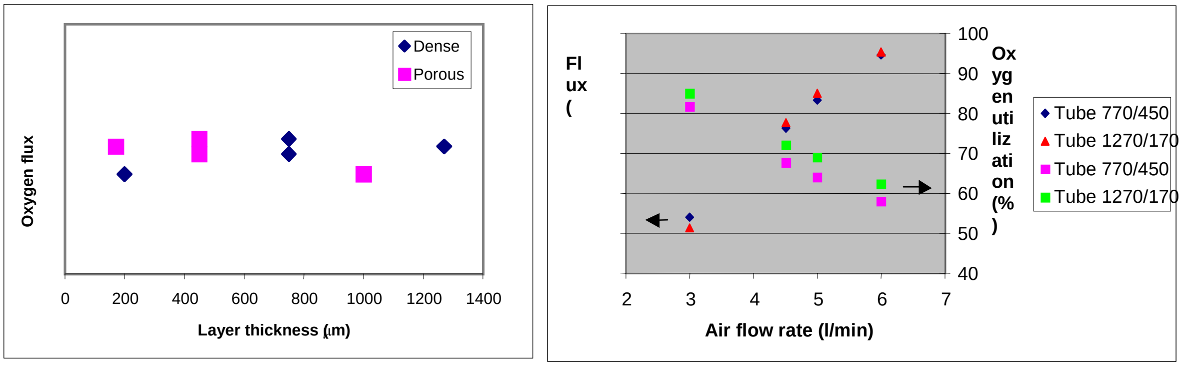

Figure 16: Results of LCM1 composite tube P-0 tests

3.3.3.1.3 LCM1/MM1 Composite Tube Test

An LCM1/MM1 substrate composite tube was prepared and loaded into a BP high-pressure P-0 reactor. Unfortunately the tube developed a leak during heat-up and the test could not be completed.

3.3.3.2 Process and Reactor Design Studies

3.3.3.2.1 Evaluation of a Novel Reactor System

A process study of an OTM reactor to allow use of less expensive was completed. The study showed cost savings of about 18% can be realized. Consequently, the novel reactor design has been adopted as the lead reactor design for the OTM syngas technology.

In addition, it was noted that the operating conditions are also suitable for making hydrogen. Thus, a flexible OTM plant could be envisaged, which could produce syngas for liquids production, hydrogen for fuel, or a combination of the above .

3.3.3.3 Architecture and Process Modeling Results

A proprietary study determined targets for the creep rates of substrate materials by evaluating the effect of element geometric parameters (tube ID and wall thickness) on time to buckle/collapse. Results are presented Figure 17.

The two main factors that affect the time to buckle are the creep rate of the material and the tube geometry (diameter and thickness) as shown in Figure 17. The high creep rate of LCM1 (~10^{-7} s^{-1} at 110% of target temperature) was the main reason last year to focus on thin membranes on improved substrates.

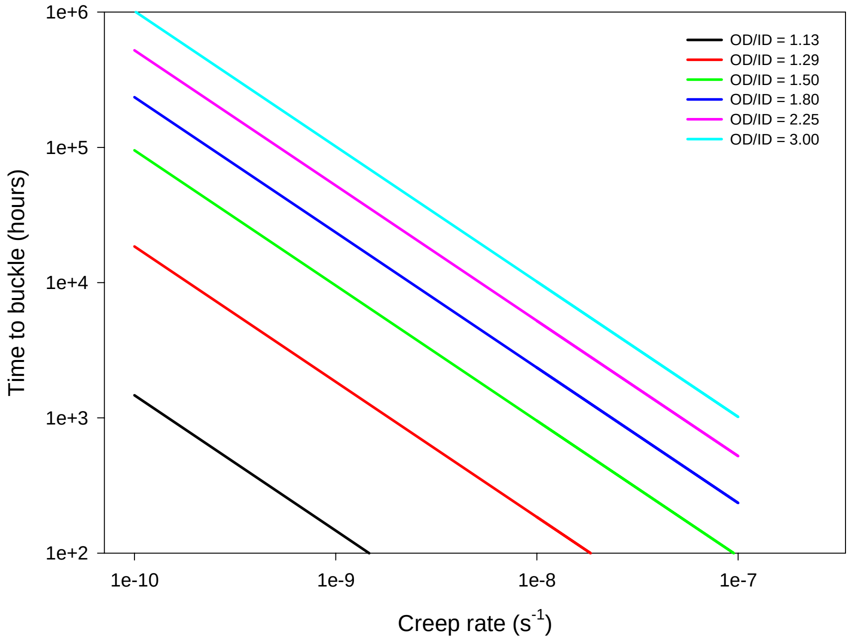

Figure 17: Time to Buckle vs. Tube Geometry and Creep Rate

A creep rate of LCM29 in the region $4x10^{-10}$ - $9x10^{-10}$ s^{-1} was measured at 110% of target temperature in air. However, examination of the creep behavior of the silicon nitride fixtures alone yields similar values for strain. Regardless, the creep rate of LCM29 is low enough to indicate that 10 years life (10^5 h) is an attainable goal for ceramic composite tubes

A second proprietary study evaluated the impact of porosity, tortuosity and wall thickness on flux rate. In addition, it determined design ranges for tube internal diameter, porosity, tortuosity and material creep rate that satisfy both creep/buckling lifetime targets and oxygen flux targets.

A third proprietary study utilized CFD modeling to assess oxygen transport through a more robust alternative architecture design. The study concluded that the porous substrate must have very large pore sizes and high porosity to provide sufficient permeability to meet oxygen flux targets.

3.4 Task 8: Fuels and Engine Testing

A matrix of UCTFs will be prepared for testing at each engine (International Truck and Engine) or fuel cell developer (Nuvera Fuel Cells). The fuel matrix will include a base stock of syngas derived Fischer Tropsch liquids and will study the addition of advanced oxygenates supplied by BP. The study will quantify the impact of fuel properties on emissions and engine (or fuel cell) system performance.

3.4.1 Diesel Engine and Exhaust Treatment

3.4.1.1 Goal - Diesel Engine and Exhaust Treatment

The goal of this task is to understand the relationship between ultra-clean fuel properties and their impact on the emissions and performance of an advanced CIDI and exhaust treatment system under development at International Truck and Engine.

3.4.1.2 Experimental - Diesel Engine and Exhaust Treatment

Detailed discussion of the test methodology used in establishing this baseline fuel database has been provided in the 4Q01 Report [Ref. 3]. Pictures and description of the SCTE are shown in the Topical Report for the Period Jan. 1 through Oct. 31, 2001 [Ref. 1].

3.4.1.3 Results and Discussion - Diesel Engine and Exhaust Treatment

3.4.1.3.1 SCTE evaluation of fuel ultra-clean diesel fuel formulations.

Two ultra-clean diesel fuels were evaluated in this budget period utilizing the SCTE rigs at International truck and Engine. The first set of tests (Set 1) compared Fischer Tropsch diesel fuel (FT diesel) supplied by Sasol, LTD to a conventional No. 2 diesel fuel. The second set of tests evaluated the effect of BP oxygenate (BPO) on a petroleum based ultra-low sulfur diesel fuel (ULS). Properties of these fuels are shown in Table 8. Results of both tests are discussed below. Complete test results for both campaigns are provided in Appendix 1.

Table 8. Characterization of diesel fuels tested in the SCTE

		Set 1		Set 2	
Fuel Property		**Baseline No. 2 Diesel**	**FT GTL Diesel**	**Baseline ULS**	**ULS + BPO**
API Gravity		**36.0**	**49.9**	**36.5**	**34.8**
Distillation, IP	**Deg F**	**370**	**327**	**364**	**317**
10%		**434**	**367**	**401**	**359**
30,%		**474**	**419**	**459**	**437**
50%		**503**	**480**	**488**	**502**
70%		**537**	**546**	**510**	**551**
90,%		**589**	**638**	**588**	**607**
End pt		**642**	**672**	**666**	**646**
Flash point, F		**167**	**135**	**170**	**133**
Viscosity @ 40 C,	**cSt**	**2.4**	**2.1**	**2.5**	**2.13**
Aromatics	**Vol. %**	**30.2**	**0.4**	**12.5**	**~11.2**
Sulfur	**PPM**	**370**	**<5**	**<10**	**6**
H/C atomic ratio		**1.82**		**1.98**	**2.05**
Carbon content	**Wt.%**				**76.7**
Hydrogen content	**Wt. %**				**13.1**
Oxygen content	**Wt. %**	**0**	**0**	**0**	**10.2**
Net heat of comb.	**Btu/Lb**	**18457**	**18884**	**18667**	**16458**
Cetane number		**47.6**	**>70**	**65**	**68**

Set 1: No. 2 Diesel versus FT Diesel

Emission performance comparisons between the FT and baseline test fuel are presented as trade-offs between NOx and soot as well as between NOx and HC in Appendix 1.1. This is the customary way to present and analyze data engine combustion data in development work. These trade-offs have been generated by changes in combinations of settings of major combustion control parameters such as injection pressure, injection timing (represented by start of combustion SOC), air/fuel ratio and concentration of EGR in intake air. Comparison between emission performance of both investigated fuels have been conducted at four points of the engine operating map designated as Mode 4, 6, 7 and 8 and considered to be the significant overall contributors to result of the HD FTP emission certification cycle. The actual data are summarized graphically in Appendix 1.1, Figures 1 through 8, and numerically in Tables 1 through 3. Tables also include definitions of operating conditions at each of the test points as well as the information on specific combinations of control settings driving obtained emission trade-offs.

As it can be seen from the presented results, the FT fuel tested in International‘s SCTE demonstrates potential for significant emission reduction over the baseline No.2 diesel fuel, however its actual advantages are specific to both the operating point and the parameter calibration specific. In general, the relative emission performance of the FT diesel fuel vs. the baseline No. 2 diesel fuel can be summarized as follows:

Mode 4 (1500rpm/10 bar BMEP):

- Range of Soot: from 8% reduction to 57% increase
- Range of NOx: reduction from 3 to 7%
- Range of HC: reduction from 15 to 53%

Mode 6 (3170rpm/3.8 bar BMEP):

- Range of Soot: reduction from 13 to 45%
- Range of NOx: reduction from 2 to 32%
- Range of HC: reduction from 26 to 43%

Mode 7 (3170rpm/7 bar BMEP):

- Range of Soot: reduction from 12 to 32%
- Range of NOx: reduction from 13 to 26%
- Range of HC: reduction from 33 to 67%

Mode 8 (3010rpm/10.5 bar BMEP):

- Range of Soot: from 40% reduction to 8% increase
- Range of NOx: reduction from 23 to 37%
- Range of HC: reduction from 73 to >90%

Set 2: Ultra-low sulfur fuel and BP oxygenate
In the second test campaign, an ultra-low sulfur diesel fuel was blended with a proprietary BP oxygenate, BPO, to yield a blend with 10% oxygen by weight. The 10% oxygen blend has a net heating value about 13% lower than the base feedstock, complicating interpretation of the test data. To ensure a meaningful and comprehensive comparison of both emission and fuel consumption performance for these fuels, the standard test matrix based on the abbreviated AVL 8-Mode test had to be run twice.

- In the first run (referred later as "constant fuel" case) the fueling rates and corresponding A/F ratios (as well as other engine settings and operating parameters) have been kept the same between baseline fuel and oxygenated fuel tests, resulting in lower torques and deteriorated fuel economy.

- In the second run (referred later as "constant torque" case) the fueling rates have been adjusted to achieve baseline level of engine torques as well as some adjustment of A/F fuel ratios applied to account for a higher energy transfer to the turbo in the real engine. Effects of those adjustments on emission and potential improvement of fuel economy were evaluated.

As in the previous discussions of the engine investigation, the results of the emission and fuel consumption performance comparisons between the ultra -low sulfur baseline fuel and the heavily oxygenated test fuel are presented here as the trade-offs between the NOx and soot as well as between the NOx and BSFC. These trade-offs have been generated by changes in combinations of settings of major combustion control parameters such as injection pressure, injection timing (represented by start of combustion SOC), air/fuel ratio and concentration of EGR in intake air. Comparison between performance of both investigated fuels have been conducted at four points of the engine operating map designated as Modes 4, 6, 7 and 8 and considered to be the significant overall contributors to result of the HD FTP emission certification cycle. The actual data are summarized graphically and tabulated numerically in Appendix 1.2. The tables include definitions of operating conditions at each of the test points as well as information on specific combinations of control settings driving obtained emission trade-offs. In addition, the tables also include the comparison of performance results obtained in a "constant fuel" runs for both the baseline and the oxygenated fuel. The results obtained from the "constant torque" case are only presented on graphs. When reviewing the full scope of presented data, an observation can be made that there is a limited amount of data for the Mode 7 "constant torque" case as well as for all the cases of Mode 8. Reason for the limited test data was due to the amount of fuel available for testing. This limitation, however, did not obscure the overall conclusions regarding the effects of investigated test fuel on engine emission and performance.

The heavily oxygenated fuel tested in International SCTE demonstrates a very significant smoke emission reduction at all operating conditions and calibration points over the baseline low sulfur fuel. The other very interesting finding is a consistent and quite substantial reduction in NOx, which persist for both "constant fuel" and "constant torque" cases. As expected, due to reduced calorific value of oxygenated fuel, the fuel mass based BSFC is increased. This increase, although somewhat mitigated in the "constant torque" case, seems to be higher than it could be explained by a lower calorific value of the fuel itself. Additional reasons of such significant deterioration in fuel economy related to specific combustion chemistry or otherwise, are not clear at this point. In general, the relative emission /BSFC performance of the oxygenated fuel vs. the base low sulfur fuel can be can be summarized as follows:

Mode 4 (1500rpm/10 bar BMEP):

- Range of Soot reduction: from 50% reduction to 80%
- Range of NOx: reduction: from 6 to 19%
- Range of BSFC increase: from 12 to 18%

Mode 6 (3170rpm/3.8 bar BMEP):

- Range of Soot reduction: from 49 to 67%
- Range of NOx: reduction: from 15 to 22%
- Range of BSFC increase: from 25 to 45%

Mode 7 (3170rpm/7 bar BMEP):

- Range of Soot reduction: from 61 to 78%
- Range of NOx reduction: from 13 to 34%
- Range of BSFC increase: from 13 to 36%

Mode 8 (3010rpm/10.5 bar BMEP):

- Range of Soot reduction: from 70 to 74%
- Range of NOx: reduction: from 8 to 9%
- Range of BSFC increase: from 20 to 23%

The highly oxygenated fuel seems to lower NOx by reducing local flame temperature, similarly to the exhaust gas recycle (EGR) mechanism. The benefit of BPO must be weighed against the increase in fuel consumption.

These tests (Set 1 and Set 2) indicate that both FT diesel and BPO can substantially reduce NOx and soot emissions.

To further explore the impact of BPO, two more SCTE tests are scheduled in 1Q03: a 5% BPO in FT diesel blend and 5% BPO in ULS. This test work will then conclude the SCTE test campaign.

3.4.1.3.2 MCTE Campaign

For a NOx reduction device to be a viable solution for future emissions regulations, the problem of NOx Adsorber poisoning by sulfur components (SO_2/SO_3) must be addressed. Apparently, periodic desulfation is one of the critical ways to purge SO_2/SO_3 out and recover the catalyst activity. A desulfation test apparatus, shown in Figure 18, has been built to study this process and gauge the effects of fuel components on its operation. An experimental campaign is underway to develop the best desulfation strategy to regenerate the NOX adsorber. One possible solution is to raise the catalyst inlet temperature to adequate levels (~600°C) while maintaining a rich exhaust stream (A/F ~13). This protocol was tested in a preliminary experiment. Conditions for the experiment were: mid-speed/mid-load condition of 1500 RPM, and 210ft-lbs. at steady state.

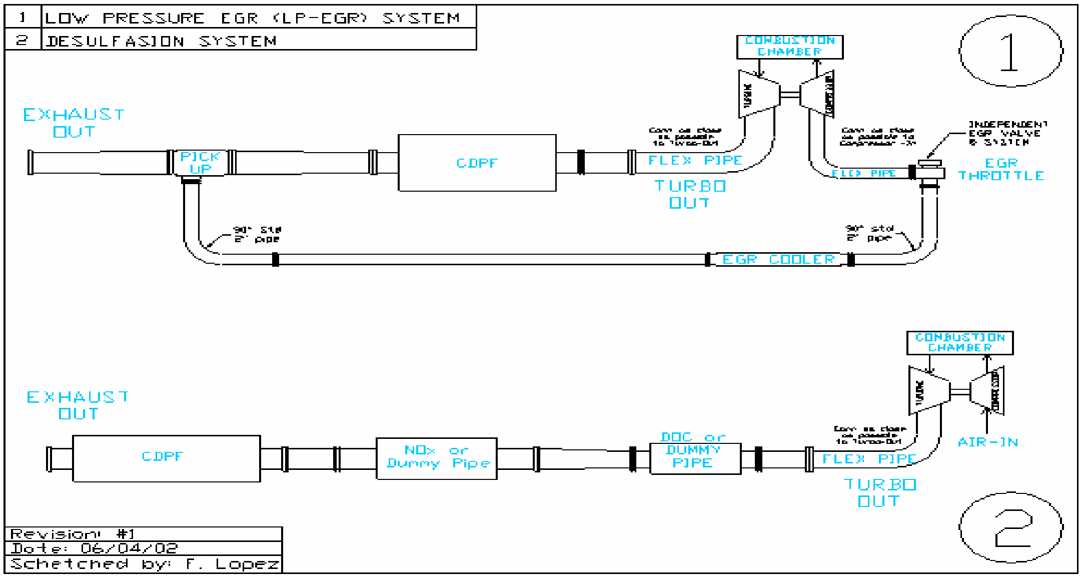

Figure 18: Desulfation test apparatus

At these engine conditions it was found that:

- ITH, EGR, and post injection are the key components to reduce A/F ratio to 13.
- Post injection is necessary to generate high HC levels (~8000 ppm) and the pre-catalyst seems critical to burn off HC and raise up the inlet temperature to >600°C.

A relatively clean NOx absorber was used to test the above desulfation protocol. The clean NOx adsorber yielded a baseline efficiency of 80% over the HD FTP cycle using the latest L/R strategy. It was then poisoned for 14 hours using a conventional No. 2 diesel fuel. After sulfur poisoning, the NOx reduction efficiency of the catalyst dropped down to 48%. The desulfation conditions were then run for 15 minutes, and the NOx absorber efficiency recovered to near 80%, indicating the preliminary desulfation process is effective.

The next step is to evaluate potential benefits of the modified fuels on the desulfation process, such as by-products control, sulfur purge efficiency and fuel penalty, etc.

3.4.2 Nuvera Fuel Cells

3.4.2.1 Goal - Nuvera Fuel Cells

The goal is to understand effect of UCTF on the fuel cell system and possibly reduce emissions on a per mile basis. The scope of phase II in the current program is to study and compare emissions produced by three alternative fuels in fuel processing / fuel cell power plant. The fuels chosen for the study were Naphtha from Sasol/Chevron, California Phase II Gasoline from Chevron Phillips and Oxygenated Naphtha blended at BP.

3.4.2.2 Experimental

Nuvera's Burner facility comprises of Nuvera's Burner module, gas and condensate sampling system, and all the process streams required for clean processing of different fuels. The experimental layout of burner facility is shown in Appendix 2.

3.4.2.3 Results and Discussion

Three fuels – GTL Naphtha, oxygenated GTL Naphtha/BPO and California Phase II RFG, were successfully processed in Nuvera's Burner Module for start-up emission study. Physical property data for these fuels are shown below in Table 9.

Table 9. Properties of fuel used in Nuvera's Burner Module for startup emission study

Fuel Properties	GTL Naphtha/BPO	GTL Naphtha	California Phase II RFG
API Gravity	71.86	73.4	60.57
Specific Gravity, 60F/60F	0.6958	0.6906	0.7367
Density, kg/m^3	695.8	690.6	736.7
C, m%	82.44	84.1	84.96
H, m%	15.82	15.9	13.02
O, m%	1.74	0	2
N, ppm	<1	<1	<1
S, ppm	1	0	32.9
Lower heating value LHV, kJ/kg	43946	44357	40983
(Air/Fuel)$_{stoich}$	14.79	15.08	14.12
Estimated molecular weight, gm/gm-mol	99.4	101.0	100.95

Exhaust gas composition was analyzed for bulk components such as carbon dioxide, water vapors and oxygen, and traces of species, such as NOx, carbon monoxide (CO) and total hydrocarbons (THC), that are governed by emission standards from the Environmental Protection Agency (EPA). In addition, process condensates were collected for analysis of water contaminants in the burner exhaust. The fuels under study were compared in terms of burner module operating conditions, exhaust compositions, start-up and steady state emissions.

To ensure repeatability of the experiments, the burning cycle of each fuel was conducted at least three times starting with the fuel ignition through the startup and steady state phase and ending with cooling burner to initial temperature.
All fuels show spikes of THC and carbon monoxide emissions at the burner startup. This is attributed to unburned fuel skipping through the module when it is lit initially. The CO spike occurred due to incomplete fuel combustion. No spikes in NOx emissions were recorded for any fuel at the startup conditions. Concentration of NOx is much less than the concentration of CO and THC

There are two principal sources of nitrogen oxide (NOx) formed during combustion: one is oxidation of atmospheric (molecular) nitrogen and another is oxidation of nitrogen-containing compounds in the fuel. During combustion of studied “clean” fuels, containing no nitrogen compounds, under lean or stoichiometric conditions the thermal mechanism is the principal source of nitrogen oxide emissions.

Integrated startup emissions for all three fuels tested are shown in Table 10. The integrated values were calculated using total amount of startup emissions divided by the amount of fuel used during respective startup time.

Table 10. Emissions at Startup

Fuel	mg/gfuel		
	CO	THC	NOx
GTL Naphtha	7.34	110.78	0.57
GTL Naphtha/BPO	5.61	78.07	0.23
Cal Phase II RFG	6.28	92.24	0.79

Table 10 shows that GTL Naphtha/BPO has the lowest CO, THC, and NOx startup emissions among all fuels tested. This can be attributed to the oxygen added to the fuel. GTL Naphtha and GTL Naphtha/BPO have almost the same fuel blend except GTL Naphtha/BPO contains 1.74% oxygen. It seems that adding oxygen to the fuel results in more complete fuel combustion and, subsequently, reducing tailpipe emissions. Oxygenated fuel also tends to provide more complete combustion of its carbon into carbon dioxide (CO_2), thereby reducing emissions of hydrocarbons and carbon monoxide. Even though both GTL Naphtha/BPO fuel and California Phase II RFG gasoline have similar oxygen concentration in the fuel (1.74 and 2 % respectively), emissions from gasoline burning are higher than emissions from GTL Naphtha/BPO. This could be explained by high percentage of aromatic compounds in California Phase II RFG, which satisfies its high octane rating.

Table 11 shows steady state emissions of three fuels averaged throughout the single burning cycle.

Table 11. Emissions throughout steady state

Fuel	mg/gfuel		
	CO	THC	NOx
GTL Naphtha	0.42	0.61	0.57
GTL Naphtha/BPO	0.41	0.61	0.23
Cal Phase II RFG	0.55	0.52	0.79

Addition of oxygen to the Naphtha blend did not affect steady state emissions of hydrocarbons and carbon monoxide as shown in Table 11. However, NOx emissions are decreased in the oxygenated Naphtha fuel blend that may be attributed to the oxygen presence in the fuel. Table 11 indicates that California Phase II RFG is the worst fuel blend among all three fuels at steady state conditions. This can be attributed to high-octane aromatics presence.

Table 12 shows average values of oxygen and carbon dioxide emissions of the three fuel blends.

Table 12. Oxygen and carbon dioxide emissions

Fuel	vol. %	
	O_2	CO_2
GTL Naphtha	13.85	6.04
GTL Naphtha/BPO	13.72	5.76
Cal Phase II RFG	11.85	10.8

Table 12 shows that GTL Naphtha and GTL Naphtha/BPO have almost the same oxygen and carbon dioxide concentrations in the burner exhausts. This is expected since both fuels have almost the same fuel compositions. It seems that adding oxygen to the Naphtha blend did not influence oxygen and carbon dioxide emissions significantly.

3.5 Task 10: Program Management

3.5.1 Goal - Task 10

The recipient shall provide technical leadership and management direction to ensure that the program delivers its goals on time, within budget and in a safe and environmentally acceptable manner. Good communications with the DOE, participants, and subcontractors will be maintained.

3.5.2 Milestones - Task 10

A detailed briefing shall be presented within (60) days of the end of the budget period. The briefings shall be given by the Recipient to explain the plans, progress, and results of the project effort, both technical and administrative.
Status:

- The Quarterly Reports for the Second Budget Period, 1st, 2nd, 3rd and 4th Quarters were completed and issued on time.

- Nuvera completed all Phase 2 experiments and the final report on time and within budget.
- A delay has been encountered in the preparation of BPO, an oxygenate supplied by BP. This fuel blending component is required to complete the SCTE test program.
- The HCCI engine tests have been delayed due to availability of certain test rigs.
- A kick-off meeting for the Second Budget Period was held on May 2, 2002 at Praxair's Tonawanda, NY research center.
- An end of the year briefing was presented to the DOE on December 12, 2002 at Praxair's Tonawanda, NY research center.
- The program remains under budget through the fourth quarter.
- A no cost extension has been requested to carry the program into 2003.

3.5.3 Discussion - Task 10

The OTM syngas program is under budget but behind schedule in some tasks. The Nuvera fuel cell testing is complete. The International diesel engine work is progressing well, but is about 4 to 6 months behind schedule due to the hiatus between completion of the 1st budget period in November, 2001 and approval of this (2nd) budget period in April, 2002. The single cylinder engine test work should be completed early next year. Thirteen drums of FT diesel fuel were obtained for the diesel engine development work. Additional quantities of BPO are also being manufactured. The production of BPO was scheduled to be completed by the end of this quarter, but a technical problem was encountered in the manufacturing process. The HCCI work at International has been delayed due to availability of the single cylinder test engine, which will be modified for HCCI studies. This should be corrected in the next budget period.

Overall, costs remain under budget. A no cost extension for the program has been requested. This should allow continuation of the program through early 2003.

4.0 Conclusions

- Two robust substrate systems (MM1, LCM29) show great promise for achieving long-term life and performance targets. Life tests on both systems are on-going.
- A suite of OTM materials have been developed that approximate the thermal expansion properties of the new substrates.
- Target flux has almost been achieved with a new, more robust composite (LCM29/LCM38) system. Architectural improvements should allow this system to achieve target flux.
- Thermal and chemical expansion properties of both membrane and substrate materials can be engineered to a certain degree by compositional manipulation.
- Several new architectures (Config.1 and 2) for the MM system appear promising based on preliminary thermal cycle tests.
- Target flux has been achieved for an MM3/LCM1 system at 1.1TT.

- The temperature boundaries of these systems are being mapped by new test procedures, including operations at 10% above the target temperature. Preliminary high temperature tests of LCM29 and MM3 substrates are very encouraging.
- A new high-pressure test rig was successfully operated at TT and 2.2TP with a dense LCM1 tube. This shows that high-pressure operations are feasible.
- A novel reactor design has been developed that lowers capital costs, improves operability, and has the flexibility to produce hydrogen as well as syngas.
- Fischer Tropsch diesel fuel shows a clear advantage in reducing NOx and soot in comparison to conventional No. 2 diesel fuel.
- The BP oxygenate show significant reductions in both NOx and soot in comparison to an ultra low sulfur petroleum derived diesel fuel.
- The lower heating value of the highly oxygenated fuel requires more fuel to achieve constant torque. Sometimes the fuel consumption is more than expected by calorific value of the fuel, suggesting other inefficiencies are being created in the combustion process.
- In the Nuvera fuel cell burner system, burning GTL Naphtha/BPO fuel resulted in the least amount of emissions among the three fuels studied
    - Adding BPO to the naphtha fuel blend reduced start-up emissions of carbon monoxide, NOx and hydrocarbons.
    - Adding oxygen to the Naphtha fuel blend did not affect the steady state emissions of carbon monoxide and hydrocarbons but resulted in reducing NOx emissions.
- Based on test results reported by both Nuvera and International, the BPO has real value for reducing emissions (hydrocarbons, NOx) from both open flame burners and internal combustion diesel engines.

5.0 References

1. Robinson et al, Topical Report for “Development of OTM Syngas Process and Testing of Syngas-Derived Ultra-clean Fuels in Diesel Engines and Fuel Cells”, US DOE Award No. DE-FC26-01NT41096, Budget Period 1, October 2001.
2. Robinson et al, Quarterly Project Status Report for Period ending September 30, 2002 for “Development of OTM Syngas Process and Testing of Syngas-Derived Ultra-clean Fuels in Diesel Engines and Fuel Cells”, US DOE Award No. DE-FC26-01NT41096, December 2002.
3. Robinson et al, Quarterly Project Status Report for Period ending December 31, 2001 for “Development of OTM Syngas Process and Testing of Syngas-Derived Ultra-clean Fuels in Diesel Engines and Fuel Cells”, US DOE Award No. DE-FC26-01NT41096, March 2002.

Appendix 1

International Truck and Engine SCTE Fuel Results

Appendix 1.1 -- No.2 Diesel versus FT Diesel

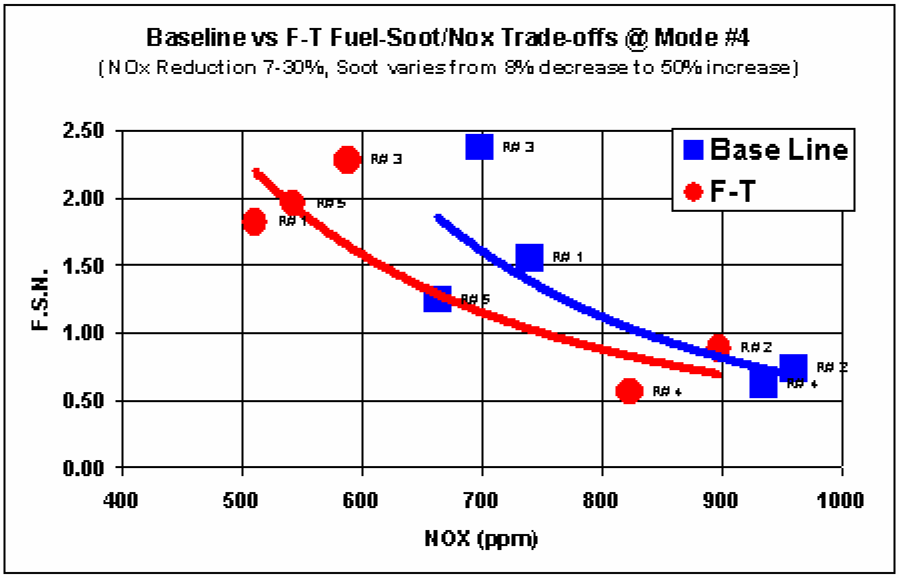

Figure 1. Baseline vs. F-T Fuel - Soot/NOx Trade-offs @ Mode 4

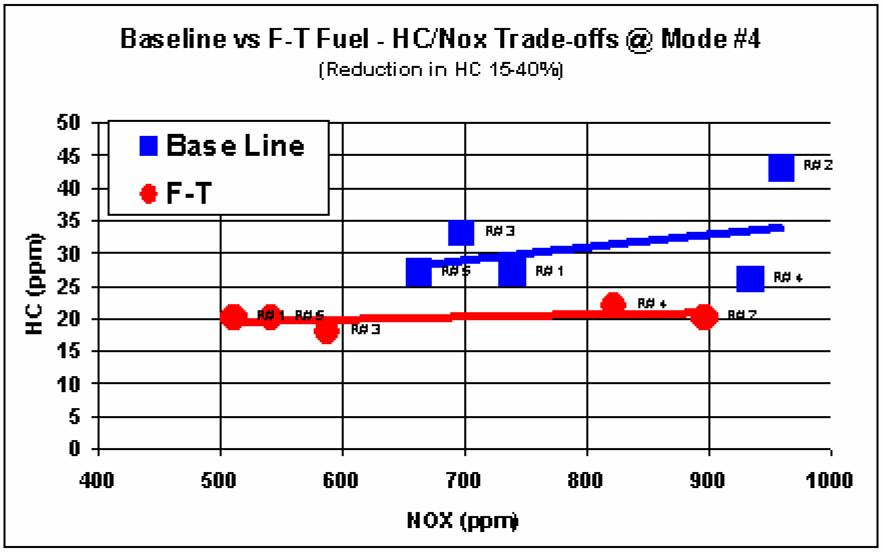

Figure 2. Baseline vs. F-T Fuel - HC/NOx Trade-offs @ Mode 4

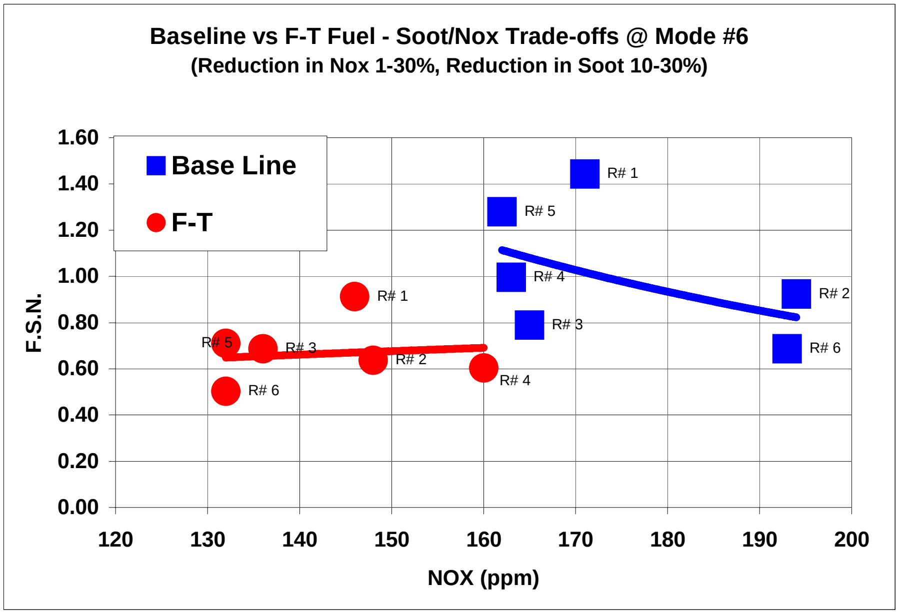

Figure 3. Baseline vs. F-T Fuel - Soot/NOx Trade-offs @ Mode 6

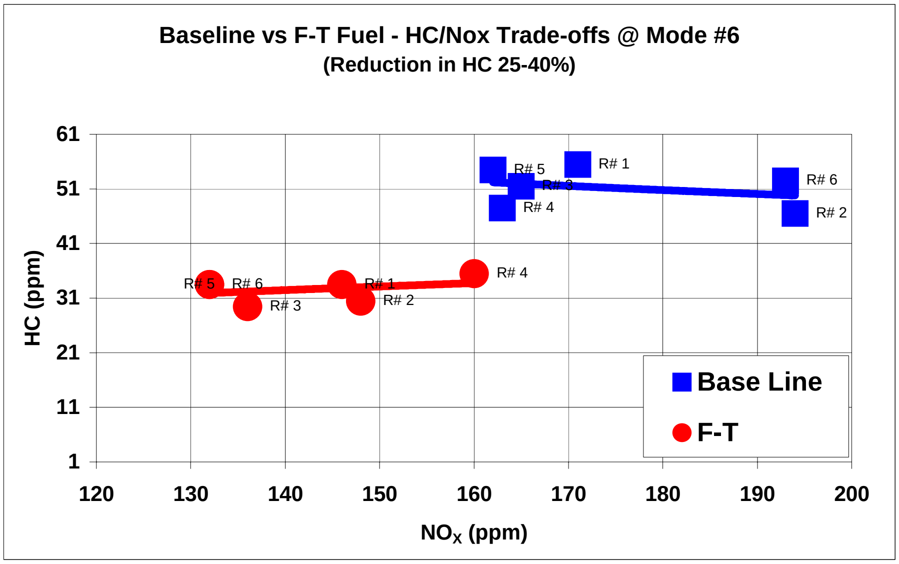

Figure 4. Baseline vs. F-T Fuel - HC/NOx Trade-offs @ Mode 6

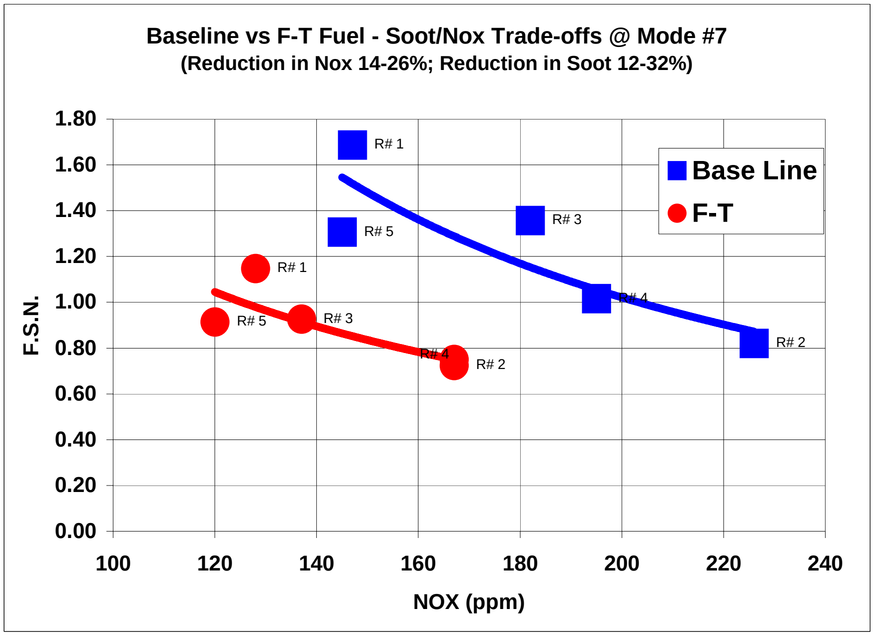

Figure 5. Baseline vs. F-T Fuel - Soot/NOx Trade-offs @ Mode 7

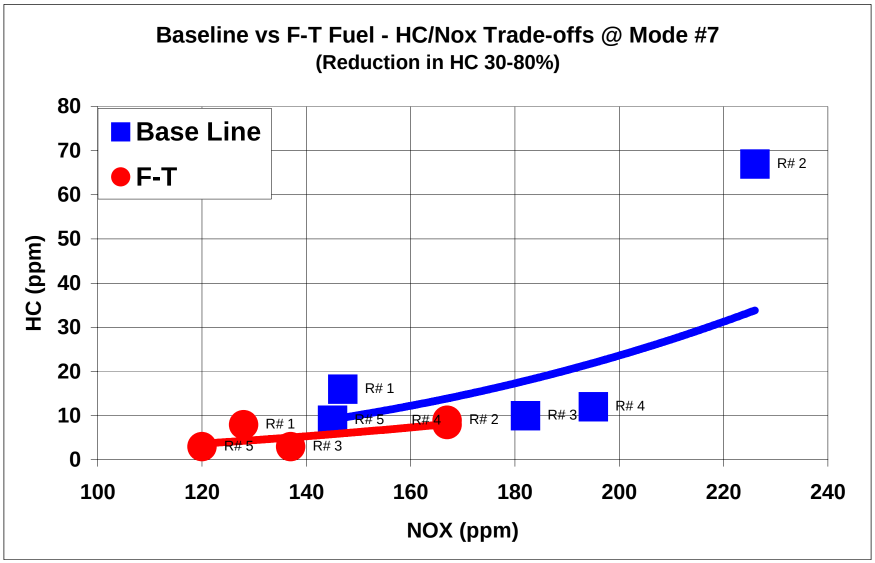

Figure 6. Baseline vs. F-T Fuel - HC/NOx Trade-offs @ Mode 7

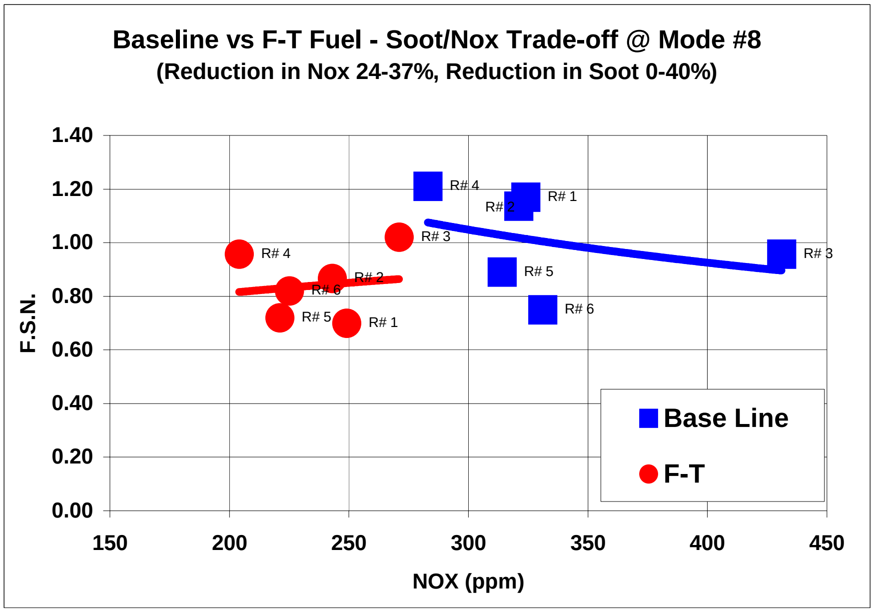

Figure 7. Baseline vs. F-T Fuel - Soot/NOx Trade-off @ Mode 8

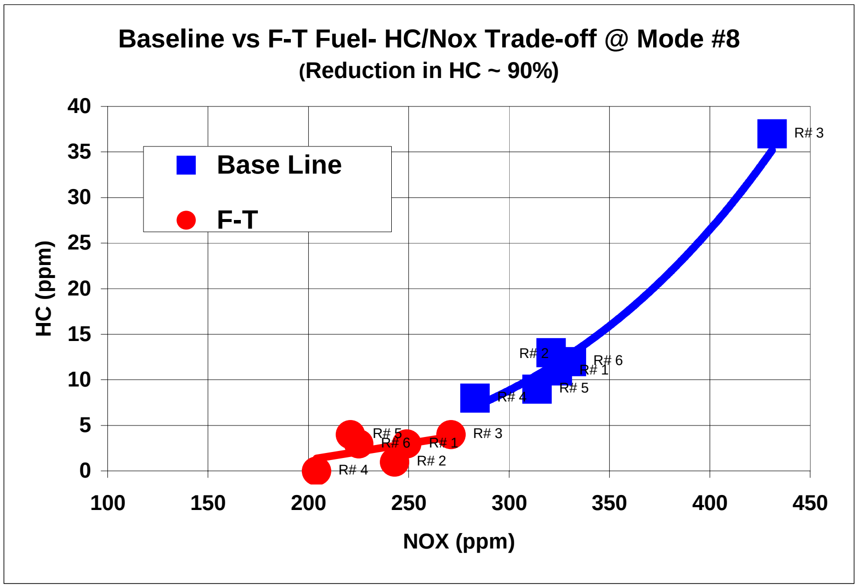

Figure 8. Baseline vs. F-T Fuel - HC/NOx Trade-off @ Mode 8

Table 1. Test Data at Mode 4

Mode #4																
Run#		1	1	d%	2	2	d%	3	3	d%	4	4	d%	5	5	d%
Fuel		BL	FT		BL	FT		BL	FT		BL	FT		BL	FT	
Engine Speed	rpm	1493	1498		1503	1497		1510	1497		1496	1496		1503	1507	
Torque	lb-ft	47.1	47.5		43.7	49.4		44.5	45.4		46.2	48.2		44.8	45.6	
NOx	ppm	740	511	-31	960	897	-7	698	588	-16	935.0	823.0	-12	663	542.0	-18
HC	ppm	27	20	-26	43	20	-53	33	18	-45	26.0	22.0	-15	27	20.0	-26
AVL smoke	FSN	1.55	1.82	17	0.7	0.9	20	2.4	2.3	-4	0.6	0.6	-8	1.24	2.0	57
ICP	Mpa	11	11		10.7	10.7		10.6	10.7		12.0	12.1		12	12.1	
Air Fuel Ratio		21.7	21.5		24.3	24.3		21.6	21.5		23.8	23.5		21.0	20.9	
EGR	%	5.5	5.7		0.7	0.6		3.1	3.0		4.1	3.9		5.8	6.1	
SOC-main	deg CA ATDC	4	4		4.0	4.0		8.0	8.0		4.0	0.4		6	6.0	
BSFC	lb/hp-hr	0.367	0.372	1	0.399	0.359	-10	0.388	0.394	2	0.362	0.360	-1	0.382	0.373	-2
Fuel Flow	lb/hr	5.43	5.41		5.39	5.41		5.51	5.49		5.29	5.30		5.45	5.42	

Table 2. Test Data at Mode 6

Mode #6																			
Run#		1	1	d%	2	2	d%	3	3	d%	4	4	d%	5	5	d%	6	6	d%
Fuel		BL	FT		BL	FT		BL	FT		BL	FT		BL	FT		BL	FT	
Engine Speed	rpm	3168	3171		3168	3170		3170	3170		3169	3171		3169	3171		3169	3172	
Torque	lb-ft	17.0	17.7		14.6	16.1		15.4	15.8		15.6	15.6		15.1	15.7		14.6	15.7	
NOx	ppm	171	146	-15	194	148	-24	165	136	-18	163.0	160.0	-2	162	132.0	-19	193	132.0	-32
HC	ppm	55	33	-40	46	30	-35	51	29	-43	47.0	35.0	-26	54	33.0	-39	52	33.0	-37
AVL smoke	FSN	1.44	0.91	-37	0.9	0.6	-31	0.8	0.7	-13	1.0	0.6	-39	1.28	0.7	-45	0.69	0.5	-27
ICP	Mpa	17	17		17.1	17.1		17.1	17.1		19.2	19.1		17	17.1		19	19.1	
Air Fuel Ratio		30.7	30.8		33.5	33.6		29.9	29.5		32.8	32.0		29.5	29.7		32.4	32.5	
EGR	%	16.4	16.1		9.3	10.1		12.8	12.1		14.6	14.0		13.0	13.5		8.6	8.9	
SOC-main	deg CA ATDC	6	6		8.0	8.0		10.2	10.0		6.0	6.0		8	8.5		10	10.0	
BSFC	lb/hp-hr	0.563	0.546	-3	0.594	0.594	0	0.624	0.609	-2	0.594	0.594	0	0.614	0.599	-2	0.639	0.604	-5
Fuel Flow	lb/hr	7.43	7.44		7.53	7.53		7.64	7.62		7.43	7.43		7.42	7.43		7.61	7.62	

Table 3. Test Data at Mode 8

Mode #8																			
Run#		1	1	d%	2	2	d%	3	3	d%	4	4	d%	5	5	d%	6	6	d%
Fuel		BL	FT		BL	FT		BL	FT		BL	FT		BL	FT		BL	FT	
Engine Speed	rpm	3010	3009		3009	3012		3008	3012		3010.4	3010.5		3010	3009		3010	3009	
Torque	lb-ft	45.6	46.6		48.2	49.6		49.2	51.1		45.0	45.6		44.5	46.2		46.2	47.0	
NOx	ppm	324	249	-23	321	243	-24	431	271	-37	283.0	204.0	-28	314	221.0	-30	331	225.0	-32
HC	ppm	11	3	-73	13	1	-92	37	4	-89	8.0	0.0	-100	9	4.0	-56	12	3.0	-75
AVL smoke	FSN	1.17	0.70	-40	1.1	0.9	-24	1.0	1.0	7	1.2	1.0	-21	0.89	0.7	-19	0.75	0.8	9
ICP	Mpa	24	24		24.0	24.1		24.0	24.3		26.2	26.2		28	27.1		28	26.9	
Air Fuel Ratio		24.2	24.3		24.6	24.8		24.5	24.6		24.2	24.2		25.6	26.1		26.0	26.0	
EGR	%	6.3	6.1		9.3	10.0		11.3	12.2		10.6	11.0		9.8	9.7		11.8	12.1	
SOC-main	deg CA ATDC	6	7		3.0	3.0		0.0	0.0		6.0	6.0		6	6.0		3	3.0	
BSFC	lb/hp-hr	0.525	0.485	-8	0.485	0.447	-8	0.469	0.428	-9	0.532	0.487	-9	0.525	0.474	-10	0.491	0.451	-8
Fuel Flow	lb/hr	14.59	14.62		14.20	14.24		14.00	14.03		14.60	14.49		14.28	14.32		13.80	13.81	

Appendix 1.2 -- ULS Diesel and ULS with 10% Oxygen

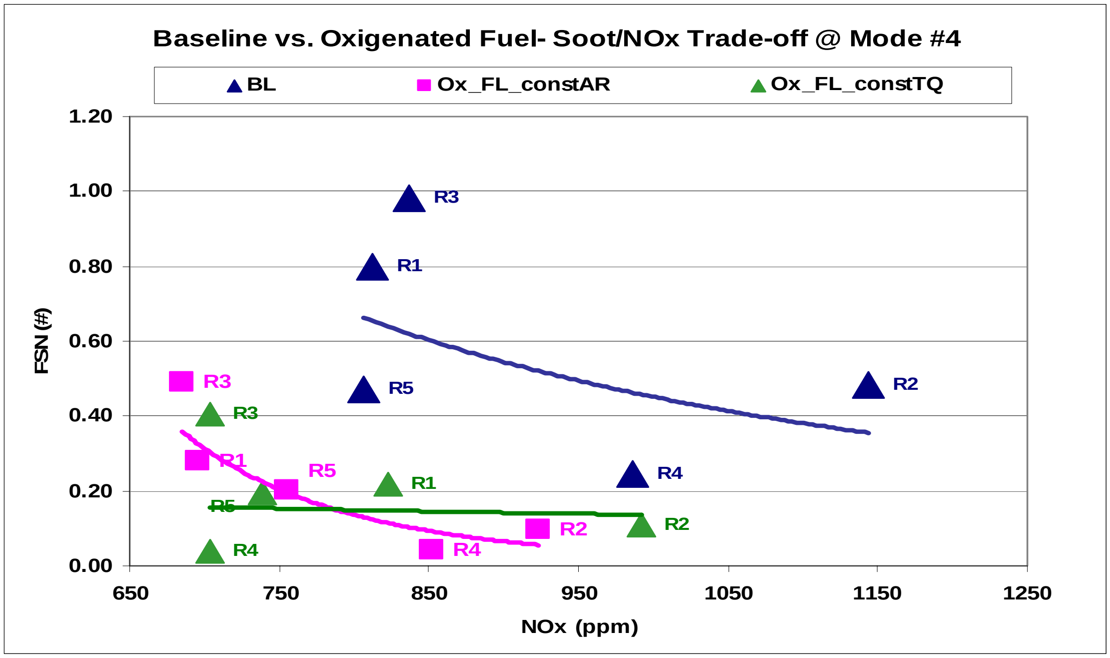

Fig 1

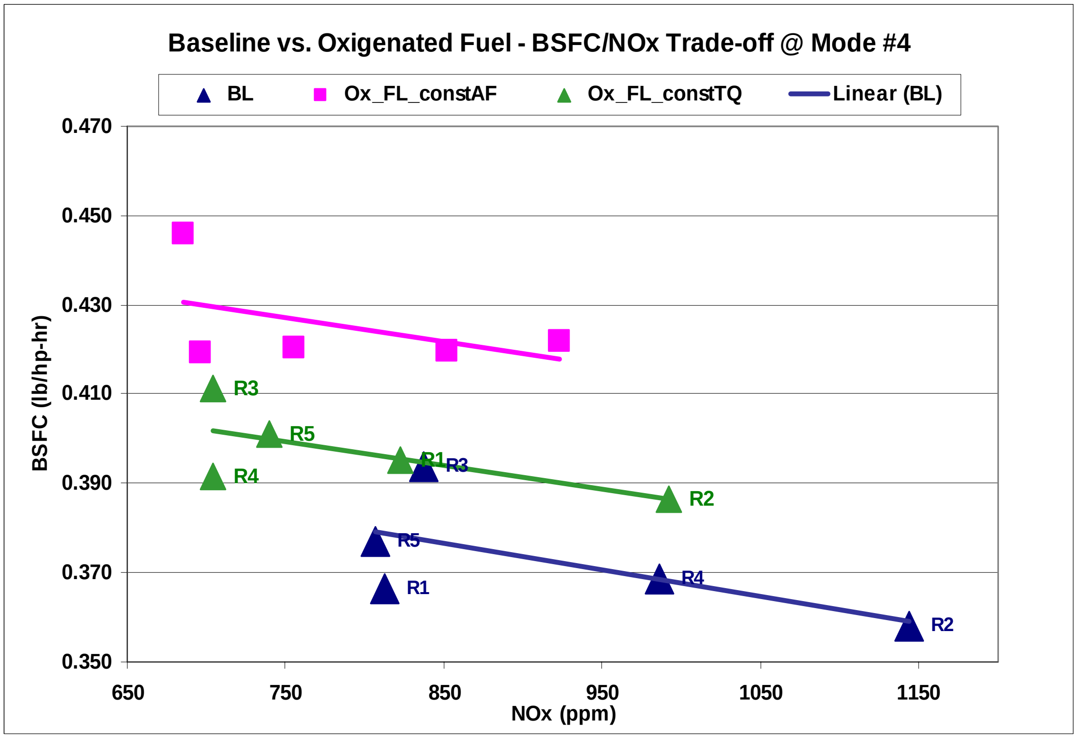

Fig 2

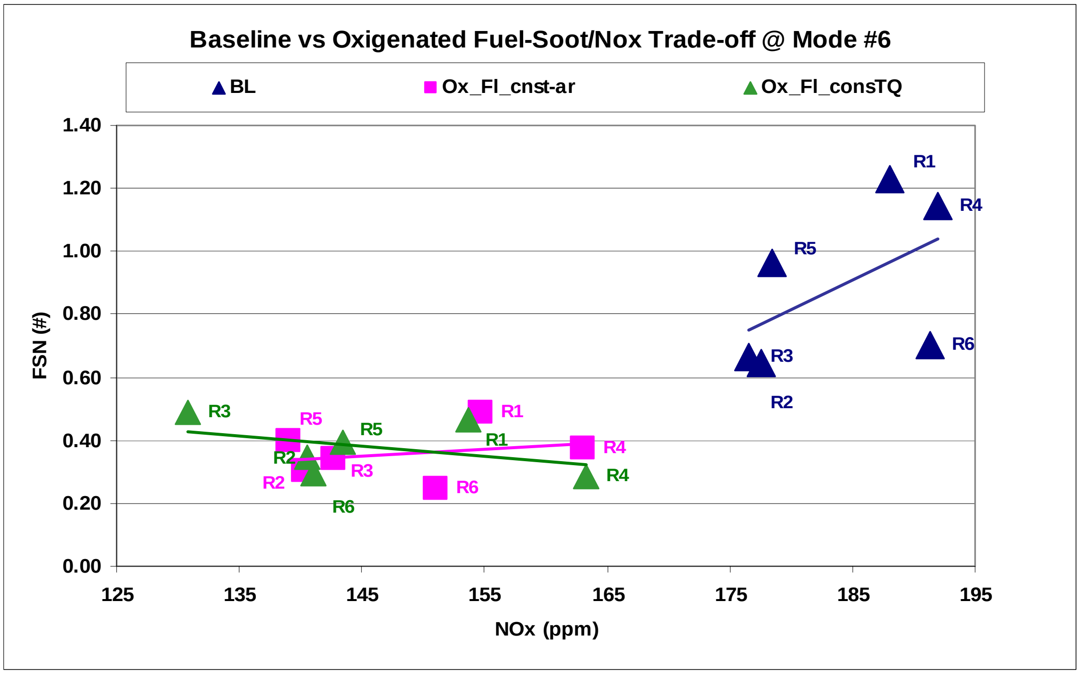
Baseline vs Oxigenated Fuel-Soot/Nox Trade-off @ Mode #6
▲ BL
■ Ox_Fl_cnst-ar
▲ Ox_Fl_consTQ
FSN (#)
1.40
1.20
1.00
0.80
0.60
0.40
0.20
0.00
125
135
145
155
165
175
185
195
NOx (ppm)
R1
R4
R5
R6
R3
R2
R3
R5
R5
R1
R1
R4
R2
R3
R2
R4
R6
R6

Fig. 3

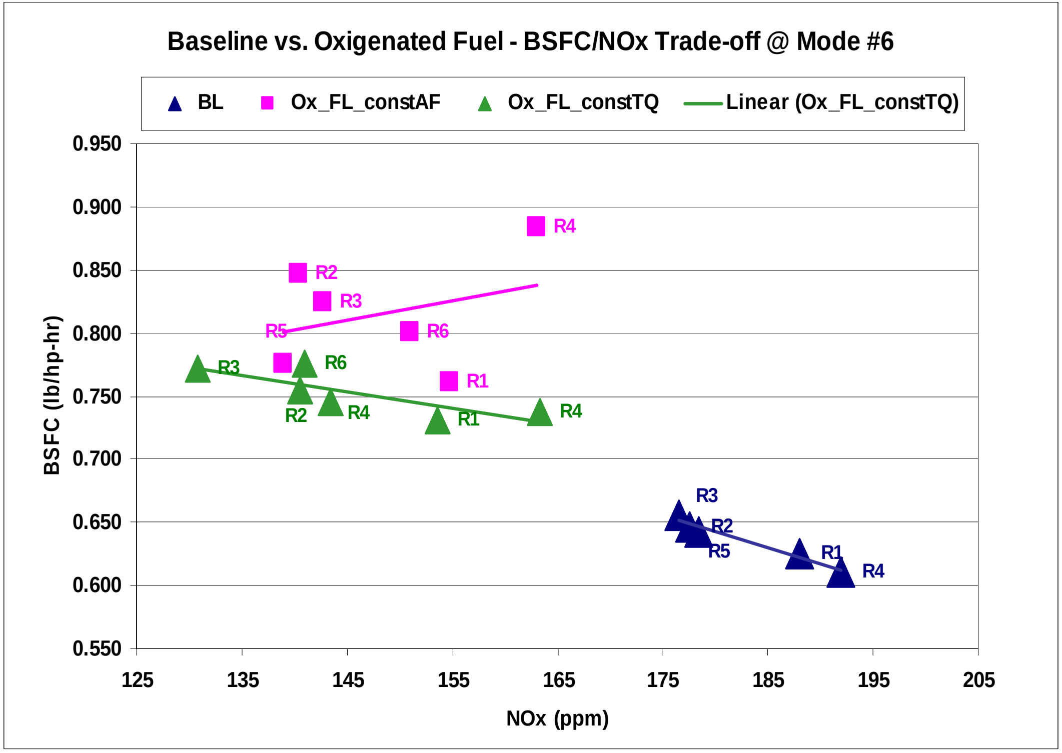
Baseline vs. Oxigenated Fuel - BSFC/NOx Trade-off @ Mode #6
▲ BL
■ Ox_FL_constAF
▲ Ox_FL_constTQ
Linear (Ox_FL_constTQ)
BSFC (lb/hp-hr)
0.950
0.900
0.850
0.800
0.750
0.700
0.650
0.600
0.550
125
135
145
155
165
175
185
195
205
NOx (ppm)
R4
R2
R3
R5
R6
R3
R6
R1
R2
R4
R1
R4
R3
R2
R5
R1
R4

Fig. 4

FINAL REPORT APPENDIX II

Topical Report—Budget Period 2

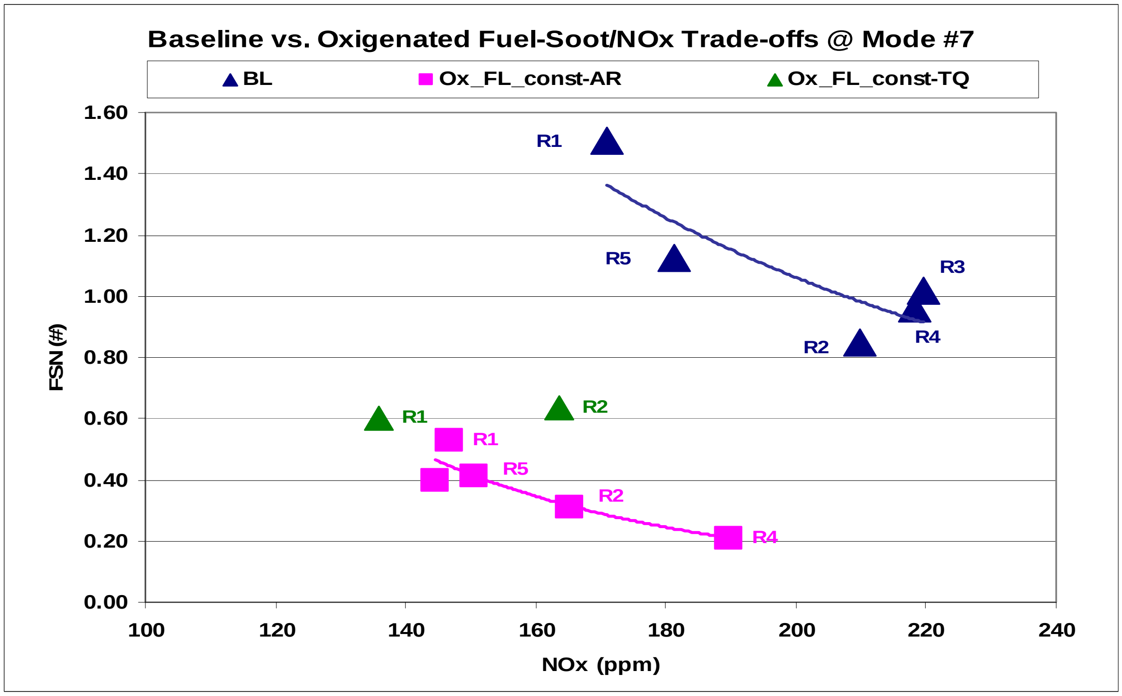

Fig. 5

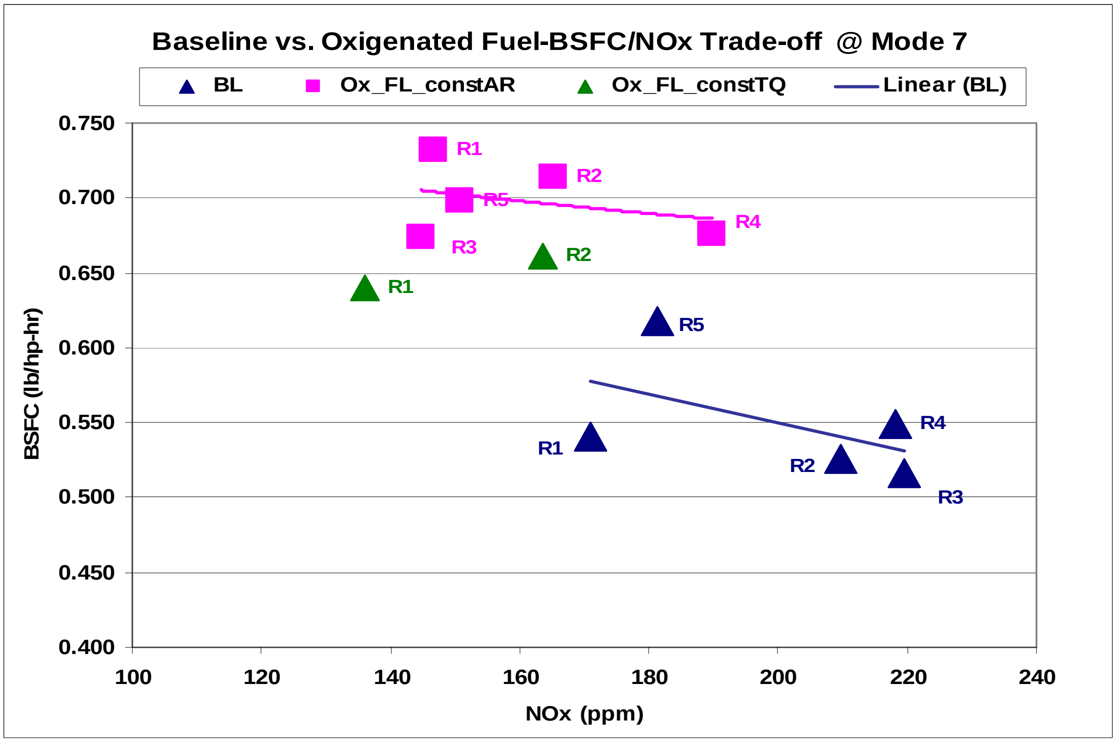

Fig. 6

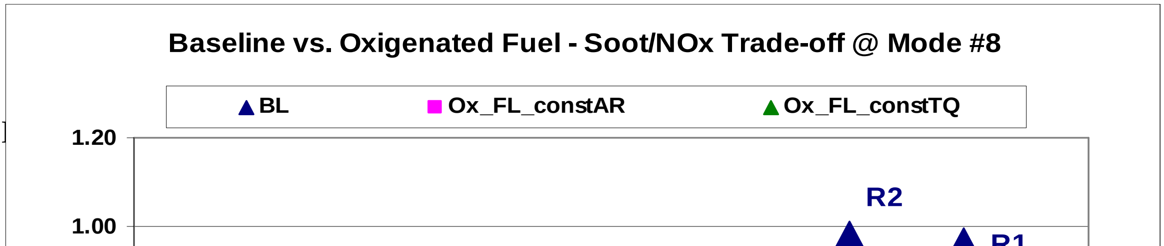

Fig.7

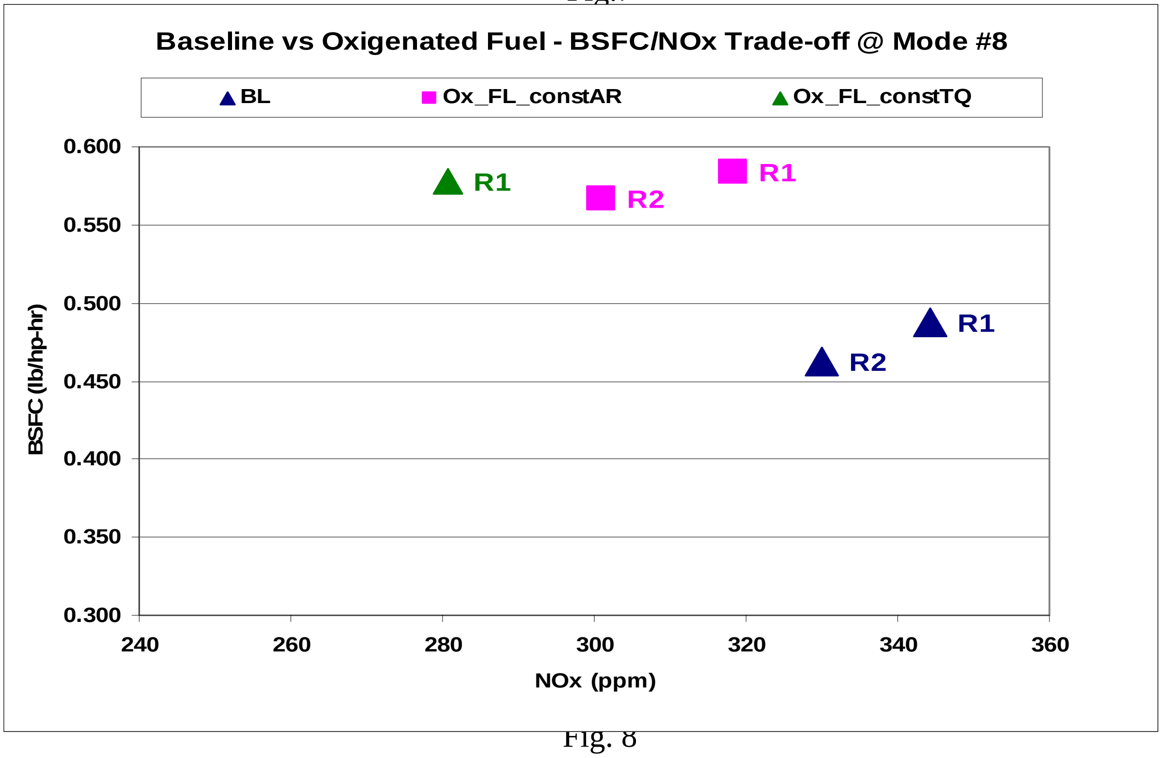

Fig. 8

Table 1

Mode #4

Run#		1	1	d%	2	2	d%	3	3	d%	4	4	d%	5	5	d%
Fuel		BL	OX		BL	OX		BL	OX		BL	OX		BL	OX	
Engine Speed	rpm	1503	1507		1503	1497		1510	1497		1496.5	1496.5		1503	1507.4	
Torque	lb-ft	47.0	40.4	-14	48.1	40.3	-16	44.5	38.7	-13	45.9	39.3	-14	45.2	40.5	-10
NOx	ppm	812	696	-14	1144	923	-19	837	685	-18	985.7	852.0	-14	807	755.3	-6
HC	ppm	62	24	-61	60	22	-63	54	27	-51	42.7	26.5	-38	52	28.3	-45
AVL smoke	FSN	0.80	0.28	-65	0.5	0.097	-80	0.98	0.49	-50	0.25	0.043	-82	0.47	0.203	-57
ICP	Mpa	11	11		10.7	10.7		10.6	10.7		12.0	12.1		12	12.1	
Air Fuel Ratio		21.7	21.7		24.5	24.4		21.7	21.8		23.8	24.0		20.8	20.6	
EGR	%	6.1	6.1		0.6	0.9		3.0	3.8		4.8	4.7		6.0	6.1	
SOC-main	deg CA ATDC	4	4		4.0	4.0		8.0	8.0		4.0	0.4		6	6.0	
BSFC	lb/hp-hr	0.366	0.419	14	0.358	0.422	18	0.394	0.446	13	0.369	0.420	14	0.377	0.420	12

Table 2

Mode #6

Run#		1	1	d%	2	2	d%	3	3	d%	4	4	d%	5	5	d%	6	6
Fuel		BL	OX		BL	OX		BL	OX		BL	OX		BL	OX		BL	OX
Engine Speed	rpm	3170	3169		3170	3168		3169	3168		3169	3167		3172	3167		3169	3166
Torque	lb-ft	14.9	11.3	-24	14.4	9.8	-32	14.4	10.4	-27	15.1	8.8	-42	14.3	11.0	-23	14.1	10.6
NOx	ppm	188	155	-18	178	140	-21	177	143	-19	192.0	163.0	-15	178	139.0	-22	191	151.0
HC	ppm	70	33	-53	69	30	-57	65	29	-55	54.8	35.0	-36	56	33.0	-41	59	33.0
AVL smoke	FSN	1.23	0.49	-60	0.6	0.3	-53	0.7	0.3	-49	1.1	0.4	-67	0.96	0.4	-59	0.70	0.2
ICP	Mpa	17	17		17.1	17.1		17.1	17.1		19.2	19.1		17	17.1		19	19.1
Air Fuel Ratio		30.1	30.3		33.2	33.1		30.0	29.9		32.6	32.7		29.7	29.8		32.6	32.6
EGR	%	15.8	15.7		10.1	10.3		12.3	12.2		14.1	14.2		13.2	13.4		9.8	9.4
SOC-main	deg CA ATDC	6	6		8.0	8.0		10.2	10.0		6.0	6.0		8	8.5		10	10.0
BSFC	lb/hp-hr	0.625	0.762	22	0.646	0.847	31	0.656	0.824	26	0.611	0.884	45	0.643	0.776	21	0.659	0.801
Fuel Flow	lb/hr	7.47	7.46		7.53	7.53		7.63	7.62		7.46	7.44		7.45	7.42		7.64	7.63

Table 3

Mode #7

Run#		1	1	d%	2	2	d%	3	3	d%	4	4	d%	5	5	d%
Fuel		BL	OX		BL	OX		BL	OX		BL	OX		BL	OX	
Engine Speed	rpm	3168	3167		3169	3166		3169	3168		3170.2	3168.9		3169	3169	
Torque	lb-ft	31.1	21.6	-31	31.4	21.7	-31	32.8	23.8	-27	28.8	22.1	-23	26.2	22.6	-14
NOx	ppm	171	147	-14	210	165	-21	220	145	-34	218.3	189.7	-13	181	150.7	-17
HC	ppm	31	21	-32	29	23	-21	19	25	30	21.0	21.0	0	33	21.0	-37
AVL smoke	FSN	1.51	0.53	-65	0.85	0.31	-63	1.02	0.40	-61	0.96	0.21	-78	1.13	0.41	-63
ICP	Mpa	22	22		24.0	24.1		24.1	24.0		26.1	26.2		26	26.0	
Air Fuel Ratio		28.7	28.5		29.9	29.9		27.8	27.8		28.7	28.8		28.2	28.0	
EGR	%	13.4	13.2		8.2	8.8		12.4	12.0		13.2	13.2		12.3	11.9	
SOC-main	deg CA ATDC	9	9		9.0	9.0		9.0	9.0		7.1	7.0		11	11.0	
BSFC	lb/hp-hr	0.541	0.732	35	0.526	0.714	36	0.516	0.674	31	0.549	0.676	23	0.618	0.698	13
Fuel Flow	lb/hr	11.95	11.97		11.81	11.83		12.03	12.04		11.55	11.52		12.02	12.07	

Table 4

Mode #8

Run#		1	1	d%	2	2	d%
Fuel		BL	OX		BL	OX	
Engine Speed	rpm	3008	3009		3009	3007	
Torque	lb-ft	46.4	37.6	-19	47.7	37.9	-21
NOx	ppm	344	318	-8	330	301	-9
HC	ppm	17	39	133	13	23	79
AVL smoke	FSN	0.96	0.29	-70	1.1	0.30	-74
ICP	Mpa	24	24		24.0	24.1	
Air Fuel Ratio		24.1	24.1		24.2	24.2	
EGR	%	6.4	6.0		9.6	10.2	
SOC-main	deg CA ATDC	6	7		3.0	3.0	
BSFC	lb/hp-hr	0.487	0.584	20	0.462	0.567	23
Fuel Flow	lb/hr	14.63	14.61		14.24	14.24	

Appendix 2

Nuvera Fuel Cells Final Report

PRAXAIR INC./
NUVERA FUEL CELLS

FINAL REPORT

Development of OTM Syngas Process and Testing of Syngas Derived Ultra-clean Fuels in Diesel Engines and Fuel Cells.

Re: DE-FC26-01NT41096

Nuvera Fuel Cells

Nuvera Fuel Cell, Inc.
Acorn Park
Cambridge,
Massachusetts
02140-2390

Project Liaison James Cross
Project Manager Olga Polevaya
Project Engineers Rafey Khan, Piyush Pilaniwalla

Date December, 23, 2002

Summary.

Nuvera Fuel Cells conducted fuel testing within the scope of subcontract to Praxair Inc as a part of DOE initiated and funded Ultra Clean Transportation Fuel (UCTF) program in the area of alternative transportation fuel formulation, emissions and fuel cell power system demonstration. Growing interest in PEM fuel cells as a potential propulsion system for transportation vehicles initiated development of the advanced fuel-making technologies for improving environment and meeting fuel vehicles emission targets. These technologies will enable production of ultra-clean transportation fuels, alternative to gasoline but utilizing it's infrastructure and being cost competitive at the same time. Nuvera Fuel Cells have been investigating autothermal reforming for the series of fuels such as gasoline, methanol, ethanol, diesel and naphthas. Previous efforts were concentrated on the parametric study of syngas production efficiencies and reforming operating conditions. The purpose of the current project was to understand effect of UCTF on the fuel cell system and possibly reduce emissions on a per mile basis.

Funding schedule suggested conducting the program in two phases.

- Phase I commenced in 2001 and was purposed to demonstrate DC power in Nuvera's state-of-art disintegrated fuel cell power train with autothermal (ATR) fuel reforming. Single ultra-clean synthetic fuel was selected for this task and then compared to conventional California Phase II Gasoline fuel for hydrogen and power production efficiency.
- Phase II was completed in 2002 and scoped testing selected fuels in Nuvera's state-of-art burner module. Three fuels including two synthetic fuels and conventional gasoline were compared in terms of start-up and steady state emissions to the environment.

The current report summarizes work conducted within the scope of both phases. Performance of all synthetic fuels tested was referenced to the performance of conventional gasoline fuel, which served the benchmark in the current program and in Nuvera's automotive state-of-art fuel processors. All studied fuels were successfully processed in Nuvera's Modular Pressurized Reactor (MPR) facility and resulted in electrical power produced by the fuel cell stack. The fuels under study were compared in terms of process efficiencies, operating conditions, reformate compositions along the power train and potential emissions to the environment. The reformate gas was analyzed for bulk composition and traces of species, representing poisons to the fuel cell stack and environment. The fuel cell stack polarization curves were recorded and the derating factors on fuel reformates were estimated relatively to operation on pure hydrogen and air. The process condensates have been analyzed at different locations for understanding potential emissions and contaminants to fuel cells and environment.

Phase I. Evaluation of hydrocarbon based fuels in the disintegrated fuel cell power train.

Phase I objectives.

Demonstrate power production and evaluate selected fuels in Nuvera's state-of-art disintegrated fuel cell power plant for hydrogen and DC power production efficiency and emissions to the environment.

Experimental.

Two fuels were selected for the studies. California Phase II certified Gasoline was obtained from Chevron Phillips. This commercially available fuel meets the current strict emission standards of the state of California. The second fuel was a Fischer Tropsch naphtha obtained from the Sasol-Chevron joint venture. This is highly paraffin fuel with essentially no sulfur, nitrogen or aromatics, as presented in Table 1.

Table 1. Fuels specifications.

Characteristics	Naphtha	lifornia Phase II RFG
n/Carbon ratio	2.25	1.8
pm	<1	35
s, Vol. %	0.5	28.1
Vol. %	0.5	7.5
gravity at 60 F, g/l	.6906	0.7377
eating Value, LHV, BTU/LB	9130	18553

Both fuels under study were processed into hydrogen containing reformates in Nuvera's disintegrated Modular Pressurized facility (MPR), shown in Fig. 1.

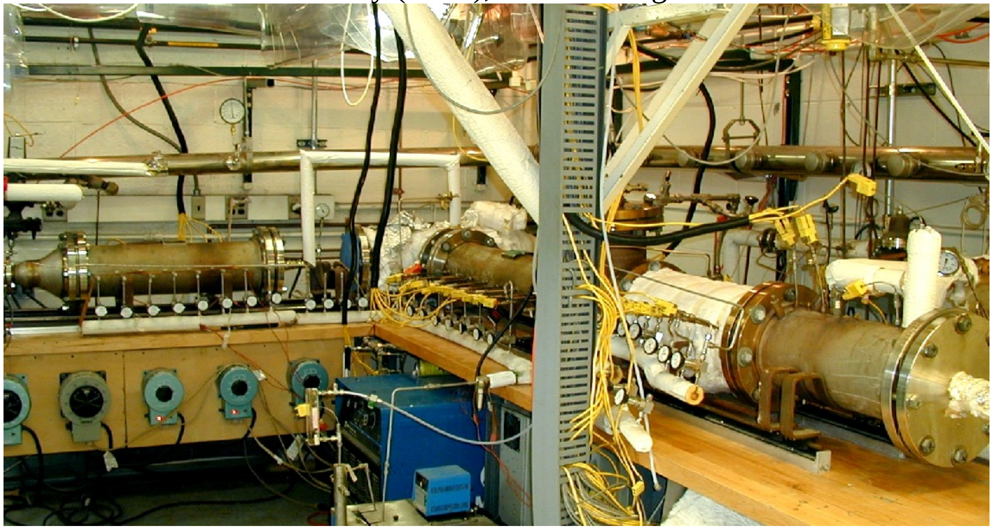

Figure 1. Modular Pressurized Facility (MPR). The upstream section, including ATR and WGS sections.

This pilot plant facility comprises the totality of fuel cell based power-producing functionality, including temperature management modules, fuel reforming spool, high- and low-temperature Water-Gas-Shifts (WGS), optional sulfur capture module, two-stage preferential-oxidation based CO cleanup, and flexible PEM fuel cell test stand shown in Fig. 2.

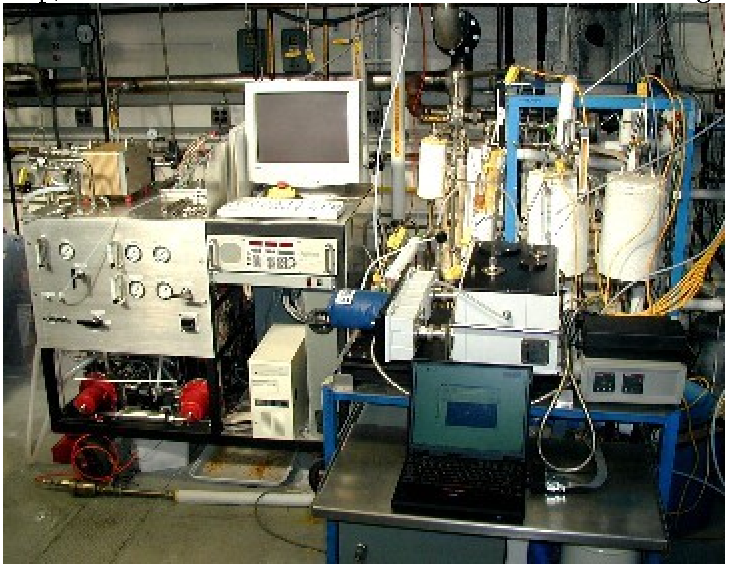

Figure 2. MPR Downstream Section, including reformate clean up and fuel cell test stand.

The maximum firing rate for the front-end assembly, including preheat, ATR and WGS sections are 140 kWth (based on the Lower Heating Value (LHV) of the fuel; for the downstream assembly, they are 40 kWth of hydrogen flowrate. Because of the differences in ratings between the upstream and downstream sections, provisions for bypassing the excess of reformate flow to the exhaust manifold have been incorporated into the assembly – a flow diagram illustrating this is shown in Figure 3.

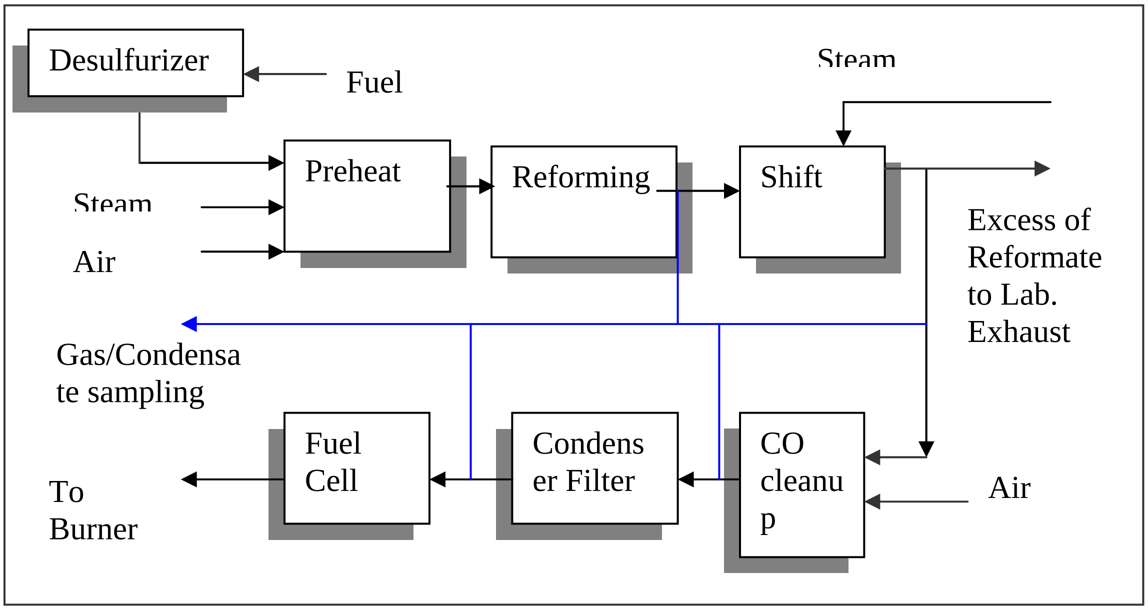

Figure 3. Experimental layout of the disintegrated power train.

Nuvera's custom desulfurization module, external to the MPR, was installed to decrease the initial concentration of sulfur in gasoline from 35 parts per million to less than 1 ppm, which is tolerated by the catalyst modules the fuel processing train comprises of. Gasoline was desulfurized prior to inletting reforming section of the MPR train. The sulfur level before and after the adsorption traps were measured in real time during the experimental runs using the UV fluorescence sulfur detector with a lower detection limit of 200 ppb of sulfur. Sampling ports for sulfur analysis were located at the desulfurizer exit and at the exit of CO clean-up section. Resulting concentration of sulfur at the exit of desulfurization module was recorded below the referenced detection limit.

Results and discussion.

The fuel specifications were analyzed and a matrix of operating conditions for fuel reforming suggested. In all the experiments the operating pressure was maintained constant at 30 psig at the reformer inlet, while fuel cell stack operating downstream pressure was maintained at 22 psig allowing pressure decrease along the fuel processor, fuel cell and clean-up reactors.

Each fuel was mixed with the steam, preheated for vaporization and sent to the ATR section, containing Nuvera's proprietary catalytic module. In all the experiments the fuel thermal input has been maintained at 60 KW based on the lower heating value (LHV) of the fuel with the fixed equivalence ratio and steam-to-carbon ratio. Equivalence ratio (ϕ) is calculated as

ϕ = (actual fuel flow/ actual air flow)/ (stoichiometric fuel flow/ stoichiometric air flow).
Steam-to-carbon (S/C) ratio is calculated as
S/C = molar steam flow/ molar carbon flow.

Increasing both ϕ and steam-to-carbon ratio result in higher hydrogen yield but require higher process heat input in case of high steam-to carbon ratio and risk of carbon formation at the catalyst or high methane slip in case of increasing equivalence ratio. Higher ϕ also yields less process heat release to satisfy the entire system heat balance requirements and results in lowering temperature profile inside the reformer risking to elevated methane slip or potential poisons to all catalytic modules and the fuel cell.

Equivalence ratio of air to fuel was originally planned to maintain at 3.65 for both fuels to maximize the hydrogen yield. In case of naphtha processing we were able to maintain the equivalence ratio close to the designed value and satisfy the required temperature profile in the fuel processor at the same time. During gasoline fuel processing ϕ had to be lowered to 3.36 to maintain the required temperature profile in the reactor and avoid skipping non-converted aromatics. Steam-to-carbon ratio was maintained at 3.4 in all the experiments. The reformate gas has been further processed in the WGS reactors followed by the cleanup from carbon monoxide. Both fuels were successfully processed in Nuvera's MPR facility and the reformates were considered "clean" and contained no poisons to the fuel cell stack.

Maintaining designed temperature profile in multiple reactors, required to process sulfur containing gasoline, is a complicated task, and additional restrictions were imposed on the controls and operating strategy. Stability of the operating regime reflected consistency of the reformate composition data, recorded over the running time, through the wider deviation of bulk gas concentrations from the average values in case of gasoline reforming, shown in Table 2.

Another source of the measurement error in the experiment was gas chromatograph (GC). All the steady state concentrations recorded by GC are reproduced within the GC measurement error.

Table 2. Fuel Processing data of Naphtha vs. Gasoline.

eformate bulk composition	**a Reformate composition**	**e Reformate composition**
en, Vol.%, dry base	0.49	- 1.91
n, , Vol.%, dry base	0.68	- 2.32
dioxide, Vol.%, dry base	0.16	- 0.30
e, Vol.%, dry base	0.01	0.08

Analysis of carbon mass balance based on GC measurements of reformate composition allowed comparing amount of carbon processed into CO, CH_4 and CO_2 to the initial amount of carbon inletting the processor as a fuel. The carbon balance is calculated for every processed fuel at each load point during the steady state operation to verify that no carbon formation occurred. Another direct indication of carbon formation is pressure drop along the reformer. Significant carbon formation would result in increase of pressure drop, which was not observed in any of studied cases. Multiple samples were collected at the steady state to ensure repeatability. Collected samples were conditioned and sent to a specially configured GC. Detection limit of oxygen concentration measured by GC was 0.1 mol.%. No oxygen was detected at any point beyond the low detection limit.

Hydrogen production efficiency η_{HP} is calculated as

$$\eta_{HP} = H_2 \text{ flow} * LHV_{H2} / \text{Fuel flow} * LHV_{Fuel}$$

The above expression is well suited for hydrogen production efficiency of entire fuel processor. To estimate hydrogen production efficiency of each section of the fuel processor, the above expression can be converted into equation

$$\eta_{HP} = 201.63\ (Y^{d}_{H2} / \Sigma Y^{d}_{Ci}) * (Cw\% / LHV_{Fuel}) * X_f,$$

where

Cw% is the carbon weight percentage of the fuel,
Y^{d}_{H2} is the hydrogen dry volume concentration from GC data,
ΣY^{d}_{Ci} is the sum of hydrogen dry volume concentrations of CO, CH_4 and CO_2 from GC data,
LHV_{Fuel} is the lower heating value of the fuel, kJ/kg
X_f is the conversion ratio of the fuel defined as $(N_{CO}+N_{CH4} + N_{CO2})/m*N_{fuel}$
N_{ii} – is the mole flow rate of component i,
m is the carbon number of the fuel defined as $C_mH_nO_o$.

Nuvera's model takes into account both material balance and chemical reaction equilibrium to predict the outcome of fuel processing at the designed operating conditions. The model, implemented in Hysis software, calculates theoretical equilibrium composition of all reaction species at the temperature values experimentally verified in the MPR power train.

GTL Naphtha fuel processing resulted in the highest hydrogen yield and hydrogen production efficiency, which was predicted by model calculations and could be attributed to its highest H/C ratio. The increasing trend in hydrogen production with increasing H/C ratio is obtained experimentally for both fuels studied and confirmed by the model prediction shown in Figure 4 and 5. Methane slip was slightly higher in case of gasoline processing affected by lower operating temperature profile.

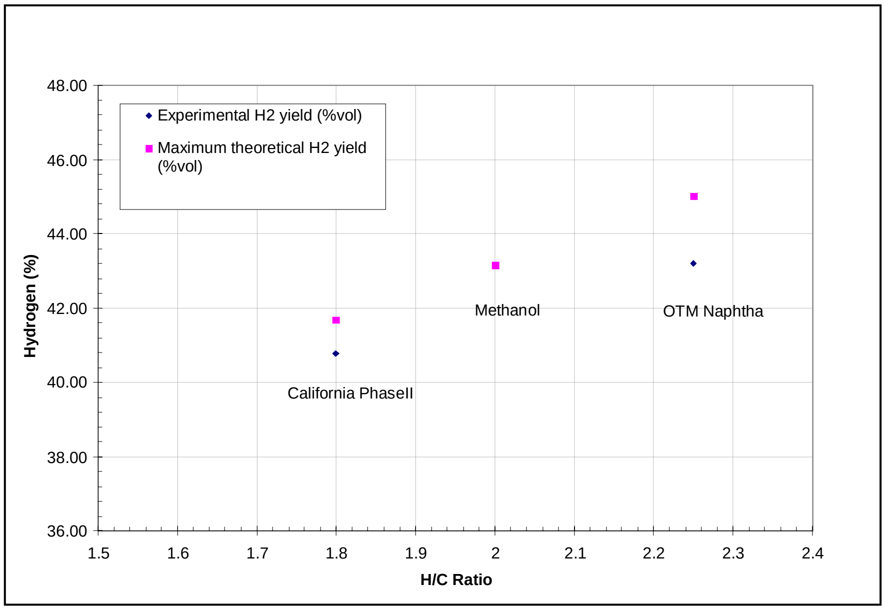

Figure 4. Hydrogen yield (experimental vs. theoretical) data at the entrance to fuel cell stack for fuels with different hydrogen-to-carbon ratios. Oxygen concentration in the fuel is accounted in methanol case for comparison.

The difference between theoretical and experimental points for gasoline fuel is about 0.8 volumetric percents of hydrogen , which is within the experimental error of 1.9 vol.%, this point was obtained with, as shown in Table 2.The difference between theoretical and experimental points for naphtha fuel is about 1.5 vol. % of hydrogen , which is higher than the experimental error of 0.49, this point was obtained with, as shown in Table 2. Higher difference between experimental and theoretical values recorded in naphtha processing versus gasoline was attributed to operating strategy of the clean-up section purposed to decrease the concentration of carbon monoxide below 20 ppm. This strategy was sacrificial to the concentration of hydrogen in the reformate stream. Since the current study was purposed on characterization of the entire power train, it was very important to balance all the subsystems within certain operating ranges, close to optimal to specific section but without sacrificing performance of another section of the power train at the same time, including the fuel cell stack.

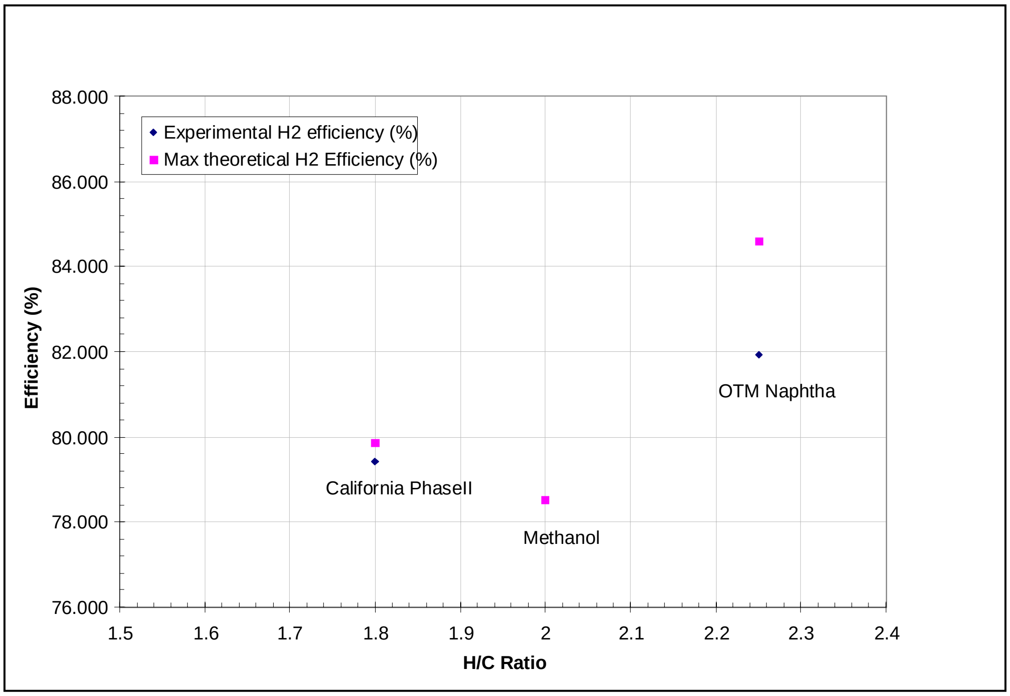

Figure 5. Hydrogen production efficiency (experimental vs. theoretical) at the entrance to fuel cell stack for fuels with different hydrogen-to-carbon ratios. Oxygen concentration in the fuel is accounted in methanol case for comparison.

To prove the good fuel conversion – close to equilibrium of the shift reaction- we compared the theoretical model to the experimental data at the exit of LTS section, presented below in Figures 6 and 7. For both studied fuels experimental data are close to the data predicted by modeling within the error ranges.

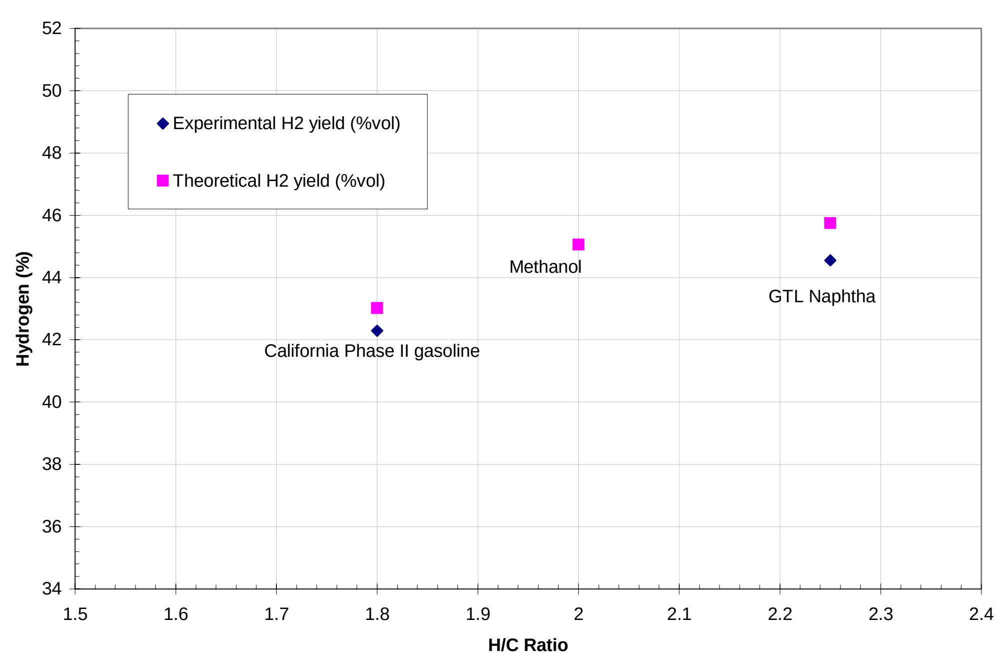

Figure 6. Hydrogen yield at the exit of LTS section (experimental vs. theoretical) data.

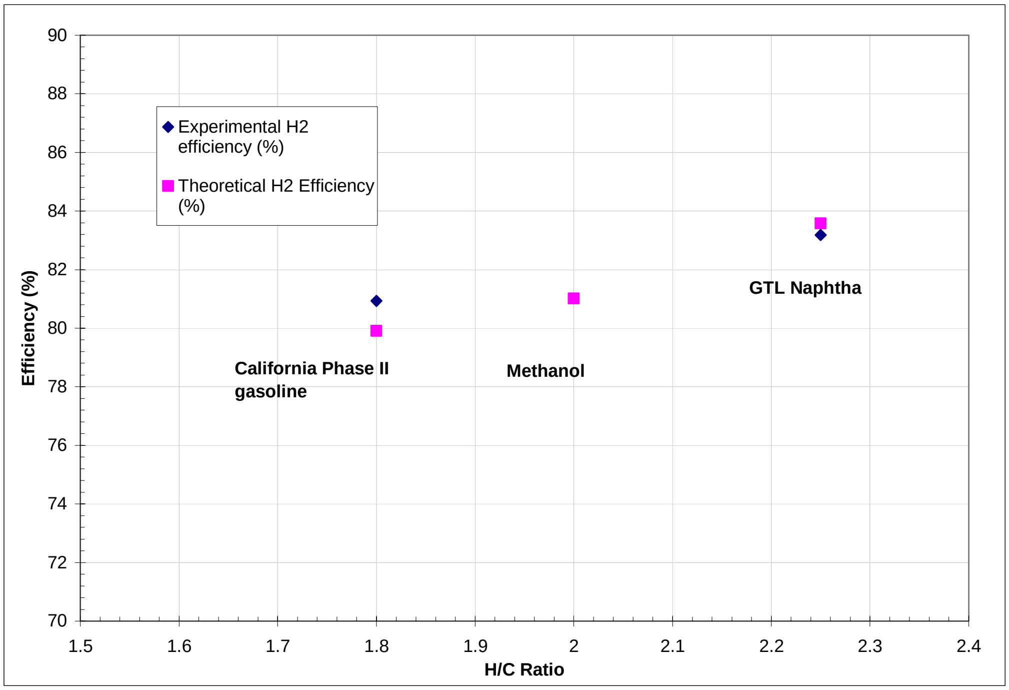

Figure 7. Hydrogen production efficiency at the exit of LTS section (experimental vs. theoretical) data.

Reformate flow was split after the LTS section of the fuel processor, in order to adhere to the maximum PROX throughput specification of 40 kW_{th}. Actual flow sent through the PROX was maintained at about 12 kW_{th}, based on the fuel cell stack size selected and the objective of running at realistic conditions (anode stoichiometries from 1.4-1.8). Carbon monoxide concentration at the PROX exit was varying in time, but consistently below 20 ppm in all fuel experiments.

The FTIR technique (model MIDAC 2001) had been used to detect species at low concentrations in both fuel reformates in the gas phase. The FTIR had been calibrated for aromatic species and ammonia. The sample to the FTIR was collected at the exhaust of clean-up section of the reforming process, which was the entrance to the fuel cell stack. In both studied reformates concentrations of above species were below detection limit of the FTIR.

As a complement to gas-phase analysis, process condensate was collected and analyzed for water-soluble species in the reformate streams, including volatile organic compounds (VOC), ammonia, metal ions and other potential contaminants. Samples were collected at two different locations:
(1) at the exit of CO cleanup section – fuel cell anode entrance
(2) at the fuel cell anode exhaust

At the exit of CO cleanup section low concentrations of aromatic compounds have been detected in the reformate condensates. The detected levels were close to the detection limit, varied from

25 to 100 ppbv depending on sample dilution. Ammonia concentration in the condensate of the gasoline reformates after CO cleanup section was detected under 3 ppm. The total organic carbon (TOC) level varied below 5 ppm at the end of the power train for both fuel reformates. No above species have been detected in the condensates at the exit of the fuel cell stack operated on gasoline or naphtha reformates. For those species found elevated above the detection limit in the condensate analysis, but not detected in the gas phase, an estimation of the level in the gas phase was made based on partitioning equilibrium (Henry’s Law). At a temperature of 25°C, the coefficient between the gas and liquid phases for ammonia is ~2.7. This means that 1-2 mg NH3/liter of water in the liquid phase would correspond to approximately less than one ppm of ammonia in the gas phase. This calculated concentration is difficult to detect even using FTIR due to the low detection limit.

The fuel cell stack used is shown in Figure 2, consisted of 30 cells and produced more than 3.25 KW of electrical DC power operating on pure hydrogen and air.

The difference in hydrogen concentration in gasoline and naphtha reformates was insignificant to change the polarization characteristics of the fuel cell, shown in Figure 8.

The same stack was used for power generation on both fuel reformates. The base line polarization curve was recorded on hydrogen/air before introducing reformates to the stack and between the expriments with different fuels. There was no signs of short-term performance degradation caused by feeding the stack anode with neither of the reformate streams. The reformate flow entering the stack was maintained constant and equivalent to 12 kW of the fuel thermal input.

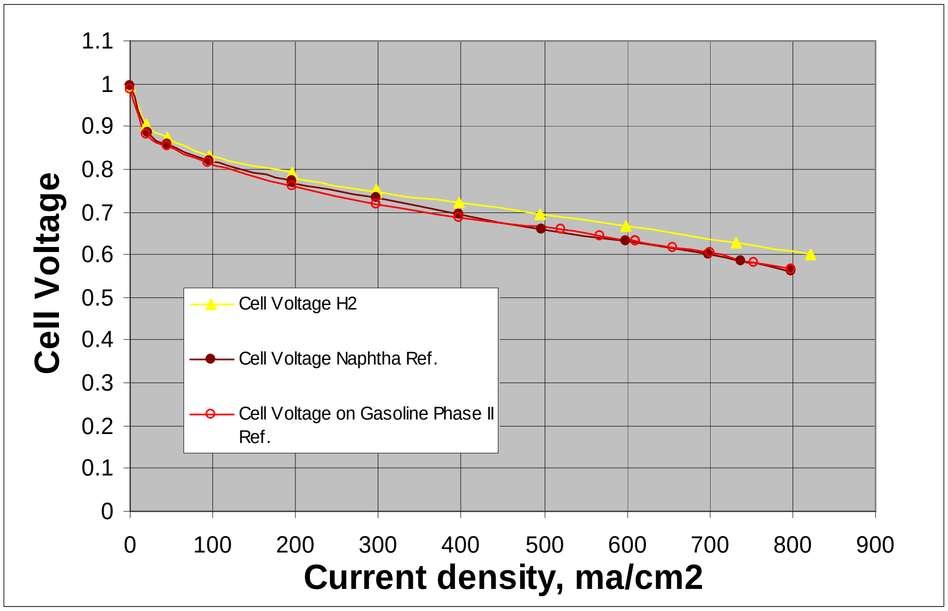

Figure 8. Polarization curves recorded on Naphtha and Gasoline Phase II ATR reformates vs. hydrogen/air performance.

It is possible to estimate the gross efficiency, denoted $_{DC,gross}$, experimentally recorded at the MPR-fuel cell setup, as a ratio of the gross electrical power produced by the fuel cell to the calculated fuel input equivalent to the fuel processor (12 kWe, as previously stated).

$_{DC,gross}$ = 3.25 kWe/ 12 kWth = 27% (LHV basis)

For a laboratory demonstration with no process optimization as in this study, this number is reasonable. In an integrated system, higher efficiencies would be achieved effected by anode hydrogen utilization and supplementing fuel to the burner. The specific operating conditions of the stack were as follows:

- Cathode stoichiometry of 2 was maintained constant at all the points on polarization.
- Anode flow was maintained constant at all the points on polarization chart equivalent to anode stoichiometry of ~1.5 at the highest current density reached.
- The stack temperature was maintained at 70ºC measured at the cathode exhaust. The cathode air inletting the stack was humidified at the temperature of 65ºC above 80 % of relative humidity using external to the stack Nuvera's humidification module. The stack has an internal cooling loop utilizing deionized water as a coolant.
- The DC power produced by the stack was recorded and sustained by the electronic Dynoload operated in the constant current mode.
- Both anode and cathode of the stack were maintained at 2.5 bara of downstream pressure in all the fuel reformate experiments.
- The fuel cell had been running on every fuel reformate for about one hour to allow stabilization of cell voltages at the current density up to 800 mamp/cm^2 and recording fuel cell utilization confirmed by GC analysis of inlet and outlet anode flow composition. GC measurement also served as a confirmation of total amount of hydrogen presented in the incoming reformate flow after PROX and condenser units. At the end of each fuel cell run the polarization curve shown in Figure 8 was recorded.

The derating factor on fuel reformates versus operation on pure hydrogen is calculated as the difference between voltage sustained by the fuel cell on pure hydrogen and fuel reformate at the same operating current density. This approach defines the performance or voltage derate, denoted $_V$, and, on both reformates, is estimated at 4.5% of power at 400 mA/cm2 of current density and about 7% at 600 mA/cm^2 versus power production on pure hydrogen at the corresponding current densities. The power production curves are shown in Fig.9

D

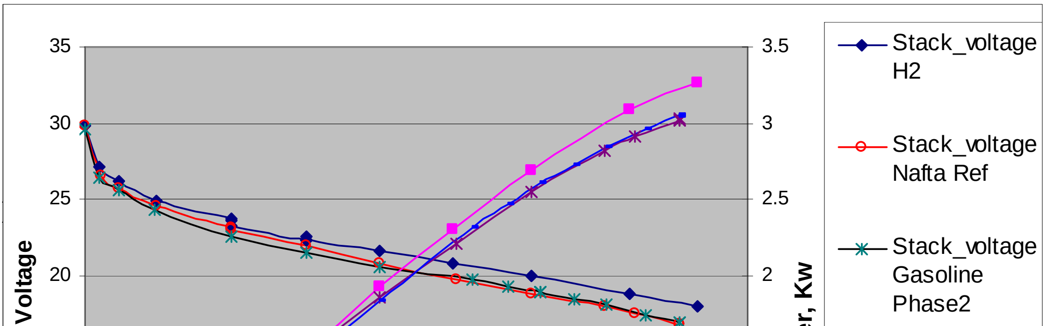

Figure 9. Power production of 30 cell stack on Naphtha and gasoline reformates vs. pure hydrogen.

Maintaining high hydrogen utilization at the fuel cell anode at the elevated current densities is a technical challenge associated with the decreased concentration of hydrogen along it's consumption and increased dilutants – nitrogen, carbon dioxide and water- at the exit of the stack. Maintaining water balance to avoid stack flooding represent current state-of-the art technology along with the insights of the fuel cell stack , adding complexity to the issue of reformate utilization and ,finally, efficiency. Mapping hydrogen utilization by the fuel cell stack operating on fuel reformate to the current density would result in the stack sizing tradeoff issues versus operating efficiency and would be the subject of separate study.

Conclusions of Phase I.

- GTL Naphtha and California Phase II RFG were successfully processed into fuel cell quality reformate in Nuvera's ATR based modular pressurized facility.
- DC power production was demonstrated in Nuvera's fuel cell stack on both fuel reformates studied.
- Both fuels were studied for hydrogen yield and reforming efficiency and experimental data were compared to the theoretical simulation data.
- Hydrogen yield and reforming efficiency demonstrated by naphtha processing were higher than for gasoline fuel, which was predicted by system analysis of both fuels. Since gasoline contained sulfur, the power train configuration had an increased complexity and maintaining stable temperature profile became a challenging task in comparison to naphtha processing.
- The power production in the fuel cell stack was not effected by operating on different fuel reformates, since hydrogen partial pressure in the reformate streams varied insignificantly.
- The gross efficiency of the power production in fuel cell is estimated at 27%, considering 3.25 kW electrical output of the stack and the fuel thermal input of 12 kW. In the stand-alone fuel cell power plant more parameters affect efficiency. Hydrogen utilization at the anode and necessity of fuel supplement in the burner would strongly influence the overall power plant efficiency.
- Both fuel reformates were considered equivalent in terms of containing no carbon monoxide emissions in the fuel cell exhaust stream to the burner, however, reformate condensates contain micro quantities of "potential bad actors" such as ammonia and aromatics in both fuels studied. Longevity of the fuel cell operation and effects of potential contaminants at micro levels should be the subject of a separate study.

Phase II. Testing of Syngas-Derived Ultra-Clean Fuels in Nuvera's burner module for start-up emission study.

Phase II objectives.

Evaluate selected fuels: GTL naphtha, oxygenated GTL naphtha and California Phase II RFG in Nuvera's burner module and compare emissions produced in the fuel processing/fuel cell power plant. The GTL naphtha was oxygenated with a proprietary oxygenate compound, designated BPO, provided by BP.

Experimental.

Nuvera's Burner facility comprises of Nuvera's Burner module, gas and condensate sampling system, and all the process streams required for clean processing of different fuels. The experimental layout of burner facility is shown in Figure 10.

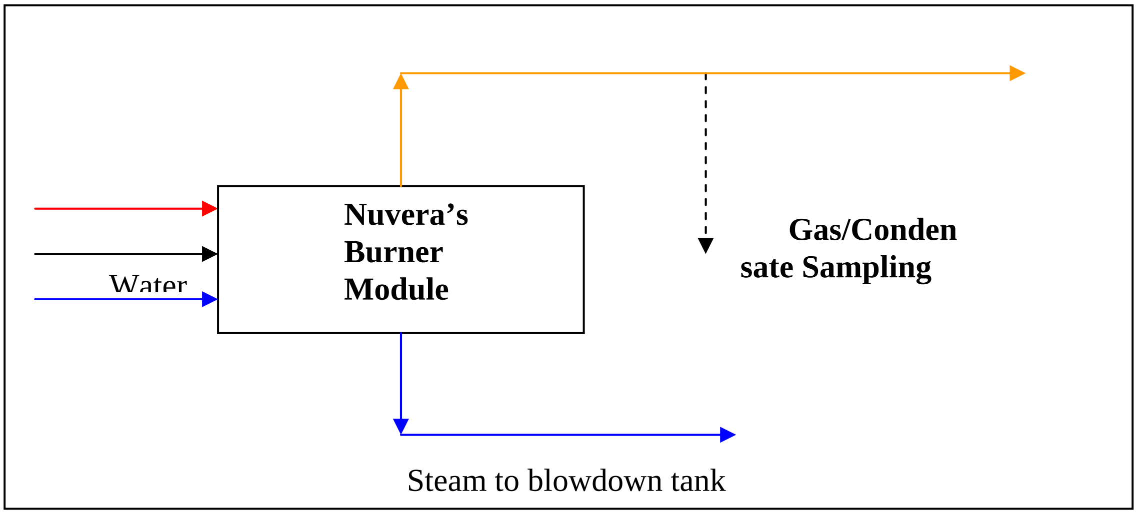

Figure 10: Experimental layout of Nuvera's Burner Module.

Table 3 below contains some characteristics of the fuels studied.

Table3: Properties of fuel used in Nuvera's Burner Module for startup emission study.

Fuel Properties	Oxygenated GTL Naphtha	GTL Naphtha	California Phase II RFG
API Gravity	71.86	73.4	60.57
Specific Gravity, 60F/60F	0.6958	0.6906	0.7367
Density, kg/m^3	695.8	690.6	736.7
C, m%	82.44	84.1	84.96
H, m%	15.82	15.9	13.02
O, m%	1.74	0	2
N, ppm	<1	<1	<1
S, ppm	1	0	32.9
Lower heating value LHV, kJ/kg	43945.89	44357.44	40983.13

$(Air/Fuel)_{stoich}$	14.79	15.08	14.12
Estimated molecular weight, gm/gm-mol	99.4	101.0	100.95

Table 4 below shows operating conditions of the burner module on all studied fuels. To start fuel ignition a slightly rich mixture of fuel and air (air-to-fuel equivalence ratio between 1.2 to 1.4) is introduced to the burner. As soon as the burner is lit, the equivalence ratio is decreased to a lean condition (typically below 0.95) to minimize hydrocarbon emissions.

Table 4: Operating parameters of Nuvera's Burner Module on three fuels studied.

Operating Parameters	**GTL Naphtha**	**Oxygenated GTL Naphtha**	**California Phase II RFG**
Thermal input, based on LHV, kW	12	12	12
Start-up air-to-fuel equivalence ratio	1.39	1.4	1.41
Steady state air-to-fuel equivalence ratio	0.95	0.95	0.95
Operating pressure, bars	1.01325	1.01325	1.01325

Details of Nuvera's gas sampling system and analyzers used in the study are collected in Table 5, showing ranges of concentrations the burner exhaust gas was analyzed for.

Table 5: Emission species and concentrations analyzed.

Emissions Species	**Units**	**Maximum Analysis Range**	**Analyzer Unit**
CO	ppm	1000 ppm	Horiba infrared analyzer model number VIA-510
CO	vol %	50%	Horiba infrared analyzer model number VIA-510
CO2	vol %	25%	Horiba infrared analyzer model number VIA-510
NOx	ppm	2000 ppm	Horiba chemiluminescence analyzer model number CLA-510SS
O2	vol %	50%	Horiba magnetic pressure analyzer model number MPA-510
THC	ppm	30000 ppm	Horiba flame ionization analyzer model number FIA-236

Results and discussion.

All studied fuels were successfully processed in Nuvera's Burner Module for start-up emissions. Exhaust gas composition was analyzed for bulk components such as carbon dioxide, water vapors and oxygen, and traces of species, such as NOx, carbon monoxide (CO) and total hydrocarbons (THC) that are governed by emission standards from the Environmental Protection Agency (EPA). In addition, process condensates were collected for analysis of water contaminants in the burner exhaust. The fuels under study were compared in terms of burner module operating conditions, exhaust compositions, start-up and steady state emissions.

In order to compare emissions from Nuvera's Burner module to the EPA standards, recorded concentrations of emission species in parts per million (ppm) are presented in milligrams per gram of fuel (mg/gfuel) units in Figure 11, 12, and 13 for naphtha, oxygenated naphtha and California Phase II RFG respectively

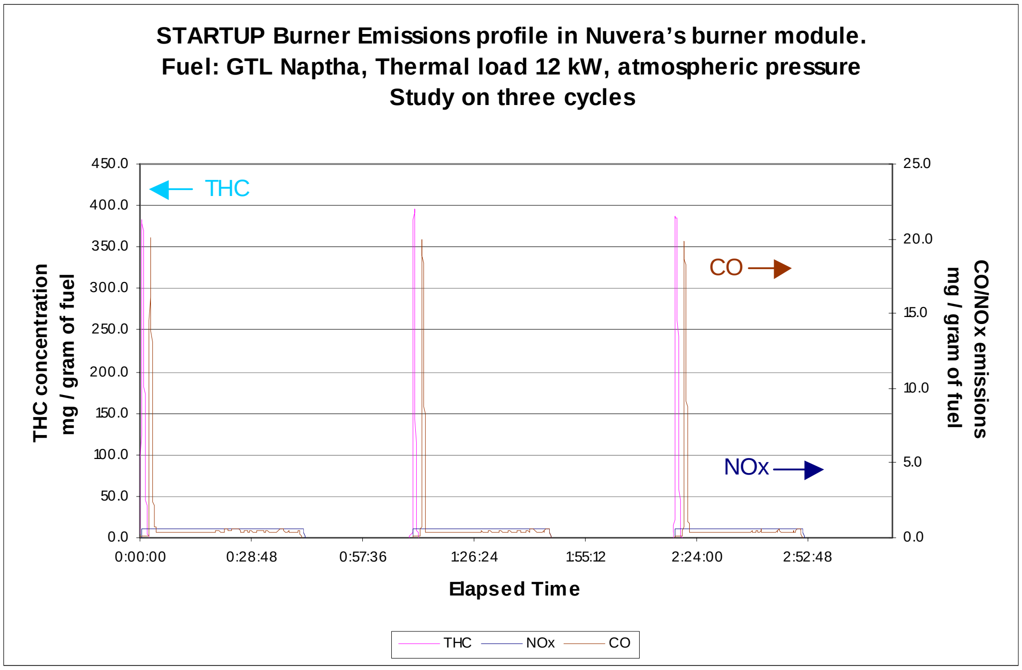

Figure 11: Burner emissions on GTL Naphtha.

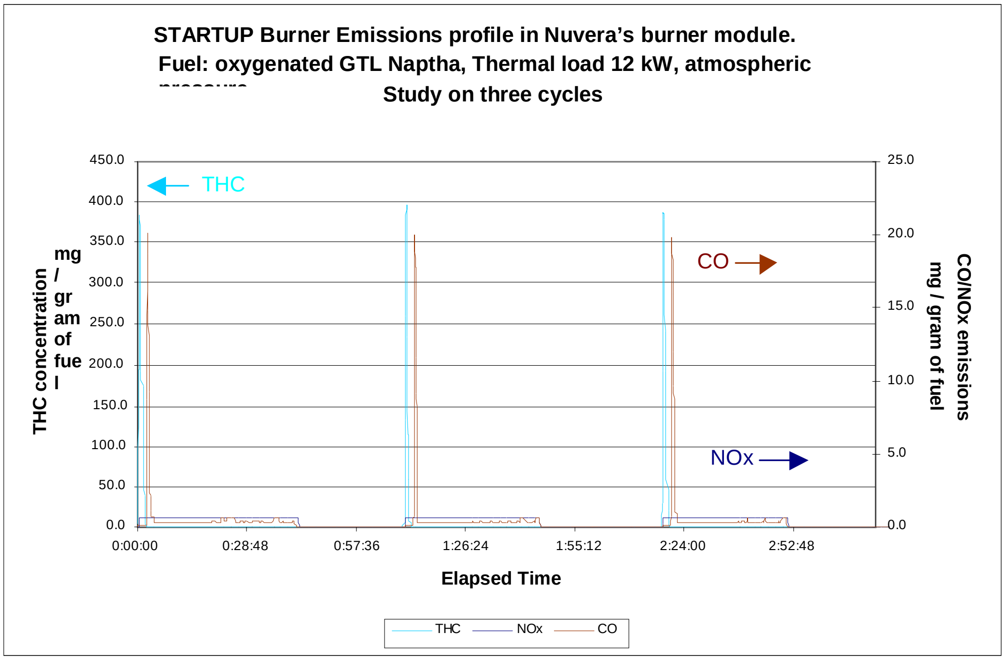

Figure 12: Burner emissions on oxygenated GTL naphtha.

D

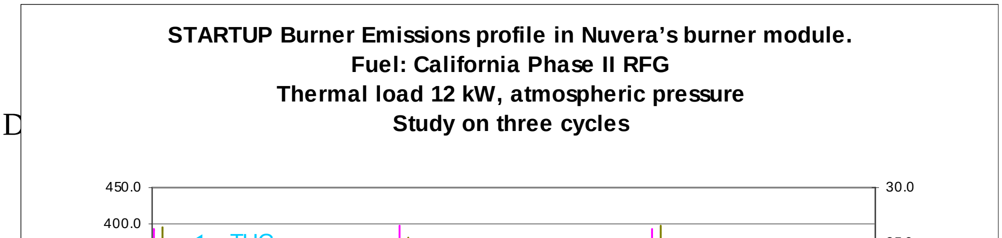

Figure 13: Burner emissions on California Phase II RFG.

To ensure repeatability of the experiments, the burning cycle of each fuel was conducted at least three times starting with the fuel ignition through the startup and steady state phase and ending with cooling burner to initial temperature. All concentration profiles are highly repeatable for each fuel as shown in Figures 11,12 and 13.

All fuels show spikes of THC and carbon monoxide emissions at the burner startup. This is attributed to unburned fuel skipping through the module when it is lit initially. The CO spike occurred due to incomplete fuel combustion. No spikes in NOx emissions were recorded for any fuel at the startup conditions. Concentration of NOx is much less than the concentration of CO and THC as shown in Figure 11,12 and 13. Comparison of NOx concentration profiles at the startup conditions is shown in Figure 14 for all fuels studied.

There are two principal sources of nitrogen oxide (NOx) formed during combustion: one is oxidation of atmospheric (molecular) nitrogen and another is oxidation of nitrogen-containing compounds in the fuel. During combustion of studied “clean” fuels, containing no nitrogen compounds, under lean or stoichiometric conditions the thermal mechanism is the principal source of nitrogen oxide emissions

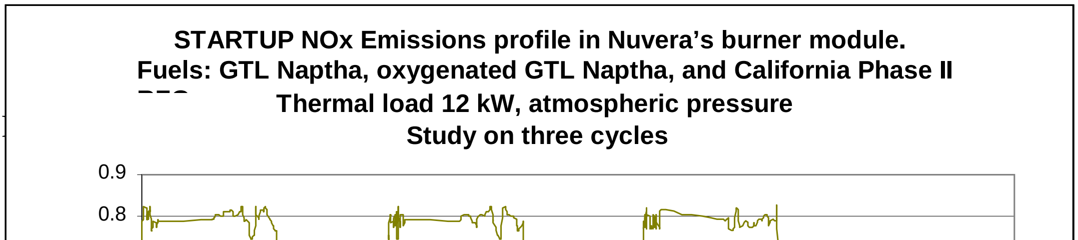

Figure 14: NOx emissions profile of studied fuels.

Integrated startup emissions for all three fuels tested are shown in Table 6 and are reported on the mass basis in milligrams per gram of every fuel and in gram of emission species per driving mile. To present the recorded data in the latter units, the current Corporate Average Fuel Economy (CAFÉ) standard of 27.5 miles per gram of fuel was used in calculation. The integrated values were calculated using total amount of startup emissions divided by the amount of fuel used during respective startup time.

Table 6: Emissions at startup.

FUEL	**mg per gram of fuel**			**gram per mile**		
	CO	**THC**	**NOx**	**CO**	**THC**	**NOx**
GTL Naphtha	7.34	110.78	0.57	0.70	10.53	0.05
Oxygenated GTL Naphtha	5.61	78.07	0.23	0.54	7.48	0.02
California Phase II RFG	6.28	92.24	0.79	0.64	9.35	0.08

Table 6 shows that oxygenated GTL naphtha has the lowest CO, THC, and NOx startup emissions among all fuels tested. This can be attributed to the oxygen added to the fuel. GTL naphtha and oxygenated GTL naphtha have almost the same fuel blend except oxygenated GTL naphtha contains 1.74% oxygen. It seems that adding oxygen to the fuel results in more complete fuel combustion and, subsequently, reducing tailpipe emissions. Oxygenated fuel also tends to provide more complete combustion of its carbon into carbon dioxide (CO_2), thereby reducing emissions of hydrocarbons and carbon monoxide. Even though both oxygenated GTL naphtha fuel and California Phase II RFG gasoline have similar oxygen concentration in the fuel (1.74 and 2 % respectively), emissions from gasoline burning are higher than emissions from oxygenated GTL naphtha. This could be explained by high percentage of aromatic compounds in California Phase II RFG, which satisfies it’s high octane rating.

Emissions recorded during steady state combustion are shown respectively for all fuels studied in Figures 15, 16, and 17

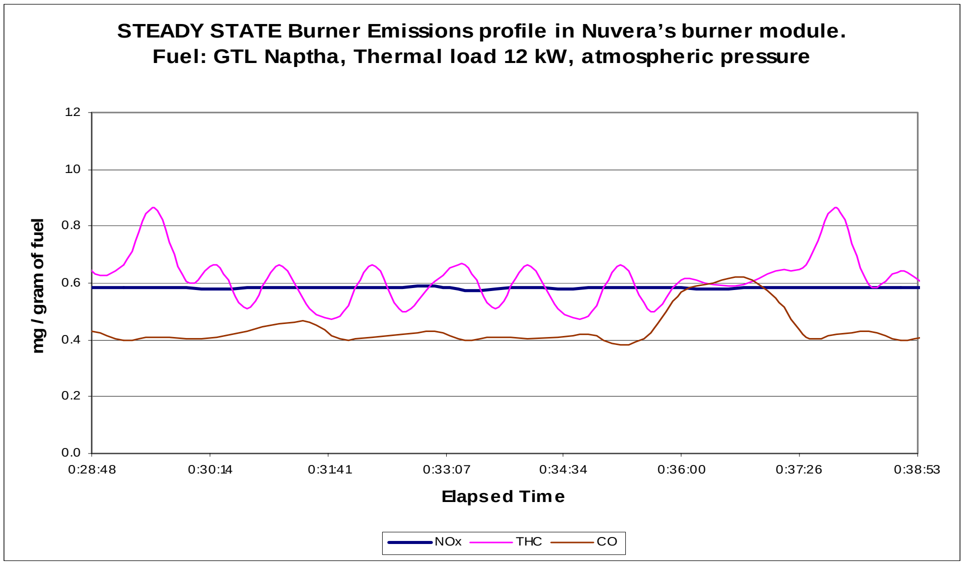

Figure 15. Steady state burner emission on GTL naphtha.

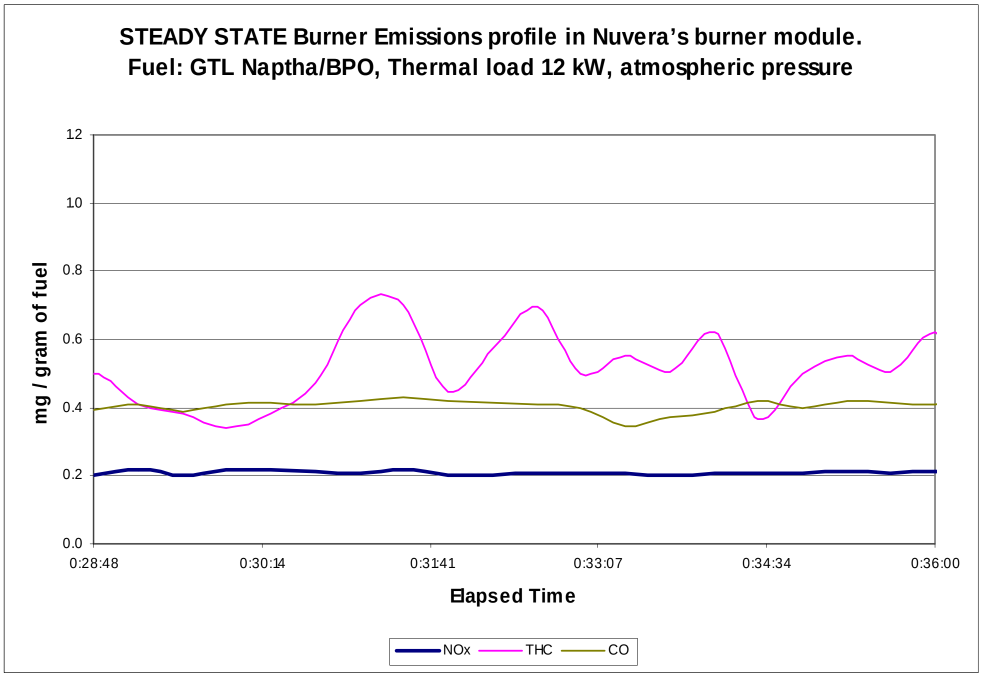

Figure 16. Steady state burner emissions on oxygenated GTL naphtha.

I

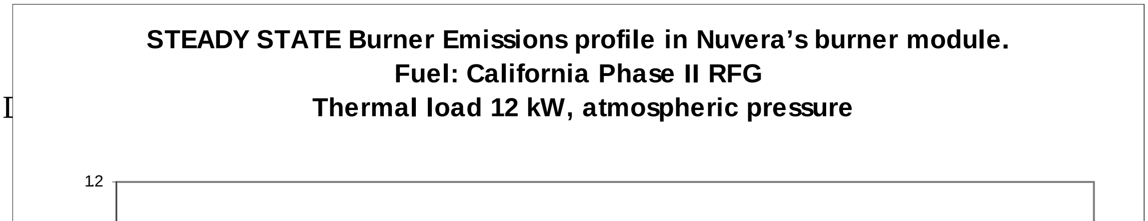

Figure 17. Steady state burner emissions on California Phase II RFG.

Table 7 shows steady state emissions of three fuels averaged throughout the single burning cycle. Note, that quality of Nuvera's burner exhaust gas satisfied all the Federal standards for light duty vehicles including ULEV requirements for CO and Nox, as shown below.

Table 7. Emissions throughout steady state.

FUEL	**mg per gram of fuel**			**gram per mile**		
	CO	**THC**	**NOx**	**CO**	**THC**	**NOx**
Federal Standard for Light Duty Vehicle – Tier 1				4.2	0.31	0.6
Federal Standard for Light Duty Vehicle – Ultra Low Emission Vehicles (ULEV)				2.1	-	0.3
GTL Naphtha	0.42	0.61	0.57	0.040	0.058	0.054
oxygenated GTL Naphtha	0.41	0.61	0.23	0.039	0.058	0.022
California Phase II RFG	0.55	0.52	0.79	0.056	0.053	0.080

Addition of oxygen to the naphtha blend did not effect steady state emissions of hydrocarbons and carbon monoxide as shown in table 7. However, NOx emissions are decreased in the oxygenated naphtha fuel blend that may be attributed to the oxygen presence in the fuel. Table 7 indicates that California Phase II RFG produced the highest amount of poisons to the environment on the absolute mass basis, and from this point could be considered the worst fuel blend among all three fuels at the steady state conditions. This can be attributed to high-octane aromatics presence. At the same time gasoline produced less total hydrocarbons than synthetic fuel blends.

Nuvera developed specific FTIR technique to get insights on what hydrocarbon species were released from the burner. The FTIR was calibrated for methane at 15 ppm. The FTIR spectra of the burner exhaust gas showed levels of methane close to the recorded by flame ionization detector concentrations of THC for all three fuels studied. The found phenomenon could be specific to the performance of the catalyst in the burner rather than fuel inherited, since fuels of different structure were burned resulting in dominating amount of methane in the THC emissions.

Table 8 shows average concentrations of bulk gases in the burner exhaust: oxygen and carbon dioxide for all three fuel blends.

Table 8. Oxygen and carbon dioxide emissions.

	vol. %	
Fuel	**O_2**	**CO_2**
GTL Naphtha	13.85	6.04
Oxygenated GTL Naphtha	13.72	5.76
Cal Phase II RFG	11.85	10.8

GTL naphtha and oxygenated GTL naphtha have almost the same oxygen and carbon dioxide concentrations in the burner exhausts. This is expected since both fuels have almost the same fuel compositions. It seems that adding oxygen to the Naphtha blend didn't influence oxygen and carbon dioxide emissions significantly.

In addition to the gas phase analysis process condensates were collected at the burner exhaust and analyzed for volatile organic compounds, metal ions, ammonia, aldehydes and other poisons to the environment, results are shown in Table 9. All condensates had been collected in steady state condition, while running fuels through the burner in the steady state. Several condensate samples were collected from the same operating regime to ensure repeatability

Table 9. Condensate analysis.

Fuel	NH3, ppmv	Acetaldehyde, ppmv	Formaldehyde, ppmv	Benzene, ppbv	Toluene, ppbv	Ethyl Benzene, ppbv	Xylenes, total, ppbv
GTL naphtha	1.8-2.1	0.13	1.35	Below detection limit (Bdl)	Bdl	Bdl	Bdl
Oxygenated GTL naphtha	1.1-1.5	0.05	1.29	Bdl	Bdl	Bdl	Bdl
Ca. Phase II gasoline	1.2	0.0002	0.0057	6-7	33-38	12-16	53-68

All fuel condensates contained ammonia and aldehydes, while no aromatic compounds were detected in naphtha's condensates as expected from the fuel structure. Presence of micro quantities of ammonia and aldehydes in the liquid phase suggests that these species are presented in the gas phase as well according to the equilibrium. Example of partitioning between gas and liquid phase for ammonia is described in the phase I of the current report. Analogically this analysis is applicable to aldehydes.

Condensate analysis of volatile organic compounds served an indirect confirmation that most of the THC emissions were not of organic origin but rather methane recognized by the FTIR analysis. Even in the case of gasoline condensates the total concentration of VOC found was around hundreds of parts-per-billion, corresponding through Henry's law to low part-per-million levels of VOC in the gas phase, which was significantly less than the levels of THC recorded by flame ionization detector and methane found by the FTIR.

FINAL REPORT APPENDIX II

Budget Period 2 Topical Report

Conclusions of Phase II.

- GTL naphtha, oxygenated GTL naphtha and California Phase II gasoline were successfully tested in Nuvera's Burner Facility for start-up and steady state emissions.
- Exhaust gases from all fuels tested were analyzed for bulk gases such as carbon dioxide and oxygen and emissions of CO, NOx, and total hydrocarbons.
- Burner condensates were collected for analysis of potential contaminants to the environment in the liquid state.
- Adding oxygen to the naphtha fuel blend reduced start-up emissions of carbon monoxide, NOx and hydrocarbons.
- Adding oxygen to the naphtha fuel blend did not effect the steady state emissions of carbon monoxide and hydrocarbons but resulted in reducing NOx emissions.
- Adding oxygen to the naphtha fuel blend did not affect the oxygen and carbon dioxide emissions.
- Burning oxygenated GTL naphtha resulted in the least amount of emissions among the three fuels studied due to oxygen presence and lack of high-octane aromatics.
- Hydrocarbon emissions consisted of mostly methane, not VOC compounds.
- All processed fuels produced fewer emissions than Federal standards require for Light Duty Vehicles on a per mile basis in the steady state conditions. Oxygenated naphtha resulted in the least absolute amount of emissions on a per mile basis. California phase II gasoline proved to yield the highest emissions in the steady state.
- Oxygenated naphtha was mostly clean among all fuels at the startup conditions, while GTL naphtha produced higher emissions than gasoline fuel.
- All fuel after-burner condensates contain micro levels of ammonia and aldehydes. Gasoline fuel condensate also contained ppb levels of aromatic compounds. It is possible to speculate on the level of micro contaminants found in the liquid phase for the gas phase, however, it would be the subject of further research beyond the scope of the current program.

FINAL REPORT APPENDIX III

Topical Report – Budget Period 3

Development of OTM Syngas Process and Testing of Syngas Derived Ultra-clean Fuels in Diesel Engines and Fuel Cells

Budget Period 3

Topical Report

For Reporting Period Starting January 1, 2003 thru December 31, 2004

Principal Authors:
E.T. (Skip) Robinson, Principal Investigator, Torix
John Sirman, Program Administrator, Praxair
Prasad Apte, Ceramic Manufacturing Manager, Praxair
Xingun Gui, Chief Engineer, Advanced Combustion and Control,
International Truck and Engine Corp.
Tytus R. Bulicz, Project Development Engineer,
International Truck and Engine Corp.
Dan Corgard,, Senior Development Engineer, Future Technology,
International Truck and Engine Corp.
Siv Aasland, Staff Engineer, Statoil
Kjersti Kleveland, Staff Engineer, Statoil
Ann Hooper, Process Supervisor, Foster Wheeler
Leo Bonnell, Process Supervisor, Foster Wheeler
John Hemmings, Director, Technology and Chemicals, Foster Wheeler
Jack Chen, Senior Development Associate, Praxair
Bart A. van Hassel, Senior Development Associate, Praxair

Report Issue Date: May, 2005
DOE Cooperative Agreement No. DE-FC26-01NT41096

Submitting Organizations:

Primary:
Praxair, Inc.
P.O. Box 44
175 East Park Drive
Tonawanda, NY 14150

Subcontractors:

Statoil ASA
Postuttak
N-7005 Trondheim, Norway

International Truck and Engine Corp.
10400 W. North Avenue
Melrose Park, IL 60160
Naperville, IL 60566

Foster Wheeler USA Corporation
2020 Dairy Ashford Road
Houston, TX 77077

Torix, Inc
7165 Hart St., Suite B
Mentor, OH 44060

BP America Production Company
150 W. Warrenville Road
Mail Code H-5,

DISCLAIMER

ABSTRACT

This topical report summarizes work accomplished for the Program from January 1, 2003 through December 31, 2004 in the following task areas:

Task 1: Materials Development
Task 2: Composite Development
Task 4: Reactor Design and Process Optimization
Task 8: Fuels and Engine Testing
    8.1 International Diesel Engine Program
Task 10: Program Management

Most of the key technical objectives for this budget period were achieved. Only partial success was achieved relative to cycle testing under pressure

Major improvements in material performance and element reliability have been achieved. A breakthrough material system has driven the development of a compact planar reactor design capable of producing either hydrogen or syngas. The planar reactor shows significant advantages in thermal efficiency and costs compared to either steam methane reforming with CO2 recovery or autothermal reforming. .

The fuel and engine testing program is complete The single cylinder test engine evaluation of UCTF fuels begun in Budget Period 2 was finished this budget period. In addition, a study to evaluate new fuel formulations for an HCCI engine was completed.

FINAL REPORT APPENDIX III

Topical Report – Budget Period 3

TABLE OF CONTENTS

List of Tables Page

List of Figures

List of Acronyms

ATR	Auto-thermal reforming
BDC	Bottom dead center
BPO	BP Oxygenate
BSFC	Brake Specific Fuel Consumption
CI	Compression ignition
CIDI	Compression ignition, direct injection
ECR	Effective compression ratio
EGR	Exhaust gas recirculation
F-T	Fischer-Tropsch
FTGTL	Fischer Tropsch Gas to Liquids
GHR	Gas heated reformer
IMEP	Indicated Mean Expanded Pressure
IVC	Intake valve closing
IVO	Intake valve opening
HCCI	Homogeneous Charge Compression Ignition
LCM	Lead candidate material
MCTE	Multi-Cylinder Test Engine
MM	Alternative material systems
OTM	Oxygen Transport Membrane
OTM-2	Compact planar reactor design optimized for F-T syngas production
OTM-3	Compact planar reactor design optimized for low emission hydrogen production
P-0	Small bench scale test reactors capable of testing single OTM tubes up to 8 inches in length at elevated pressures and temperature.
SCTE	Single Cylinder Test Engine
SMR	Steam methane reforming
TDC	Top dead center
TF	Target Flux
TFd	Target flux for dense disks
TFc	Target flux for composite systems
TP	Target Pressure
TT	Target Temperature
ULS	Ultra-low Sulfur
ULSD	Ultra-low Sulfur Diesel
VVA	Variable valve actuation

1.0 Executive Summary

In this budget period, the program has two major goals:

- OTM Syngas and Hydrogen Technology: lower capital costs, lower operating costs, lower emissions and smaller footprint compared to conventional syngas or hydrogen plants. The baseline technology for comparison of large scale hydrogen production costs is steam methane reforming.
- UCTF in Advanced Diesel Engines: understanding of UCTF impact on contemporary diesel engine performance and emissions and potential of new HCCI engines and fuels to meet longer term performance and emissions targets.

The specific objectives and status are summarized below:

- *Develop a durable OTM system for hydrogen that meets interim cyclability, flux and life targets*.
    - In an extended life test, demonstrate an oxygen flux 0.6TF, 500 hours and 10 thermal and compositional cycles without degradation at TT. This critical goal was achieved with the proprietary film/substrate system LCM61/MM2. Most recently a flux of 0.7TF has been achieved at 0.9TF with a similar system.

    - Demonstrate the same performance in a pressurized reactor at 0.9TT and 1.38 TP. One system has achieved partial success at 0.8TT and 1.38TP. Stress analyses models indicate the OTM should survive the higher pressure. Failures in testing are believed to be the result of apparatus design that places additional stress on the system. This is being addressed.

- *Determine performance and economic targets for an OTM hydrogen system to achieve a 20% economic advantage over conventional steam methane reforming. Evaluate performance targets for the compact planar reactor to achieve a 20% reduction in syngas capital costs relative to conventional autothermal reforming with cryogenic oxygen for FTGTL.*
    - This study evaluated several different configurations of OTM based reactors including stand alone and modified SMR reactors. The study showed that the OTM-3 compact planar reactor is a step change improvement in hydrogen production costs if CO_2 capture is desired or mandated.
    - A benchmarking study to assess technical and cost targets for the OTM-2 compact planar reactor versus conventional ATR FTGTL was completed. Cost targets for the OTM technology to achieve a 20% advantage relative to ATR in a 25,000 BPD FTGTL plant were determined at two pressure levels. In addition it was shown that at full FTGTL reactor pressure, the OTM-2 design can achieve a syngas capital cost reduction of 28 to 44%

- *Select reactor type (planar versus tubular) by 2Q04.*
    - Complete. A compact planar reactor design (OTM-2) which utilizes the MM2 substrate system was selected for large scale syngas production. A similar reactor design, OTM-3, was selected for hydrogen production.

- *Complete BP and International Truck and Engine fuel testing and engine development program by 2Q04.*
    - This task was completed in the 4Q04 with the successful conclusion of the HCCI fuel evaluation work.

Under the revised scope of work for this budget period, work was performed only under Tasks 1, 2, 4, 8 and 10. A brief summary of results by task is shown below:

Task 1, Material Development
The goal of this task is to develop superior materials for fabricating OTM elements. The approach is to develop two types of materials with different functions– a robust substrate for mechanical strength and an OTM film material for oxygen transport. Both materials must be chemically and physically compatible.

The primary substrate materials, LCM65 or MM2, were chosen early in this budget period. Both of these materials have little or no chemical expansion and exhibit excellent high temperature strength and creep properties. Work thus focused on developing OTM film materials that are robust and compatible with LCM29 and MM2 . To this end, forty nine new membrane materials were fabricated and characterized in Budget Period 3. One system has met our flux, life and cycle goals, LCM61/MM2. Other materials show great promise for improving performance and durability under more severe conditions.

Task 2, Composite Element Development
Numerous disk and tubular elements were fabricated for flux and life/durability testing. A new fabrication technique for making thin OTM films has been developed. This new method has resulted in significant improvements in flux. Work continues to optimize this fabrication process.

The LCM61/MM2 system successfully completed two life/cycle durability tests. This achievement satisfies one of the key goals of this budget period.

A larger scale planar test element (4 in by 4 in.) has been fabricated. This process will be adapted to fabricate planar channels and sub-sections in the next budget period.

Task 4, Reactor Design and Process Optimization
Evaluations of the OTM technology for hydrogen applications were completed. The results show significant thermal efficiency and cost advantages, especially if greenhouse gas control is required. A compact planar reactor design has been developed through computer modeling of the chemical and physical processes (chemical reactions, heat and mass transfer). Interestingly, the limiting design parameter in most cases is heat transport, not oxygen flux. A low pressure syngas application has been identified with early commercialization potential.

A benchmarking study to determine target OTM equipment costs for a 25,000 BPD FTGL plant was completed. The benchmark syngas technology is autothermal reforming with cryogenic oxygen. The study evaluated cost tradeoffs for both a low and high pressure OTM syngas reactor design. The study showed that the OTM -2 reactor design can achieve cost reductions of 28 to 44% relative to the benchmark technology at full FTGTL pressure.

Task 8, Fuels and Engine Testing

The SCTE diesel test work with syngas derived ultra-clean fuels was completed. Fischer Tropsch diesel combined with a proprietary BP syngas derived oxygenate showed substantial reduction in all air emissions targets (NOx, soot, carbon monoxide) over most of the test nodes.

In addition, work on the HCCI fuel and engine development task was completed. A model of the 4.5L V6 diesel engine was developed using GT-Power Cycle Simulator software.. The model was used to evaluate valve timings and lift profiles strategies and guide the HCCI engine development and fuel testing program. The study concluded that a variable valve actuation system capable of simultaneous control of intake valve closing and intake valve lift at fixed intake valve opening has a significant potential for becoming the HCCI enabling technology.

BP developed a matrix of fuel components and conducted a blending study of 24 test fuel mixtures. Three fuels were selected for testing in the single cylinder HCCI test engine. The three fuels contained both diesel and gasoline fuel components and were more volatile than diesel but less volatile than gasoline.

The three fuels were compared against a benchmark ULS diesel fuel. An experimental design was used to evaluate three engine parameters: EGR, swirl and No. 2 injection timing. All fuels showed substantial reduction in soot versus the ULS base fuel. Fuels 2 and 3 achieved significant reductions in NOx as well as soot. However all fuels showed an increase in hydrocarbon emissions relative to the base fuel. No deterioration in fuel consumption (BSFC) was observed with the three HCCI fuels. These experiments are the foundation for a more in-depth study of fuel properties and engine parameters

Task 10, Project Management

All progress reports were completed and submitted on time. All key objectives were completed. A six month no-cost extension was granted to allow completion of Task 8. and part of Task 2.

We participated in a DOE sponsored peer review in Houston June, 2003. In addition, three progress update meetings were held with the DOE in July 2003, June 2004 and December 2004. A paper was submitted for the Spring AIChE meeting, under the natural gas utilization topic in April 2004 and a similar paper was presented at the March 2003 ACS meeting.

2.0 Introduction

The DOE's Office of Fossil Energy created strategic partnerships targeted at the development and verification of advanced fuel-making processes that utilize fossil feedstocks. These processes will enable the production of ultra-clean transportation fuels that improve the environment, while also expanding and diversifying the fossil resource base. In response to the DOE's solicitation for research and development leading to the production of ultra-clean transportation fuels from fossil resources, Cooperative Agreement number DE-FC26-01NT41096 for work entitled "Development of OTM Syngas Process and Testing of Syngas-Derived Ultra-clean Fuels in Diesel Engines and Fuel Cells" was awarded to Praxair.

The objectives of this project are: (1) develop an advanced syngas technology, based on Oxygen Transport Membranes (OTMs), that will provide a step change reduction in the cost of converting natural gas to a spectrum of liquid transportation fuels and thereby improve the prospects for meeting vehicle emissions targets with cost competitive ultra clean transportation fuels (UCTFs); (2) evaluate the performance of, and emissions from selected syngas-derived UCTFs in advanced vehicle propulsion systems, including advanced diesel engines with post treatment and fuel cells; and 3) develop an optimized UCTF/diesel engine/exhaust after treatment system capable of meeting emission regulations beyond 2007.

The scope of work was modified for this budget period to include development of the OTM syngas technology for hydrogen production. Hydrogen is an ultra-clean fuel and a co-product of syngas, and is an integral part of the OTM commercialization roadmap.

3.0 Progress and Results by Task

3.1 Task 1: Materials Development

3.1.1 Goal - Task 1

The Recipient shall fabricate, test and characterize OTM film and substrate materials with the goal of developing a more robust and cost effective OTM element in comparison to the lead candidate material, LCM1.

3.1.2 Experimental - Task 1

The experimental facilities and methods in Task 1 were described in detail in the Topical Report for Budget Period 1 [Ref. 1].

3.1.3 Task 1 Results and Discussion

The goal of this task is to develop superior materials for fabricating OTM elements. The approach is to develop two types of materials with different functions– a robust substrate for mechanical strength and an OTM film material for oxygen transport. Both materials must be chemically and physically compatible.

3.1.3.1 Substrate materials

The primary substrate materials, LCM65 or MM2, were chosen early in this budget period. Both of these materials have little or no chemical expansion and exhibit excellent high temperature strength and creep properties. These materials are close analogs of the materials selected at the end of Budget Period 2 (LCM29 and MM1).. Materials work is focusing on improving the performance and durability of the oxygen transport membrane material.

3.1.3.2 Membrane materials

The focus of this subtask is to develop OTM film materials that are robust and compatible with LCM29 and MM2 . To this end forty nine new membrane materials were fabricated and characterized in Budget Period 3.

In addition, a review of all prior interaction studies between membrane material components and substrate candidates was completed to guide optimization studies. Two membrane components were shown to be the key factors effecting high temperature performance and life. A number of material formulations have been developed that eliminate these components. Table 1 shows the flux results of five new materials without the undesirable components. All of these materials achieved acceptable fluxes at TT, but some (LCM 74, 77 and 80) were found to be unstable after prolonged exposure at TT. LCM74 and LCM80 were retested at 0.8TT. At this temperature the materials were stable and showed no sign of decomposition or phase change.

Table 1: Normalized flux results of membrane candidate materials

Disc	Fuel composition	TT	0.9 TT	0.8 TT	E_a
LCM74	70%H_2/30%CO_2	0.8 TF	-	-	79 kJ/mole
	85%H_2/15%CO_2	**1.2 TF**	0.6TF	0.3TF	
LCM77	70%H_2/30%CO_2	0.9TF	-	-	72 kJ/mole
	85%H_2/15%CO_2	**1.1TF**	0.6TF	0.3TF	
LCM78	70%H_2/30%CO_2	1.2TF	-	-	62 kJ/mole
	85%H_2/15%CO_2	**1.4TF**	0.7TF	0.4TF	
LCM79	70%H_2/30%CO_2	1.0TF	-	-	94 kJ/mole
	85%H_2/15%CO_2	**1.1TF**	0.5TF	0.2TF	
LCM74	70%H_2/30%CO_2	-	-	0.4TF	-
	85%H_2/15%CO_2	-	-	0.4TF	
LCM80	70%H_2/30%CO_2	-	-	0.2TF	-
	85%H_2/15%CO_2	-	-	0.3TF	
LCM81	70%H_2/30%CO_2	1.0TF			89* kJ/mole

Thermal and chemical expansion of these materials were measured in a Baehr Dilatometer DIL 802 and compared to other membrane materials. Results of thermal expansion measurements in air are shown below in Table 2.

Chemical expansion behavior of these materials was also measured relative to air at 0.9TT. Table 2 shows the relative expansion in three different gas compositions which represent a pO_2 range from ~ 10^{-5} to ~ 10^{-13} bar.

Table 2: Thermal and chemical expansion behavior of membrane materials

Material	Normalized Average TEC	Chemical expansion At 0.9TT Relative to air (%)		
		in CO_2	*1%CO in CO_2*	*5%CO in CO_2*
LCM7	1.21	0	0.02	0.035
LCM82	1.19	0	0	0.03
LCM15	1.53	0.13	>0.24	
LCM87	1.10	0	0.03	0.07
LCM40	1.16	0	0.03	0.20
LCM83	1.29	0.02	0.07	0.08
LCM84	1.27	0.015	0.06	
LCM85	1.29	0.02	0.07	0.085
LCM86	1.29	0.02	0.06	
LCM77*	1.16	-0.06*	-0.04	
LCM80*	1.17	-0.05*	-0.03	
LCM74*	1.18	-0.04*	-0.02	0.13-0.15¤

Many of these materials show good expansion behaviour relative to air (less than 0.1 %), however some materials (*) contract at reduced pO_2. Based on the behaviour of similar materials, this is an unexpected result that may be advantageous.

More recent tests have focused on materials with promising high temperature stability and conductivity properties. Results of conductivity tests are shown below in Figure 1..

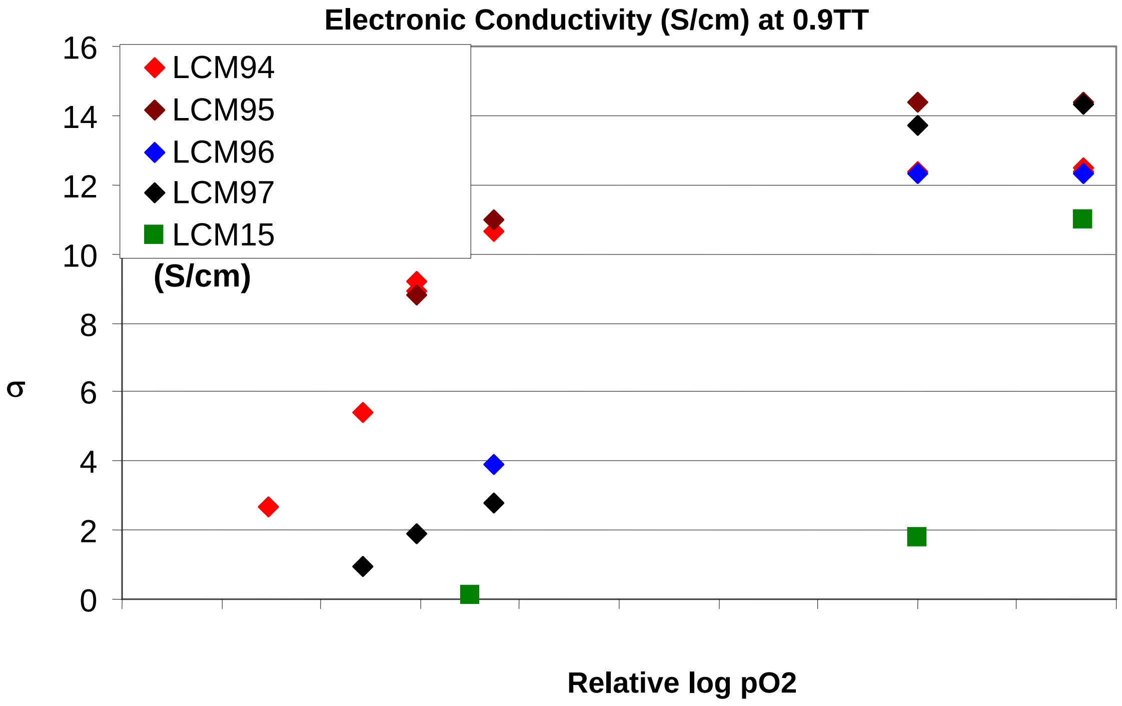

Figure 1: High temperature conductivity of OTM candidates

In comparison to our benchmark material, LCM15, these new materials exhibit significantly higher conductivity at low pO2.

Thermal and chemical expansion behaviour of these materials was also measured. Results are summarized below in Table 3 LM94 and 95 both show good chemical expansion behaviour. More testing is planned with these materials

Table 3 : Thermal and chemical expansion of LCM65 type film candidates.

New Materials	Normalized TEC	**Chemical expansion at 0.9TT** relative to air (%)				
		CO_2	*1%C in CO_2*	*5%CO inCO_2*	*25%CO in CO_2*	*75%CO in CO_2*
LCM94	**1.06**	**0**	**0**	**0.05**	**0.13**	**0.24**
LCM95	**1.00**	**0**	**0.03**	**0.08**	**0.16**	**0.25**
LCM96	**1.22**	**0**	**0.31**	**0.41**	**0.54**	
LCM97	**1.16**	**0**	**0.18**	**0.21**	**0.24**	

The above OTM materials are targeted for the LCM12 system. A number of materials are also being developed for the MM2 system. These include LCM71-73, LCM75, LCM83, 84, LCM88-93, and LCM98

Results of the LCM90-93 are encouraging. These materials show substantially improved chemical expansion behaviour in comparison to the benchmark LCM15. Fluxes of these materials are adequate and high temperature stability is expected to be good. Cycling results of some of these materials are reported later and show good robustness.

Table 4: Thermal and chemical expansion of MM2 type film candidates.

	Normalized TEC	***Chemical expansion at 0.9 TT*** *relative to air (%)*			
		CO_2	1%C in CO_2	5%CO inCO_2	25%CO in CO_2
LCM15	**1.55**	**0.120**	**0.24**	**0.24**	**0.24**
LCM93	**1.40**	**0.058**	**0.11**	**0.12**	
LCM92	**1.37**	**0.043**	**0.097**	**0.11**	**0.14**
LCM91	**1.31**	**0.033**	**0.078**	**0.090**	**0.13**
LCM90	**1.32**	**0.027**	**0.064**	**0.079**	**0.13**

3.2 Task 2: Composite Development

3.2.1 Goal - Task 2

The Recipient shall develop advanced composite OTM elements and the techniques for fabricating these elements at the bench scale. The goal is to develop robust, low cost, high flux elements that can survive multiple temperature and fuel composition cycles while maintaining structural integrity at target pressure differentials.

Milestone:

- In an extended life test, demonstrate an oxygen flux of 0.6TF, 500 hours and 10 thermal and compositional cycles without degradation at TT.

3.2.2 Experimental - Task 2

The experimental facilities and methods in Task 2 were described in detail in the Topical Report for the Period Jan. 1 through Oct. 31, 2001 [Ref. 1].

3.2.3 Results and Discussion - Task 2

Composite development focused on the LCM61/MM2 system. Figure 2 below shows that these materials have very similar thermal expansion characteristics.

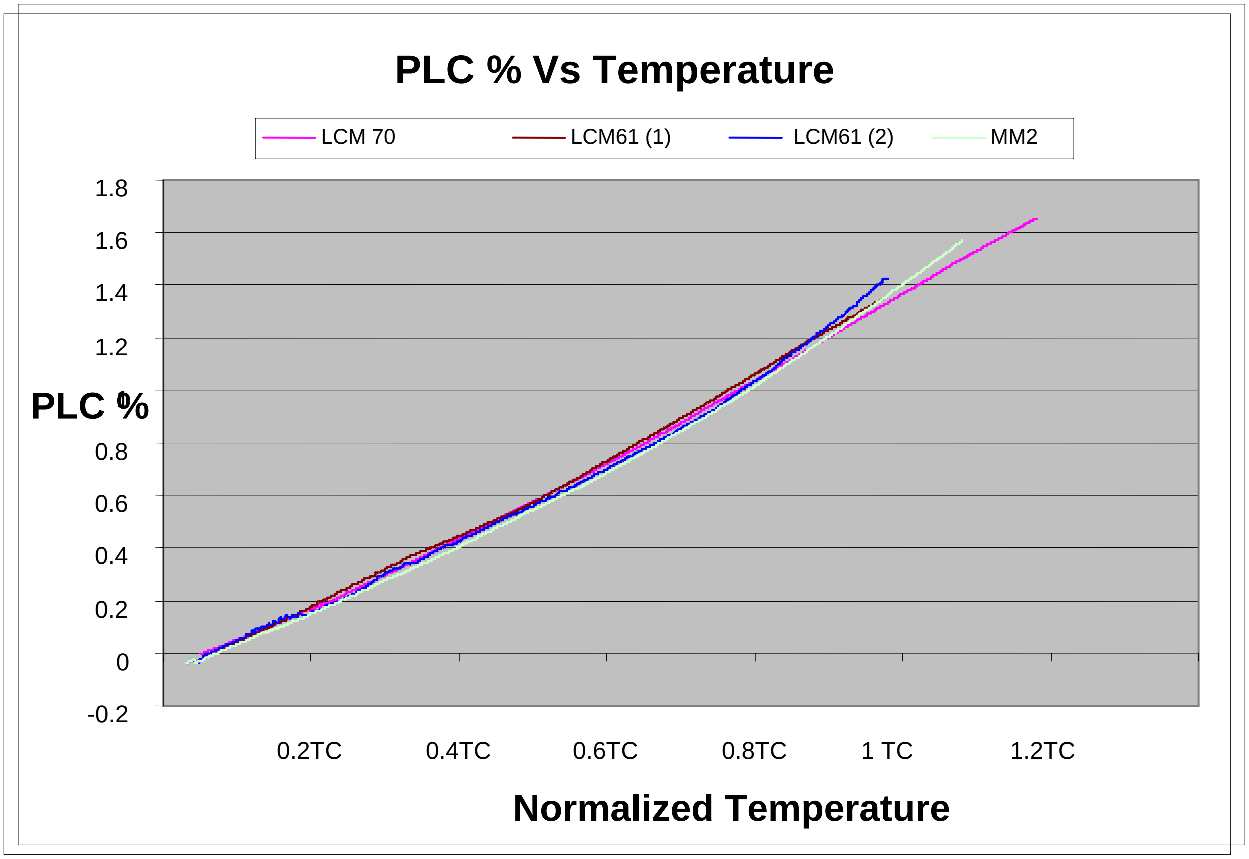

Figure 2: Thermal expansion behavior of MM2 and OTM material candidates

An LCM61 on MM2 disk was fabricated and tested in the disk reactor. The disk achieved a flux of 0.4TFc at TT. The disk was subjected to ten thermal and twelve compositional cycles. The disk was removed after the fourth cycle and examined. The disk showed no signs of cracking or leaking, per both physical examination and a pressurized gas permeability test. The disk was reloaded and completed another six thermal cycles. The flux did not degrade, nor did the measured leak rate increase during the 336 hour test. Again, the disk showed no signs of cracking or corrosion after the severe life and durability test. This is a very important confirmation of the LCM61/MM2 system.

A second test of the LCM61 on MM2 disk was performed in the disk reactor. The disk achieved a flux of 0.6TFc at TT and maintained this flux for over 500 hours. The disk was also subjected to ten thermal and twelve compositional cycles. The flux performance and temperature cycling are shown in Figure 3.

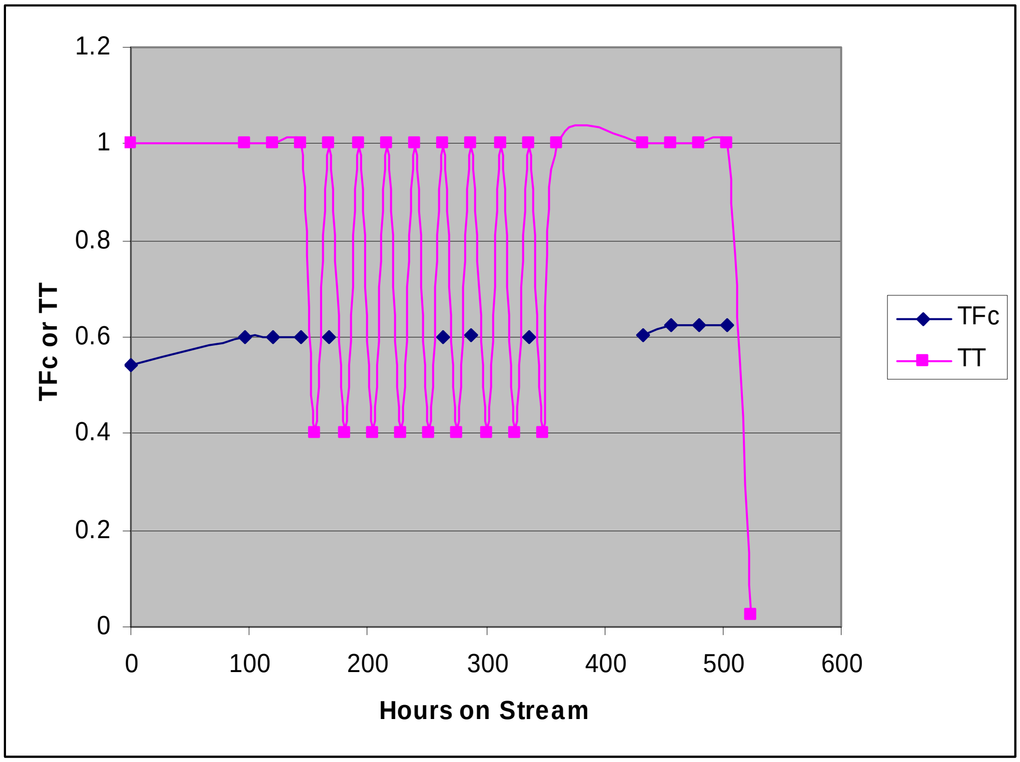

Figure 3: Life and cycle test results for LCM61/MM2 composite disk

The disk was removed after the final cycle and examined. The disk showed no signs of cracking or delamination. SEM analysis also showed no stress cracks of any kind. Photographs of the disk are shown below in Figure 4. This achieved a major Budget Period 3 milestone for flux, life and durability.

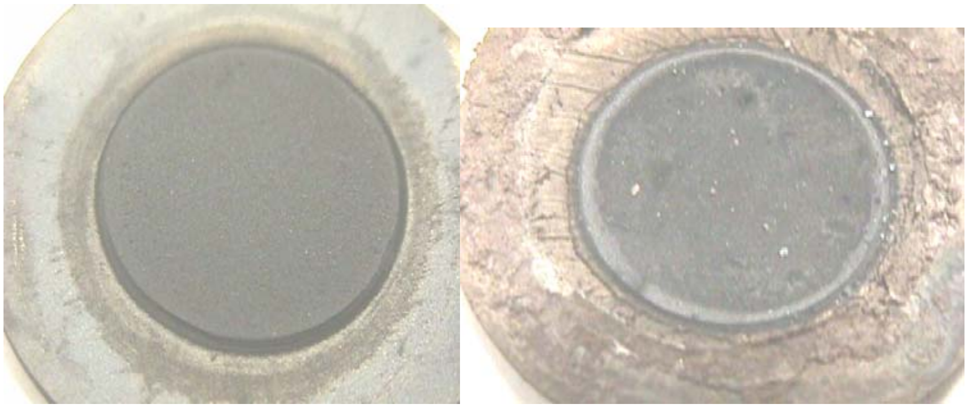

LCM61/MM2 disk ***before*** LCM61/MM2 disk ***after***

Figure 4: Before and after photographs of LCM61/MM2 composite disk

An LCM62 on MM2 composite disk was fabricated and run for 480 hours at TT. The disk achieved a steady flux of 0.6TFc. The sample was then subject to 10 thermal cycles and 12 compositional cycles. Although flux did not degrade over this time, micro-cracks were observed in the sample after removal from the test reactor. The cracks may be attributable to chemical expansion in the LCM62. For this reason LM62 will be abandoned.

A new system, LCM89/MM1, was prepared and subjected to oven cycle tests. The film material showed no signs of cracking or spalling after 80 cycles from room temperature to 0.9TT. The first 10 cycles were conducted at a rate of 2^{o}C/minute and the final 70 were cycled at 5^{o}C/minute. The samples were held at 0.9TT for 1 hour before cooling.

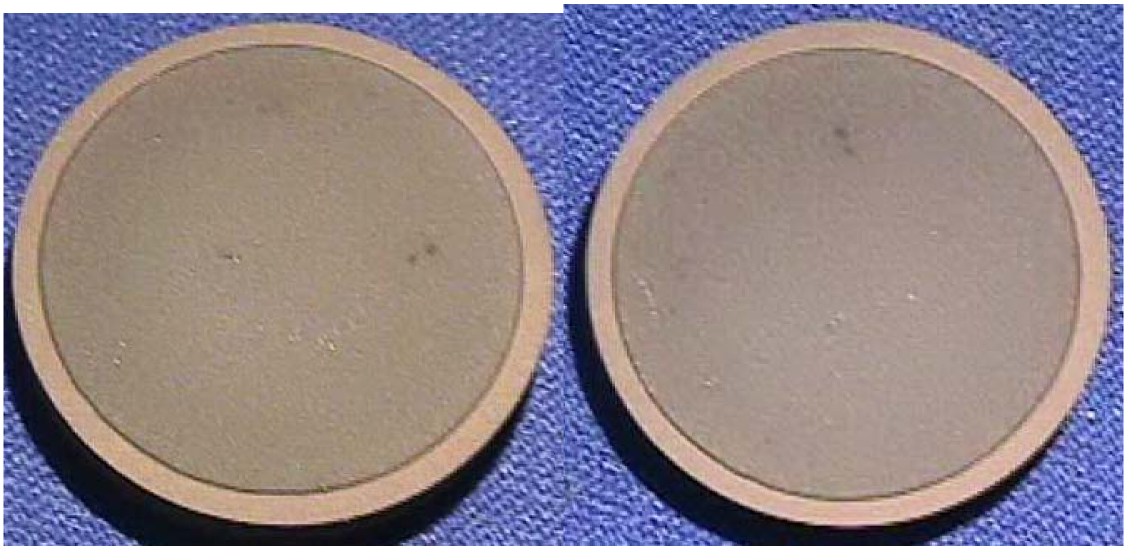

Before oven cycling **After 80 cycles**

Figure 5: Oven cycle test results for LCM88/MM2 composite disk coupon

This new system promises to be more stable at high temperatures

In addition, a new film application technique is being developed that produces robust, dense, but very thin OTM films. An LCM761/MM2 disk made by this technique with a 50 micron film, achieved a flux of 0.64TF at 0.9TT. A second disk completed a 480 life/cycle test at 0.9TT. It achieved a steady flux of 0.60 TF.

3.3 Task 4: Reactor Design and Process Optimization

3.3.1 Goal - Task 4

Develop the commercial OTM syngas and hydrogen processes, including reactor design and catalyst deployment, reactor components (seals, internals, isolation devices, high temperature tube sheet, etc), and ancillary processes (feed pre-treatment, pre-heat, syngas cooling). Task 4 includes the operation of bench scale units, P-0, which are used to evaluate small OTM elements (tubes or disks) at high pressure. Task 4 also includes mathematical modeling, process scale up and economic evaluation.

Milestones:

- Demonstrate robust performance of an OTM system in a pressurized reactor at 0.9TT and 1.38TP
- Determine performance and economic targets for an OTM hydrogen system to achieve a 20% economic advantage over conventional steam methane reforming.
- Evaluate performance targets for the compact planar reactor to achieve a 20% reduction in syngas capital costs relative to conventional autothermal reforming with cryogenic oxygen for FTGTL.
- Select reactor type (planar versus tubular) by 2Q04

3.3.3 Experimental - Task 4

The experimental facilities and methods in Task 4 were described in detail in the Topical Report for the Period Jan. 1 through Oct. 31, 2001 [Ref. 1].

3.3.4 Results and Discussion

3.3.4.1 High pressure disk reactor

A high disk pressure reactor was built. It is capable of prolonged operation at 1.4TP and 0.9TT. LCM61/MM2 disks with 1.0 mm substrates had film failures, ostensibly due to deformation of the substrate under the hydraulic pressure differential of 1.3 TP. Subsequent tests with a 1.5 mm substrate survived three pressure and thermal cycles from room temperature to 0.8TT and ambient pressure to 0.56TP.

3.3.4.2 OTM Reactor Study

The development of a new class of OTM materials has allowed us to reevaluate the tubular OTM element strategy. These new materials are amenable to planar geometries with small channels and passages. Consequently, a new reactor design has been developed in this Budget Period, employing a fundamentally new architecture based on planar, not tubular element fabrication. Details of this reactor design are proprietary and patent pending. This compact design has unique advantages in terms of thermal efficiency, emissions control and obviously plant size and footprint area. Computer modeling of the chemical and physical processes (heat and mass transfer) has shown that the limiting design parameter is heat transport, not oxygen flux.

Two planar reactor designs have been developed. The OTM-2 reactor is optimized for producing high pressure syngas for FTGTL applications. The OTM-3 reactor is optimized for producing hydrogen and sequestering CO_2. The OTM membrane operates at a much lower pressure differential than the OTM-2 reactor configuration.

The reactor design is staged to allow optimal use of materials based on process severity. A low temperature inlet region will employ less expensive structural and OTM materials. The high temperature stage, if required, (it depends on product application) will employ suitable structural and OTM materials, which generally become more expensive as design temperature increases.

Currently the LCM61/MM2 system is adequate for the low temperature stage. Some improvements in film durability are required for the second stage, which t is the prime focus of the materials development team.

3.3.4.3 Foster Wheeler OTM Hydrogen Study

Foster Wheeler has completed an evaluation of OTM technology for producing hydrogen from natural gas. The base case is a 100 MMSCFD Gulf Coast steam methane reforming (SMR) hydrogen plant utilizing Foster Wheeler furnace technology and a conventional PSA for hydrogen purification. The study also compared advanced OTM designs to an SMR plant with a gas heated reformer (SMR/GHR). This configuration will produce the highest yield of hydrogen per mole of methane feed. An OTM process configuration and reactor design was developed that exceeded the SMR/GHR hydrogen yield efficiency and almost eliminates the production of NOx. In addition, all waste gases are nitrogen free, thus greatly facilitating carbon dioxide sequestration. A comparison of the cases is shown below in Table 5.

Table 5: Hydrogen study results

	Units	SMR Base Case	SMR/GHR Case	Best OTM Case
H2 yield	Mole H2 /Mole CH4	2.44	2.74	2.86
NOx production	Ton/Yr	142	105	Nil
Export steam	KLb/Hr	191	Nil	Nil
OPEX	$MM/yr	80.6	71.5	70.7
Steam credit	$MM/yr @$5.50/klb	9.1	0.0	0.0
Net OPEX	$MM/yr	71.5	71.5	70.7

The results show that OTM is efficient at converting methane to hydrogen and can do so without direct air combustion of fuel, which will create NOx. The OTM however requires a large blower to supply air to the membranes and thus has a non-trivial power cost penalty. This can be reduced by lowering the pressure drop of air through the OTM reactor membrane passages and improving the recovery of oxygen in the reactor, both of which are development goals for the next phase of the program.

This study showed that the OTM process has a distinct thermal efficiency advantage for producing hydrogen from natural gas. In addition, the OTM-3 planar \ reactor , which is explained in more detail below, has an added benefit of producing almost zero NOx while easily sequestering over 95% of the potential CO2 emissions. A follow-up study by Foster Wheeler shows that the cost of capturing CO2 with the OTM GSR is well under 50% of the cost of conventional amine scrubbing technology when more or less complete CO2 removal is required. Further this system will recover 100% of the available CO2 (compared to 92% for the most efficient amine configuration), will emit almost no NOx and yield considerably more hydrogen than conventional SMR. These results are shown below in Table 6.

Table 6. Economic Comparison of OTM-3 and Conventional SMR for hydrogen production with CO2 recovery and compression.

Parameter	Units	SMR with CO2 recovery of syngas and flue gas	OTM-3 Case
H2 yield	Mole H2 /Mole CH4	1.45	2.57
Electricity	KW	2,663	18,220
CO2 production	TPD	3,359	2,018
CO2 emissions	TPD	284	-
CO2 Recovery		92%	100%
Estimated NOx emissions	Ton/Yr	346.2	Nil
TOTAL COSTS, $/year		181,599,405	112,330,036
Hydrogen cost	$/MSCF	2.49	2.49
CO2 Cost w/compression	$/T	76.09	31.31

Note that a significant amount of energy is required in both cases to compress the CO_2 to pipeline pressure (3300 psig). It should be immediately apparent that the hydrogen yield for the OTM-3 case is comparable to conventional technology without CO_2 recovery, whereas in the SMR case, the yield is closer to 60%. This is a consequence of the vast amount of natural gas required as fuel to raise steam for the amine systems..

Looked at slightly differently, in the case where CO2 has no value, but instead must be sequestered at a cost of $10 per ton. The SMR –Amine system above produces hydrogen at $5.38/MSCF, while the GSR is able to produce hydrogen at $3.32/MSCF. In this context, it is clear that the penalty for CO2 sequestration in the GSR case is modest and potentially affordable, while with conventional technology it is very large.

Seen in this light, the GSR is an enabling technology for the hydrogen economy.

The OTM-3 reactor scheme results in an extremely compact configuration as shown in Figure 6 This technology could be a BACT candidate for hydrogen if both CO_2 and NOx become regulated pollutants.

Figure 6. Comparison of Conventional Hydrogen SMR Plant with Amine CO2 Recovery and the OTM GSR Technology.

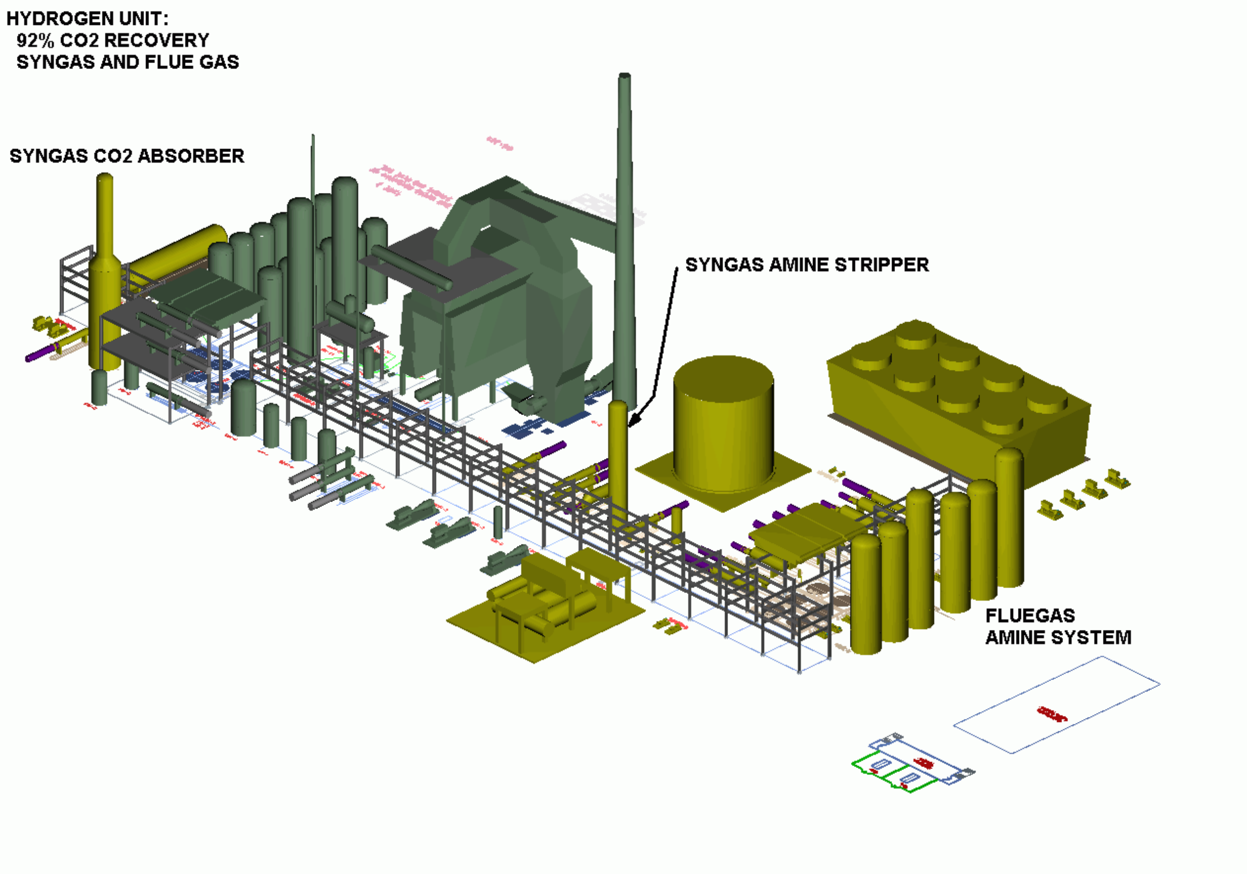

6a—Conventional SMR with PSA and Amine Scrubbing to Recover 92% of total CO_2 emissions by scrubbing high pressure syngas and low pressure flue gas

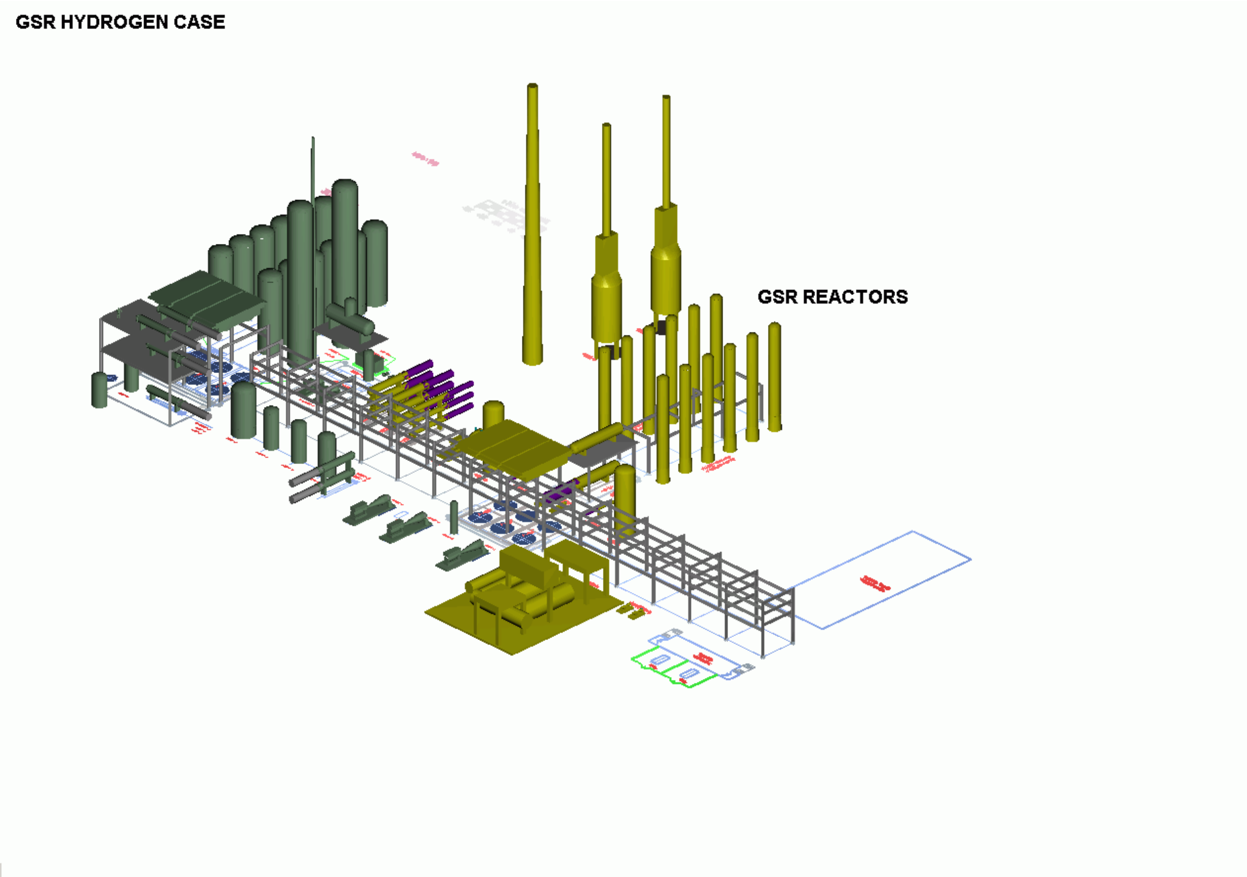

6b—OTM-3 Hydrogen Plant with ~ 100% CO2 Recovery

3.3.4.4 FTGTL Application

Foster Wheeler has completed a study of a 25,000 BPD OTM based Fischer Tropsch Gas to Liquids plant (FTGTL). The purpose of this study is to update our understanding of the economic incentives and cost and performance targets for the new OTM technology which has been developed. Results are shown below in Table 7.

Table 7: Cost Targets for OTM Equipment in a 25,000 BPD FTGTL Plant

Savings from ATR Base Case	Cost of Production Plus ROI ($/bbl)	OTM Equipment Target Cost ($MM)
5%	25.50	163.2
10%	24.16	130.7
15%	22.82	98.0
20%	21.48	65.4

The OTM-2 reactor was sized and costed for the above 25,000 BPD GTL plant. Two reactor designs were evaluated. The “A” design employs a single high temperature material for the entire reactor length. The “b” design stages the reactor so that lower cost materials can be used in lower temperature regions of the reactor. In addition, the “B” reactors configured so that ID and FD fans can be used to supply fresh air and remove the depleted air from the reactor. A cost comparison is shown below in Table 8.

The OTM-2 planar reactor design shows cost reductions relative to conventional ATR with cryogenic oxygen of 28 to 44%. This shows that the economic potential for the OTM planar type reactor is very robust.

Table 8: Cost Comparison of OTM-2 Syngas Process and Conventional ATR

	ATR Case **$MM**	**OTM -2 (A) with 20 psi blower** **$MM**	**OTM -2 (B) staged** **$MM**
ASU/ATR (including extra power supply)	**164.75**		
OTM Modules, Installed		**71.70**	**62.42**
Air/DA Exchangers		**12.52**	**12.52**
Syngas Cooling to 1250oF		**3.75**	**3.75**
Balance of Syngas Island	**25.40**	**19.61**	**21.65**
Air moving equipment		**30.00**	**6.25**
TOTAL	**190.15**	**137.57**	**106.58**
Saving compared to ATR		**28%**	**44%**

In addition to the high pressure syngas application FTGTL, a low pressure syngas application has been identified with early commercialization potential. This opportunity may be pursued as a means to fast track the syngas technology development. Learnings could have significant impact on large scale high pressure syngas systems.

3.3.4.5 CFD Modeling

A CFD model with a mass transport and membrane kinetic code was completed for the high pressure disk reactor utilizing subroutines developed for other reactor models. The model has been used to understand thermal profiles in the OTM membrane and surrounding reactor shell and internal devices. The model shows the non-isothermal behavior of the oxygen membrane transport process and the effect of the relatively large internal reactor surface area on methane conversion. With proper calibration, the CFD model can be used to subtract out internal surface area effects and interpret non-isothermal reaction and transport data.

3.4 Task 8: Fuels and Engine Testing

3.4.1 Diesel Engine and Exhaust Treatment

3.4.1.1 Goal - Diesel Engine and Exhaust Treatment

The goal of this task is to understand the relationship between ultra-clean fuel properties and their impact on the emissions and performance of an advanced CIDI and exhaust treatment system under development at International Truck and Engine.

3.4.1.2 Experimental - Diesel Engine and Exhaust Treatment

Pictures and description of the SCTE are shown in the Topical Report for the Period Jan. 1 through Oct. 31, 2001 [Ref. 1].

3.4.1.3 Results and Discussion - Diesel Engine and Exhaust Treatment

In Budget Period 3 this Task focused on two goals: 1) completing the evaluation of ultra-clean transportation fuels in conventional diesel engines and 2) completing the exploratory program in HCCI engine and fuel development. Both test programs are conducted on highly instrumented single cylinder test engines (SCTE) at International's facilities in Melrose Park, Ill.

3.4.1.3.1 Ultra-clean fuel testing in conventional diesel engines.

In Budget Period 3, three ultra-clean diesel fuels were tested in the SCTE and compared to a baseline No.2 conventional diesel fuel. The three ultra-clean fuels are : 1) Fischer Tropsch (FT) diesel fuel obtained from Sasol, LTD, 2) a commercial, petroleum based, ultra-low sulfur (ULS) diesel fuel and 3) the same ULS with a BP oxygenate (BPO) blended to achieve 10% oxygen in the fuel. The fuel properties and engine performance and emission results are reported in the Budget Period 2 Topical Report. The study concluded that the FT diesel fuel shows a clear advantage in reducing NOx and soot in comparison to conventional No.2 diesel. The study also clearly showed that the BPO at 10% oxygen level (in ULS) reduces both NOx and soot in comparison to that ULS fuel. .Thus this syngas derived additive may be useful in improving the emission performance of the "cleanest" commercial diesel fuels available today. The high oxygenate level however resulted in fuel consumptions that were higher than expected based on fuel calorific content, suggesting that some other in-efficiencies in engine performance were occurring due to the BPO. [Ref. 3] Thus a second test with only 5% oxygenate was planned for Budget Period 3. These results are reported below.

3.4.1.3.1.1 Test Objective

Objective of this phase is to evaluate the steady-state emission performance in a Single Cylinder Test Engine (SCTE) of the ultra- low sulfur diesel fuel blended with BP oxygenate (BPO) to yield 5 wt.% oxygen content and compare to the tests results from Budget Period 2. The 5% oxygenate fuel was prepared by BP Research in Naperville, Ill. Using an ultra-low sulfur diesel fuel supplied by International. Detailed discussion of the general test methodology used in establishing the engine data sets for this program has been provided in the 4Q01 Report. [Ref. 2]

Table 9. Summarizes inspections of the ULS and ULS with 5% oxygen.

Table 9: SCTE fuel inspections

		ULS Base Fuel	ULS 5%O Blend
Cetane #		**47.6**	**66.7**
Destilation	**deg F**		
Initial Point		**364**	**339**
10	**%**	**401**	**397**
30	**%**	**459**	**469**
50	**%**	**488**	**517**
70	**%**	**510**	**559**
90	**%**	**588**	**614**
End Point		**666**	**653**
Carbon	**m%**		**81.1**
Hydrogen	**m%**		**13.6**
O avg,	**m%**		**5.22**
Specific Gravity		**0.842**	**0.83**
Total Sulfur	**Mass ppm**	**<10**	**5**
Aromatics	**Vol %**	**29**	**27**
Flashpoint	**deg F**	**170**	**133**
Viscosity @ 40C	**cSt**	**2.5**	**2.13**
H/C Ratio		**1.82**	
Net Heat Of Comb	**BTU/lb**	**18457**	**17659**

3.4.1.3.1.2. Test Description

In its general outline the test is similar to the test conducted in the period Starting July 1, 2002 and Ending September 30, 2002 when the fuel blend with 10% oxygenate was evaluated. Because of the passage of time between these tests, the configuration of the SCTE testing facility has been changed to address requirements of progressing technology. Therefore, some details of the general set-up and engine operating points in the current test differ somewhat from the 2002 tests as follows:

- Engine is now configured with the Common Rail (CR) Injection System and accordingly optimized combustion system consisting of a different combustion chamber geometry and injector nozzle spray pattern;
- Injection strategy now includes the pilot injection and post injection needed to control the NOx emission levels required by the ’07 EPA rules.
- Speed and load conditions of four test points: Mode 4, 6, 7 and 8 have changed somewhat relatively to the original definitions due to certain shifts in location of the sensitive emission control areas of the engine operating map,
- Based on the previous experience with the oxygenated fuel testing, where both “constant fuel” and “constant toque” tests protocols were used and produced similar engine performance trends, it was decided to employ a “constant fuel” approach only for these tests..

3.4.1.3.1.3. Discussion of Test Data

As in the previous discussions of the engine investigation, the results of the emission and fuel consumption performance comparisons between the ultra low sulfur baseline fuel and the 5% oxygenated test fuel are presented here as the trade-offs between the NOx and Soot as well as between the NOx and BSFC. These trade-offs have been generated by changes in combinations of settings of major combustion control parameters such as injection timing of various injection events (represented by start of combustion, SOC), air/fuel ratio and concentration of EGR in intake air. Comparison between performance of both investigated fuels have been conducted at four points of the engine operating map designated as Mode 4, 6, 7 and 8 and considered to be the significant overall contributors to result of the HD FTP emission certification cycle. The actual discussed data are summarized graphically and tabulated numerically in Appendix I, Fig.1, Fig.2 and Table 2 for Mode 4, Fig.3, Fig.4 and Table 3 for Mode 6, Fig.5, Fig. 6 and Table 4 for Mode 7, and finally, in Fig.7, Fig. 8 and Table 5 for Mode 8.. Tables include definitions of operating conditions at each of the test points as well as the information on specific combinations of control settings driving obtained emission trade-offs. The tables also include the comparison of performance results obtained for both the baseline and the 5% oxygenated fuel. Fig.1, Fig. 3, Fig.5 and Fig. 7, in addition to Nox-Soot trade-off, include also the data sets representing Indicated Mean Expanded Pressure (IMEP) which is a measure of cycle work performed by expanding cylinder charge on the piston. The inserts imbedded in these figures show overlays of the Heat Release Rates (HRRs) for pairs of compared fuels for specific test settings delineated by the circles. This additional information is provided to demonstrate the differences in an actual combustion process caused by the fuels.

Based on review of these data, the following observation can be made:

- When comparing the results obtained with 10% oxygenated fuel, the 5% oxygenated fuel is showing much lower reduction in IMEP at fixed fuelling conditions relative to the base fuel. Actually, for the certain calibrations of some operating points increase in IMEP, directly correlated to improvement in gravimetric fuel consumption, could be achieved. One of the reasons for this more desirable performance of 5% oxygenated fuel is that its calorific value is closer to that of base fuel.

- Comparisons of Heat Release Rates show that almost in all cases there are visible differences in start and progression of combustion of oxygenated and base fuels which also can contribute to improvement in thermo-efficiency of the process. In addition to the presence of extra oxygen in the mixture, the higher cetane number of oxygenated fuel seems also to play a role in modifying combustion.

- Smoke reduction at all operating conditions and calibration points over the baseline fuel is quite evident. While at some operating conditions the extent of this reduction is lower than levels observed with the 10% oxygenate blend, in general, decrease in smoke is significant. Interestingly, in the case of the pilot injection which is known for its significant smoke penalty with conventional fuel, the 5% oxygenate blend provides consistent reduction in smoke by 60 to 80%. One of possible explanation of this phenomenon is that the higher concentration of active radicals is being formed in the pilot phase of oxygenated fuel combustion which intensifies the oxidation of soot later in the cycle.

- As with previous highly oxygenated fuel there is a consistent and quite substantial reduction in NOx, which persist for all cases but the pilot injection strategy. Considering a relatively low level of NOx due to the pilot injection strategy and the high concentration of EGR used in this test coupled with highly oxidizing combustion environment demonstrated by very significant soot reduction, such behavior of a NOx seems to be not unexpected.

In general, the relative emission/BSFC performance of the oxygenated fuel vs. the base low sulfur fuel can be can be summarized as follow:

Mode 4 (1000rpm/4 bar IMEP with pilot injection strategy)
- Range of Soot reduction: from 66% reduction to 87%,
- Range of NOx increase: from 5 to 25%
- Range of BSFC: from 2% improvement to 32% deterioration

Mode 6 (2060rpm/10 bar IMEP with post-injection strategy):
- Range of Soot reduction: from 23 to 46%
- Range of NOx: reduction from 4 to 28%
- Range of BSFC: from 10% improvement to 11% deterioration

Mode 7 (3108rpm/7.5 bar IMEP with single injection strategy):
- Range of Soot reduction: from 4 to 26%
- Range of NOx: from 13% reduction to 2% increase
- Range of BSFC: from18% improvement to 3% deterioration

Mode 8 (3000rpm/17.5 bar IMEP):
- Range of Soot reduction: from 16 to 26%
- Range of NOx: reduction from 15 to 21%
- Range of BSFC deterioration: from 2 to 10%

3.4.1.3.1.4 General Conclusions from Oxygenated Fuels Testing

1. The testing of low sulfur fuel blends with 10% and 5% BPO oxygenate provides strong evidence of significant soot reduction potential for this type of fuel in diesel engines
2. While the soot reduction capability seems to be proportional to an oxygenate concentration, even the lower concentration blends provide a significant soot reduction benefit. Since the calorific value of the lower concentration blends differ less from the calorific value of base fuel, the penalty in gravimetric BSFC is also lower.
3. Presence of an oxygenate seems to be modifying the chemical kinetics of diesel fuel burn, allowing for significant reduction of soot even in the highly sooting modes of combustion such as the pilot injection and the high EGR
4. Interestingly, the oxygenated fuels tested have consistently demonstrated reduction in the NOx emission relative to base fuel. Mechanism of this reduction must also be related to reaction kinetics but is not well understood

3.4.1.3.2 HCCI engine and fuel development

3.4.1.3.2.1 Introduction

The Homogeneous Charge Compression Ignition (HCCI) combustion process is considered to be a very strong candidate solution for meeting extremely stringent 2010 EPA diesel emission regulations. In theory it offers very significant in-cylinder NOx and Soot reduction while still maintaining the superior diesel fuel economy advantage. If successfully developed and implemented HCCI technology could significantly reduced the complexity and cost of diesel after-treatment systems.

In its principle, the HCCI calls for some degree of homogenization of in-cylinder air/fuel mixture based on injection of the fuel early in the compression stroke. A Serious challenges associated with this concept is control of the ignition delay to prevent start of combustion occurring significantly prior to TDC (top dead center) while allowing sufficient time for charge homogenization. The strongest factors that affect the ignition delay in diesel combustion are the fuel properties and charge temperature and pressure histories prior to TDC, which can be controlled by a parameter called an effective compression ratio (ECR) and defined in Compression Ignition (CI) engines as:

ECR=(Ptdc/Pim)^(1/1.36)

Where:

Ptdc – pressure of charge at TDC
Pim – intake manifold pressure

It is known that the flexible intake and exhaust valve timings as well as valve lift profiles offered by a Variable Valve Actuation (VVA) system can provide certain degree of ECR modulation which can become, in turn, a valuable HCCI technology enabler. Analytical study has been, therefore, undertaken to determine the best VVA strategy capable of providing the widest range of ECR modulation as well as maintaining reasonably low charge temperature in cylinder prior to TDC.

3.4.1.3.2.2 Scope of Analysis

The simulation of in-cylinder conditions and engine performance as affected by wide range variations in the valve timings and lift profiles has been conducted using the International V6 4.5l engine model developed in GT-Power Cycle Simulator software. Scope and range of simulation domain is as follows:

1. Varying the intake and exhaust valve opening and closing events at fixed valve lifts - see Table 9
2. Varying the intake valve closing event (IVC) and lift at fixed intake valve opening (IVO) – see Figure 7
3. Shifting the intake valve lift profile at fixed valve lift – see Figure 8
4. Varying the intake valve lift at fixed IVO and IVC – see Figure 9

Three engine operating points have been examined. They are 2000 RPM 50% load, 800 RPM 50% load and 3300 RPM 50% load.

Table 10: Scope and range of engine simulation domain
(Crank angle values corresponding to valve events are based on convention: TDC start of intake=-360; TDC firing=0; TDC end of exhaust=360)

Case #	IVO	IVC	EVO	EVC
1	-250	-90	90, 132, 180	250, 310, 376
2	-250	-129	90, 132, 180	250, 310, 376
3	-250	-180	90, 132, 180	250, 310, 376
4	-312	-90	90, 132, 180	250, 310, 376
5	-312	-129	90, 132, 180	250, 310, 376
6	-312	-180	90, 132, 180	250, 310, 376
7	-377	-90	90, 132, 180	250, 310, 376
8	-377	-129	90, 132, 180	250, 310, 376
9	-377	-180	90, 132, 180	250, 310, 376

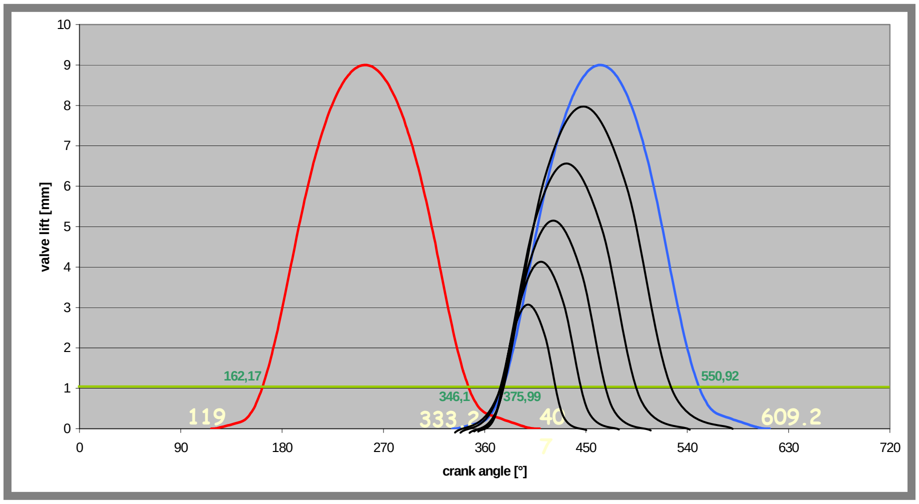

Figure 7: Intake Valve Closing w/variable lift duration

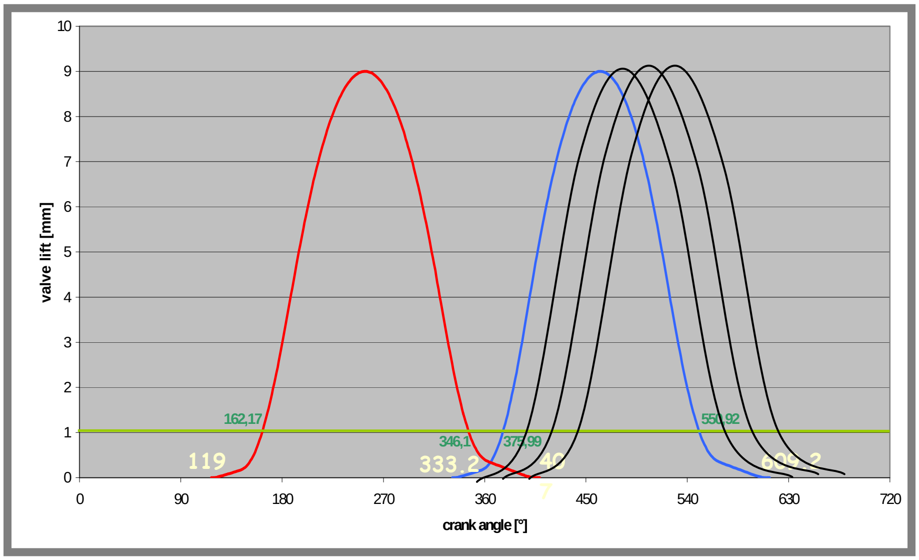

Figure 8: Valve event phasing

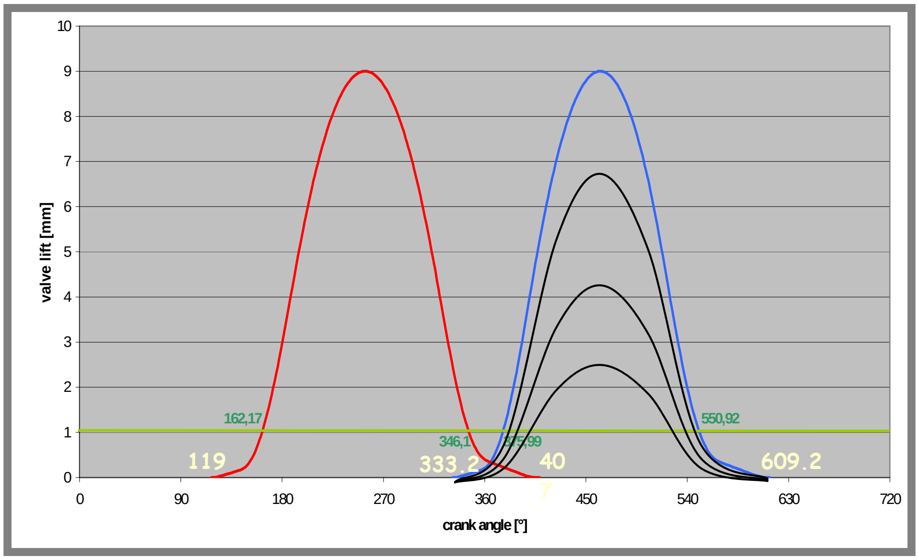

Figure 9: Variable lift with fixed duration

3.4.1.3.3 Discussion of Results

Results of the full factorial evaluation of effects of the intake and exhaust valve events variations (at 2000 rpm/ 50% load point) on ECR are presented in Fig. 10. As can be seen by changing the valve events alone available range of ECR modulation is rather limited. More detailed analysis of simulation data also has revealed that the cases producing lower ECR values are associated with significant fuel penalty and/or significant reduction of cylinder mass flow.

Simulation outputs from extensive sweeps of the IVC/lift modulation, the intake valve lift profile phasing and the intake valve lift modulation with fixed profile duration have been comprehensively summarized in Fig. 11. This graph illustrates the trade-offs between range of ECR available for these different VVA control strategies and the fuel consumption gain/penalty relative to the current product baseline. These correlations are plotted for several operating conditions to confirm prevailing trends.

Review of this graph leads to conclusion that the most effective VVA strategy capable to produce wide range of ECR at favorable fuel consumption potential is the IVC/lift modulation. This strategy can modulate ECR within the range of 11 to 18 with potential for BSFC improvement of 2-4%.

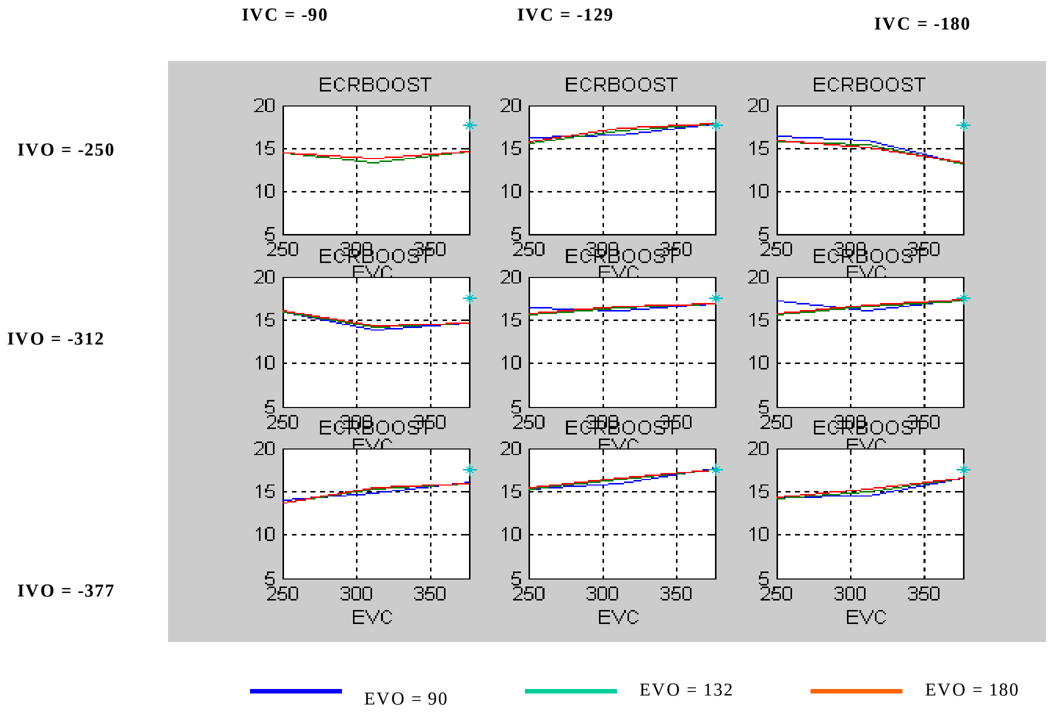

Figure 10: Results of the full factorial evaluation of effects of the intake and exhaust valve events variations (at 2000 rpm/ 50% load point) on ECR

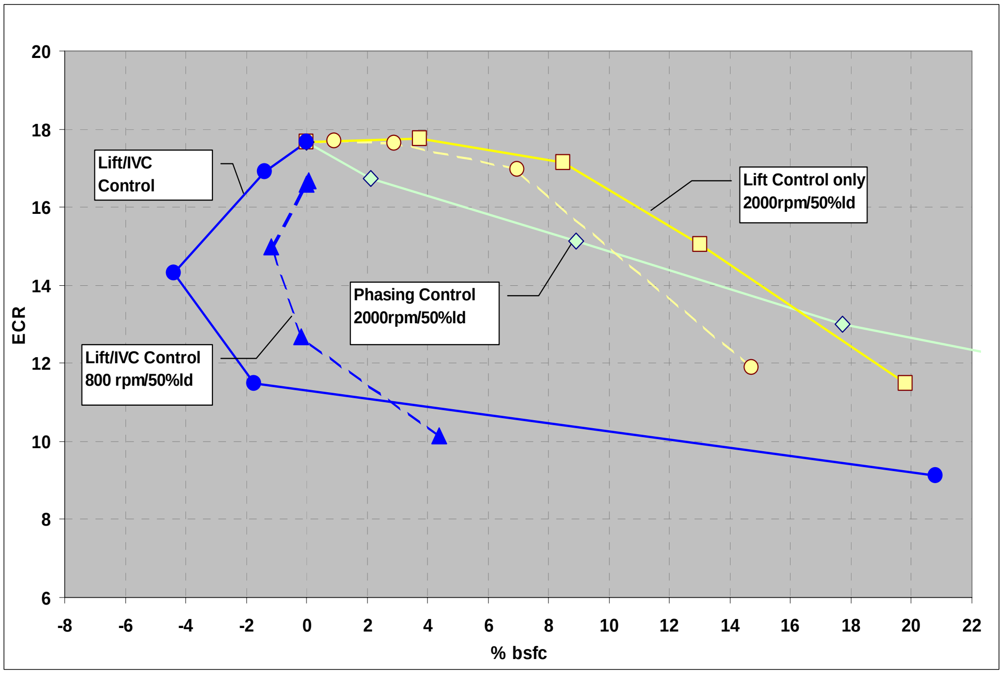

Figure 11: Summary of effect of ECR on BSFC for simulated valve strategies

3.4.1.3.4 Engine simulation conclusions

- VVA system capable of simultaneous control of intake valve closing and intake valve lift at fixed intake valve opening has a significant potential of becoming the HCCI enabling technology.
- Such VVA system coupled with diesel fuel having enhanced HCCI properties (such as lower CN and lower volatility) may allow to extend effective HCCI combustion rpm/load range.

3.4.1.3.5 Fuel characterization and blending study

BP has acquired 10 fuel components for blending studies. These materials are summarized below in Table 11. Twenty four blends were prepared and tested for RVP, IQT ignition delay and cetane number as shown in Table 12 . Complete results are shown in Appendix 3.

Table 11: HCCI fuel components for blending studies

		Blending Component Properties							
	Mid-Range		**Approximate**		**Estimated Qualitative**			**Approximate**	
Material	**Boiling Pt, F**		**Cetane**		**Ignition Delay**			**Octane**	
D2	500		49		Short			unknown	
D2A	500		30		Medium			unknown	
D1H	420		50		Short			unknown	
D1L	420		40		Medium			unknown	
HNP	220		unknown		Long			50	
HNA	330		unknown		Very Long			100	
LNA	230		unknown		Very Long			120	
LNP1	200		unknown		Very Long			100	
LNP2	200		unknown		Long			0	
LNP3	135		unknown		Very Long			85	

D = diesel; N = naphtha; A = aromatic; P= paraffinic;, L= light, low; H = heavy, high

Table 12. HCCI Fuel Candidate Blending Results

	Blends by Weight %											
Blend	**1**	**2**	**3**	**4**	**5**	**6**	**7**	**8**	**9**	**10**	**11**	**12**
D2	100	50	50	50								
D2A												
D1H					100	50	50	50				
D1L									100	50	50	50
HNP		50				50				50		
HNA			50				50				50	
LNA												
LNP1				50				50				50
LNP2												
LNP3												
Test Data	**1**	**2**	**3**	**4**	**5**	**6**	**7**	**8**	**9**	**10**	**11**	**12**
Rvp	0.36	1.45	0.23	3.15	0.15	1.33	0.26	3.05	0.22	1.36	0.28	3.02
IQT ignition delay	4.066	4.628	8.039	5.524	4.612	5.035	8.862	6.088	5.632	5.674	10.99	7.164
IQT cetane number	48.86	43.3	27.99	37.21	43.44	40.22	26.15	34.42	36.63	36.41	22.67	30.42

Blend	**13**	**14**	**15**	**16**	**17**	**18**	**19**	**20**	**21**	**22**	**23**	**24**
D2	50	50									25	
D2A			100	50					50	50		25
D1H						50		50				25
D1L	50			50	50		50				25	
HNP												25
HNA										50		
LNA		50			50	50			50			
LNP1											25	
LNP2							50	50				
LNP3											25	25

Test Data	**13**	**14**	**15**	**16**	**17**	**18**	**19**	**20**	**21**	**22**	**23**	**24**
Rvp	0.29	0.91	0.08	0.55	0.88	0.87	1.54	1.52	0.78	0.23	4.03	3.35
IQT ignition delay	4.407	6.827	10.71	6.991	7.761	9.782	5.29	4.775	28.32	24.11	5.824	6.073
IQT cetane number	45.28	31.53	23.05	30.97	28.7	24.46	38.58	42.11	13.2	14.34	35.65	34.49

Based on the blending results above, three fuel blends were selected for HCCI testing. The three blends and their properties are shown below in Table13. These fuels provide a range of IQT cetane and aromaticity and some variation in volatility. Note that all fuels will be somewhat similar to JP4 in volatility, and will therefore require additional precautions in fuel handling, such as adequate grounding to prevent static ignition.

Table 13 – Selected fuel blends for HCCI single cylinder engine testing

Table 7
Engine Test Blends (55 gallons)

Engine Test Blend	**21507-31-1**	**21507-31-2**	**21507-31-3**
Test	**Fuel 1**	**Fuel 2**	**Fuel 3**
API Gravity, °API	44.65	51.98	48.41
Specific Gravity, 60F/60F	0.8033	0.7712	0.7865
Distillation			
Initial Boiling Point, °F	119.5	201.9	149.8
10% distilled, °F	205.1	208.9	20839
20% distilled, °F	222.2	213.5	216.8
30% distilled, °F	231.3	217.9	224.7
40% distilled, °F	241	226.6	235.1
50% distilled, °F	254.3	242.9	249.1
60% distilled, °F	271.5	290.6	278.6
70% distilled, °F	303.8	377.3	339.1
80% distilled, °F	346.1	404.5	377.4
90% distilled, °F	385.2	443	429.2
Final Boiling Point, °F	541.6	489.9	537
Reid vapor pressure, psi	2.64	1.49	2.05
Carbon, mass %	86.66	85.8	86.42
Hydrogen, mass %	11.91	13.82	12.9
Nitrogen, ppm	25	<1	12
Sulfur, ppm	293	5	143
SFC Aromatics, vol%	60.02	28.69	44.88
Lower heating value, BTU/lb	17872.45	19066.2	18297.13
Lower heating value, BTU/gal	119563.5	122453.9	119846.4

3.4.1.3.6 HCCI Engine Test Results

The complete HCCI test results are shown in Appendix 2. Performance of the above three fuels were compared to the ULS base fuel shown in Table 9

Although the scope of this work has been limited primarily to investigation of the engine emission performance at a single operating point, the results show the undisputable advantages of customizing hydrocarbon fuel blends to achieve clean HCCI type diesel combustion. Reducing cetane number and increasing fuel volatility. a re both required to achieve good performance in the HCCI engine. . All of the “HCCI” fuels have demonstrated very significant potential in reducing soot emissions relative to the base ULS diesel fuel. Fuel # 3 has demonstrated best performance in the sense that, for the optimized soot-NOx trade-off point, the approximately 90% reduction in soot was coupled to approximately 30% reduction in NOx , relative to the best point for the base fuel.

It needs to be emphasized that there are certain chemical properties related to combustion kinetics of the fuel which at present time are not well understood
In order to fully evaluate the potential of these fuels and the HCCI engine, more extensive engine mapping and fuel composition studies are necessary.

3.5 Task 10: Program Management

3.5.1 Goal - Task 10

The recipient shall provide technical leadership and management direction to ensure that the program delivers its goals on time, within budget and in a safe and environmentally acceptable manner. Good communications with the DOE, participants, and subcontractors will be maintained.

3.5.2 Milestones - Task 10

A detailed briefing shall be presented within (60) days of the end of the budget period. The briefings shall be given by the Recipient to explain the plans, progress, and results of the project effort, both technical and administrative.

- Status: A briefings were presented to DOE management on June 8th , 2004. at Praxair Technical Center in Tonawanda, NY and December 14th, 2004 in Morgantown, WV

3.5.3 Discussion - Task 10

All progress reports were completed and submitted on time. All key objectives were completed. A 6 month no-cost extension was granted to allow completion of Task 8. and part of Task 2.

We participated in a DOE sponsored peer review in Houston on June , 2003. In addition, three briefings were held with the DOE: July 2003, June 2004. and December, 2004.

A paper was submitted for the Spring AIChE meeting, under the natural gas utilization topic in April 2004 and a similar paper was presented at the March 2003 ACS meeting. The program remains under budget through the second quarter, 2004.

4.0 Conclusions

- An advanced material system LCM61/MM2 has met our flux, life and cyclabiltiy targets for this budget period. This material system is suitable for the first stage of a high pressure OTM hydrogen or syngas process; a more robust film material is required for the higher temperature second stage.
- Several promising high temperature OTM film material candidates have been fabricated and are undergoing testing.
- The LCM61/MM2 and several LCM65 systems are suitable for a low pressure syngas application which could be commercialized early on, as part of an integrated technology development roadmap.
- A new fabrication technique has been developed that allows the manufacture of thin, dense OTM films on porous substrates.
- An OTM-3 reactor has been shown to have a very high hydrogen yield with almost no NOx emissions. The reactor is also very efficient at capturing CO2.
- The OTM-3 will reduce the costs of recovering the carbon dioxide created from reforming natural gas .by 50% or more. This device could be a BACT candidate

for hydrogen production if NOx and CO2 are regulated pollutants and would therefore be significantly advantaged over SMR.

- The OTM-2 reactor shows potential to reduce ATR syngas capital costs by 28 to 44% based on a 25,000 BPD FTGL plant with cryogenic oxygen.
- Adding the BP oxygenate at a 5% oxygen level to conventional ultra-low sulfur diesel fuel significantly reduces soot and NOx emissions with only minimal impact on fuel consumption and engine efficiency.
- The HCCI engine promises to be the next generation internal combustion engine which will be capable of meeting 2010 EPA emission regulations. The engine promises to reduce soot and NOx formation in the cylinder with no loss of efficiency, thereby reducing the need or complexity of after-treatment technology.
- VVA system capable of simultaneous control of intake valve closing and intake valve lift at fixed intake valve opening has a significant potential of becoming the HCCI enabling technology.
- The HCCI fuel will likely resemble JP4 in volatility, but will have specific ignition delay and cetane requirements to achieve optimal performance.
- The best fuel found in this study has an aromatic content of ~ 45 volume percent and a Reid vapor pressure of ~ 2 psi. with an estimated IQT cetane of 25

5.0 References

1. Robinson et al, Topical Report for “Development of OTM Syngas Process and Testing of Syngas-Derived Ultra-clean Fuels in Diesel Engines and Fuel Cells”, US DOE Award No. DE-FC26-01NT41096, Budget Period 1, October 2001.

2. Robinson et al, Quarterly Project Status Report for Period ending December 31, 2001 for “Development of OTM Syngas Process and Testing of Syngas-Derived Ultra-clean Fuels in Diesel Engines and Fuel Cells”, US DOE Award No. DE-FC26-01NT41096, March 2002.

3. Robinson, et al, Topical Report for ““Development of OTM Syngas Process and Testing of Syngas-Derived Ultra-clean Fuels in Diesel Engines and Fuel Cells”, US DOE Award No. DE-FC26-01NT41096, Budget Period 2, February 2003.

Appendix 1

International Truck and Engine SCTE Results

Baseline vs Oxygenated Fuel Soot/Nox Trade-off @ Mode #4

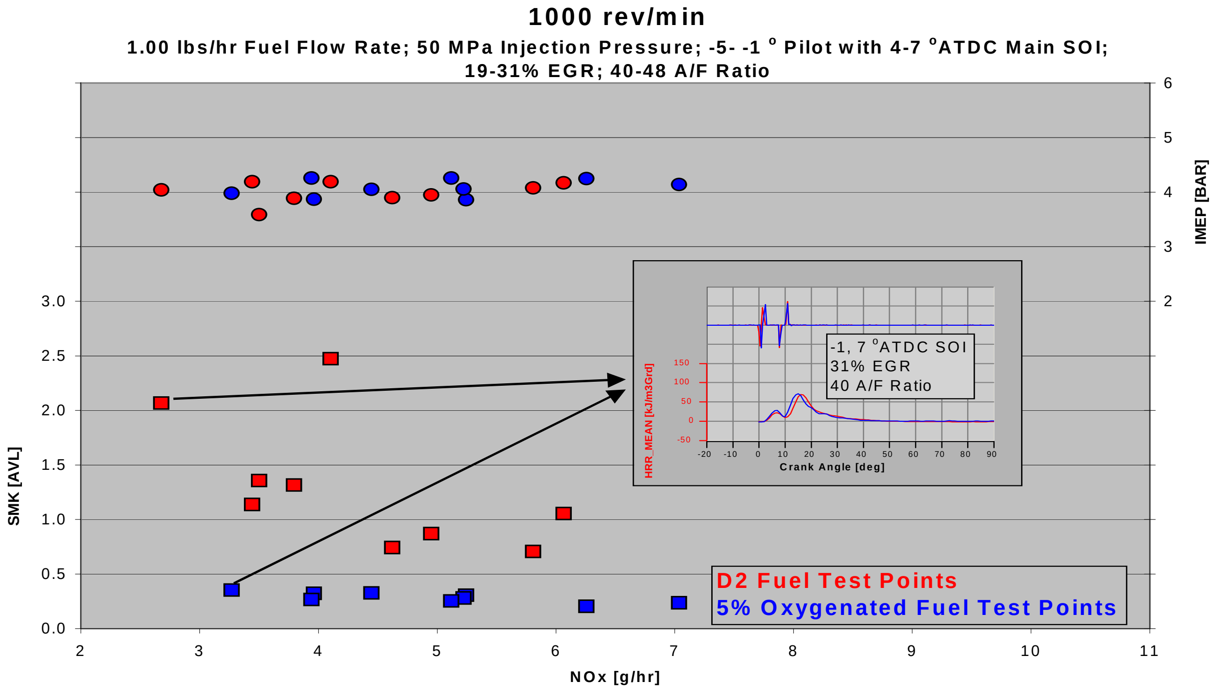

Fig 1

Baseline vs Oxygenated Fuel BSFC/Nox Trade-off @ Mode #4

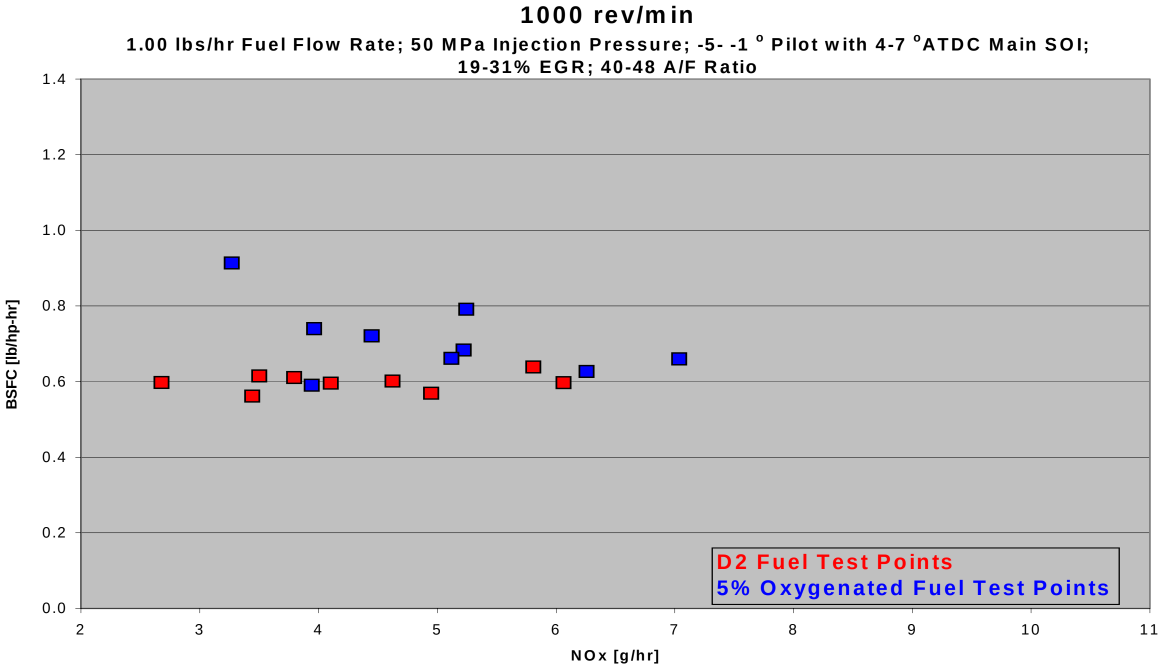

Fig 2

Baseline vs Oxygenated Fuel Soot/Nox Trade-off @ Mode #6

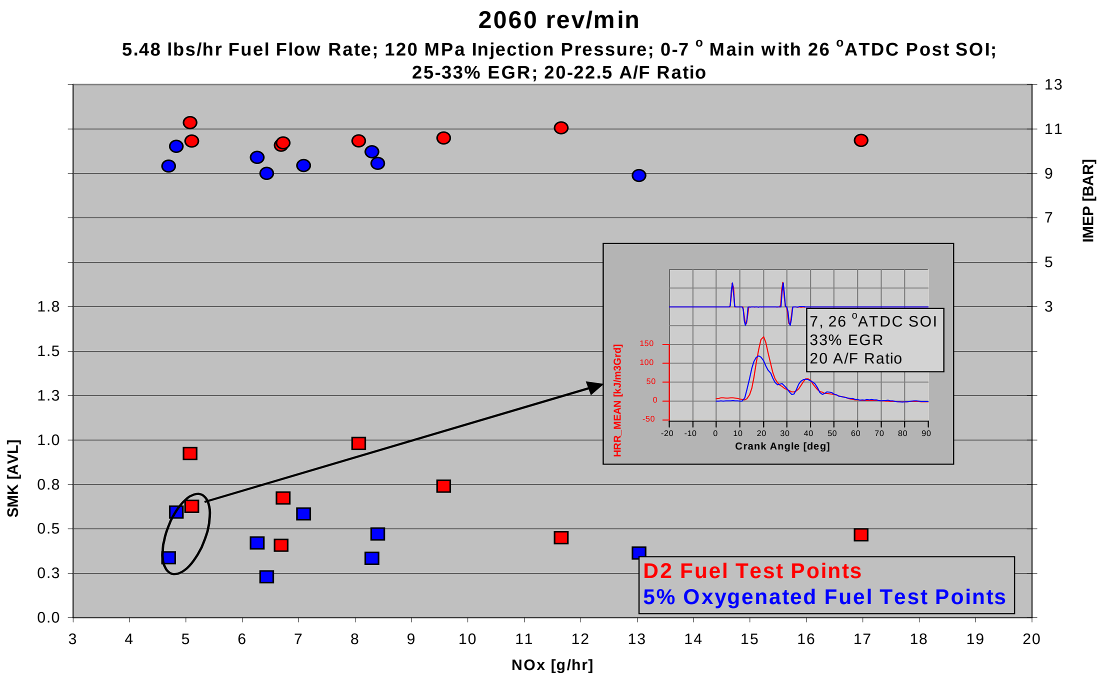

2060 rev/min

5.48 lbs/hr Fuel Flow Rate; 120 MPa Injection Pressure; 0-7 ° Main with 26 °ATDC Post SOI; 25-33% EGR; 20-22.5 A/F Ratio

Fig. 3

Baseline vs Oxygenated Fuel BSFC/Nox Trade-off @ Mode #6

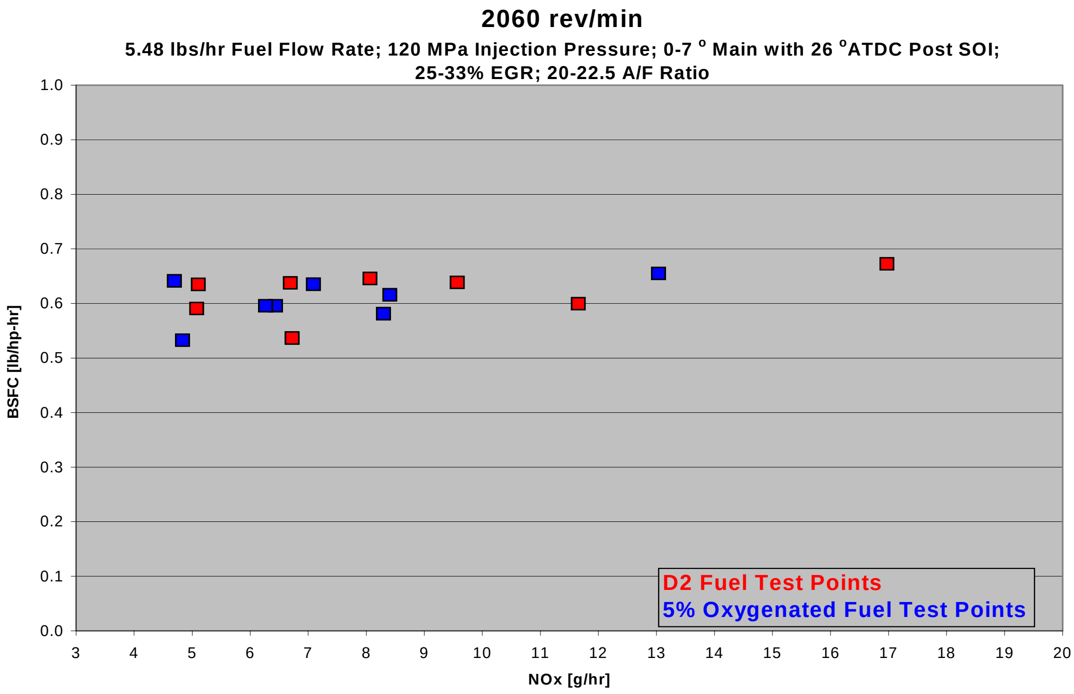

2060 rev/min

5.48 lbs/hr Fuel Flow Rate; 120 MPa Injection Pressure; 0-7 ° Main with 26 °ATDC Post SOI; 25-33% EGR; 20-22.5 A/F Ratio

Fig. 4

Baseline vs Oxygenated Fuel Soot/Nox Trade-off @ Mode #7

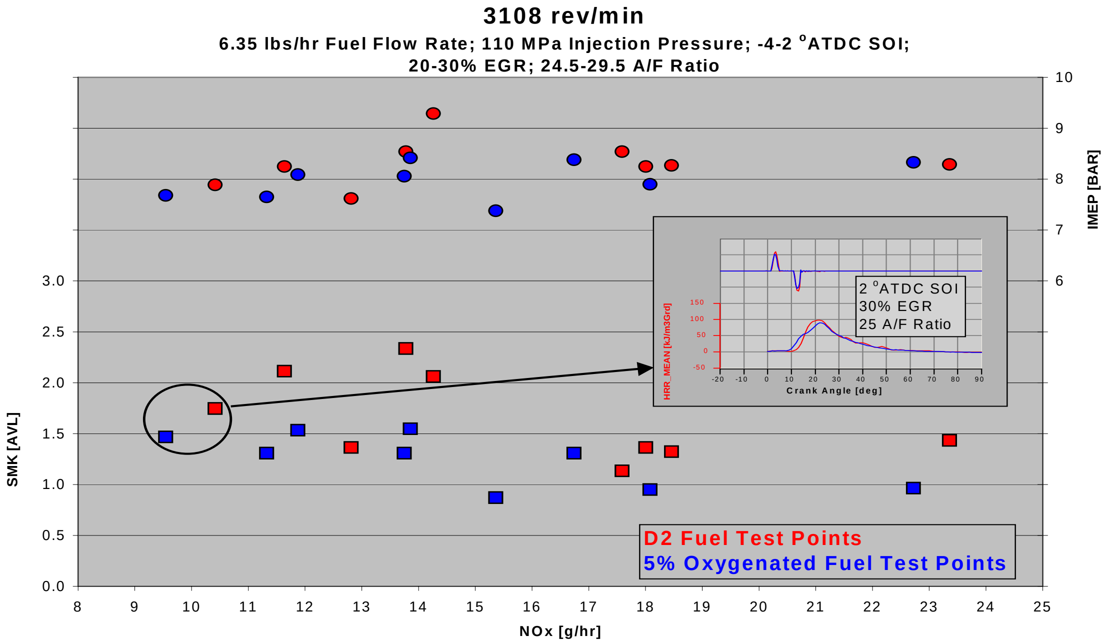

Fig. 5

Baseline vs Oxygenated Fuel BSFC/Nox Trade-off @ Mode #7

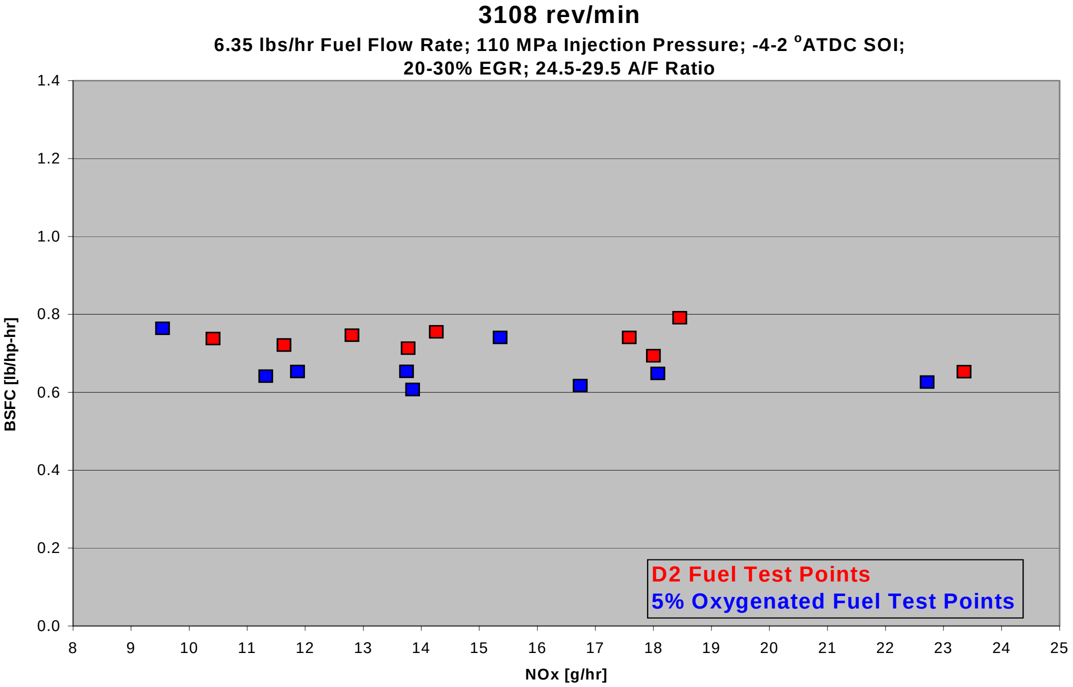

Fig. 6

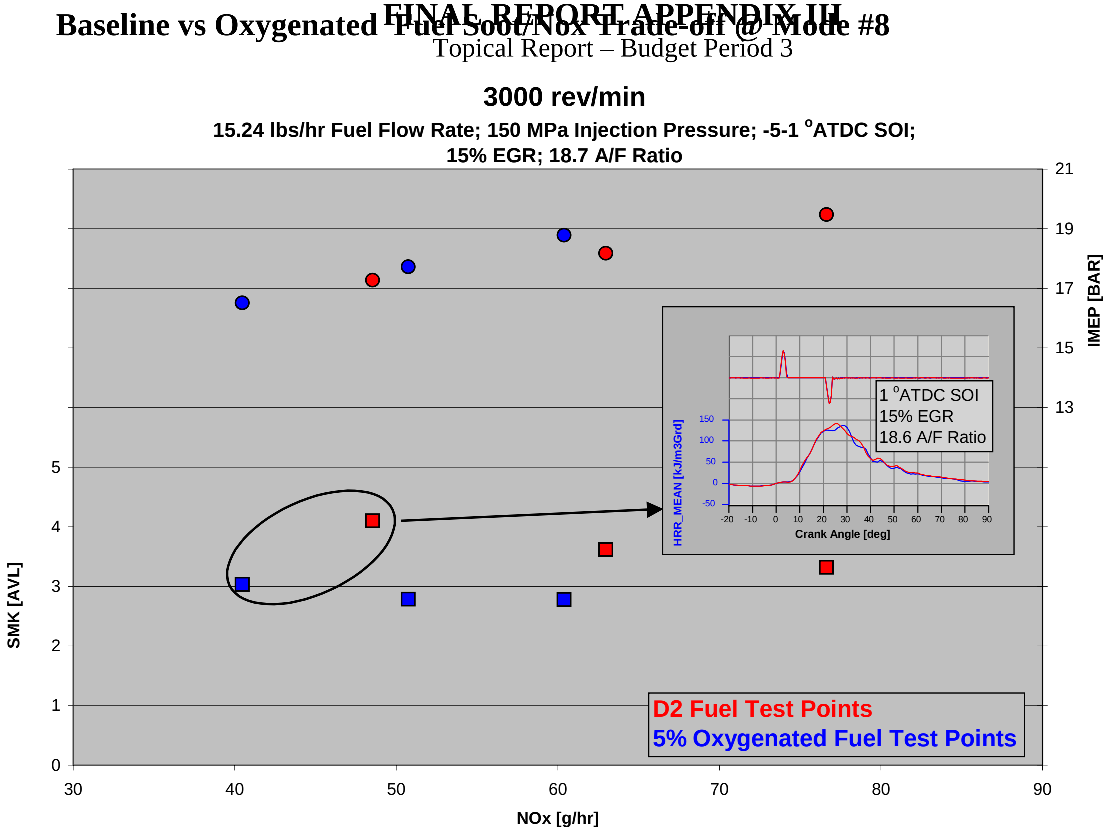
Baseline vs Oxygenated Fuel Soot/Nox Trade-off @ Mode #8
3000 rev/min
15.24 lbs/hr Fuel Flow Rate; 150 MPa Injection Pressure; -5-1 °ATDC SOI;
15% EGR; 18.7 A/F Ratio
SMK [AVL]
IMEP [BAR]
NOx [g/hr]
0
1
2
3
4
5
13
15
17
19
21
30
40
50
60
70
80
90
HRR_MEAN [kJ/m3Grd]
150
100
50
0
-50
-20
-10
0
10
20
30
40
50
60
70
80
90
Crank Angle [deg]
1 °ATDC SOI
15% EGR
18.6 A/F Ratio
D2 Fuel Test Points
5% Oxygenated Fuel Test Points

Fig. 7

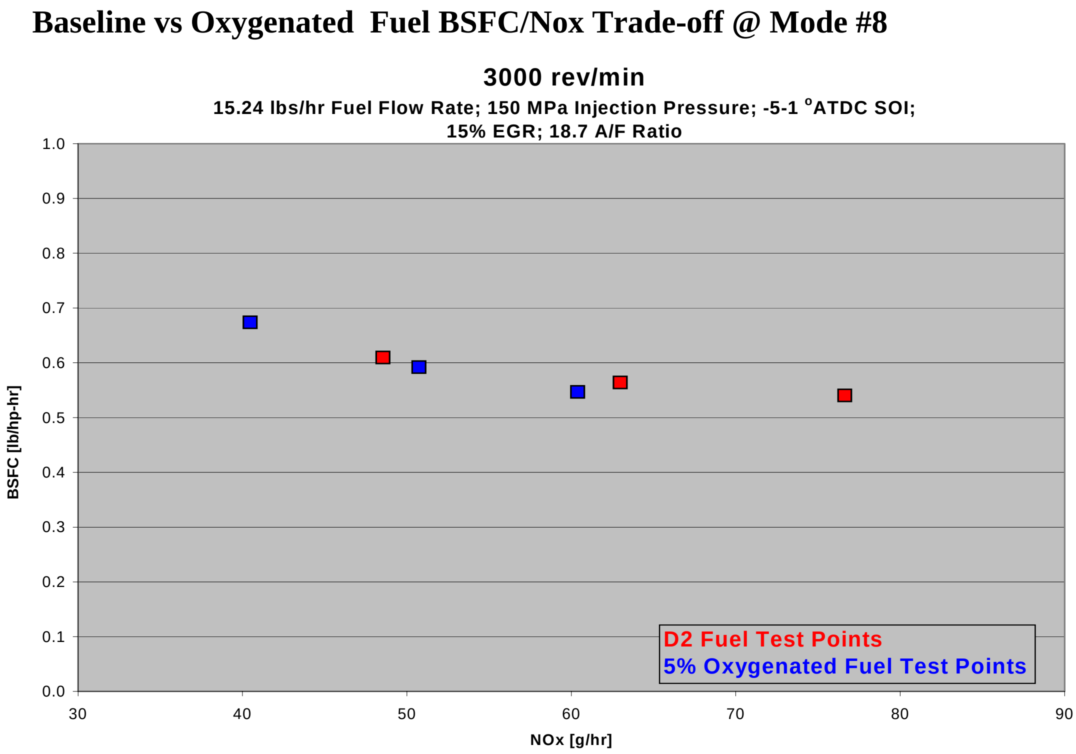
Baseline vs Oxygenated Fuel BSFC/Nox Trade-off @ Mode #8
3000 rev/min
15.24 lbs/hr Fuel Flow Rate; 150 MPa Injection Pressure; -5-1 °ATDC SOI;
15% EGR; 18.7 A/F Ratio
BSFC [lb/hp-hr]
NOx [g/hr]
0.0
0.1
0.2
0.3
0.4
0.5
0.6
0.7
0.8
0.9
1.0
30
40
50
60
70
80
90
D2 Fuel Test Points
5% Oxygenated Fuel Test Points

Fig 8

Table 2a

Run#		1	1	d%	2	2	d%	3	3	d%	4	4	d%	5	5
Fuel		BL	OX		BL	OX		BL	OX		BL	OX		BL	OX
Engine Speed	rpm	1005	1003		1004	1004		1007	1003		1007	1004		1006	1003
Torque	ft-lbs	9.1	8.2	-10	8.2	8.5	4	9.5	6.6	-31	9.0	8.0	-11	8.5	8.7
IMEP	bar	4.2	4.1	-1	4.1	4.3	4	4.2	3.9	-8	4.0	4.1	3	3.9	4.3
NOx	ppm	175	200	14	168	178	6	118	151	28	152	160	5	142	157
HC	ppm	386	324	-16	381	306	-20	490	375	-23	463	341	-26	291	356
AVL smoke	FSN	1.05	0.24	-77	0.71	0.20	-72	2.47	0.31	-87	0.87	0.28	-68	0.74	0.25
Injection Pressure	MPa	50	50		50	50		50	49		50	50		49	50
Air Fuel Ratio		45.6	46.5		47.1	47.4		43.9	47.7		45.3	42.4		45.6	40.4
EGR	%	21.8	19.5		20.8	21.0		20.9	19.0		24.8	26.7		24.6	24.1
SOC-pilot	deg CA ATDC	-4	-5		-2	-3		2	1		-4	-5		-2	-3
SOC-main	deg CA ATDC	6	5		8	7		10	9		6	5		8	7
BSFC	lb/hp-hr	0.60	0.66	10	0.64	0.63	-2	0.60	0.79	32	0.57	0.68	19	0.60	0.66
Fuel Flow	lb/hr	1.04	1.03		1.01	1.01		1.08	0.99		0.98	1.05		0.97	1.10

Table 4a

Run#		1	d%	2	d%	3	d%	4	d%	5
Fuel		BL		BL		BL		BL		BL
Engine Speed	rpm	3108		3110		3108		3107		3108
Torque	ft-lbs	14.6		13.6		16.3		14.3		14.4
IMEP	bar	8.5		8.3		8.3		7.6		9.3
NOx	ppm	143		149		190		106		118
HC	ppm	329		262		265		245		245
AVL smoke	FSN	1.13	-23	1.32	-28	1.43	-33	1.36	-4	2.06
Injection Pressure	MPa	110		109		109		109		109
Air Fuel Ratio		29.5		26.2		26.3		25.6		25.2
EGR	%	21.8		20.1		20.8		26.6		27.8
SOC-main	deg CA ATDC	9		5		0		9		4
BSFC	lb/hp-hr	0.74		0.79		0.65		0.75		0.75
Fuel Flow	lb/hr	6.38		6.35		6.28		6.33		6.42

Table 2b

Run#		6	6	d%	7	7	d%	8	8	d%	9	9	d%
Fuel		BL	OX		BL	OX		BL	OX		BL	OX	
Engine Speed	rpm	1005	1003		1006	1003		1006	1000		1006	997	
Torque	ft-lbs	8.3	7.4	-11	8.7	7.5	-14	9.4	9.0	-4	9.0	5.8	-36
IMEP	bar	3.6	3.9	8	3.9	4.1	4	4.2	4.3	2	4.0	4.0	-1
NOx	ppm	109	123	13	123	144	17	110	128	16	88	106	20
HC	ppm	444	367	-17	395	382	-3	267	337	26	391	355	-9
AVL smoke	FSN	1.36	0.32	-76	1.32	0.33	-75	1.14	0.27	-76	1.15	0.35	-70
Injection Pressure	MPa	50	50		50	50		49	50		50	49	
Air Fuel Ratio		44.7	42.1		41.4	40.6		42.0	41.7		40.3	41.4	
EGR	%	25.7	26.2		31.2	30.9		30.2	29.6		31.4	30.3	
SOC-pilot	deg CA ATDC	2	1		-4	-5		-2	-3		2	1	
SOC-main	deg CA ATDC	10	9		6	5		8	7		10	9	
BSFC	lb/hp-hr	0.61	0.74	21	0.61	0.72	18	0.56	0.59	5	0.60	0.75	25
Fuel Flow	lb/hr	0.98	1.04		1.01	1.03		1.01	1.01		1.03	1.01	

Table 4b

Run#		6	d%	7	d%	8	d%	9	d%
Fuel		BL		BL		BL		BL	
Engine Speed	rpm	3107		3105		3106		3108	
Torque	ft-lbs	15.4		14.6		14.9		15.1	
IMEP	bar	8.3		7.9		8.3		8.5	
NOx	ppm	149		88		98		116	
HC	ppm	268		234		253		327	
AVL smoke	FSN	1.36	-4	1.75	-16	2.11	-27	2.34	-34
Injection Pressure	MPa	109		109		109		109	
Air Fuel Ratio		25.6		24.8		25.1		24.9	
EGR	%	27.0		29.3		30.3		29.7	
SOC-main	deg CA ATDC	0		9		5		0	
BSFC	lb/hp-hr	0.69		0.74		0.72		0.71	
Fuel Flow	lb/hr	6.33		6.39		6.35		6.37	

Table 3a

Run#		1	1	d%	2	2	d%	3	3	d%	4	4	d%
Fuel		BL	OX		BL	OX		BL	OX		BL	OX	
Engine Speed	rpm	2061	2059		2059	2058		2	2058		2066	2059	
Torque	ft-lbs	23.3	24.1	3	20.8	21.3	2	21.9	23.5	7	26.0	23.5	-10
IMEP	bar	11.1	10.0	-10	10.5	8.9	-15	10.3	9.0	-12	10.4	9.7	-6
NOx	ppm	130	93	-28	184	144	-22	78	75	-4	78	73	-6
HC	ppm	462	232	-50	388	313	-19	327	238	-27	313	217	-31
AVL smoke	FSN	0.45	0.33	-27	0.47	0.36	-23	0.41	0.23	-44	0.67	0.42	-37
Injection Pressure	MPa	118	120		118	119		117	118		118	119	
Air Fuel Ratio		21.8	21.7		22.4	22.0		20.8	20.8		20.9	20.8	
EGR	%	25.3	27.2		25.2	26.7		31.9	31.1		30.6	31.4	
SOC-main	deg CA ATDC	9	8		4	4		12	9		9	8	
SOC-post	deg CA ATDC	32	32		31	32		32	32		32	32	
BSFC	lb/hp-hr	0.60	0.58	-3	0.67	0.66	-1	0.64	0.60	-6	0.54	0.60	11
Fuel Flow	lb/hr	5.48	5.48		5.48	5.48		5.48	5.48		5.48	5.48	

Table 3b

Run#		5	5	d%	6	6	d%	7	7	d%	8	8	d%
Fuel		BL	OX		BL	OX		BL	OX		BL	OX	
Engine Speed	rpm	2062	2062		2062	2058		2062	2058		2060	2058	
Torque	ft-lbs	21.9	22.7	4	22.0	21.8	-1	23.6	26.3	11	21.6	22.0	2
IMEP	bar	10.6	9.5	-11	10.5	9.3	-11	11.3	10.2	-9	10.5	9.4	-11
NOx	ppm	111	97	-13	62	57	-8	62	59	-5	99	87	-12
HC	ppm	340	303	-11	268	233	-13	290	225	-22	351	254	-28
AVL smoke	FSN	0.74	0.47	-36	0.63	0.34	-46	0.92	0.59	-36	0.98	0.58	-41
Injection Pressure	MPa	118	120		117	120		119	119		120	120	
Air Fuel Ratio		20.9	21.0		19.9	19.9		19.8	19.8		19.7	19.7	
EGR	%	31.7	30.9		32.5	32.8		32.2	32.3		32.6	31.5	
SOC-main	deg CA ATDC	4	4		12	9		9	8		4	4	
SOC-post	deg CA ATDC	32	32		32	32		32	32		32	32	
BSFC	lb/hp-hr	0.64	0.62	-3	0.63	0.64	2	0.59	0.53	-10	0.65	0.64	-2
Fuel Flow	lb/hr	5.48	5.48		5.48	5.48		5.48	5.48		5.48	5.48	

Table 5

Run#		1	1	d%	2	2	d%	3	3	d%
Fuel		BL	OX		BL	OX		BL	OX	
Engine Speed	rpm	2998	3002		2998	3000		2997	2999	
Torque	ft-lbs	49.6	48.4	-2	46.8	45.0	-4	44.0	39.6	-10
IMEP	bar	19.5	18.8	-4	18.2	17.7	-3	17.3	16.5	-4
NOx	ppm	358	284	-21	289	237	-18	223	189	-15
HC	ppm	22	79	259	23	56	143	23	50	117
AVL smoke	FSN	3.32	2.78	-16	3.62	2.78	-23	4.10	3.03	-26
Injection Pressure	MPa	150	148		149	148		149	148	
Air Fuel Ratio		18.5	18.6		18.8	18.6		18.8	18.6	
EGR	%	14.7	15.5		14.5	15.2		14.3	15.5	
SOC-main	deg CA ATDC	0	0		3	3		6	6	
BSFC	lb/hp-hr	0.54	0.55	2	0.57	0.59	4	0.61	0.67	10
Fuel Flow	lb/hr	15.31	15.13		15.27	15.23		15.31	15.24	

Appendix 2
International Truck and Engine HCCI Test Results

Evaluation of HCCI Fuels in Diesel Single-Cylinder Test Engine

Background

In the last decade the search for new technological ways of controlling in-cylinder emission of diesel engine without compromising its traditional advantages of a high fuel economy and superior torque characteristics has increased interest in the alternative modes of diesel combustion. Traditional diesel combustion is known as a mixing controlled process in which fuel is injected in the form of a high pressure fuel jet into the high pressure and high temperature air, ignited very soon thereafter, and then undergo both combustion and mixing while injection lasts. While high efficiency of this type of combustion is very well established the heterogeneity of air-fuel mixture formed in such process imposes certain practical limits on reduction ability of emissions such as Nox and soot. One of the alternative modes of diesel combustion which recently gained the significant interest is a Homogeneous Charge Compression Ignition (HCCI) combustion. Conceptually, in this case, the fuel is injected significantly ahead of its ignition, allowed to pre-mix thoroughly with air to form a homogenous charge and then self-ignited and burned., usually, with a much lower amount of soot and Nox emission being formed. It needs to be understood, however, that despite of apparent simplicity of this concept the abundant amount of conducted research has indicated existence of many technological barriers inhibiting successful application of the HCCI concept in today's diesel technology

Work Objective

It is well known that some of these barriers are related to the fuel properties. For a successful HCCI combustion the fuel needs to mix fast with an air and, additionally, to have prolonged ignition delay allowing for the complete fuel-air premix and shift of the ignition point into the vicinity of TDC position of the piston. The fuel volatility and the cetane number (CN) are clearly the properties which enhance these processes, accordingly.
The objective of this work, therefore, has been to formulate three different blends of the hydrocarbon based fuels having a distinctly different volatility and CN properties, test them in the diesel single cylinder test engine operating in the HCCI-like mode of combustion and to compare their relative emission performance against the baseline obtained for ULS base fuel.

Test Fuels

The extensive study of multi-component blends of hydrocarbon fuels has been performed by BP-AMOCO to generate concise matrix of test fuels characterized by relatively wide ranges of volatility and CN that would be still compatible with ignitibility and combustion constrains typical for diesel combustion. As result of this study three test fuel have been selected and custom fabricated for purpose of this work:

- Test fuel #1 – 90%/10% blend of gasoline aromatics (petroleum naphtha) and No 2 Diesel
- Test fuel #2 – 35%/65% blend of kerosene (petroleum distillate) and gasoline aromatics (petroleum naphtha)
- Test fuel #3 - 50%/50% blend of test fuel #1 and test fuel #2

The ULS fuel has been used as the baseline. Fig. 1 schematically shows the composition of these test fuels.

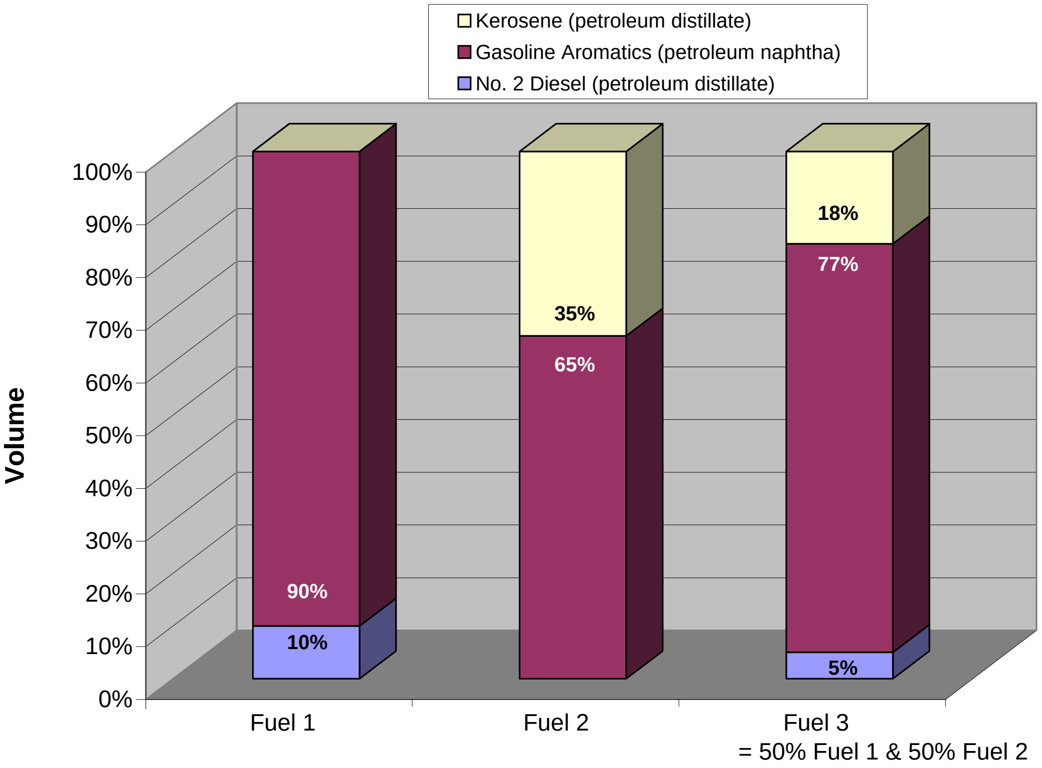

Fig 1

Description of Engine Test

Testing has been conducted on ITEC Single-Cylinder Test Engine (SCTE) with the 95mm bore x 104mm stroke cylinder –crank module having displacement of .75l. In order to enable the HCCI-like combustion the piston for this test has been modified to reduced compression ratio (CR) of 15 and engine has been equipped with common rail injection system capable of multiple injection. In addition, the SCTE had a wide range of exhaust gas re-circulation (EGR) control and had a special intake port swirl modulating device allowing to vary amount of the air-fuel mixing during pre-mix phase of HCCI-like combustion. To ensure good quality of results comparison the all fuel tests have been run at 2000rpm and 4.5 bar BMEP load. Such conditions have been well established as conducive to maintain the stable and consistent HCCI-like combustion.

Type of HCCI-like combustion selected in this work (ideal HCCI combustion in which entire amount of fuel is perfectly pre-mixed with available air is not realistic to be achieved in real diesel !) was a partially premixed combustion based on a triple-shot injection process. This mode has been demonstrated to have significant potential for the emission improvement relative to the conventional single-shot injection during the work with conventional diesel fuel prior to this investigation. In the triple-shot injection the first very early injection premixes optimized amount of the fuel which "cool" burn is initiated by second injection. Relatively low temperature combustion continues throughout this phase till the beginning of a final injection which burns fast but relatively clean. Although details of this mode of combustion is not fully understood yet it is believed to be dependant strongly on a kinetics of reactions involved.

Finally, the test methodology applied in this work involves Statistical Design of Experiment (DOE). This methodology is capable to provide a widest possible interrogation domain of important engine control parameters and corresponding emission responses of individual fuels tested. In addition, as it will become evident in the discussion of results, DOE allows to better understand effects of the individual control parameters on performance (responses) under investigation. The specific test design used was a central composite Box- Benhken array in which three control parameters, namely the EGR level, start of injection of second injection shot and intake port swirl level have been varied through three levels resulting in the15-point test for each fuel. Fig 2 illustrates configuration of parameters and levels relevant for this test design. The levels of the main test parameters have been pre-optimized and selected for each of individual fuels according to their specific combustion characteristics. Some other parameters, external to DOE array (such as injection pressure, timing and quantity of the first injection and quantity of second injection) have been optimized with respect to observed responses – primarily Nox, soot and BSFC – for each set of DOE parameter settings.

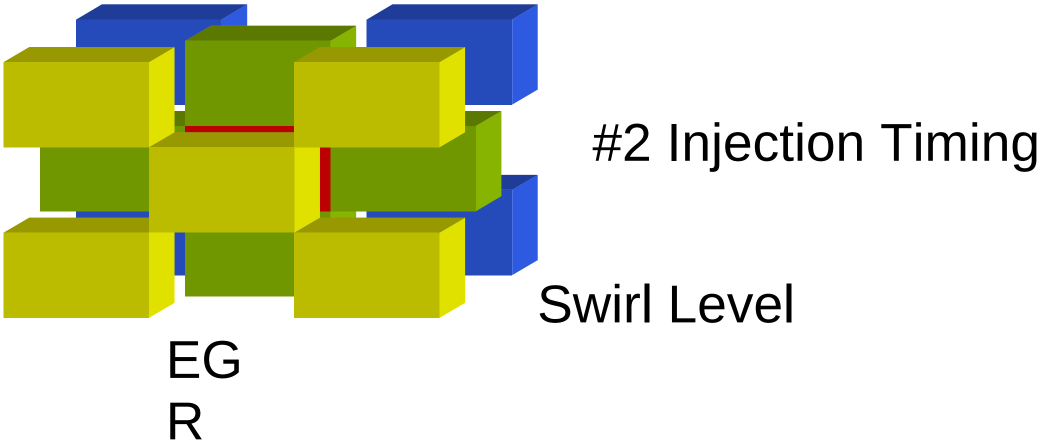

Fig 2

Discussion of Results

The results of the soot-Nox trade-offs obtained from DOE based parameter sweeps (with external parameters optimized for each point) are shown in Fig. 3. From the cursory look at this graph, by comparing the scatters of test points for individual fuels it is becoming evident that all “HCCI” fuels demonstrate very significant reduction in soot emission. Test fuel #1, for the values of BSNOx >.2 g/hp-hr shows lowest smoke number <.1 FSN which is apprx by a factor of ten lower than lowest smoke obtained with base fuel. This level of soot emission represents almost “smokeless” combustion. Although observed reductions in the Nox for the “HCCI” fuels, relative to base fuel, are not so dramatic as the reductions in soot, they are still very significant. Table 1 summarizes BSNOx and soot values recorded for **the best** Nox-soot trade-off points with the base fuel and individual “HCCI” fuels and evaluates relative improvements (or penalties) with respect to base fuel

Table 1

	Base Fuel	Fuel #1		Fuel #2		Fuel #3	
	Value	Value	%diff to base	Value	%diff to base	Value	%diff to base
BSNOx,g/hp-hr	0.15	0.17	10.00	0.09	-43.33	0.10	-33.33
Soot, FSN	1.35	0.40	-70.37	0.20	-85.19	0.10	-92.59

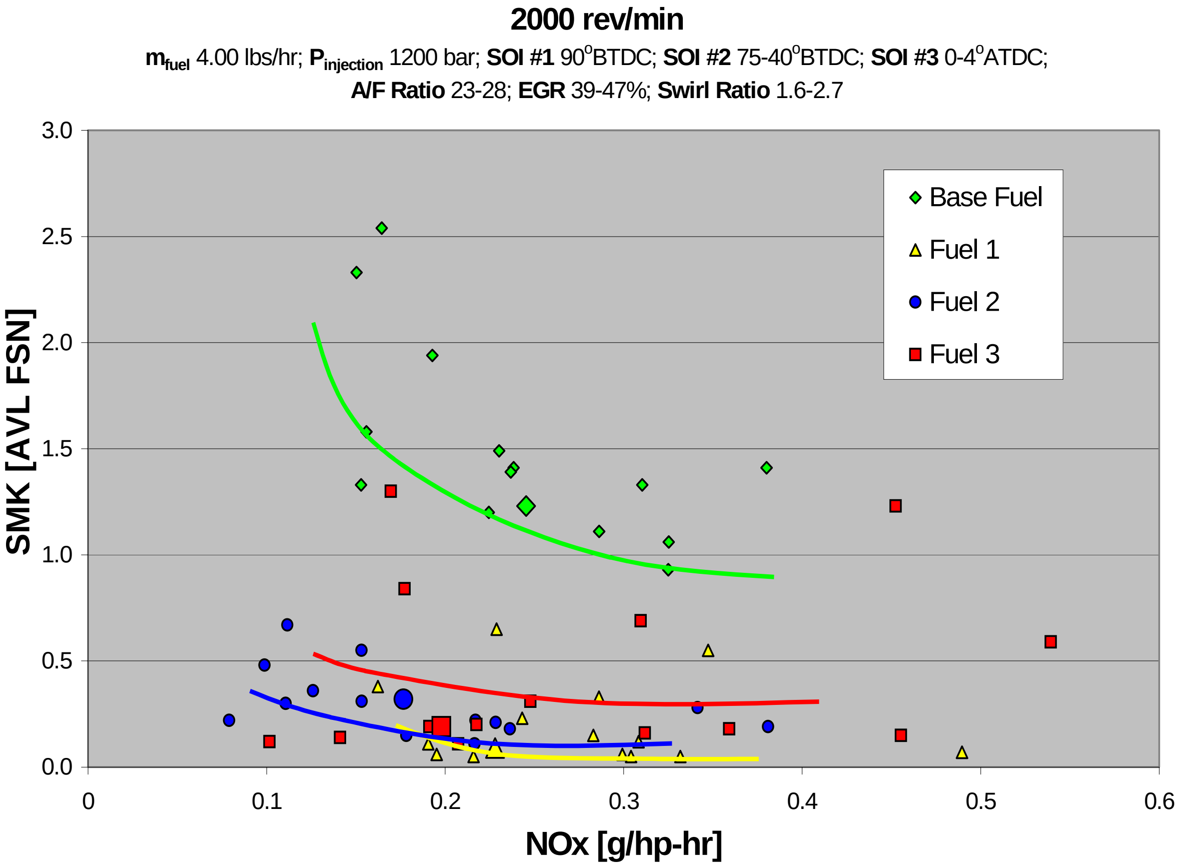

Fig 3

Fig. 4 provides the comparison of HC emission and break specific fuel consumption (BSFC) for “HCCI” fuels and base fuel. As it is typical for an HCCI-like combustion “HCCI” fuels show increase in the HC emission levels relative to the base fuel. Interestingly, fuel #1 – primarily gasoline-like aromatics – produces highest level of HC than other two blends. This behavior correlates with the fact that fuel #1 have been showing some difficulty in reliable ignition and stable combustion. Actually, both fuel #1 and fuel #3 have required, at certain test points, auxiliary intake air heating to stabilize the ignition, It is, most probably, indicating that selected compression ratio CR=15 was somewhat too low for these fuels. Review of the BSFC for the base and the “HCCI” fuels does not indicate any significant deterioration in fuel consumption for “HCCI” fuels. In order, however, to make a fair judgment on this issue the calorific values of base and “HCCI” fuels would need to be carefully taken into account, which has not been done.

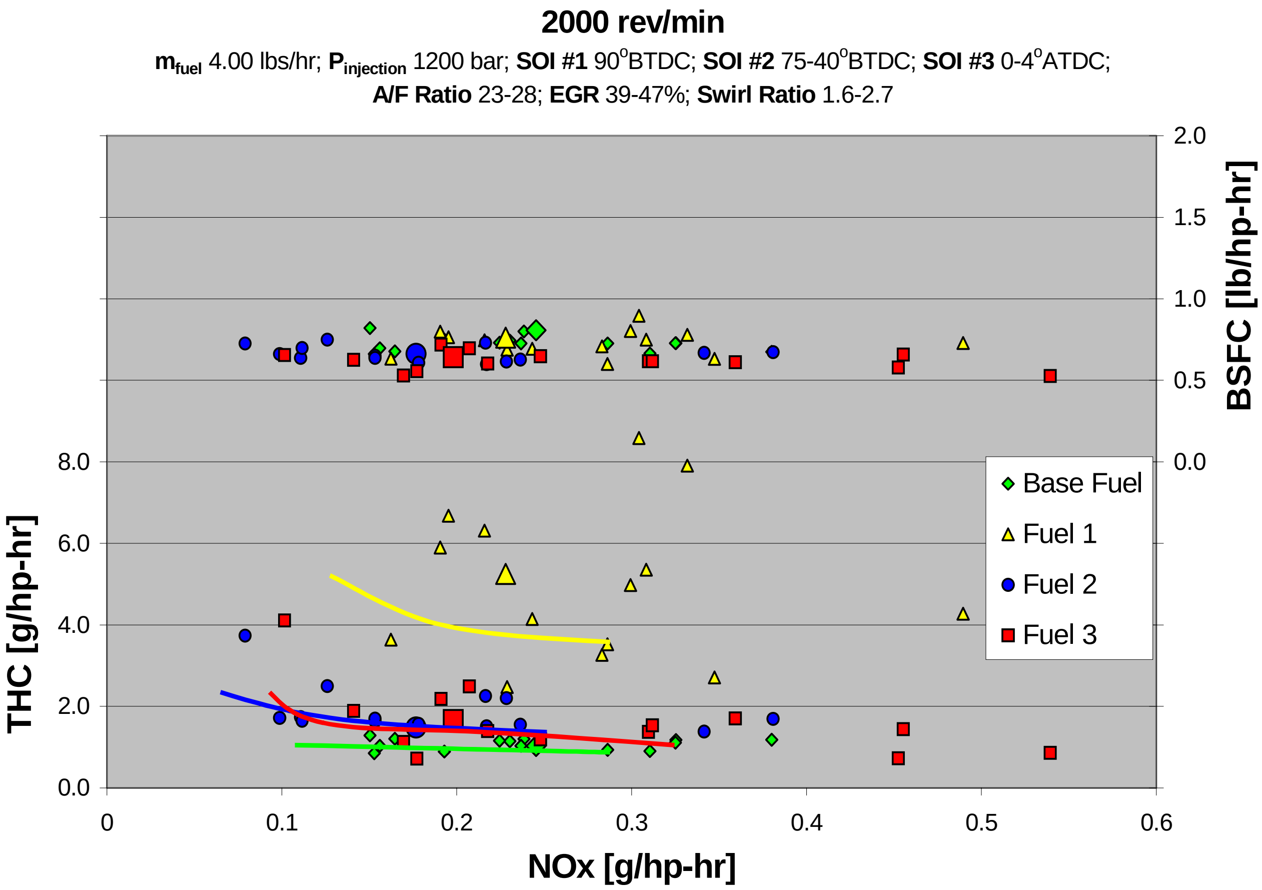

Fig. 4

To provide some insight into combustion thermodynamics of evaluated fuels the cylinder pressures have been measured and then post-processed to obtain corresponding traces of Apparent Heat Release Rates (AHRR). In internal combustion engine research an AHHR is considered to be an approximate "signature" of combustion process. To allow for a meaningful comparison of AHRRs between the base and test fuels, the cylinder pressures shown in Fig. 5 have been measured at the EGR, injection timing and intake swirl settings being selected as close as possible. Enlarged points of the data sets corresponding to individual fuels shown in Fig 3 are representative of those conditions for which cylinder pressure measurements have been taken. Fig 6. shows AHRRs obtained from cylinder pressures shown in Fig. 5. The traces shown in the upper sections of Fig. 5 and Fig. 6 represent the injection timing commands for individual injection events executed for each of the fuels. As it can be seen the timing strategy applied to individual fuels is almost identical assuring that observed differences in the cylinder pressures and corresponding AHRRs are result of the differences in combustion of different fuels and not the result of injection strategy. Review of both of the cylinder pressures and AHRRs traces clearly indicates very significant differences in combustion

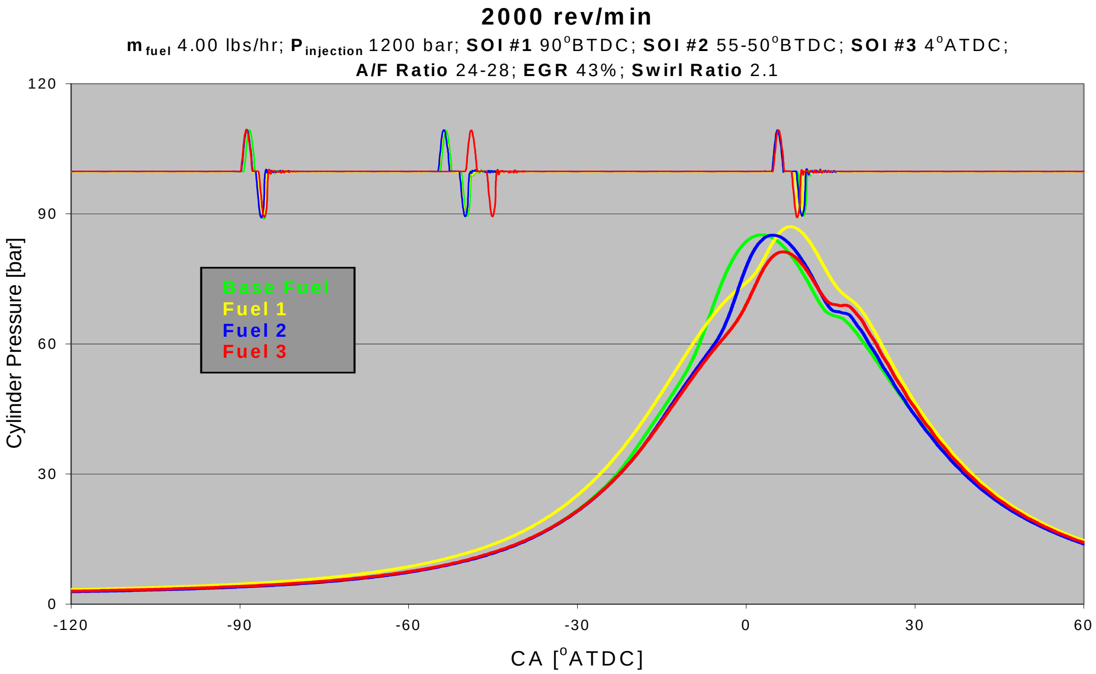

Fig 5
Cylinder Pressure Traces

between different fuels – a feature that can be attributed to the different fuel specific chemical kinetics involved.

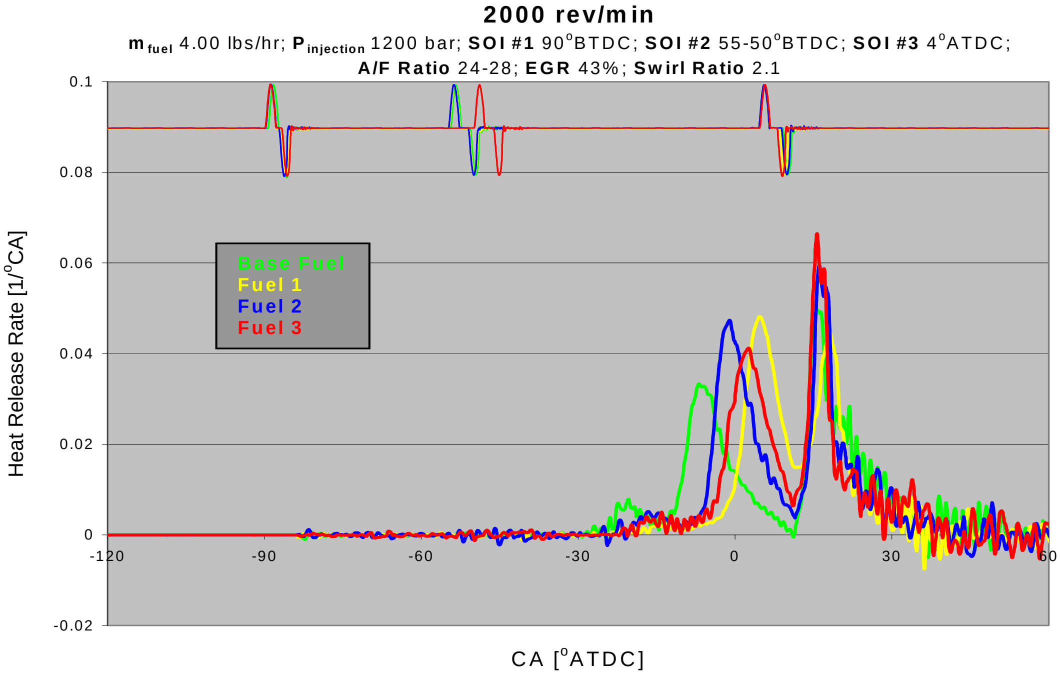

Fig. 6

AHRRs Traces

From the comparison of first "humps" of heat release rates in Fig.6 it can be clearly seen that ignition delay for all of the "HCC" fuels is longer than of the base fuel. This means that the more of "HCCI" fuel is premixed with the air before the ignition event. Also, the first AHRR "hump" for "HCCI" fuels is lower and more spread out than the one for the base fuel indicating that the "cool" flame reaction rates are lower for "HCCI" fuel than for base fuel. More of premixed "HCCI" fuel causes much higher second AHRR hump what could suggest existence of a higher local temperatures in the combustion space and , therefore, higher smoke and Nox. But, since the "HCCI" fuel- air mixture is better homogenized and locally leaner the local temperatures are, most probably, actually not much higher than in case of the poorly homogenized based fuel-air mixture and the production of Nox is contained. On the other hand, the higher local air-fuel ratios related to the better charge homogenization lead to reduction of the soot.

Use of the DOE methodology allows to evaluate the general trends of effects that the DOE control parameters - i.e. the EGR, timing of second injection and the intake swirl - have on main response characteristics under investigation –i.e. Nox and soot - for individual fuels. Fig. 7 shows respective response plots for base fuel, Fig. 8 response plots for fuel #1, Fig. 9 response plots for fuel #2 and, finally, Fig. 10 response plots for fuel #3.
The principal observations that can be made out of the analysis of the response plots for individual fuels are as follows:

- Decreasing amount of EGR has a decreasing effect on Nox regardless of fuel – a characteristic well established for conventional diesel fuel
- There seems to be an optimum in EGR level helping soot reduction for the fuel #1 and fuel #3 while the fuel #2 shows a monotonic deteriorating effect of increasing EGR on smoke, typical for the conventional diesel fuel represented by base fuel
- "V"-shaped response of the Nox to timing of second injection, which is apparent for all fuels, indicates that the range of this parameter was very well optimized with respect to Nox in DOE array
- Smoke production for all "HCCI" fuels is evidently reduced by advancing start of second injection while the base fuel shows optimum in smoke for the mid-level of second injection; These difference in the smoke responses is probably related to the difference in fuel volatility and its co-effect on mixing
- As expected, in general, swirl seems to have stronger effect on soot than on Nox formation; there are definite optima in a level of swirl with respect to smoke for all fuels except for fuel #2 which prefers lower swirl.
- Nox formation for fuel #1 seems to be relatively strongly increasing with increasing swirl; all other fuels show either a low sensitivity of Nox to swirl – like the base fuel and fuel #2 or show the optimum in swirl for Nox – case of the fuel #3

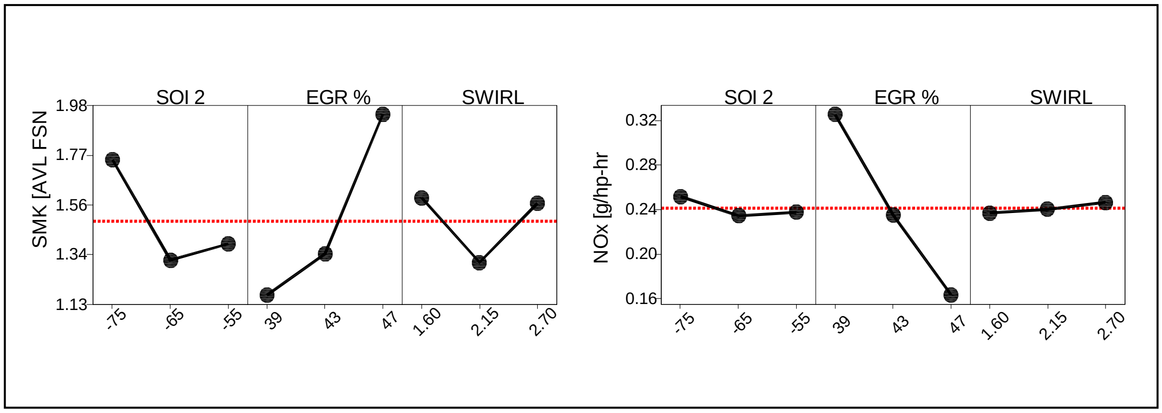

Fig. 7
Response Plots for Base Fuel

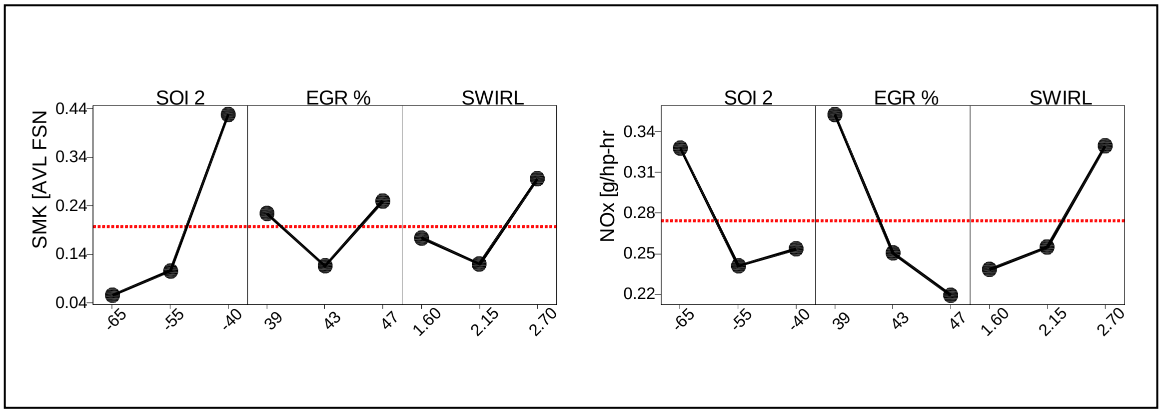

Fig. 8
Response Plots for Fuel #1

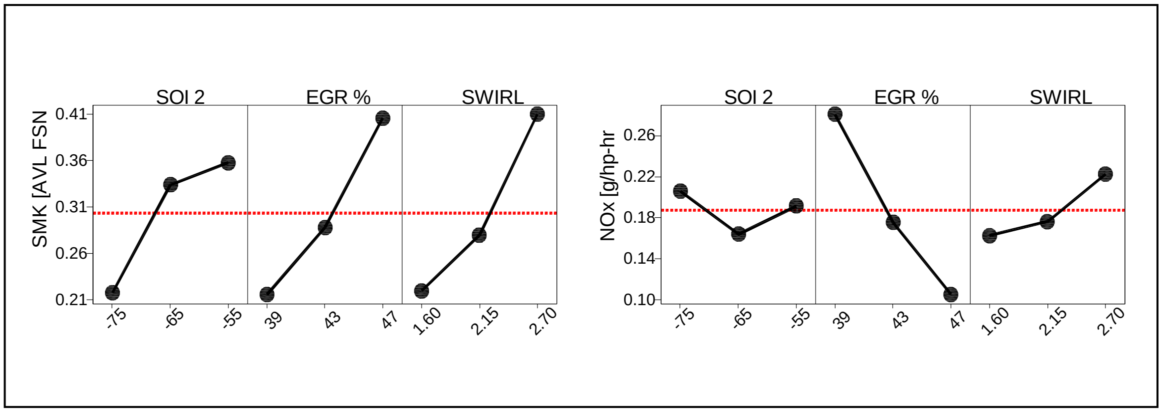

Fig. 9
Response Plots for Fuel #2

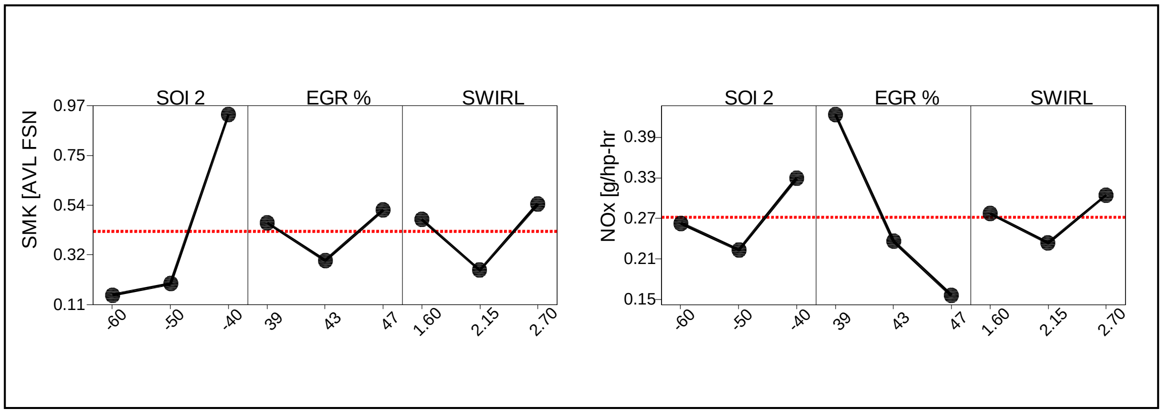

Fig. 10

Response Plots for Fuel #3

Conclusions

Although the scope of this work has been limited primarily to investigation of the engine emission performance on single operating point the results show the undisputable advantages of customized hydrocarbon fuel blends for a clean HCCI type diesel combustion. Optimized lower cetane number and increased volatility of fuel are clearly the physical properties enhancing its HCCI diesel combustion compatibility. It needs to be emphasized that there are also certain chemical properties related to a combustion chemical kinetics of the fuel that make it suitable for HCCI use which at present time are not well understood . All of the “HCCI” fuels have demonstrated very significant potential in reducing emission of soot relative to the base diesel fuel. Fuel # 3 has demonstrated best performance in the sense that, for the optimized soot-Nox trade-off point, the approximately 90% reduction in soot was coupled to approximately 30% in Nox reduction, relative to the best point for base fuel.

In order to fully evaluate the potential of tested fuels the more extensive engine mapping would be necessary. Considering the complexity of the HCCI process and its investigation the much more extensive program would be needed to complete such a task.

Appendix 3
BP Preparation of HCCI Fuels

Development of OTM Syngas Process and Testing of Syngas Derived Ultra-clean Fuels in Diesel Engines and Fuel Cells
Budget Period 3
DOE Cooperative Agreement No. DE-FC26-01NT41096
Task 8: Fuel and Engine Testing

Date: October 30, 2004
Author: Leslie R. Wolf
Global Fuels Technology
BP Amoco Oil
150 W. Warrenville Rd.
Naperville, Il. 60563-8460

Summary

Laboratory scale fuel blends were made using ten different gasoline or distillate refinery blending components. Testing of these blends for ignition and volatility properties allowed the determination of blending characteristics for these properties. From these results, three larger scale (55 gallons) blends with selected ignition quality and volatility were produced.

Results and Discussion

The ten refinery streams described in Table 1 were blended according to the compositions shown in Table 2 to make laboratory scale samples. These samples were tested for Reid vapor pressure, single-plate distillation (ASTM D86) and ignition quality (IQT tester). Test results are shown in Table 3.

Table 1

Material	Description
D2	High cetane full boiling range No. 2 diesel fuel
D2A	Low cetane heavy aromatic distillate
D1H	High cetane No. 1 diesel fuel
D1L	Low cetane No.1 diesel fuel
HNP	Low octane heavy paraffinic naphtha
HNA	High octane heavy aromatic naphtha
LNA	High octane light aromatic naphtha
LNP1	High octane light paraffinic naphtha
LNP2	Low octane light paraffinic naphtha
LNP3	Intermediate octane very light paraffinic naphtha

From the data in Table 3, blending characteristics for IQT cetane number and density (API gravity) were developed (see Appendix 1 for discussion of IQT cetane number relative to ASTM D613 cetane number). It was found that IQT cetane number blended as a linear volume fraction weighted sum. Density could be calculated assuming ideal mixing (i.e. no volume change).

Table 2

Blends by Mass %

Blend	1	2	3	4	5	6	7	8	9	10	11	12
D2	100	50	50	50								
D2A												
D1H					100	50	50	50				
D1L									100	50	50	50
HNP		50				50				50		
HNA			50				50				50	
LNA												
LNP1				50				50				50
LNP2												
LNP3												

Blend	13	14	15	16	17	18	19	20	21	22	23	24
D2	50	50									25	
D2A			100	50					50	50		25
D1H						50		50				25
D1L	50			50	50		50				25	
HNP												25
HNA										50		
LNA		50			50	50			50			
LNP1											25	
LNP2							50	50				
LNP3											25	25

Table 3

Test Results

Blend	1	2	3	4	5	6	7	8	9	10	11	12
Rvp	0.36	1.45	0.23	3.15	0.15	1.33	0.26	3.05	0.22	1.36	0.28	3.02
Ignition delay	4.066	4.628	8.039	5.524	4.612	5.035	8.862	6.088	5.632	5.674	10.989	7.164
IQT Cetane number	48.86	43.3	27.99	37.21	43.44	40.22	26.15	34.42	36.63	36.41	22.67	30.42
Sp. Gr.	0.8383	0.7741	0.8567	0.7674	0.8184	0.7650	0.8460	0.7585	0.8257	0.7681	0.8498	0.7616
Blend	**13**	**14**	**15**	**16**	**17**	**18**	**19**	**20**	**21**	**22**	**23**	**24**
Rvp	0.29	0.91	0.08	0.55	0.88	0.87	1.54	1.52	0.78	0.23	4.03	3.35
Ignition delay	4.407	6.827	10.71	6.991	7.761	9.782	5.29	4.775	28.319	24.105	5.824	6.073
IQT Cetane number	45.28	31.53	23.05	30.97	28.7	24.46	38.58	42.11	13.2	14.34	35.65	34.49
Sp. Gr.	0.8323	0.8528	0.9413	0.8798	0.8462	0.8422	0.7440	0.7551	0.9053	0.9086	0.7524	0.7733

Table 4 gives blending values for density and IQT cetane derived from data in Table 3.

Table 4
Blending Properties

Material	Blending Density	Blending IQT Cetane Number
D2	0.8388	50.0
D2A	0.9426	22.1
D1H	0.8201	43.3
D1L	0.8240	38.2
HNP	0.7182	36.8
HNA	0.8758	6.5
LNA	0.8683	10.0
LNP1	0.7070	25.6
LNP2	0.6888	40.0
LNP3	0.6676	32.9

Blend distillation data are given in Table 5. Figure 1 summarizes the volatility described by 10%, 50% and 90% evaporated temperatures as a function of the IQT cetane number.

Engine Test Fuels

Engineers at International Truck and Engine Company (IT&E) selected property ranges for engine test fuels. High volatility (i.e. low distillation temperatures) and cetane ranging from very low (16) to moderate (35) were desired. Estimated properties for six blends were calculated to span the desired property ranges. Table 6 shows the composition of the six blends and calculated properties. From these six blends, IT&E engineers selected three blends: P2, P3, and P6. These three blends were blended at 55 gallons scale. In addition to the blend components, lubricity improver was added at 0.01 to 0.02% to provide adequate fuel system protection. Table 7 shows test results on the final blends.

Table 6 Proposed Blends, Mass %

Material\Blend	P1	P2	P3	P4	P5	P6
D2A	10	10		10	5	5
D1L			35	25	17.5	17.5
HNA	35	25	10	10	22.5	17.5
LNA	15	25	10	10	12.5	17.5
LNP1	40	40			20	20
LNP2			45	45	22.5	22.5
Calculated IQT Cetane	16	16	35	36	26	26
Estimated T10	174	169	212	214	203	217
Estimated T90	445	438	393	462	414	431

Table 5
Blend Distillation Temperatures

Blend	1	2	3	4	5	6	7	8	9	10	11	12
0%	334.7	193.8	302.8	110.7	368.2	192.7	314.8	115.8	319.2	197.7	308.2	112.4
5%	386.9	203.1	336.6	141.4	387.7	207.9	345	176.6	349.3	216.1	332.9	171.6
10%	401.3	210.1	337.7	177.5	390.5	215.2	347.4	196	354.8	226	334.8	194.6
20%	429	221.6	345.9	210.2	399.6	228.6	352	222.7	366.3	239.8	340.9	223.9
30%	453.5	234	353.6	232.2	408.1	243	357.4	246.4	378.4	252	346.1	245.1
40%	476.9	251.9	363.9	253.9	415.9	266.7	363.4	273.6	391	269.9	351.9	267.5
50%	499.7	283.5	380.5	290.9	424.5	306.8	372.2	316.8	403.7	294.1	358.3	298.9
60%	522.7	351.7	409.5	375.9	434.4	368.9	384.1	383.7	416.7	332.7	367.8	349.8
70%	547.6	441.4	462.9	441.8	446.1	406.5	402.4	408.4	432.2	373.2	383.2	386.5
80%	574.7	498.9	521.1	496.4	460.3	428.5	427.3	427.2	450.7	410.5	407.9	409.6
90%	608.1	550.8	574.6	551.3	479.6	455.8	458.2	456.5	476.3	447.6	445.1	446.4
95%	632.8	583.8	608.5	583.6	496.4	474.1	478.8	476.9	498.3	474.9	471.3	474.4
100%	655.6	623.8	636.3	626	514.8	497.8	503.8	498.4	524.7	491.5	508	505.7
Recovery	98.5	94.5	98.6	94.2	98	97.8	98.7	98.2	98.4	97.6	99.1	97.2
Residue	1.4	1.9	1.3	1.7	1.3	1.2	1.2	1.5	1.4	2	1.3	1.4
Loss	0.1	3.2	0.1	3.8	0.7	0.9	0.1	0.3	0.2	0.4	0	1.3

Blend	13	14	15	16	17	18	19	20	21	22	23	24
0%	329.4	230.4	339.1	327.4	232.1	232	196.7	199.8	227.8	318.4	138.2	145.6
5%	360.2	236.1	433	358.3	241.2	239.2	204.9	202.7	230.8	334.5	155.5	158.5
10%	365.1	237.1	452.8	372.7	241.8	241.2	208.8	206	231.8	341	163.9	165
20%	384.6	240	476.5	396.7	245.7	246	215.6	215	233.7	352.6	179.8	174.9
30%	403.2	244.9	492.7	416.5	251	251.3	220.1	220.2	243.9	359.5	202.8	189.1
40%	422.6	256.9	505.2	437.8	261.3	264.8	230.3	233.3	259.7	373.3	237.1	218.2
50%	442.8	296.3	518.4	457.4	282.9	302.4	253.3	256.4	293.7	395.9	277.5	276.9
60%	464.6	425.7	533.7	478	343	392.6	329.3	375.8	471.6	441.2	354.4	366.5
70%	490.9	478	552.8	501.7	394.4	417.9	386.4	410.6	503.5	494.6	409.1	432.9
80%	525.5	525.5	581.5	530.3	422	437.6	415.5	428	528.8	532.7	448.3	463.9
90%	575.3	578.3	630.1	580.5	457.3	462.9	453.4	456.2	584	584.6	512.2	507.8
95%	610.1	611.4	670.4	629.5	488.2	482.8	483.5	476.4	630.3	633.8	563.7	569.3
100%	630.2	629.7	680.9	644	510.6	502.2	508.4	497.5	631	636.2	580.5	581.6
recovery	98.1	98	97.2	97	97.5	98	97.4	96.8	95.8	96.6	96.9	96.2
residue	1.8	1.8	1.5	2.4	1.4	1.5	1.7	1.5	2.5	2.9	2.5	3
Loss	0.2	0.2	1.2	0.6	1	0.5	0.8	1.5	1.6	0.5	0.6	0.7

Figure 1
Volatility Range - Ignition Quality Map

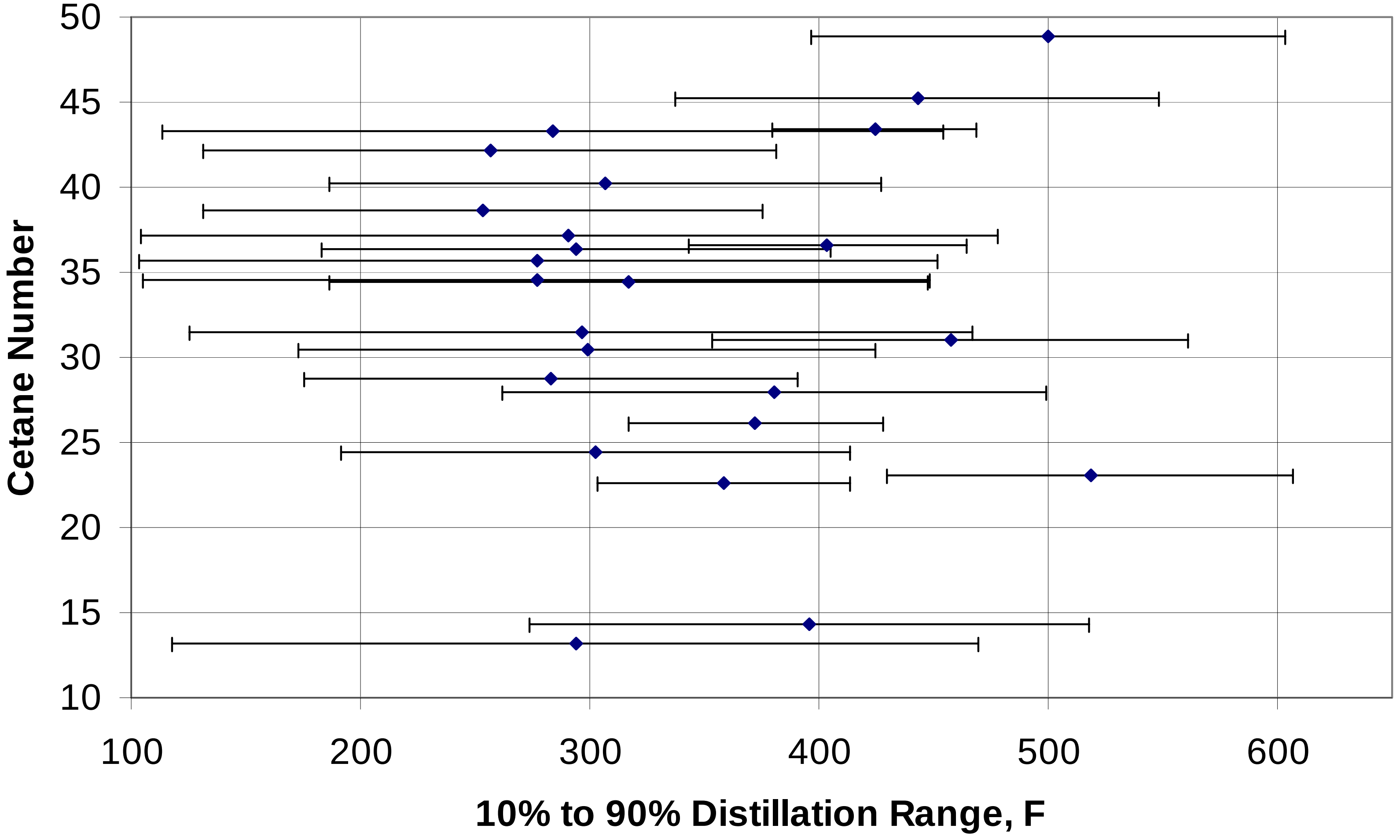

Table 7
Engine Test Blends (55 gallons)

Engine Test Blend	**21507-31-1**	**21507-31-2**	**21507-31-3**
Test	Fuel 1	Fuel 2	Fuel 3
API Gravity, °API	44.65	51.98	48.41
Specific Gravity, 60F/60F	0.803293	0.771201	0.786504
Distillation			
Initial Boiling Point, °F	119.5	201.9	149.8
10% distilled, °F	205.1	208.9	20839
20% distilled, °F	222.2	213.5	216.8
30% distilled, °F	231.3	217.9	224.7
40% distilled, °F	241	226.6	235.1
50% distilled, °F	254.3	242.9	249.1
60% distilled, °F	271.5	290.6	278.6
70% distilled, °F	303.8	377.3	339.1
80% distilled, °F	346.1	404.5	377.4
90% distilled, °F	385.2	443	429.2
Final Boiling Point, °F	541.6	489.9	537
Reid vapor pressure, psi	2.64	1.49	2.05
Carbon, mass %	86.66	85.8	86.42
Hydrogen, mass %	11.91	13.82	12.9
Nitrogen, ppm	25	<1	12
Sulfur, ppm	293	5	143
SFC Aromatics, vol%	60.02	28.69	44.88
Lower heating value, BTU/lb	17872.45	19066.2	18297.13
Lower heating value, BTU/gal	119563.5	122453.9	119846.4
Cetane Number			
IQT Cetane Number			

Appendix 1
Test Methods and Descriptions

Test methods reported used in this work are based on the standard ASTM methods or standardized in-house methods given in Table A1. A short description is also provided.

Table A1
Test Methods

Test	Method	Description
API Gravity, °API	ASTM D4052	Calculated from specific gravity data
Specific Gravity, 60F/60F	ASTM D4052	Specific gravity at 60ºF compared to water at 60ºF by calibrated oscillating tube
Distillation	ASTM D86	Single-plate, atmospheric distillation
Reid vapor pressure, psi	ASTM D5191	Dry vapor pressure equivalent at 100ºF, instrumental method
Carbon, mass %	BP internal method	Instrumental, high precision
Hydrogen, mass %	BP internal method	Instrumental, high precision
Nitrogen, ppm	ASTM D5762	Instrumental, chemilumenescence detection
Sulfur, ppm	ASTM D5453	Instrumental, UV fluorescence
SFC Aromatics, vol%	ASTM D5186	Supercritical Fluid Chromatography
Lower heating value, BTU/lb	ASTM D4809	Bomb calorimetry
Cetane Number	ASTM D613	Engine test*
IQT Cetane Number	ASTM D6890	AET instrumental**

*The ASTM D613 single-cylinder, compression ignition engine test measures cetane number by determination of critical compression ratio at which the fuel ignites. The engine compression ratio is varied manually to find the minimum required to ignite the fuel. This is the standard method with the cetane scale defined by zero equal to performance of methyl naphthalene and one hundred equal to performance of n-hexadecane. In practice, heptamethyl nonane, cetane number 15, is used in place of methyl naphthalene. Intermediate cetane numbers are defined by volumetric mixtures of the two pure chemicals. For example, 40 cetane number is the performance for a mixture of 70.6 volume % heptamethyl nonane and 29.4 volume % n-hexadecane.

** The ASTM D6890 method uses the ignition quality tester (IQT) instrument made by AET. This instrument injects sample into a heated, air-pressurized chamber and measures the time delay (milliseconds) until a rapid pressure rise is observed. The delay time is related to ignition quality and is correlated to the ASTM D613 cetane number by an equation based on the time delays of the same two chemicals, heptamethyl nonane and n-hexadecane, and their mixtures.